Combining model detail with large scales

A simulation framework for population viability analyses in changing and disturbed environments

Dissertation

submitted by
Johannes A. Leins

for the degree of
Doctor of Natural Sciences
(Dr. rer. nat.)
in the academic discipline of "Ecology"

University of Potsdam
Faculty of Science
Institute of Biochemistry and Biology

Department of Ecological Modelling

Date of disputation: 16th February 2023

First Supervisor: Prof. Dr. Volker Grimm
Second Supervisor: Prof. Dr. Dr. Martin Drechsler
Reviewers: Prof. Dr. Boris Schröder-Esselbach
Prof. Dr. Bernd Blasius

Published online on the
Publication Server of the University of Potsdam:
https://doi.org/10.25932/publishup-58283
https://nbn-resolving.org/urn:nbn:de:kobv:517-opus4-582837

Summary

The global climate crisis is significantly contributing to changing ecosystems, loss of biodiversity and is putting numerous species on the verge of extinction. In principle, many species are able to adapt to changing conditions or shift their habitats to more suitable regions. However, change is progressing faster than some species can adjust, or potential adaptation is blocked and disrupted by direct and indirect human action. Unsustainable anthropogenic land use in particular is one of the driving factors, besides global heating, for these ecologically critical developments. Precisely because land use is anthropogenic, it is also a factor that could be quickly and immediately corrected by human action.

In this thesis, I therefore assess the impact of three climate change scenarios of increasing intensity in combination with differently scheduled mowing regimes on the long-term development and dispersal success of insects in Northwest German grasslands. The large marsh grasshopper (LMG, *Stethophyma grossum*, Linné 1758) is used as a species of reference for the analyses. It inhabits wet meadows and marshes and has a limited, yet fairly good ability to disperse. Mowing and climate conditions affect the development and mortality of the LMG differently depending on its life stage.

The specifically developed simulation model HiLEG (*Hi*gh-resolution *L*arge *E*nvironmental *G*radient) serves as a tool for investigating and projecting viability and dispersal success under different climate conditions and land use scenarios. It is a spatially explicit, stage- and cohort-based model that can be individually configured to represent the life cycle and characteristics of terrestrial insect species, as well as high-resolution environmental data and the occurrence of external disturbances. HiLEG is a freely available and adjustable software that can be used to support conservation planning in cultivated grasslands.

In the three case studies of this thesis, I explore various aspects related to the structure of simulation models per se, their importance in conservation planning in general, and insights regarding the LMG in particular. It became apparent that the detailed resolution of model processes and components is crucial to project the long-term effect of spatially and temporally confined events. Taking into account conservation measures at the regional level has further proven relevant, especially in light of the climate crisis. I found that the LMG is benefiting from global warming in principle, but continues to be constrained by harmful mowing regimes. Land use measures could, however, be adapted in such a way that they allow the expansion and establishment of the LMG without overly affecting agricultural yields.

Overall, simulation models like HiLEG can make an important contribution and add value to conservation planning and policy-making. Properly used, simulation results shed light on aspects that might be overlooked by subjective judgment and the experience of individual stakeholders. Even though it is in the nature of models that they are subject to limitations and only represent fragments of reality, this should not keep stakeholders from using them, as long as these limitations are clearly communicated. Similar to HiLEG, models could further be designed in such a way that not only the parameterization can be adjusted as required, but also the implementation itself can be improved and changed as desired. This openness and flexibility should become more widespread in the development of simulation models.

Zusammenfassung

Die globale Klimakrise trägt maßgeblich dazu bei, dass sich Ökosysteme verändern, die Artenvielfalt sinkt und zahlreiche Spezies vom Aussterben bedroht sind. Viele Arten sind prinzipiell in der Lage, sich wandelnden Bedingungen anzugleichen oder ihre Habitate in geeignetere Regionen zu verlagern. Allerdings schreitet der Wandel schneller voran als sich einige Spezies anpassen können oder die mögliche Anpassung wird durch direkte und indirekte menschliche Eingriffe blockiert und gestört. Gerade die nicht-nachhaltige Landnutzung durch den Menschen ist neben der Klimaerhitzung einer der treibenden Faktoren für diese ökologisch kritischen Entwicklungen. Gleichzeitig ist sie durch ihre unmittelbare menschliche Ursache ein Faktor, der sich kurzfristig und schnell korrigieren ließe.

Zu diesem Zweck untersuche ich in dieser Dissertation, wie sich drei Klimawandelszenarien ansteigender Intensität im Zusammenspiel mit unterschiedlich terminierten Mahdregimen im Nordwestdeutschen Grünland auf die langfristige Entwicklung und Ausbreitung von Insekten auswirken. In der Untersuchung fungiert die Sumpfschrecke (*Stethophyma grossum*, Linné 1758) als Bezugsspezies. Sie ist in Feucht- und Nasswiesen zu Hause und zu räumlicher Ausbreitung fähig, auch wenn sie nur eingeschränkt mobil ist. Mahd und Klimabedingungen wirken sich je nach Lebensstadium unterschiedlich stark auf die Entwicklung und Mortalität der Sumpfschrecke aus.

Das eigens entwickelte Simulationsmodell HiLEG (*Hi*gh-resolution *L*arge *E*nvironmental *G*radient) dient als Werkzeug zur Untersuchung und Projektion der Überlebens- und Ausbreitungswahrscheinlichkeit unter verschiedenen Klima- und Landnutzungsszenarien. Es ist ein räumlich explizites, stadien- und kohortenbasiertes Modell, das individuell konfiguriert werden kann, um den Lebenszyklus und die Charakteristiken terrestrischer Insektenarten sowie hochaufgelöste Umweltdaten und das zeitlich variierende Auftreten externer Störfaktoren abzubilden. HiLEG ist eine frei verfügbare Software und kann zur Unterstützung bei der Planung von Umweltschutzmaßnahmen in kultiviertem Grünland verwendet werden.

In den drei Fallstudien dieser Arbeit habe ich verschiedene Aspekte in Bezug auf die Struktur von Simulationsmodellen an sich, deren Bedeutung im Naturschutz im Allgemeinen und Erkenntnisse für die Sumpfschrecke im Speziellen untersucht. Es zeigte sich, dass die detaillierte Auflösung der Modellprozesse und –komponenten entscheidend ist, um den langfristigen Effekt räumlich und zeitlich begrenzter Ereignisse projizieren zu können. Insbesondere in Anbetracht der Klimakrise hat sich die gesteigerte Relevanz von Naturschutzmaßnahmen auf regionaler Ebene herausgestellt. Ich konnte außerdem bestätigen, dass die Sumpfschrecke zwar im Prinzip von der Klimaerwärmung profitiert, aber weiterhin durch ungeeignete Mahdregime beschränkt wird. Bewirtschaftungspläne könnten allerdings in dem Sinne angepasst werden, dass sie die Ausbreitung und Etablierung der Sumpfschrecke erlauben, ohne sich über die Maßen auf den Ertrag der Landwirtschaft auszuwirken.

Insgesamt können Simulationsmodelle wie HiLEG einen wichtigen Beitrag und Mehrwert für die Planung von Naturschutzmaßnahmen und Politikinstrument leisten. Richtig eingesetzt beleuchten die Simulationsergebnisse Aspekte, die durch subjektive Bewertung und Erfahrung einzelner Akteure möglicherweise übersehen würden. Auch wenn es in der Natur von

Modellen liegt, dass sie Einschränkungen unterworfen sind und nur Ausschnitte der Realität abbilden, sollte dies kein Hindernis für ihren Einsatz sein, solange diese Limitierungen klar kommuniziert werden. Analog zu HiLEG könnten Modelle so konzipiert werden, dass nicht nur ihre Parametrisierung nach Bedarf angepasst, sondern auch die Implementierung selbst beliebig verbessert und verändert werden kann. Diese Offenheit und Flexibilität sollte sich bei der Entwicklung von Simulationsmodelle stärker durchsetzen.

Contents

List of Figures

List of Tables

1 General Introduction

Worldwide, ongoing global change is causing the degradation of ecosystems and the loss of biodiversity, often even including the extinction of individual species (IPCC, 2022), if they cannot adapt in time. Species have a variety of adaptation strategies (Mawdsley et al., 2009) to cope in a changing environment, including distribution shifts, changes in life cycle timing and phenology, aligned demographic rates, such as fecundity, and range expansion (Bridle et al., 2014). In practice, however, wildlife is often incapable to respond quickly enough to such change (Parmesan et al., 1999) and thus additional human action is required to prevent biodiversity loss and assist the species' adaptations, or at least not inhibit them. While global institutions set the overall framework to halt climate change and biodiversity loss, it is becoming increasingly clear that these policies are insufficient and additional local and regional action is needed to achieve the worldwide objective (Moloney et al., 2018). There is an increasing demand regarding such actions to demonstrate their benefits to people and ecosystems upfront (Carpenter et al., 2009). For this purpose, both good knowledge of the system and of the potential prospects for regional policies and action are required to assess the success of a conservation objective (Hulme, 2005). Simulation models based on this knowledge could be a valuable tool for decision-making in conservation planning, yet they are rarely used for such assessments, despite their documented value. Decisions are still rather based on subjective judgment and stakeholder experience (Addison et al., 2013), which can lead to unintended consequences at worst. For this very reason, it can be important not only to build useful simulation models, but also to promote them and make them freely available.

1.1 Motivation

With this work, I address a number of challenges around biodiversity conservation under climate change and intend to support stakeholders in conservation planning in two ways. First, by providing an open access simulation model for those who need a tool to identify suitable measures for the conservation of grassland insects in a changing and disturbed environment. Second, by conducting case studies of a selected species to show what practical use such a model can have for stakeholders and what specific recommendations can be drawn from the study results for the conservation management of a grassland community. Although my approach is limited to a specific area, I believe that, on the one hand, contributions at all levels and scales of the global ecosystem are necessary to achieve the overall objective in a worldwide crisis. On the other hand, I am convinced that even specific results can help to draw general conclusions, to better understand the bigger picture and to have a starting point to approach similar problems.

1.2 Translating Micro-scale Experiments to Macro-scale Studies – Introducing the HiLEG Simulation Model

The present work introduces the simulation model HiLEG (*Hi*gh resolution *L*arge *E*nvironmental *G*radient) that allows analyzing the viability of a population as function of species parameters and a combination of environmental conditions. Both, population characteristics and environmental data can be individually predefined and adjusted for a simulation. The model aims at highlighting the relevance and potential impact of scale and resolution on wide-range and long-term results. Not only on the temporal and spatial scale, but also in the level of detail of a species' life cycle.

For this purpose, HiLEG makes use of scaling data and insights from micro-scale experiments to the regional- and state-level, and of spatially interpolating environmental data to match species-relevant resolutions. The scaling approach of HiLEG may miss the details of local population viability and distribution. It can, however, project the effect of environmental change and land use on regional population development sufficiently well to assess the relative performance of alternative management options.

Apart from the general purpose of simulation models to explore potential system context and development, the idea behind the described approach is threefold. First, to function as a tool for decision-makers to analyze where, when and how to preferably implement suitable land use measures taking into account the interests of both local stakeholders and conservation biologists. Second, to allow such analyses even with limited field data by upscaling and interpolating available data. Third, to include detailed system processes, in particular the life cycle of the species in question, even on the large scale to prevent overlooking their potential long-term effects.

Especially the second and third idea address aspects that many simulation studies still forgo at least to some extent (Pe'er et al., 2013), despite their potential relevance (Radchuk et al., 2013; Radchuk et al., 2014; Szewczyk et al., 2019). Surely the outcome of numerous modelling studies would change when increasing model resolution and including detailed system processes.

1.3 Endemic Species Require Relief from Multiple Stressors

Endemic species are threatened by a variety of stressors, most of which are directly or indirectly anthropogenic in origin (Munns, 2006), including the alteration of spatial structures, unsuitable land use and changing climate conditions. It is well known that the individual effects of such stressors can interact or reinforce each other, but studies often ignore the complexity of these combined effects (Oliver & Morecroft, 2014), despite their relevance for the protection of a species or ecological communities. Some species can adapt to a changing environment, evade disturbances or track shifting climate conditions (Mawdsley et al., 2009), but for others it is unclear whether they require assistance to keep up when migrating and to reduce their risk of extinction (Robillard et al., 2015).

Precisely because many of the stressors are human in origin, they can also be eliminated or reduced by human action of varying effort (Heller & Zavaleta, 2009). Among others, these actions include structural measures such as restoration, dispersal corridors or stepping stones,

but also changes in management such as reducing harmful (farming) practices, lowering intensive agriculture or changing land use schedules. Establishing refuges of suitable microclimate and structure (Cowan et al., 2021) or adapting management strategies to climate change (Hulme, 2005), for example, are two viable strategies on the regional scale to protect existing populations within a disturbed cultivated environment. It is, however, advisable to analyze the success of such measures in advance in order to avoid conflicts between the interests of regional stakeholders and those of species conservation (Rounsevell et al., 2006).

1.4 Diversification and Adaptation of Land use Practices as Factor in Conservation Planning

The most immediate and straightforward conservation measure in agriculturally intensive countries such as Germany is, in theory, the proper adaptation of land use practices. Intensity and timing of local land use practices could be adapted in a quick and easy manner, especially if the adaptation does not require any additional knowledge or technology. If such measures are additionally applied in a spatially and temporally more heterogeneous manner, different species and the overall biodiversity of a region could benefit (Benton et al., 2003). With some tradeoffs for both, biodiversity and agricultural production could even benefit at the same time (Brussaard et al., 2010).

Despite these benefits, the intensification of cultivated landscapes in Germany is advancing (Bundesamt für Naturschutz, 2017). There is even a debate about releasing ecological priority areas for agricultural use in the interest of food security (Dahm, 2022), although there are more sustainable options, such as rethinking the use of land for biofuel production (Franco et al., 2010) or a transformation towards a more plant-based diet (Mottet et al., 2017; Poore & Nemecek, 2018). Given the prevailing focus on high-yield agriculture, it may be challenging to convince farmers or other stakeholders to adapt their practices. Even more so as the design and spatial targeting of existing policies and measures has proven inefficient in the past (Meyer et al., 2015).

It is therefore essential to provide scientific evidence of the potential advantages related to diversification and adaptation of land use practices and conservation measures, not only on an abstract global level but also on a practical regional or local scale (Moloney et al., 2018). The advantages of applying conservation measures at the landscape level are widely recognized but rarely applied (Nguyen et al., 2022). Will et al. (2021) further emphasize that process-based models, despite their potential to contribute to the understanding of complex systems problems, rarely influence actual policy making. The authors recommend, among other things, the use of models to demonstrate different assumptions as a basis for discussion with stakeholders, and to ensure the availability of and accessibility to data and results. In terms of achieving disclosure with models, it can thus be particularly helpful to demonstrate the positive effects of focused and carefully timed measures.

1.5 Study Environment and Study Species

The analyses in this thesis evolve around the viability and range expansion of the large marsh grasshopper (LMG, *Stethophyma grossum*, Linné 1758) in cultivated grasslands of Northwest

Germany and its surroundings that are subject to climate change in scenarios of increasing severity.

The study region (Figure 1.1) includes Northwest Germany with its four federal states (Bremen, Hamburg, Schleswig-Holstein, Lower Saxony) and adjacent regions (parts of other federal states as well as Denmark and the Netherlands). It is subdivided into 968 terrestrial climate cells (Figure 3.1) with an area of 12×12 km^2 each. The federal state of Schleswig-Holstein is further subdivided (Figure 4.2) into 72,969 grassland cells with a defined area of 250×250 m^2 each, where the spatial grassland structure (e.g. level of fragmentation) differs depending on the sub region (Figures 4.2B and C, and 5.2, LEFT). Details on the spatial distribution of climate and grassland cells can be found in Sections 2.2, 3.2.1, 4.2.1 and 5.2.1.

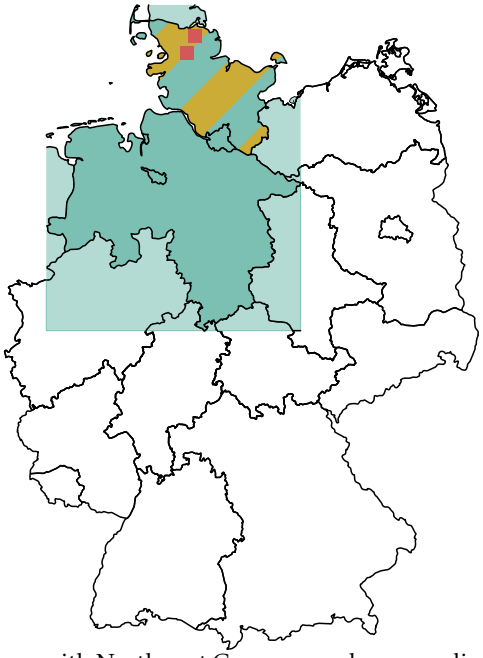

Figure 1.1: Outline map of Germany with Northwest Germany and surroundings in green (study region of Chapter 3), Schleswig-Holstein brown-green striped (Chapter 4), and the sub regions used in Chapter 5 marked by pink squares

The LMG (Figure 1.2) inhabits wet meadows and marshes (Ingrisch & Köhler, 1998) and is a species with limited ability to disperse (Sörens, 1996), although long distance dispersal does occasionally occur (Oppel, 2005). Its yearly life cycle has three main stages (Heydenreich, 1999), i.e., egg / larva / imago stage, while foremost the water demand of the egg stage binds the species to wet grasslands (Koschuh, 2004). Due to its former status as endangered species (Winkler, 2000; Winkler & Haacks, 2019), its role as indicator for the quality of grasslands (Keller et al., 2012; Keßler et al., 2012) and as likely beneficiary of climate change (Trautner & Hermann, 2008; Poniatowski et al., 2018a), it is a species well-suited for studying both the interplay of external drivers regarding population development and the range expansion into uninhabited territories. There are two types of external drivers influencing the LMG's life cycle considered in this work. The first are the climate conditions (Ingrisch, 1983; Wingerden et al., 1991) at a populations habitat, the second is anthropogenic land use in the form of grassland mowing (Malkus, 1997; Marzelli, 1997). For more details regarding the LMG and its adaption in terms of the simulation model see Sections 2.2, 2.7 3.2.2 and 4.2.2.

The climate conditions influencing the species' life cycle stem from projection data (Keuler et al., 2016) of daily resolution until the year 2080 for each of the 968 climate cells described

Figure 1.2: A female adult of the large marsh grasshopper, *Stethophyma grossum* (photo: Daniel Konn-Vetterlein). The specimen remained unharmed and was released to its natural habitat after taking photos.

above. These projections were calculated for three different scenarios of *Representative Concentration Pathways of* CO_2 (RCP) of increasing severity (RCP2.6, RCP4.5 and RCP8.5). To match the resolution of the 72,969 grassland cells in the state of Schleswig-Holstein, the climate data was upscaled using bilinear interpolation. The climate parameters considered relevant for the life cycle of the LMG that were taken from the available data are *surface temperature*, *precipitation* and (change in) *soil moisture content*. A comprehensive description of the climate data, parameters and their modification can be found in Sections 2.6, 3.2.3, 4.2.3 and Appendix A.1.

The grasslands of the study region are subject to mowing schedules of different predefined timing (Section 2.5, Table 2.4). Grassland mowing has an exclusively lethal effect on the target species, yet to a different extent depending on its life stage. Potentially positive effects of mowing are either ignored or implied for this study. Sections 2.7.1.6, 3.2.4, 4.2.4 and 5.2.1 give a more detailed description of both timing and effects of grassland mowing.

1.6 Thesis Outline

The remainder of this thesis has three parts structured into five chapters. In the only chapter of Part I, the basic version of the modelling framework HiLEG and its implementation, as well as two model extensions are introduced following the ODD (Overview, Design concepts, Details) protocol (Grimm et al., 2006; Grimm et al., 2020). These versions of HiLEG were used in three case studies. Part II contains one chapter for each of the three studies. Since the present thesis is a cumulative work, these chapters are organized like journal articles:

Chapter 3 is published in *Ecological Modelling* as
Leins, J.A., Banitz, T., Grimm, V., Drechsler, M., 2021. *High-resolution PVA along large environmental gradients to model the combined effects of climate change and land use timing: lessons from the large marsh grasshopper. Ecological Modelling 440, 109355.*

It projects the local effects of environmental conditions and land use on a grasshopper species in 968 climatically distinct regions of Northwest Germany over three future time periods and under three scenarios of climate change. Specifically, the following research questions are addressed:

(1) How do population density and viability shift regionally, given different climate change scenarios?

(2) Which mowing schedule has the least negative impact on the overall population density and viability in the study region?

(3) Does the mowing impact severity depend on the spatial location (with its specific climate)?

The results show that in most parts of the study region the grasshopper would benefit from climate change alone, especially higher temperatures, though regionally uncertain events of extended droughts could substantially inhibit egg development. Unsuitably scheduled grassland mowing, on the other hand, was the determining factor preventing long-term survival of a local grasshopper population, at least if it occurred in a critical phase during late spring and summer. Exclusively mowing before and after this phase allowed for species survival or even positive development, yet, such timing of land use might be unpopular with stakeholders. Regionally, the window of problematic mowing shifted depending on the temperature-driven development speed of a population and could thus provide the opportunity for more popular conservation-related land use schedules, if the vegetation period does not shift in the same way. The key to identifying the relevance of small-scale process for long-term effects was to include the species' detailed life cycle together with high-resolution climate data into the model implementation. In terms of conservation management, it is recommended to implement adaptive measures to be able to react to the changing environmental conditions.

Chapter 4 is published in *Ecology and Evolution* as
Leins, J.A., Grimm, V., Drechsler, M., 2022. *Large scale PVA modelling of insects in cultivated grasslands: the role of dispersal in mitigating the effects of management schedules under climate change. Ecology and Evolution, 2022;12:e9063.*

The paper analyzes how the timing of regionally homogeneous mowing schedules could either promote or hinder the range expansion of a species with limited dispersal abilities depending on the severity of climate change in grasslands of the North German federal state of Schleswig-Holstein. The analysis is centered around three research questions:

(1) Are there (regional) differences in dispersal success depending on climate change scenario?

(2) Is the success of dispersal additionally affected by spatial patterns such as grassland cover?

(3) Can dispersal compensate for otherwise detrimental grassland mowing?

The analyses highlight that the state of Schleswig-Holstein has a spatial threshold roughly running from northwest to southeast in terms of climate-induced dispersal success. North resp. east of this threshold, conditions for the target species improve most under more severe climate change scenarios (CCS), while south resp. west of the threshold less severe CCS tend to allow higher dispersal success. Exception to the latter is the moderate CCS that performs better than the the minor scenario even to the south, and in general is the most robust scenario in terms of dispersal success. In the applied model setup including long distance dispersal of the species, spatial landscape structure played a minor role for the overall population development. Considering grassland mowing, regional differences shifted but the tendency regarding the northwest-southeast threshold remained. Furthermore, the study showed that there are mowing schedules still allowing range expansion that were previously considered to be mostly detrimental for a non-dispersing population. The latter finding emphasized the relevance of scale, in this case the high spatial resolution, for the reliability of model projections.

Chapter 5 is ready for submission to *Conservation Biology* as
Leins, J. A. & Drechsler, M. *Finding the right balance of conservation effort in cultivated grasslands: A modelling study on protecting dispersers in a climatically changing and anthropogenically disturbed environment.*

It addresses the issue of focused conservation planning in two highly disturbed grassland regions of different spatial configuration in North Germany to potentially assist a dispersing target species in establishing and expanding its range with the following research questions:

(1) How does the relative effort in conservation-oriented grassland management affect the population development of a species with limited dispersal ability?

(2) Are there time-critical factors that are worth considering for conservation planning in a climatically changing environment?

(3) Does the conservation effort required to meet a conservation target differ depending on the spatial landscape structure?

The study results show that already a limited amount of focused conservation effort can help a range-expanding species to cope and thrive in an otherwise disturbed environment. Yet, a species' range remains restricted to reachable sites that are suitably managed, if the level of disturbance in other sites, which are only suitable in theory, is too high. For the evaluation of newly implemented conservation measures targeting a selected species, it is vital to have in-depth knowledge about its life cycle. The simulations revealed in this respect that newly inhabited sites can take some years to show a measurable population size due to the species intrinsic delay of population development. Regarding spatial correlations, allocating conservation effort in a landscape of aggregated grasslands transpired to be considerably more effective than in a fragmented landscape. Also, it is recommended to increase spatial heterogeneity in terms of diversification of land use practices. Including these spatial considerations into the model implementation helped revealing implications easily overlooked with a more coarse setup.

In the final Part III, the overall findings of this thesis are synthesized and discussed. Furthermore, a condensed interpretation and recommendation for stakeholders regarding the key results is given along with a discussion of the limitations and conclusion concerning the implications of the thesis.

Part I

Modelling Framework HiLEG

2 The *Hi*gh-resolution *L*arge *E*nvironmental *G*radient simulation model

The model description below follows the ODD (Overview, Design concepts, Details) protocol (Grimm et al., 2006; Grimm et al., 2020). It includes the original model description (M1 and black text) used to study the effects of land use and climate change on spatially stationary populations of the large marsh grasshopper in Northwest Germany (Chapter 3); it describes extensions made to the original model (M2 and green text) to explore the additional effects on the species when adding dispersal in an environment of higher spatial resolution (Chapter 4); and it incorporates the description of changes made (M3 and pink text) to study the implications of varying conservation effort (Chapter 5).

2.1 Purpose and Patterns

M1: The *PURPOSE* of the model HiLEG (*Hi*gh-resolution *L*arge *E*nvironmental *G*radient) is to answer the following questions regarding populations of the large marsh grasshopper (LMG) Stethophyma grossum (Linné 1758) in Northwest Germany: (1) How do population density and viability shift regionally, given different climate change scenarios? (2) Which mowing schedule has the least negative impact on the overall population density and viability in the study region? (3) Does the mowing impact severity depend on the spatial location (with its specific climate)?

The empirical patterns used to ensure that the model is realistic enough for its purpose are observed features of the life cycle and their sensitivity to environmental conditions, which were taken from literature. These patterns were used for the model's design. Model output in terms of population structure, densities and persistence were not compared to data, as such data are sparse. Therefore, all model predictions are relative, not absolute. The model was implemented in C++. The source code of the model implementation and the input files used for the simulations runs are available via a GitLab repository[1].

M2: The *PURPOSE* of the model extension is to study the additional effect of dispersal on the LMG in a North German environment of realistic grassland distribution with higher spatial resolution to answer the following questions: (1) Are there (regional) differences in dispersal success depending on climate change scenario? (2) Is the success of dispersal additionally affected by spatial patterns such as grassland cover? (3) Can dispersal compensate for otherwise detrimental grassland mowing?

The species' dispersal metrics were taken from literature and known LMG habitats (Chapter 4, Figure 4.2, orange circles) adapted from survey data[2] gathered in the years 2000 to 2016, which were used to analyze some implications of regional effects. Other measures of dispersal success are relative, not absolute, due to a lack of relevant data.

[1] HiLEG GitLab repository: `git.ufz.de/leins/hileg`

[2] Provided by Landesamt für Landwirtschaft, Umwelt und ländliche Räume via our project partner Stiftung Naturschutz Schleswig-Holstein

M3: *PURPOSE* of the second extension of the HiLEG model is to study which are the implications of restricted, heterogeneous conservation effort targeting the LMG addressed by these research questions: (1) How does the relative effort in conservation-oriented grassland management affect the population development of a species with limited dispersal ability? (2) Are there time-critical factors that are worth considering for conservation planning in a climatically changing environment? (3) Does the conservation effort required to meet a conservation target differ depending on the spatial landscape structure?

Two known LMG populations on the edge of unpopulated grasslands (taken from survey data[2]) were contemplated to examine the effect of spatial composition (aggregated, fragmented) on the dispersal success of the range-expanding species in a disturbed and changing environment. Timing of land use (mowing) was coupled to the start of the vegetation period as suggest by Gerling et al. (2020).

2.2 Entities, State Variables and Scales

M1: The model has the following entities: *Grid Cells* (defining environmental conditions) and *Population* per *Grid Cell* comprised of *Life Stages* which are comprised of age-distinguished *Cohorts*. *Flows* are auxiliary entities that manage the *density transfer* between *Life Stages* or their *loss* through mortality.

M2: Instead of *Grid Cells* the model extension has two separate entities *Climate Cells* (defining large scale climate conditions in a 12×12 km^2 region) and *Grassland Cells* (defining environmental conditions, e.g. interpolated climate values, on a scale of 250×250 m^2). A *Grassland Cell* contains an initially empty *Population* entity and is considered *inhabited* if the *Population* has a non-zero *density*. Otherwise it is considered *uninhabited*. The *Flow* entities additionally connect *Grassland Cells* and handle the *density transfer* between their *Populations* during dispersal.

M1: The LMG develops through three main *Life Stages* during a year (cf. Chapter 3, Section 3.2.2). Following Ingrisch (1983) and Wingerden et al. (1991), we divided the egg / embryo stage into pre-diapause, diapause and post-diapause development (called embryo hereafter) to account for the clutch's different susceptibility to climate conditions in autumn, winter and spring. This subdivision yields five *Life Stages*: (1) pre-diapause, (2) diapause, (3) embryo, (4) larva, (5) imago. Stages (1) to (3) occur below ground, stages (4) and (5) above ground. Furthermore, stages (2) and (4) can have multiple *Cohorts*, to allow survival over several years in case of conditions during winter that are unsuitable for development, and to account for different temperature-driven development speed depending on hatching date.

M2: Dispersal only occurs between the *Populations'* imago *Life Stages* of *Grassland Cells* within a defined neighborhood.

M1: Tables 2.1 and 2.2 provide an overview of the model's life cycle and spatial entities as well as their state variables. The *Population* consists of several *Life Stages* and is characterized by the *coordinates* of its *Grid Cell* and a *minimum density* [individuals m^{-2}]. The *Population*'s *density* and *aboveground density* [both in individuals m^{-2}] are calculated from its *Life Stages' densities*. A *Life Stage* has a *name*, consists of one or more *Cohorts* and supplies a *maximum age* [days] for each of those *Cohorts*. *Cohorts* exceeding the *maximum age* or falling below the *minimum density* are considered extinct. Furthermore, a *Life Stage* has a *flag* informing whether it occurs below or above ground. The *Life Stages' density* [individuals m^{-2}] is calculated from its

Cohorts' densities and the amount of *gain* [individuals m^{-2}] from the incoming *transfer Flow* of its preceding *Life Stage*.

Cohorts are distinguished by an *ID* and have an *age* [days] and a *density* [individuals m^{-2}]. They have a *development progress* given as a ratio $\in [0,1]$ that defines if and how *density* is transferred to subsequent *Life stages*. The *development progress* is used in two different ways depending on the external *Influence* (Section 2.7.1) associated with the *transfer Flow*: (1) it is directly affected by external *Influences* and contributes to a *Flow*'s *density transfer* to the subsequent *Life Stage* if it reaches a value of 1 (Section 2.7.4); or (2) it is used within stochastic *Influences* to determine the probability and extent of contribution to the *flow rate* (Section 2.7.1, Binominal Climate, M2: renamed from Factor; Algorithm 2). Without external *Influences*, the *development progress* defaults to a value of 1.

M1: The auxiliary entity *Flow* was introduced to ease the implementation of the model. Each *Flow* is characterized by the *life stage of origin* and *life stage of destination* (empty for *mortality Flow*), a static per capita *base flow rate* [day^{-1}] and a *total flow amount* [individuals m^{-2}]. For each *Cohort* in its *life stage of origin* it has a per capita *dynamic flow rate* [day^{-1}] and a *current flow amount* [individuals m^{-2}]. These *flow rates* are calculated using external *Influences* (Section 2.7.2). The different *types* of *Flows* define the different flow processes: *trans* (transferring *density* to a subsequent stage: $1 \rightarrow 2$, $2 \rightarrow 3$, $3 \rightarrow 4$, $4 \rightarrow 5$); *repr* (reproduction from imago (no loss) to pre-diapause stage; $5 \rightarrow 1$). Additionally, all five *Life Stages* and their *Cohorts* lose *density* through *mortality* (*Flow type mort*).

M2: A fourth *Flow type disp* (dispersal) is introduced defining the *density transfer* from a *Life Stage* to the same *Life Stage* (here, imago only) of a neighboring *Population*. Potential *density loss* during dispersal of the imago *Life Stage* is handled by an additional *mortality Flow*.

M1: The *Grid Cells* comprising the environment are characterized by their *coordinate* (cell indexes), *carrying capacity* (maximum number of aboveground population that can be sustained), daily climate conditions (*temperature*, *humidity*, *contact water*) and land use schedule (*mowing day*).

M2: *Grid Cells* are replaced by the two entities *Climate Cell* and *Grassland Cell* with the indexes of the former and the geometric center of the latter belonging to the same Cartesian coordinate systems. In this coordinate system, *x-coordinates* increase from West to East and *y-coordinates* from North to South. *Climate Cells* have a unique *ID* and contain the daily climate conditions in the original spatial resolution. *Grassland Cells* take the *carrying capacity* and a *mowing schedule* while adapting the climate conditions of up to four adjacent *Climate Cells* to calculate the local climate conditions using bilinear interpolation. Both the *mowing schedules* and the bilinear interpolation will be described in more detail below.

M1: The model uses daily time steps for updating the model's states and process. This time scale also reflects the sampling of the climate data. However, the single possible mowing event per year is considered on a weekly basis. To account for this weekly frequency, a year has 364 days by definition, resulting in exactly 52 full calendar weeks $year^{-1}$. Input data (i.e., climate time series) is either cropped or expanded accordingly. Simulations were run for 20 years (7280 time steps) or stopped earlier in case all *Cohorts* of the *Population* became extinct.

M2: For each year of the climate data, February 29^{th} (if exists) and December 31^{st} are omitted to achieve 364 days. A simulation run takes 21,840 time steps (60 years) starting on January 1^{st} 2020 and ending on December 30^{th} 2079. In the case of premature extinction of all *Populations*, simulations stop earlier.

Table 2.1: Overview of the model's life cycle entities (first column) and their state variables (second column). The text in parentheses of columns one and two represents the entity's or state variable's symbol when used, e.g., in equations. The third column gives the (initial) value(s) of the state variables, the fourth column gives their units (if any). In the fifth column, a brief description of the state variable is provided. The indexes for location and time step that distinguish entities and their dynamically changing states are implied and not explicitly specified in the identifier. The parameter $A_{hab} = 62,500\ m^2$ is the habitat size modeled for a Population.

Entity (symbol)	State Variable (symbol)	Value(s)	Unit	Description
Population (P)	coordinate ($coord_{x,y}$)	$x, y \in [1, 36]$		Index of rotated pole grid coordinates (see Section 3.2.3)
	set of Life Stages (P^{stages})	$\{S^{pre}, S^{dia}, S^{emb}, S^{lar}, S^{ima}\}$		Distinguished Life Stages of the target species
	set of Flows (P^{flows}_{type})			A set of all Flows associated with this Population distinguished by their flow type (see below)
	density ($dens^{P}$)	$\sum\{dens^{pre}, dens^{dia}, dens^{emb}, dens^{lar}, dens^{ima}\}$	$ind.\ m^{-2}$	Summed Life Stage densities
	aboveground density ($dens^{P}_{above}$)	$\sum\{dens^{lar}, dens^{ima}\}$	$ind.\ m^{-2}$	Summed density of the aboveground Life Stages
	minimum density ($dens_{min}$)	$\frac{1}{A_{hab}}$	$ind.\ m^{-2}$	Minimum density of one individual per habit
Life Stage (S^{name})	name	$\in \{pre, dia, emb, lar, ima\}$		Name of the distinguished Life Stages
	set of Cohorts ($S^{name}_{cohorts}$)	$\{C^m, \ldots, C^n\}, \{m, n\} \in \mathbb{N}$		Distinguished Cohorts associated with the Life Stage
	density ($dens^{name}$)	$\sum\{dens^m, \ldots, dens^n\}, \{m, n\} \in \mathbb{N}$	$ind.\ m^{-2}$	Summed densities of the associated Cohorts
	gain ($gain^{name}$)		$ind.\ m^{-2}$	Summed total flow amount of the incoming Flows (Sections 2.7.3, 2.7.4)
	aboveground flag ($above^{name}$)	$\in \{TRUE, FALSE\}$		Boolean flag defining whether the stage occurs above ground
	maximum age ($dens^{name}_{max}$)	$\in \{210, 1700, 120, 90, 120\}$	days	Maximum age of the associated Cohorts
Cohort (C^{name})	ID	$\in \mathbb{N}$		Unique Cohort identifier
	density ($dens^{ID}$)		$ind.\ m^{-2}$	The Cohort's individual density
	age (age^{ID})		days	Age in days since Cohort creation
	development progress ($prog^{name}_{ID}$)	$\in [0, 1]$		The ratio of development compared to full development
Flow (F^{name}_{type})	type	$\in \{trans, repr, mort, disp\}$		Defines how the Flow is processed
	life stage of origin ($orig$)	$\in \{S^{pre}, S^{dia}, S^{emb}, S^{lar}, S^{ima}\}$		Life Stage used to determine the amount of flow
	life stage of destination ($dest$)	$\begin{cases} \text{mort}, & \text{if type=mort} \\ \in \{S^{pre}, S^{dia}, S^{emb}, S^{lar}, S^{ima}\}, & \text{otherwise} \end{cases}$		Life Stage receiving the amount of flow, or the amount of mortality
	set of influences (I^{name}_{type})			Environmental drivers associated with this Flow
	base flow rate ($rate^{name}_{type}$)		day^{-1}	Daily per capita base flow rate
	dynamic flow rate (dyn^{ID}_{type})		day^{-1}	Daily per capita flow rate per Cohort in the life stage of origin
	current flow amount ($amount^{ID}_{type}$)	$dens^{ID} \times dyn^{ID}_{type} \times day$	$ind.\ m^{-2}$	Amount of density flow over one day
	total flow amount ($amount^{name}_{type}$)	$\sum\{amount^m_{type}, \ldots, amount^n_{type}\}, \{m, n\} \in \mathbb{N}$	$ind.\ m^{-2}$	Summed amount (per Cohort) of density flow over one day

Abbreviations: above=aboveground, C=Cohort, coord=coordinate, dens=density, dest=destination, dev=development, dia=diapause, disp=dispersal, dyn=dynamic, emb=embryo, F=Flow, hab=habitat, ID=Cohort identifier, ima=imago, ind=individuals, lar=larva, m=meter, max=maximum, min=minimum, mort=mortality, orig=origin, P=Population, pre=prediapause, prog=progress, repr=reproduction, S=Life Stage, t=time step, trans=transfer

Table 2.2: Overview of the model's spatial entities (first column) and their state variables (second column). The text in parentheses of columns one and two represents the entity's or state variable's symbol when used, e.g., in equations. The third column gives the (initial) value(s) of the state variables, the fourth column gives their units (if any). In the fifth column, a brief description of the state variable is provided. The indexes for location and time step that distinguish entities and their dynamically changing states are implied and not explicitly specified in the identifier.

Entity (symbol)	State Variable (symbol)	Value(s)	Unit	Description
Climate Cell (Ω)	ID	$\in [1, 107] \subset \mathbb{N}$		Unique identifier of Climate Cells in Schleswig-Holstein
	$center_{x,y}$	$\{x, y\} \in \mathbb{N}$		Geometric center in coordinate system of Grassland Cells
	temperature (ω_{ts})		°C	Local surface temperature
	humidity (ω_{rhug})		%	Local relative humidity in the upper 2 cm of the ground
	contact water (ω_{cw})		$kg\ m^{-2}$	Amount of water in the upper 2 cm of the ground
Grassland Cell (G)	coordinate ($coord_{x,y}$)	$\{x, y\} \in \mathbb{N}$		Index in Cartesian coordinate system
	carrying capacity (cap_{above})	25	$ind.\ m^{-2}$	Maximum aboveground density
	climate value(s) (ω_{clim})			Calculated by weighing resp. values of adjacent Climate Cells
	mowing schedule (T_{mow})	See Table 2.4	days	Occurrence days of mowing events
	start of vegetation period (t_{veg})		day	Day on which the yearly sum of surface temperature ω_{ts} reaches 200.0 °C (see Eqn. 2.28)

Abbreviations: above=aboveground, cap=capacity, clim=climate, coord=coordinate, cw=contact water, G=Grassland Cell, ID=Climate Cell identifier, ind=individuals, kg=kilogram, m=meter, mow=mowing, rhug=relative humidity upper ground, t=time step, temp=temperature, ts=surface temperature, veg=vegetation

M1: The environment, or study region, comprises 1296 (36×36) cells, each having an area of 144 km^2 (12×12 km^2), which corresponds to the resolution of the climate input data (Section 2.6). The integer *Grid Cell* indexes (1-36) are mapped to rotated pole grid coordinates (Chapter 3, Figure 3.1). 968 *Grid Cells* are terrestrial and therefore belong to the model domain. Within a *Grid Cell* a single habitat is simulated and represents a squared virtual grassland plot with the size of 6.25 ha (250×250 m^2). *Grid Cells* and hence habitats are not connected, i.e., there is no exchange of individuals. If populations become extinct, there is no recolonization.

M2: The study region is the German federal state of Schleswig-Holstein (SH) consisting of a 107 terrestrial *Climate Cell* subset of the original data and 72,969 *Grassland Cells* representing the state's actual grassland area that were retrieved using the software DSS-Ecopay (Mewes et al., 2012; Sturm et al., 2018). Each *Grassland Cell* by definition has a size of 6.25 ha (250×250 m^2) that reflects the spatial resolution of the data quite well. *Grassland Cells* within a radius of 1,500 m are connected by the dispersal process of the imago *Life Stage*. In some cases, there are additional connections outside this radius representing long distance dispersal (LDD). The connections and dispersal processes will be described below.

M3: Two sub regions of the grasslands described above function as point of origin for the simulation of a range-expanding species, both containing a known LMG population on the edge of unpopulated territory. The regions are of different spatial composition (cf. Chapter 5, Figure 5.2B), where the northern one is spatially fragmented in terms of grassland cover around the known population and the southern one has rather aggregated grasslands. Again, *Grassland Cells* are connected by the dispersal process in a radius of 1,500 m, but LDD is ignored to focus the analysis on the actual grassland composition.

2.3 Process Overview and Scheduling

M1: In each time step and for every *Grid Cell* (M2: *inhabited Grassland Cell*), four main blocks of *PROCESSES* are executed: 'Update environmental drivers', 'Flow update', 'Life Stage update', and 'Cohort update'. The first three blocks are SCHEDULED one after the other, while 'Cohort update' is executed as a submodel of 'Life Stage update'. Algorithm 1 gives an overview of this top level scheduling. During 'Flow update' the *flow rates* and *amounts* are calculated using the *Flow*'s *life stage of origin* while depending on its *type* and specified external *Influences* (submodel 'Update environmental drivers').

M2: The *PROCESS* 'Bilinear climate interpolation' is executed each time step as a submodel of 'Update environmental drivers'. If the *life stage of destination* of a non-zero (in terms of *flow amount*) dispersal *Flow* belongs to the *Population* of an *uninhabited Grassland Cell*, the *Population* is not empty anymore and the cell thus rendered *inhabited*. In this case, the submodel 'Dispersal setup' is executed to find all *Grassland Cells* considered neighbors of the *Population* and establish a dispersal connection to each of them by creating a respective *Flow* of *type disp*.

M3: The *PROCESS* 'Start of vegetation period' is executed executed each time step as a submodel of 'Update environmental drivers' right after submodel 'Bilinear climate interpolation'.

M1: The 'Life Stage update' first handles creation (input from *Flows*) and lastly deletion (*density* falling below *minimum density*) of its *Cohorts*. In between *Cohort* creation and deletion, the submodel 'Cohort update' is executed.

Algorithm 1 Main process overview. Processes executed at each inhabited Grassland Cell and for each time step. The processes 'Bilinear climate interpolation' and 'Cohort Update' are executed as submodel of 'Update environmental drivers' and 'Life Stage update', respectively.

for all Inhabited Grassland Cells / Populations **do**
  RUN SUBMODEL('Update environmental drivers')
  for all Originating Flows **do**
    RUN SUBMODEL('Flow update')
    if $[Flow_{type} = \text{'dispersal'} \ \& \ Flow_{amount} > 0 \ \& \ Population^{target}_{density} = 0]$ **then**
      $Grassland\ Cell^{target}_{state} \leftarrow \text{'inhabited'}$
    end if
  end for
end for
for all Inhabited Grassland Cells / Populations **do**
  $Population_{density} \leftarrow 0$
  for all Life Stages **do**
    RUN SUBMODEL('Life Stage update')
    $Population_{density} \leftarrow Population_{density} + Life\ Stage_{density}$
  end for
  if $Population_{density} < min_{density}$ **then**
    $Grassland\ Cell^{target}_{state} \leftarrow \text{'uninhabited'}$
  end if
end for

2.4 Design Concepts

Basic Principles:

M1: The model uses viability, i.e., the ability of small populations to persist, as a comparative metric to identify grassland *mowing schedules* that are compatible with the projected climate conditions in a certain region. Development and mortality of the different *Life Stages* are driven by environmental factors. For this, relationships were imposed that reflect the available empirical knowledge and data.

M2: The extension uses the same comparative metrics and environmental drivers as the original study. Additionally, it applies density-independent dispersal using a fat-tailed dispersal kernel that changes depending on regional grassland cover. Relevant dispersal parameters were adapted from empirical studies of the target species.

Emergence:

M1: The relationships describing the life cycle are imposed and not emergent from first principles, such as energy budgets or adaptive decision making.

M2: The dispersal metrics are imposed by the parameter definitions such as dispersal radius.

Interaction:

M1: The model does not include direct interaction within or among different *Life Stages*. Indirect interactions are included by assuming density dependence of the mortality of larvae and imagines.

M2: Neighboring *Populations* of *inhabited Grassland Cells* indirectly interact through a dispersal process that depends on the grassland cover surrounding the originating cell.

Stochasticity:

M1: Transfer from embryo to larval (F^{emb}_{trans}, Table 2.5) and larval to imago (F^{lar}_{trans}) *Life Stage* is stochastically drawn from a binominal distribution (Section 2.7.1). The probability is influenced by temperature, *Cohort density* and *development progress*.

M2: Dispersal mortality as well as the actual dispersal from a *Population*'s imago *Life Stage* to the imago *Life Stages* of its connected *Grassland Cells* is determined stochastically using a density dependent binomial distribution. The *dispersal probability* for each connection is calculated using a predefined *base dispersal rate*, a distance dependent *dispersal preference*, a *probability* of finding the connected neighbor and a *survival probability*, where the latter two depend on grassland cover and distance between both *Grassland Cells*. The probability of dispersal mortality is derived from the summed dispersal probabilities.

2.5 Initialization

M1: The model is initialized with a *starting date*, *duration*, *mowing day* and *climate change scenario* (CCS). Additionally, each *Population* receives an *initial density* per *Life Stage*. The *carrying capacity* [individuals m^2] for the aboveground population is assumed to be the same for all *Grid Cells* to reduce the number of confounding factors in the model analysis. As the climate data only offers a single projection per RCP scenario (cf. Chapter 3, Section 3.3.2) and

location, we resampled the time series per replicate run (*seed*): for a simulation period of 20 years, we used a time frame of 30 years (simulation period ±5 years) and reordered the years by sampling with replacement. This resampling is feasible since there are no significant trends in the relevant climate parameters within such a period (K. Keuler, pers. comm.). Simulation period 2060-79 has just 26 years, because climate data was only available up to the year 2080. A list of the sampled years per *seed* and simulation period is supplied in Appendix A.2. The initial settings of the model are listed in Table 2.3.

M2: Every simulation starts on 01 January 2020 and runs for 60 years (21,840 time steps). A run is initialized with one of three *CCS*, a single *starting Population* in the *Grassland Cell* closest to the geometric center of either one of the 107 *Climate Cells* and one out of 18 *mowing schedules* (Table 2.4). Ignoring replicates, this results in a total of 5,778 distinct simulations runs. In the *Grassland Cell* of the starting *Population* the base *mowing schedule* named M20+00+44 always applies. Here, the first number of the schedule's name stands for early mowing calendar week 20 (day 133) and the last number for late mowing week 44 (day 301). The middle number defines the (additional) mowing weeks 22-38 of more intensive grassland management schedules (acronyms: M22-M38). All other cells receive the initially defined schedule. In that way, the starting location works as a rather undisturbed habitat of low-impact grassland mowing rendering it a fixed point for analyzing the dispersal process. Early mowing (day 133) for schedules M22-25 is omitted, because cuts should be at least six weeks apart, and late mowing (day 301) for schedules M35-38, because it us unnecessary due to slowed grassland growth and being economically ineffective for farmers (Gerling et al., 2022). Per replicate run, each simulation year was resampled randomly using ±10 years, e.g. the simulation year 2053 was determined using the set $\{2043, 2044, ..2063\}$. If the set would exceed the available data (e.g. for years > 2080), it is reduced accordingly.

M3: The initialization is similar to the one in M2 with some exceptions: (1) a single known population is initially placed either in spatially aggregated or fragmented grasslands of the study region (cf. Table 2.3, reg_{init}); (2) *Grassland Cells* are either subject to the *conventional mowing schedule* T_{conv} or, with probability p_{prot}, to the *protective schedule* T_{prot} (cf. Table 2.4), where that schedule at the initial cell is always T_{prot}; (3) the protected grassland probability $p_{prot} \in \{0.01, 0.02 \ldots, 0.2, 1.0\}$ (cf. Table 2.3) is defined at simulation start; (4) the timing of the *mowing schedules* is defined to be coupled to the start of the vegetation period t_{veg} (Section 2.7.7); (5) LDD remained disabled; and (6) a number of 100 replicates were run each using a distinct *random seed*.

Table 2.3: List of parameters used to initialize a simulation run and to evaluate simulation results. First column: parameter name used in text. Second column: parameter symbol when used in model equations. Third column: initial / determined value(s) resp. value options used for simulation runs. Fourth column: brief description of the parameter. Parameters below double line can be varied in principle, but are constant in the presented work. M2: rows below first single line contain relevant parameters for the dispersal process. M3: rows below second single line contain parameters used for evaluating results.

Parameter Name	Symbol	Value(s)/ Unit	Description
starting date	t_{init}	1^{st} Jan. of 2000, 2020, 2040 or 2060	The date of initial time steps translated to climate data index
mowing day	t_{mow}	none or day 134, 141,..,274	The timing of mowing per year
Climate change scenario	CCS	FF, MOD or BAU	Representative Concentration Pathways of CO_2 model
mowing schedule	T_{mow}	see Table 2.4	A set of mowing days per year
initial region	reg_{init}	$\in \{aggr, frag\}$	Definition of originating habitat (region) in terms of spatial configuration of grassland surrounding it, where aggr=aggregated and frag=fragmented
protected grassland probability	p_{prot}	$\in \{0.01, 0.02, \ldots, 0.2, 1.0\}$	Probability of grassland to be defined as protected habitat ($T_{mow} = T_{prot}$) at simulation start (cf. Table 2.4)
duration	t_Δ	7,280 or 21,840 days	Runtime in days resp. time steps
habitat area	A_{hab}	$250 \times 250\ m^2$	Area of a Grassland Cell
initial density	$dens_{init}$	$\{0, 0.016 \vee 0.725, 0, 0, 0\}$ $ind.\ m^{-2}$	The initial Population density per Life Stage in individuals m^{-2}
carrying capacity	cap_{above}	$25\ ind.\ m^{-2}$	Maximum aboveground density per square meter
climate cell size	$size_{clim}$	$12,000\ m$	Width and height of square Climate Cells
habitat size	$size_{hab}$	$250\ m$	Width and height of square habitats / Grassland Cells
dispersal radius	rad_{disp}	$1,500\ m$	Maximum distance covered by an individual (Griffioen, 1996)
base dispersal rate	$rate^{ima}_{disp}$	$0.00595\ day^{-1}$	Daily rate of furthest dispersing imagos (Malkus, 1997)
dispersal preference	$pref^{near}$	1	Preference of selecting a neighbor during the dispersal process. Higher values result in selection of closer neighbors.
sight	$sight_{disp}$	0.5	Ability to find a selected neighbor during a dispersal process
decay rate	dec_{disp}	0.04	Distance dependent probability of surviving dispersal
inhabited status	$stat_{inh}$	$\in \{occ, est, res\}$	The inhabited status of a grassland habitat, where occ=occupied, est=established, res=residential
potential range	rng_{pot}	m	The distance in meters from habitat of origin to farthest habitat (in)directly connected by rad_{disp}
realized range	rng_{inh}, $inh \in stat_{inh}$	m	The distance in meters from habitat of origin to farthest occupied / established / residential habitat
number of changing habitats	Δn_{inh}, $inh \in stat_{inh}$	$\in \mathbb{N}$	Yearly number of habitats changing their inhabited status to occupied /established /residential
population density	$dens_{occ}$	$ind.\ m^2$	Population density in $individuals\ m^2$ considering all occupied habitats in the region

FF=full force, MOD=moderate, BAU=business as usual, CCS=climate change scenario, aggr=aggregated, above=aboveground, cap=capacity, clim=climate, dec=decay, dens=density, disp=dispersal, est=established, frag=fragmented, hab=habitat, ima=imago, inh=inhabited, init=initial, m=meters, mow=mowing, occ=occupied, pot=potential, pref=preference, prot=protective / protected, rad=radius, reg=region, res=residential, rng=range, scen=scenario, stat=status, t=time step, veg=vegetation

Table 2.4: Yearly grassland mowing schedules as applied in the simulation runs. First column gives the names of the 18 mowing schedules that encode the calendar weeks of yearly mowing occurrence divided by a plus (+) symbol. An acronym of the schedule name is provided in the second column, encoding the relevant mowing week in its name. The last three columns give the actual yearly mowing days (first day of respective calendar week) per mowing schedule. Schedules that include cells containing a dash (encoded by '00' in the respective name) only have two mowing occurrences per year, all others have three. The first mowing schedule M20+00+44 represents low-impact mowing, while more intensive mowing schedules follow in the rows below the double line.
M3: Deviating timing for dynamic mowing schedules in conventionally managed (T_{conv}) and protected grasslands (T_{prot}). Mowing occurs x days after yearly start of vegetation period t_{veg} (Table 2.3).

Schedule name	Acronym	Mowing days				
M20+00+44	M00	133	-	301		
M00+22+44	M22	-	147	301		
M00+23+44	M23	-	154	301		
M00+24+44	M24	-	161	301		
M00+25+44	M25	-	168	301		
M20+26+44	M26	133	175	301		
M20+27+44	M27	133	182	301		
M20+28+44	M28	133	189	301		
M20+29+44	M29	133	196	301		
M20+30+44	M30	133	203	301		
M20+31+44	M31	133	210	301		
M20+32+44	M32	133	217	301		
M20+33+44	M33	133	224	301		
M20+34+44	M34	133	231	301		
M20+35+00	M35	133	238	-		
M20+36+00	M36	133	245	-		
M20+37+00	M37	133	252	-		
M20+38+00	M38	133	259	-		
conventional	T_{conv}	42	84	126	168	210
protective	T_{prot}	49	-	-	-	217

2.6 Input Data

M1: As input source, time series of climate data for each *Grid Cell* are used. Each climate parameter (*ts*, *pr*, *mrso*, *smt* – cf. Chapter 3, Section 3.2.3 and Appendix A.1) is read from a single NetCDF[3] data file that stores one data point per day and coordinate. Files provided for this work contain time series from 01 January 1995 to 31 December 2080 including leap years. All data points on 29 February and 31 December are removed to achieve 364 day long years (Section 2.2).

M2: Climate parameters of a *Grassland Cell* are determined using up to four terrestrial *Climate Cells* in direct squared neighborhood that in terms of their geometrical center are closest to the *coordinate* of the *Grassland Cell*. The parameter values are then calculated using bilinear interpolation (Section 2.7.6) resulting in a two-dimensionally gradual climate data resampling of higher spatial resolution (107 to 72,969 spatial data points).

2.7 Submodels

M1: Table 2.5 gives an overview of the model processes and dynamics rates. The underlying full equations are provided in Table 2.6 and the corresponding parameters in Table 2.7.

[3]Network Common Data Form (NetCDF) library documentation: `www.unidata.ucar.edu/software/netcdf/`

M2: Sections 2.7.1.7, 2.7.5 and 2.7.6 describe the dispersal process between *Populations*, the setup of a dispersal network within a neighborhood of *Grassland Cells* and the calculation of climate values for a *Grassland Cell* using bilinear interpolation of values stemming from coarse-scale parameters of adjacent *Climate Cells*.

M3: Sections 2.7.1.6 and 2.7.1.7 include descriptions of randomly selected *mowing schedules* and the calculation of discrete amounts of dispersing individuals, respectively, while Section 2.7.7 introduces the temperature driven calculation of vegetation start per year and *Grassland Cell*.

2.7.1 Update Environmental Drivers

M2: The environmental drivers are updated every time step for each *Grassland Cell*. This means here that the climate values are recalculated by bilinear interpolation (Section 2.7.6) and it is checked whether a *mowing schedule* takes effect.

M3: The timing of a mowing event (Section 2.7.1.6) can be associated with the start of the local vegetation period (Section 2.7.7), if defined accordingly at simulation start. Timing can thus change dynamically from year to year while slightly differing between *Grassland Cells*.

M1: Both *flow rates* and a *Cohort*'s *development progress* can change depending on the current value of environmental drivers or static conditions. Our model includes functions or equations – called *Influences* – that may be applied to achieve dynamic changes. Generally speaking, each *Influence* provides a factor that can mediate the effect of environmental conditions on the variables *dynamic flow rate* and *development progress* of a *Flow* or *Cohort*, respectively. This factor may be restricted to a minimum and maximum value ($f_{min} = 0$ and $f_{max} = 1$, if not specified otherwise) regardless of those conditions and contributes either in a multiplicative or additive way to the update of a *rate* or *progress*. The contribution to an *Influence's* current factor f_{inf} by a multiplicative factor f_{mult} is – as the name suggests – simply $f_{inf} \times f_{mult}$; while an additive factor f_{add} contributes via the equation

$$f_{inf} + (1 - f_{inf}) \times f_{add} \tag{2.1}$$

A factor is calculated during the update of the associated *Flow* / *Cohort*. The specific *Influences* are described below and their equations summarized in Table 2.6. *Influences* may be combined for the use in a process. The empirical basis for these equations is given below.

M1: The *Capacity Influence* is used in a logistic function that increases its factor with increasing *population density*. It restricts *Life Stages* to a maximum size by raising the mortality for large populations (Eqn. 2.2).

A *Linear Climate Influence* provides a factor that is linearly correlated with a specified climate value either in a positive or negative manner (Eqn. 2.3).

Similar to the linear correlation, an *Exponential Climate Influence* can be used to provide a factor that is exponentially correlated to a specified climate value (Eqn. 2.4).

The *Sigmoid Climate Influence* is the third option to provide a factor by correlating with a climate value (Eqn. 2.5). It allows bounding a factor to an upper and lower limit without clipping it.

Table 2.5: Overview of the model processes and their daily rates and equations. Processes (second column) are distinguished by Life Stage (first column) and referenced by their symbol (third column) as used in the model equations. The fourth column defines the equation and environmental drivers (Influences, f-symbols, cf. Table 2.6) used for calculating a cohort-specific dynamic rate. Equation segments marked with *s are simplifications of the iterative process of updating the flow rate described in Algorithm 4. Superscript letters reference the sources used to parameterize the processes and equations for the LMG (coefficients in Table 2.7): [a]Ingrisch (1983), [b]B. Schulz (pers. comm.), [c]Wingerden et al. (1991), [d]Ingrisch & Köhler (1998), [e]Helfert & Sänger (1975), [f]Helfert (1980), [g]Kriegbaum (1988), [h]Waloff (1950) , [i]Griffioen (1996), [j]Malkus (1997).

Life Stage (symbol)	Process	Process symbol	Dynamic rate (daily)	Description
pre-diapause (S^{pre})	mortality	F^{pre}_{mort}	$dyn^{ID}_{mort} = rate^{pre}_{mort} + (1 - rate^{pre}_{mort})^* \times (f^A_{sig} \times f^B_{thd} + f^C_{mow})$	The base mortality rate a increases in two cases: (1) humidity-driven $(f^A_{sig})^a$ if contact water $(f^B_{thd})^a$ is missing; (2) if mowing is scheduled $(f^C_{mow})^b$
	development	$prog^{pre}_{ID}$	$prog^{pre}_{ID} = \begin{cases} prog^{pre}_{ID} + f^D_{thd}, & if\ f^D_{thd} > 0 \\ 0, & \text{otherwise} \end{cases}$	Needs three days below 10 °C in a row $(f^D_{thd})^a$ to fully develop
	transfer	F^{pre}_{trans}	$dyn^{ID}_{trans} = \begin{cases} 1, & if\ prog^{pre}_{ID} = 1 \\ 0, & \text{otherwise} \end{cases}$	Immediately transfers to diapause stage if fully developed
diapause (S^{dia})	mortality	F^{dia}_{mort}	$dyn^{ID}_{mort} = rate^{dia}_{mort} + (1 - rate^{dia}_{mort}) \times f^E_{mow}$	The base mortality rate increases if mowing is scheduled $(f^E_{mow})^b$
	development	$prog^{dia}_{ID}$	$prog^{dia}_{ID} = \begin{cases} prog^{dia}_{ID} + \frac{f^F_{thd}}{2}, & if\ prog^{dia}_{ID} < 0.5, \\ prog^{dia}_{ID} + \frac{f^G_{thd}}{2}, & if\ prog^{dia}_{ID} \geq 0.5 \wedge f^G_{thd} \neq 0, \\ 0.5, & \text{otherwise} \end{cases}$	Needs 61 days below 5 °C to break diapause $(f^F_{thd})^{a,c}$ and afterwards three days above 10 °C in a row $(f^G_{thd})^a$ to fully develop. Temperatures > 5 °C before diapause is broken reverse development
	transfer	F^{pre}_{trans}	$dyn^{ID}_{trans} = \begin{cases} 1, & if\ prog^{dia}_{ID} = 1 \\ 0, & \text{otherwise} \end{cases}$	Immediately transfers to embryo stage if fully developed
embryo (S^{emb})	mortality	F^{emb}_{mort}	$dyn^{ID}_{mort} = rate^{emb}_{mort} + (1 - rate^{emb}_{mort})^* \times (f^H_{exp} + f^I_{sig} \times f^J_{thd} + f^K_{mow})$	The base mortality is defined by the temperature $(f^H_{exp})^c$. It increases in two cases: (1) humidity-driven $(f^I_{sig})^a$ if contact water $(f^J_{thd})^a$ is missing and / or (2) if mowing is scheduled $(f^K_{mow})^b$
	transfer	F^{emb}_{trans}	$dyn^{ID}_{trans} = rate^{emb}_{trans} \times f^L_{bin}(f^M_{exp}, f^N_{exp}, dens^{ID}, prog^{name}_{ID})$	The base transfer rate is multiplied by a temperature- $(f^M_{exp}, f^N_{exp})^c$, progress- and the density-driven hatching probability stemming from a binomial distribution (f^L_{bin})
larva (S^{lar})	mortality	F^{lar}_{mort}	$dyn^{ID}_{mort} = rate^{lar}_{mort} + (1 - rate^{lar}_{mort})^* \times (f^O_{cap} + f^P_{lin} + f^Q_{mow})$	The base mortality $rate^d$ increases with density $(f^O_{cap})^b$ and in two additional cases: (1) the temperature (f^P_{lin}) is below 10 °C and / or (2) if mowing is scheduled $(f^Q_{mow})^b$
	transfer	F^{lar}_{trans}	$dyn^{ID}_{trans} = rate^{lar}_{trans} \times f^R_{bin}(f^S_{lin}, f^T_{lin}, dens^{ID}, prog^{lar}_{ID})$	The base transfer rate is multiplied by a temperature- $(f^S_{lin}, f^T_{lin})^{e,f}$, progress- and density-driven maturation probability stemming from a binomial distribution (f^R_{bin})
imago (S^{ima})	mortality	F^{ima}_{mort}	$dyn^{ID}_{mort} = rate^{ima}_{mort} + (1 - rate^{ima}_{mort})^* \times (f^U_{cap} + f^V_{lin} + f^W_{mow} + f^X_{mow})$	The base mortality $rate^g$ increases with density $(f^U_{cap})^b$ and in three additional cases: (1) the temperature (f^V_{lin}) is below 10 °C, (2) if mowing is scheduled $(f^W_{mow})^b$ and / or (3) loss during dispersal (f^X_{bif})
	reproduction	F^{ima}_{repr}	$dyn^{ID}_{repr} = rate^{ima}_{repr}$	Fixed reproduction $rate^{d,h}$
	dispersal	$F^{ima}_{disp}(a, b)$	$dyn^{ID}_{disp} = f^Y_{bif}$	Dispersal rate from a to b depends on grassland cover around a, and is stochastically determined by a binomial distribution $(f^Y_{bif})^{i,j}$

Abbreviations: bif=binominal factor, bin=binominal climate, cap=capacity, dens=density, dia=diapause, disp=dispersal, emb=embryo, exp=exponential, f=symbol of Influence function, F=Flow, ID=Cohort identifier, ima=imago, lar=larva, lin=linear, mort=mortality, mow=mowing, pre=pre-diapause, prog=progress, repr=reproduction, sig=sigmoid, t=time step, thd=threshold, trans=transfer

Table 2.6: List of equations / functions applied for environmental drivers including numbering (first column), name as used in the text (second), symbol with subscript of name abbreviation (third) and brief description (last)

Eqn#	Name	Equation / Function (symbol)	Description
(2.2)	Capacity Influence	$f_{cap} = \left(1.0 + e^{\beta^1_{cap}\left[\frac{dens^P_{above}}{A_{hab}} - \beta^2_{cap} \times cap_{above}\right]}\right)^{-1}$	Applying carrying capacity for the aboveground population
(2.3)	Linear Climate Influence	$f_{lin} = \beta^1_{lin} + \beta^2_{lin} \times \omega_{clim}$	Linear correlation with a climate parameter
(2.4)	Exponential Climate Influence	$f_{exp} = \beta^1_{exp} + \beta^2_{exp} \times e^{\left(\beta^3_{exp}\omega_{clim}\right)}$	Exponential correlation with a climate parameter
(2.5)	Sigmoid Climate Influence	$f_{sig} = \beta^1_{sig}\left\lvert 1 - \left(1 + e^{-\beta^2_{sig}\left[\omega_{clim} - \beta^3_{sig}\right]}\right)^{-1}\right\rvert$	Sigmoid correlation with a climate parameter
(2.6)	Factor Threshold	$f_{thd} = \begin{cases} \beta^1_{thd}, & if\ \omega_{clim} \leq thd_{clim}, \\ \beta^2_{thd}, & \text{otherwise} \end{cases}$	Varying factor depending on threshold exceedance
(2.7)	Binominal Climate	$f_{bin}\left(\mu_{\Delta t}, \sigma_{\Delta t}, dens^{ID}, prog^{name}_{ID}\right)$	This factor is a climate-, density- and progress-driven probability stemming from a binomial distribution. See Algorithm 2 for details
(2.8)	Land Use Influence	$f_{mow} = \begin{cases} mort_{mow}, & if\ t_{mow} = t \\ 0, & \text{otherwise} \end{cases}$	Increased mortality if mowing occurs
(2.9)	Binominal Factor	$f_{bif}\left(\beta^1_{bif}, dens^{ID}\right)$	Density-driven probability stemming from a binomial distribution of a predefined mean (factor). See Algorithm 3 for details

Abbreviations: above=aboveground, bif=binominal factor, bin=binominal climate, cap=capacity, clim=climate, dens=density, exp=exponential, hab=habitat, ID=Cohort identifier, lin=linear, mort=mortality, mow=mowing, prog=progress, sig=sigmoid, t=time step, thd=treshold

A *Factor Threshold* is used with either of the above *Influences*. It allows applying two different values depending on whether a defined climate threshold is exceeded (Eqn. 2.6). It can be used, for instance, to either enable another *Influence* (threshold exceeded, factor = 1) or disable it (threshold not exceeded, factor = 0). An iterative use of this *Influence* is possible to apply thresholds for multiple climate values.

The *Binomial Climate (M2: renamed from Factor)* is an *Influence* that depends on climate conditions and a *Cohort*'s *density* and *development progress*. It stochastically determines its factor by drawing from a binomial distribution (Eqn. 2.7, Algorithm 2). In other words, it defines which share of a *Cohort* population (*density*) is affected by an event (e.g. death). The binomial distribution is approximated by the cumulative distribution of a standard normal distribution. Their mean and standard deviation are calculated using one of the above *Climate Influences*. In that way, population statistics stemming from climate-driven stochastic processes can be translated to a dynamic factor like *mortality rate*.

M1: *Land Use Influence* is a timed event that increases the mortality of a *Cohort* differently depending on its *Life Stage*. In our model, land use is defined as a mowing event that occurs once a year (Eqn. 2.8). M2: The model extension adds the option to provide a *mowing schedule* that defines a set of days per year on which land use occurs.

M2: The *Binomial Factor* works similarly to the *Binomial Climate Influence* described above but deviates in two aspects. First, mean and standard deviation are calculated using a predefined

probability factor only. Second, it just uses a *Cohort*'s *density* for the calculation ignoring the *development progress* (Eqn. 2.9, Algorithm 3).

Algorithm 2 'Binominal Climate' (M2: renamed from Factor) function to calculate a flow rate using a stochastically determined flow amount taken from a binominal distribution that is emulated by a normal distribution. The flow probability used to calculate the flow amount is taken from cumulative normal standard deviations using climate-dependent mean and standard deviation of flow duration. The resulting absolute flow rate is the ratio from flow amount to Cohort density. Finally, the applied relative flow rate takes development progress – or rather previously determined flow amount – into account to ensure flow of full density after maximum flow duration / full progress is reached.

function INFLUENCE('Binominal Climate', $\mu_{\Delta t}$, $\sigma_{\Delta t}$, $Cohort^{ID}$) ▷ $\mu_{\Delta t}$ and $\mu_{\Delta t}$: climate-dependent ▷ mean flow duration and standard deviation
  $density \leftarrow dens^{ID}$ ▷ get the Cohort's density
  $progress \leftarrow prog_{ID}$ ▷ get the Cohort's (development) progress
  $max_{\Delta t} \leftarrow \mu_{\Delta t} + 3 \times \sigma_{\Delta t}$ ▷ climate-dependent maximum flow duration
  $age \leftarrow max_{\Delta t} \times progress$ ▷ climate-dependent relative Cohort age
  $diff_{tod} \leftarrow frac(age - \mu_{\Delta t})\sigma_{\Delta t}$ ▷ today's age difference to mean duration
  $diff_{tom} \leftarrow frac(age + 1 - \mu_{\Delta t})\sigma_{\Delta t}$ ▷ tomorrow's age difference to mean duration
  $p_{trans} \leftarrow CDF(diff_{tom}) - CDF(diff_{tod})$ ▷ flow probability; CDF: cumulative standard normal distribution
  $\mu_{amount} \leftarrow density \times p_{trans}$ ▷ mean flow amount
  $\sigma_{amount} \leftarrow \sqrt{\mu_{amount} \times (1 - p_{trans})}$ ▷ standard deviation of flow amount
  $n_{amount} \leftarrow NORM(\mu_{amount}, \sigma_{amount})$ ▷ draw from normal distribution (NORM) to determine amount
  $r_{abs} \leftarrow fracn_{amount}density$ ▷ absolute flow rate
  $r_{rel} \leftarrow 0$ ▷ relative flow rate

  if $progress < 1$ **then**
    $r_{rel} \leftarrow \frac{r_{abs}}{1 - progress}$
  end if
  if $r_{rel} > 1$ **then**
    $r_{rel} \leftarrow 1$
  end if
  $progress \leftarrow progress + r_{rel}$
  return r_{rel}
end function

Algorithm 3 The 'Binominal Factor' function calculates a flow rate using a stochastically determined flow amount taken from a binominal distribution that is emulated by a normal distribution. The predefined probability factor is used directly as mean value of the distribution and indirectly to calculate the standard deviation. The resulting flow rate is the ratio of flow amount compared to Cohort density.

function INFLUENCE('Binominal Factor', p_{flow}, $Cohort^{ID}$) ▷ p_{flow}: predefined probability factor
  $density \leftarrow dens^{ID}$ ▷ get the Cohort's density
  $\mu_{amount} \leftarrow density \times p_{flow}$ ▷ mean flow amount
  $\sigma_{amount} \leftarrow \sqrt{\mu_{amount} \times (1 - p_{flow})}$ ▷ standard deviation of flow amount
  $n_{amount} \leftarrow NORM(\mu_{amount}, \sigma_{amount})$ ▷ draw from normal distribution (NORM) to determine amount
  $r_{flow} \leftarrow \frac{n_{amount}}{density}$ ▷ flow rate
  if $r_{flow} > 1$ **then**
    $r_{rel} \leftarrow 1$
  end if
  return r_{flow}
end function

M1: In the following, we describe the life cycle processes of the LMG separately for each life stage and define the environmental drivers influencing them. The parametrization for the belowground life stages is mainly adapted from *temperature* experiments conducted by Wingerden et al. (1991) and *soil moisture* and *contact water* experiments by Ingrisch (1983). For the

aboveground population, data from different sources was used (Sections 2.7.1.4 and 2.7.1.5) – not all of them including LMG explicitly. The parameter values for the impact of grassland were established following personal communication with B. Schulz (Section 2.7.1.6).

M2: Information incorporated to estimate and validate the dispersal process (Section 2.7.1.7) of the LMG are an empirical 'mark and recapture' study by Malkus (1997), field studies by Griffioen (1996) and Marzelli (1994), as well as two experiments using genetic markers to measure distances between populations (Keller, 2012; Van Strien, 2013).

Table 2.7: List of coefficients (third column) used to parameterize the Influences' equations (second column, Table 2.6) as used to modify the processes (first column, Table 2.5) of the target species. Superscript letters reference the sources used to parameterize the processes and influences for the LMG: [a]Ingrisch (1983), [b]B. Schulz (pers. comm.), [c]Wingerden et al. (1991), [d]Ingrisch & Köhler (1998), [e]Helfert & Sänger (1975), [f]Helfert (1980), [g]Kriegbaum (1988), [h]Waloff (1950) , [i]Griffioen (1996), [j]Malkus (1997)

Process symbol	Influences	Base rate of process and / or coefficients of influences
F^{pre}_{mort}		$(rate^{pre}_{mort} = 8.164147 \times 10^{-4})^{a}$
	f^{A}_{sig}	$(\beta^{A1}_{sig} = 0.357,\ \beta^{A2}_{sig} = 17.183,\ \beta^{A3}_{sig} = 0.703,\ \omega^{A}_{clim} = \omega_{rhug})^{a}$
	f^{B}_{thd}	$(\beta^{B1}_{thd} = 1,\ \beta^{B2}_{thd} = 0,\ \omega^{B}_{clim} = \omega_{cw},\ thd^{B}_{clim} = 0\ kg\ m^{-2})^{a}$
	f^{C}_{mow}	$(mort^{C}_{mow} = 0.05)^{b}$
$prog^{pre}_{ID}$	f^{D}_{thd}	$(\beta^{D1}_{thd} = \frac{1}{3},\ \beta^{D2}_{thd} = 0,\ \omega^{D}_{clim} = \omega_{ts},\ thd^{D}_{clim} = 10°C)^{a}$
F^{dia}_{mort}	f^{E}_{mow}	$(rate^{pre}_{mort} = 8.164147 \times 10^{-4})^{a},\ (mort^{E}_{mow} = 0.05)^{b}$
$prog^{dia}_{ID}$	f^{F}_{thd}	$(\beta^{F1}_{thd} = \frac{1}{61},\ \beta^{F2}_{thd} = \frac{-1}{182},\ \omega^{F}_{clim} = \omega_{ts},\ thd^{F}_{clim} = 5°C)^{a,c}$
	f^{G}_{thd}	$(\beta^{G1}_{thd} = 0,\ \beta^{G2}_{thd} = \frac{1}{3},\ \omega^{G}_{clim} = \omega_{ts},\ thd^{G}_{clim} = 10°C)^{a}$
F^{emb}_{mort}	f^{H}_{exp}	$(\beta^{H1}_{exp} = 6.949 \times 10^{-3},\ \beta^{H2}_{exp} = 5.45 \times 10^{-8},\ \beta^{H3}_{exp} = 0.4743,\ \omega^{H}_{clim} = \omega_{ts})^{c}$
	f^{I}_{sig}	$(\beta^{I1}_{sig} = 0.351,\ \beta^{I2}_{sig} = 40,\ \beta^{I3}_{sig} = 0.975,\ \omega^{I}_{clim} = \omega_{rhug})^{a}$
	f^{J}_{thd}	$(\beta^{J1}_{thd} = 1,\ \beta^{J2}_{thd} = 0,\ \omega^{J}_{clim} = \omega_{cw}, thd^{J}_{clim} = 0\ kg\ m^{-2})^{c}$
	f^{K}_{mow}	$(mort^{K}_{mow} = 0.05)^{b}$
F^{emb}_{trans}	f^{M}_{exp}	$(\beta^{M1}_{exp} = 7.991,\ \beta^{M2}_{exp} = 1069.98,\ \beta^{M3}_{exp} = -0.2248,\ \omega^{M}_{clim} = \omega_{ts})^{a}$
	f^{N}_{exp}	$(\beta^{N1}_{exp} = 0.9251,\ \beta^{N2}_{exp} = 126.3933,\ \beta^{N3}_{exp} = -0.1978,\ \omega^{N}_{clim} = \omega_{ts})^{a}$
F^{lar}_{mort}		$(rate^{lar}_{mort} = 0.0358)^{d}$
	f^{O}_{cap}	$(\beta^{O1}_{cap} = -1.5,\ \beta^{O2}_{cap} = 0.85)$
	f^{P}_{lin}	$(f^{P}_{max} = 0.95,\ \beta^{P}_{lin}1 = 1.9,\ \beta^{P2}_{lin} = -0.19,\ \omega^{P}_{clim} = \omega_{ts})$
	f^{Q}_{mow}	$(mort^{Q}_{mow} = 0.95)^{b}$
F^{lar}_{trans}	f^{S}_{lin}	$(\beta^{S1}_{lin} = 83,\ \beta^{S2}_{lin} = -1.679,\ \omega^{S}_{clim} = \omega_{ts})^{e,f}$
	f^{T}_{lin}	$(\beta^{T1}_{lin} = -2.2188,\ \beta^{T2}_{exp} = 0.2188,\ \omega^{T}_{clim} = \omega_{ts})^{e,f}$
F^{ima}_{mort}		$(rate^{ima}_{mort} = 0.0475)^{g}$
	f^{U}_{cap}	$(\beta^{U1}_{cap} = -1.5,\ \beta^{U2}_{cap} = 0.85)$
	f^{V}_{lin}	$(f^{V}_{max} = 0.95,\ \beta^{V1}_{lin} = 1.9,\ \beta^{V2}_{lin} = -0.19,\ \omega^{V}_{clim} = \omega_{ts})$
	f^{W}_{mow}	$(mort^{W}_{mow} = 0.95)^{b}$
	f^{X}_{bif}	$(\beta^{X1}_{bif} = mort^{ima}_{disp}$, see Eqn. 2.16)
F^{ima}_{repr}		$(rate^{ima}_{repr} = 1.3)^{d,h}$
F^{ima}_{disp}	f^{Y}_{bif}	$(\beta^{Y1}_{bif} = rate^{ima}_{disp}(a,b)$, see Eqn. 2.11$)^{i,j}$

Abbreviations: bif=binominal factor, dia=diapause, disp=dispersal, emb=embryo, exp=exponential, f=symbol of Influence function, F=Flow, ID=Cohort identifier, ima=imago, lar=larva, lin=linear, mort=mortality, mow=mowing, pre=pre-diapause, prog=progress, repr=reproduction, sig=sigmoid, thd=treshold, trans=transfer

M1: The values for *base rates* and the *coefficients* used to parameterize the *Influences* as applied for the processes of the target species are listed in Table 2.7. A verbal description on their usage for the target species is given in the following subsections.

2.7.1.1 Pre-diapause Life Stage

M1: The first sub-stage of the belowground population represents the LMG's clutch after oviposition and before diapause. Following the study of Ingrisch (1983), we define that it requires three consecutive days below a *temperature* of 10 °*C* to start diapause thus develop into the next life stage (*Factor Threshold*, Eqn. 2.6). The intrinsic *mortality rate* rapidly increases if the eggs experience pre-winter drought stress caused by missing *contact water* (Ingrisch, 1983) (*Factor Threshold*, Eqn. 2.6). The increased mortality is calculated using the *Sigmoid Climate Influence* (Eqn. 2.5) driven by *humidity*.

2.7.1.2 Diapause Life Stage

M1: The diapause life stage occurs mainly during winter and is mostly unaffected by climate conditions in terms of our model. Therefore, the intrinsic *mortality rate* remains constant. We defined that it needs to experience a total of 61 days below 5 °*C* to break diapause (*Factor Threshold*, Eqn. 2.6). By that, we followed the cold treatments in the studies by Ingrisch (1983) and Wingerden et al. (1991), though with a shorter period of time to avoid stagnation in slightly warmer winters. Additionally, a too early indication of spring is prevented by defining that the life stage requires three consecutive days of at least 10 °*C* to develop into the next life stage (*Factor Threshold*, Eqn. 2.6). The diapause life stage can have multiple *Cohorts*, i.e., one for each consecutive year of unsuitable conditions (diapause not broken).

2.7.1.3 Embryo Life Stage

M1: This life stage is the most complex in our model. Mortality is influenced by three climate parameters while the temperature-driven hatching process (transfer to larval stage) is stochastically determined by the stage's *density* and *development progress*. Following Wingerden et al. (1991) we established the *mortality rate* using the fact that a *temperature* of 22.2 °*C* yields the highest hatching success rate (∼ 82 %) while the rate drops with both lower and higher *temperatures* (*Exponential Climate Influence*, Eqn. 2.4). At the same time higher *temperatures* decrease the mean hatching time from 45 days at 15.0 °*C* to 8 days at 37.5 °*C* (*Exponential Climate Influence*, Eqn. 2.4). In our model, the *base mortality rate* is in fact mainly determined by *temperature*. Similar to the pre-diapause life stage it can further increase in the case of post-winter drought stress caused by missing *contact water* (Ingrisch, 1983) (*Factor Threshold*, Eqn. 2.6). This additional mortality is calculated using the *Sigmoid Climate Influence* (Eqn. 2.5) driven by *humidity*. As mentioned above, the timing and amount of hatching eggs is stochastically determined (*Binomial Climate* [M2: renamed from Factor], Eqn. 2.7). The hatching probability increases with *development progress* and higher *temperatures*. Mean and standard deviation defining the binomial distribution to draw the probability from are factors that are correlated with the *temperature* (*Exponential Climate Influence*, Eqn. 2.4).

2.7.1.4 Larva Life Stage

M1: The larval life stage has multiple *Cohorts*, i.e., one for each hatching day per year of the previous embryo stage. These larva *Cohorts* are processed independently. High *temperatures* increase the development speed of larvae. We used the development traits found in three related grasshopper species (Helfert & Sänger, 1975; Helfert, 1980) to calculate temperature-driven mean and standard deviation (*Linear Climate Influence*, Eqn. 2.3). Both are then applied to stochastically determine the density- and progress-dependent transfer (or rather development) of a larva *Cohort* to the imago life stage (*Binomial Climate* [M2: renamed from Factor], Eqn. 2.7). The larva *base mortality rate* was adopted by averaging the parameters of two related grasshopper species (Ingrisch & Köhler, 1998, Tab. 16). It increases with *aboveground population density* (*Capacity Influence*, Eqn. 2.2) allowing a maximum of 25 individuals m^{-2} (B. Schulz, pers. comm.) and by definition with *temperatures* below 10 °C (*Linear Climate Influence*, Eqn. 2.3).

2.7.1.5 Imago Life Stage

M1: Similar to the larval stage, the *base mortality rate* for the imago life stage was adopted using the daily survival rates of four related grasshopper species determined by Kriegbaum (1988). It increases with *aboveground population density* (*Capacity Influence*, Eqn. 2.2) allowing a maximum of 25 individuals m^{-2} (B. Schulz, pers. comm.) and by definition with *temperatures* below 10 °C (*Linear Climate Influence*, Eqn. 2.3). The daily *transfer* or rather *oviposition rate* of 1.3 was defined including several considerations. First of all, an LMG egg pod contains 11-14 eggs (Waloff, 1950) and reproduction is delayed up to two weeks after maturation (Ingrisch & Köhler, 1998). Furthermore, we assumed that half of the LMG population is female and that a female lays up to three egg pods during a lifetime of 60 days. In terms of our model, oviposition is not influenced by any external drivers.

2.7.1.6 Land Use

M1: As mentioned above, land use in our model is a representation of grassland mowing that occurs once per year on the first day of the same calendar week. It affects the belowground population (life stages 1-3) less severely than the aboveground population (4-5) by increasing the stage's *mortality rate* additively by 0.05 (below ground) and 0.95 (above ground), respectively (B. Schulz, pers. comm.).

M2: Disturbance through land use occurs on 2-3 days per simulation year depending on initially defined *mowing schedule* (Table 2.4).

M3: Depending on the protected grassland probability p_{prot}, the *mowing schedule* occurring in each *Grassland Cell* is determined randomly at simulation start. That is, either the conventional schedule T_{conv} with five cuts or the protective schedule T_{conv} with two cuts per year (cf. Table 2.4). Depending on the schedules' definitions the cuts occur x days after the start of a year's vegetation period (Section 2.7.7).

2.7.1.7 Dispersal

M2: In terms of the model extension, the dispersal rate from the imago *Life Stage* of *Population* P_a to the same stage of each neighboring *Population* $P_n \in N_a$ is stochastically determined (*Binomial Factor*, Eqn. 2.9) every time step using a *base dispersal rate* ($rate_{disp}^{ima} = 0.00595\ day^{-1}$) and a pre-calculated *dispersal probability* (Eqn. 2.11). We determined the base dispersal rate by defining those individuals as dispersers that traveled the largest distance during one day (1 out of 168) in a 'mark and recapture' study by Malkus (1997). The *dispersal mortality rate* is calculated using the inverse of the dispersal rate (Eqn. 2.16). Following the maximum covered distance of LMG individuals described by Griffioen (1996), dispersal is defined to remain within a radius (rad_{disp}) of $1,500\ m$, in principle. In regions of low grassland cover, however, dispersal outside this radius (LDD) can occur to account for the LMG's flight ability (Sörens, 1996). Section 2.7.5 describes in detail, how the neighborhood (both inside and outside of the dispersal radius) of each *Population* is defined and the values of the dispersal process are determined.

M3: To prevent unrealistic low population size in newly inhabited cells, the amount of dispersing individuals is truncated to discrete numbers in terms of habitat size A_{hab}. Discrete here means that the size of one individual is defined as $\frac{1}{A_{hab}}\ ind.\ m^{-2}$ and the calculated dispersing amount must be a manifold of this individual size. Dispersing amount below the next largest manifold remains in the *life stage of origin*.

2.7.2 Flow Update

M1: During 'Flow update', the state variables *total flow amount*, *current flow amount* and *dynamic flow rate* (Table 2.5) are iteratively recalculated using the *Cohorts* associated with the *life stage of origin* (Algorithm 4). If there are any external *Influences* (Section 2.7.1) associated with this *Flow*, they change the *dynamic flow rate* depending on their *type*.

2.7.3 Life Stage Update

M1: The submodel 'Life stage update' (Algorithm 5) calculates a *Life Stage*'s *total density* from the *density* of its subordinate *Cohorts* and its *gain* from the incoming *transfer Flow* of its preceding *Life Stage*. The *gain* is then used to determine whether to create a new *Cohort* from it or add it to an existing *Cohort*. Furthermore, overaged *Cohorts* or such of *density* below the minimum are erased.

Algorithm 4 Submodel 'Flow update'. All associated Flows of the defined Population are iteratively updated by this submodel. Sequence of update is irrelevant. Algorithm describes the update of a single Flow. Equations of influence functions are listed in Table S1-5.

function SUBMODEL('Flow update')
  $amount \leftarrow 0$ ▷ total flow amount
  $origin \leftarrow Flow_{origin}$ ▷ Flow's Life Stage of origin
  for all $Cohort^{ID} \in origin_{Cohorts}$ **do**
    $amount^{ID} \leftarrow 0$ ▷ Cohort's flow amount
    $rate^{ID} \leftarrow 0$ ▷ Cohort's flow rate
    $progress \leftarrow prog_{ID}$ ▷ Cohort's (development) progress
    if $Flow_{type} =$ *'mortality' OR* $progress \geq 1$ **then**
      if $Flow_{type} =$ *'mortality' AND* $age^{ID} \geq age^{max}_{origin}$ **then**
        $amount^{ID} \leftarrow 1$
      else
        $rate^{ID} \leftarrow Flow_{rate}$ ▷ set to Flow's base rate
        for all $Influence \in Flow_{Influences}$ **do**
          $factor_{Influence} \leftarrow$ SUBMODEL('Influence')
          if $Influence_{type} =$ *'additive'* **then**
            $rate^{ID} \leftarrow rate^{ID} + factor_{Influence} \times (1 - rate^{ID})$
          else if $Influence_{type} =$ *'multiplicative'* **then**
            $rate^{ID} \leftarrow rate^{ID} \times factor_{Influence}$
          end if
        end for
      end if
    end if
  end for
  $amount^{ID} \leftarrow rate^{ID} \times density^{ID}$
  $amount \leftarrow amount + amount^{ID}$
end function

Algorithm 5 Submodel 'Life Stage update'. All associated Life Stages of a Population are iteratively updated using this submodel. The pseudocode describes the update of a single Life Stage.

function SUBMODEL('Life Stage update')
  $density \leftarrow 0$ ▷ total density
  $gain \leftarrow 0$ ▷ total density gain
  $created_{Cohort} \leftarrow false$ ▷ was a new Cohort created?
  for all $Flow \in Stage_{input}$ **do** ▷ loop over incoming Flows of (Life) Stage
    $gain \leftarrow gain + Flow_{amount}$ ▷ add total flow amount to gain
    if $gain \geq density^{min}_{Stage}$ **then**
      if $Stage_{Cohorts} = \emptyset$ *OR* $multi^{Cohort}_{Stage} = true$ **then** ▷ empty set of Cohorts or multiple allowed
        $Cohort^{gaining} \leftarrow$ CREATE COHORT($gain$) ▷ Cohort with gain as initial density
        $created_{Cohort} \leftarrow true$
      else
        $Cohort^{gaining} \leftarrow Stage_{Cohorts}(1)$ ▷ get Cohort from top of Stage's Cohorts
        $density^{gaining} \leftarrow density^{gaining} + gain$
      end if
    end if
  end for
  for all $Cohort^{ID} \in Stage_{Cohorts}$ **do**
    RUN SUBMODEL('Cohort update')
    if $density^{ID} < density^{min}_{Stage}$ **then**
      remove $Cohort^{ID}$ *from* $Stage_{Cohorts}$
    else
      $density \leftarrow density + density^{ID}$
    end if
  end for
  if $created_{Cohort} = true$ **then**
    $Stage_{Cohorts}(1) \leftarrow Cohort^{gaining}$ ▷ put new Cohort on top of Stage's Cohorts
  end if
end function

2.7.4 Cohort Update

M1: During 'Cohort update', *density* and *development progress* of a *Cohort* a recalculated (Algorithm 6). First, *loss* of *density* is calculated using the outgoing *transfer Flow* of the *Cohort*'s parent *Life Stage*. Then, *gain* (if any) is added to the *density* and reset to zero afterwards. Finally, the *development progress* is increased using external influences, if there were defined any. Otherwise it is set to a value of 1.

Algorithm 6 Submodel 'Cohort update'. All associated Cohorts of the defined Life Stage are iteratively updated by this submodel. Sequence of update is irrelevant. Pseudocode describes the update of a single Cohort. Equations of influence functions are listed in Table S1-5.

function SUBMODEL('Cohort update', ID) ▷ using ID of updating Cohort
  $loss \leftarrow 0$ ▷ total density loss
  $parent \leftarrow Cohort_{parent}$ ▷ Cohort's parent Life Stage
  for all $Flow \in parent_{output}$ **do** ▷ loop over outgoing Flows of parent Life Stage
    if $Flow_{type} \neq$ *'reproduction'* **then**
      $loss \leftarrow loss + Flow^{ID}_{amount}$ ▷ add Cohort-specific flow amount to loss
    end if
  end for
  $density \leftarrow density + (gain - loss)$ ▷ update Cohort density with potential gain and loss
  $gain \leftarrow 0$ ▷ reset (externally updated) gain
  $progress_{temp} \leftarrow 1$ ▷ temporary buffer for potential development progress
  for all $Influence \in Development_{Influences}$ **do** ▷ loop over development Influences, if any
    $factor_{Influence} \leftarrow$ SUBMODEL('Influence')
    $progress_{temp} \leftarrow factor_{Influence} \times progress_{temp}$
  end for
  $progress \leftarrow progress + progress_{temp}$
  if $progress < 0$ **then**
    $progress \leftarrow 0$
  else if $progress > 1$ **then**
    $progress \leftarrow 1$
  end if
end function

2.7.5 Dispersal Setup

M2: The submodel 'Dispersal setup' is called every time the *life stage of destination* of an empty *Population* is subject in a non-zero *dispersal Flow* (in terms of *flow amount*), in other words, if dispersal is directed to an *uninhabited Grassland Cell* (for the first time). In this case, the submodel locates all *Populations* $P_b \in N_a \subset R$ in the study region R belonging to the sub region or neighborhood N_a of *Population* P_a in the now *inhabited* cell G_a and establishes a connection to each of them by creating a *dispersal Flow* between the imago *Life Stages* of the formerly empty *Population* (*life stage of origin*) and the respective neighboring *Population* (*life stage of destination*). *Populations* considered a neighbor $P_b \in N_a$ are determined in two ways: (1) all *Populations* inside a predefined dispersal radius (home range); and (2) the nearest *Population* in either one of eight cardinal directions [North (N), Northeast (NE), East (E), Southeast (SE), South (S), Southwest (SW), West (W), Northwest (NW)], in case there are no cells found inside the home range in this direction (LDD). Identifying *Populations* inside the home range is straight forward using the Euclidean distance $dist_{a,b}$ [in meters] between two *Grassland Cells* G_a and G_b:

$$dist_{a,b} = \sqrt{(coord^a_x - coord^b_x)^2 + (coord^a_y - coord^b_y)^2} \times size_{hab} \tag{2.10}$$

If $dist_{a,b} \leq rad_{disp}$ (Table 2.3), the cells belong to the same neighborhood. Finding potential neighbors for LDD into one of the cardinal directions $DIR = N, NE, E, SE, S, SW, W, NW$ requires additional information about the surroundings of the source *Grassland Cell* G_a. If none of the *Populations* $P_c \in N_a^{dir}$ fulfills the home range constraint $dist_{a,c} \leq rad_{disp}$, the nearest cell $P_{LDD} \in N_{a,LDD}^{dir} \subset N_a^{dir}$ is selected as long distance neighbor in direction dir. Here, N_a^{dir} represents a set of all *Populations* located within a 90-degree angle in direction $dir \in DIR$ of cell G_a and $N_{a,LDD}^{dir}$ a subset of slightly narrowed angle outside the dispersal radius. Using this method, potential long distance neighbors are identified for all directions of DIR. Figure 4.5 of Chapter 4 geometrically illustrates the selection of LDD neighbors. A detailed definition of cells belonging to each of the narrowed subsets will follow below. Having identified all *Populations* belonging to the neighborhood N_a, the *flow rate* $rate_{disp}^{ima}(a,b)$ for each dispersal *Flow* originating in G_a and destined in G_b is determined using the base dispersal rate defined for the *Life Stage* of interest (here, $rate_{disp}^{ima}$ for the LMG's imago stage) and a species-specific *dispersal probability* $p_{a,b}^{disp}$ (Eqn. 2.11):

$$rate_{disp}^{ima}(a,b) = rate_{disp}^{ima} \times p_{a,b}^{disp} \tag{2.11}$$

$$p_{a,b}^{disp} = pref_{a,b} \times p_{a,b}^{find} \times p_{a,b}^{surv} \tag{2.12}$$

The *dispersal probability* itself (Eqn. 2.12) is calculated using a *preference factor* to select the destined *Population* depending on the distance to all neighbors (Eqn. 2.13), a probability to find the selected neighbor during the dispersal process (Eqn. 2.14) and a probability to survive the dispersal (Eqn. 2.15):

$$pref_{a,b} = \frac{1/dist_{a,b}^{pref^{near}}}{\sum_{P_n \in N_a} dist_{a,n}^{pref^{near}}} \tag{2.13}$$

$$p_{a,b}^{find} = \left(rGrass_{a,b}^{at}\right)^{1-sight_{disp}} \tag{2.14}$$

$$p_{a,b}^{surv} = \exp^{-decay_{disp} \times (1-rGrass_{a,b}^{to}) \times dist_{a,b}} \tag{2.15}$$

Table 2.3 contains the parameter values used to define the dispersal process of the LMG and their usage is described in the following. The size of the parameter $pref^{near} \geq 0$ in Eqn. 2.13 defines to what extent nearby cells are preferred over more distant ones, where a value of zero leads to equal preference independent of the distance. Finding a selected neighbor (Eqn. 2.14) depends on the relative grassland cover $rGrass_{a,b}^{at}$ in the same distance as the destined cell (i.e., the actual number of *Grassland Cells* relative to the potential number), and the ability of the species to locate suitable neighbors given by the parameter $sight_{disp} \in [0,1]$, where a value of zero defines a success rate equal to the grassland ratio and a value of one a 100 % success rate. The probability to survive the dispersal process (Eqn. 2.15) depends on the relative grassland cover $rGrass_{a,b}^{to}$ in the perimeter of a radius lower than the distance to the destined cell and a distance dependent decay rate $decay_{disp} \in [0,1]$, where a value of zero equals 100 % and a value of one equals minimum survival probability. Furthermore, the dispersers are subject to dispersal mortality which is the difference of the sum of all the dispersal probabilities multiplied by the *base dispersal rate*:

$$mort_{disp}^{ima} = \left(1 - \sum_{P_n \in N_a} p_{a,n}^{disp}\right) \times rate_{disp}^{ima} \tag{2.16}$$

Finally, the eight sub regions $N_{a,LDD}^{dir} \subset R$ representing all cells found outside the dispersal radius in the direction $dir \in DIR$ of an originating *Grassland Cell* G_a are determined as follows:

$$N_a^N = \{\forall G_n \in R \backslash \{G_a\} \mid dist_{a,n}^x < dist_{a,n}^y \wedge coord_y^n < coord_y^a \wedge dist_{a,n} > rad_{disp}\} \tag{2.17}$$
$$N_a^{NE} = \{\forall G_n \in R \backslash \{G_a\} \mid coord_x^n > coord_x^a \wedge coord_y^n < coord_y^a \wedge dist_{a,n} > rad_{disp}\} \tag{2.18}$$
$$N_a^E = \{\forall G_n \in R \backslash \{G_a\} \mid coord_x^n > coord_x^a \wedge dist_{a,n}^y < dist_{a,n}^x \wedge dist_{a,n} > rad_{disp}\} \tag{2.19}$$
$$N_a^{SE} = \{\forall G_n \in R \backslash \{G_a\} \mid coord_x^n > coord_x^A \wedge coord_y^n > coord_y^a \wedge dist_{a,n} > rad_{disp}\} \tag{2.20}$$
$$N_a^S = \{\forall G_n \in R \backslash \{G_a\} \mid dist_{a,n}^x < dist_{a,n}^y \wedge coord_y^a > coord_y^a \wedge dist_{a,n} > rad_{disp}\} \tag{2.21}$$
$$N_a^{SW} = \{\forall G_n \in R \backslash \{G_a\} \mid coord_x^n < coord_x^a \wedge coord_y^a > coord_y^a \wedge dist_{a,n} > rad_{disp}\} \tag{2.22}$$
$$N_a^W = \{\forall G_n \in R \backslash \{G_a\} \mid coord_x^n < coord_x^a \wedge dist_{a,n}^y < dist_{a,n}^x \wedge dist_{a,n} > rad_{disp}\} \tag{2.23}$$
$$N_a^{NW} = \{\forall G_n \in R \backslash \{G_a\} \mid coord_x^n < coord_x^a \wedge coord_y^n < coord_y^a \wedge dist_{a,n} > rad_{disp}\} \tag{2.24}$$

We defined the sub regions in such a way that each of them overlaps with both neighbors in clockwise and counterclockwise direction to minimize LDD to cases where the area in direction of interest is largely empty within the home range. Figure 4.5 (Chapter 4) visualizes the areas belonging to either of the sub regions.

2.7.6 Bilinear Climate Interpolation

M2: This submodel is called every time step to achieve heterogeneous, gradual values at the location of each *Grassland Cell* using bilinear interpolation of the climate data from the closest adjacent neighbors. This is done by weighing the distances from a *Grassland Cell* G_a to the center of the (up to) four *Climate Cells* $\{\Omega_{a,NE}, \Omega_{a,SE}, \Omega_{a,SW}, \Omega_{a,NW}\}$ into secondary cardinal directions of G_a. The resulting bilinear weights $w_{bilin}^{a,dir}$ are multiplied with their respective climate values $\omega_{clim}^{a,dir}$ and then summed to achieve the value at G_a. The interpolated climate value ω_{clim}^a for cell G_a is then calculated as follows.

$$\omega_{clim}^a = \sum_{dir \in DIR_{sec}} w_{bilin}^{a,dir} \times \omega_{clim}^{a,dir} \tag{2.25}$$
$$w_{bilin}^{a,dir} = 1 - \frac{(size_{clim} - dist_{a,dir}^x) \times (size_{clim} - dist_{a,dir}^y)}{(size_{clim})^2} \tag{2.26}$$
$$dist_{a,dir}^{xy} = |coord_{xy}^a - center_{xy}^{a,dir}| \times size_{hab} \tag{2.27}$$

Here, $DIR_{sec} \subset DIR$ (see Section 2.7.5) are the secondary cardinal directions $\{NE, SE, SW, NW\}$ and $\omega_{clim}^{a,dir}$ is the projected value in the *Climate Cell* $\Omega_{a,dir}$ into direction dir of G_a. Parameters $size_{clim}$ of a *Climate Cell* and $size_{hab}$ of a *Grassland Cell* were introduced

in Table 2.3. The value $dist^{xy}_{a,dir}$ for the distances in x- or y-direction are calculated using the respective *coordinate* of the geometric center of a *Climate Cell* ($center^{a,dir}_{x,y}$, Table 2.3). Figure 4.4 (Chapter 4) illustrates the calculation of the weights for a single *Grassland Cell* using a simplified geometric example. Please refer to Appendix B.3 for a description of the mapping between *Climate* and *Grassland Cells*, and a reference to the calculated weights.

2.7.7 Start of Vegetation Period

The start of the vegetation period t_{veg} in a *Climate* or *Grassland Cell* is calculated using the *surface temperature* ω_{ts}. Following Gerling et al. (2020), this period starts when the *yearly temperature sum* surpasses 200.0 °C. Adapting their calculation to the *surface temperature* ω_{ts} used in the present model gives the following equation:

$$
\begin{aligned}
sum_{ts} &= \sum_{i=1}^{I} (x \times \omega^i_{ts}) \forall I \in \{1,2,\ldots,364\} \; until \; sum_{ts} \geq 200.0\,°C, \\
x &= \begin{cases} 0.5, & if\ 1 \leq i \leq 31 \\ 0.75, & if\ 32 \leq i \leq 59 \\ 1.0 & if\ i \geq 60 \end{cases}, \\
\omega^i_{ts} &= \begin{cases} 0, & if\ \omega^i_{ts} < 0 \\ \omega^i_{ts}, & \text{otherwise} \end{cases}
\end{aligned}
\tag{2.28}
$$

Here, sum_{ts} is the *summed surface temperature*, ω^i_{ts} is the *mean surface temperature* (ignoring negative values) on day i of a year, and x is a weight including the *temperature* values of January and February with only 50 % and 75 % of their extent. The value of t_{veg} equals the day i where t_{sum} reaches 200.0 °C.

Part II

From Model to Application: Case Studies of the Large Marsh Grasshopper

3 High-resolution PVA along large environmental gradients to model the combined effects of climate change and land use timing: lessons from the large marsh grasshopper

An article with similar content to this chapter is published as: *Leins, J. A., Banitz, T., Grimm, V., & Drechsler, M. (2021). High-resolution PVA along large environmental gradients to model the combined effects of climate change and land use timing: lessons from the large marsh grasshopper. Ecological Modelling 440, 109355. DOI: 10.1016/j.ecolmodel.2020.109355*

Abstract

Both climate change and land use regimes affect the viability of populations, but they are often studied separately. Moreover, population viability analyses (PVAs) often ignore the effects of large environmental gradients and use temporal resolutions that are too coarse to take into account that different stages of a population's life cycle may be affected differently by climate change. Here, we present the *Hi*gh-resolution *L*arge *E*nvironmental *G*radient (HiLEG) model and apply it in a PVA with daily resolution based on daily climate projections for Northwest Germany. We used the large marsh grasshopper (LMG) as the target species and investigated (1) the effects of climate change on the viability and spatial distribution of the species, (2) the influence of the timing of grassland mowing on the species and (3) the interaction between the effects of climate change and grassland mowing. The stage- and cohort-based model was run for the spatially differentiated environmental conditions temperature and soil moisture across the whole study region. We implemented three climate change scenarios and analyzed the population dynamics for four consecutive 20-year periods. Climate change alone would lead to an expansion of the regions suitable for the LMG, as warming accelerates development and due to reduced drought stress. However, in combination with land use, the timing of mowing was crucial, as this disturbance causes a high mortality rate in the aboveground life stages. Assuming the same date of mowing throughout the region, the impact on viability varied greatly between regions due to the different climate conditions. The regional negative effects of the mowing date can be divided into five phases: (1) In early spring, the populations were largely unaffected in all the regions; (2) between late spring and early summer, they were severely affected only in warm regions; (3) in summer, all the populations were severely affected so that they could hardly survive; (4) between late summer and early autumn, they were severely affected in cold regions; and (5) in autumn, the populations were equally affected across all regions. The duration and start of each phase differed slightly depending on the climate change scenario and simulation period, but overall, they showed the same pattern. Our model can be used to identify regions of concern and devise management recommendations. The model can be adapted to the life cycle of different target species, climate projections and disturbance regimes. We show with our adaption of the HiLEG model

that high-resolution PVAs and applications on large environmental gradients can be reconciled to develop conservation strategies capable of dealing with multiple stressors.

Highlights:

- Explore spatial viability of terrestrial species given dynamic external drivers
- High-resolution climate data are coupled to a demographic locust[1] population model
- Climate change alone would benefit the locust in Northwest Germany
- Climate and land use interact nontrivially thus timing of mowing gets crucial
- Smart conservation planning should adapt mowing schedule to locally varying climate

Key words: climate change, land use, population viability analysis, stage-based model, high resolution, environmental gradients

3.1 Introduction

In terrestrial ecosystems, land use and climate change are two dominant factors driving biodiversity loss (Millennium Ecosystem Assessment, 2005). The risk of species loss can be estimated using simulation models that support population viability analysis (PVA) in changing environments. PVAs are used to assess the viability of species and populations as a function of species parameters such as the population growth rate, environmental conditions such as food availability and anthropogenic impacts such as the fragmentation and deterioration of habitats (Coulson et al., 2001; Beissinger & McCullough, 2002). These analyses are of great value in conservation biology to decide where, when and how which species should be protected.

While PVAs are widely performed (Pe'er et al., 2013; Stephens, 2016; Chaudhary & Oli, 2020), most of them address small areas, build on aggregated demographic rates and use low temporal resolutions (e.g., years). In recent years, however, it has become increasingly clear that three interrelated factors need to be considered in PVAs to broaden their scope. First, a large spatial extent can be important to capture relevant environmental gradients. Second, considering all life stages, i.e., the full life cycle of a species is relevant (Radchuk et al., 2013) because stages respond in different (Levy et al., 2015) or even contrary ways (Cordes et al., 2020) to changes in the environment caused, for example, by climate change. Third, the high temporal resolution of climate data has proven relevant for improving modeling results (Radchuk et al., 2014), for instance, to capture the impact of extreme conditions (Ma et al., 2015). The second and third factors are interrelated, as capturing the response of different life stages to external conditions requires high-resolution data. Yet, to our knowledge, only few studies so far use such highly resolved external drivers, especially in combination with spatial gradients and distinguishing different life stages (Thompson et al., 2012; Green et al., 2014; Bonnot, 2016; Schmidt & Zinkernagel, 2017).

Here, we present the *Hi*gh-resolution *L*arge *E*nvironmental *G*radient (HiLEG) model, a spatially differentiated stage- and cohort-based simulation model that allows us to use daily time steps, to mechanistically examine the interrelations between population dynamics and external drivers, such as climate and land use. The HiLEG model is designed to be used

[1] The term *locust* was used in the original article, but assigned the target species to an incorrect group within the family of *Acrididae*. In the other chapters of this work, the more general term *grasshopper* is used instead

for different terrestrial animal species by specifying a corresponding set of parameters and external drivers along large environmental gradients.

We use climate data with a daily temporal resolution and a spatial resolution of $12 \times 12\ km^2$ grid cells and that widely cover Northwest Germany. In each climate cell, a representative patch of grassland is considered. Similar to a sensitivity analysis, the comparison of the model results for different climate cells allows the exploration of the dependence of population viability on climate change and land use as well as the interaction between the two factors.

Experimental data on the impact of climate parameters such as temperature, precipitation and soil moisture on population dynamics are usually scarce and uncertain, which is also the case in the present study. The output of the model simulations is thus too uncertain to make quantitative predictions on the future development or viability of a target species. However, relative predictions and comparative analyses are usually robust to data uncertainty (Drechsler et al., 2003; McCarthy & Possingham, 2014), for example, if they address the influence of an environmental factor on the ranking of habitats or land use measures with regard to their suitability for a species. The present PVA is such a relative analysis.

As a first application, we parametrized the HiLEG model for the well-studied large marsh grasshopper (LMG, *Stethophyma grossum*) in cultivated grasslands of Northwest Germany and simulated its population dynamics for the years 2000-2079, given different climate change scenarios and schedules for grassland mowing. The LMG prefers wet meadows and marshes as habitats, while its life stages are affected differently by climate conditions and the timing of grassland mowing: Warm temperatures accelerate hatching and larva development while spring and autumn droughts degrade eggs located below ground. Mowing is highly lethal for larvae and imagines because they can hardly escape the harvesters. The LMG is partly considered threatened in the federal states of Northwest Germany (Winkler, 2000) and therefore of high relevance for local conservation agencies. While recent studies project this species will benefit from elevated temperatures caused by climate change (Trautner & Hermann, 2008; Poniatowski et al., 2018a), they state that extended droughts and anthropogenic disturbances such as mowing and grazing – depending on their timing – can still pose a threat to its survival (Poniatowski et al., 2018a; Löffler et al., 2019).

Our model allows simulating the combined effects of different scenarios of climate change and mowing schedules on LMG population dynamics. Therefore, it helps to evaluate possible conservation measures by assessing how the timing of grassland mowing can be altered to adapt to climate-induced shifts in the LMG life cycle. To this end, the model considers temporal changes and spatial heterogeneity in essential climate variables. In principle, our model is also able to consider spatial heterogeneity in other factors, such as habitat size, food competitors, predators and land use. However, the aim of the model is not to investigate real land use patterns with spatially heterogeneous mowing dates or other heterogeneous features in the study region. Rather, our model aims to solve the problem of coupling high-resolution climate data into a demographic model and investigating how the dynamics of local LMG populations are affected by the locally changing climate and selected mowing schedules. Specifically, the following questions are addressed: (1) How do population density and viability shift regionally, given different climate change scenarios? (2) Which mowing schedule has the least negative impact on the overall population density and viability in the study region? (3) Does the mowing impact severity depend on the spatial location (with its specific climate)?

3.2 Material and Methods

Our case study involves four main components: the study region (Northwest Germany and the surrounding areas), the target species (LMG), climate data (projections until 2080) and land use (grassland mowing). These components are described in the following subsections. Furthermore, the HiLEG model, which simulates the interplay between these components, is introduced in Section 3.2.6.

3.2.1 Study Region

The study region is Northwest Germany and the surrounding areas (Figure 3.1), for which climate projections were available (Section 3.2.3). More precisely, those regions are the federal states of Schleswig-Holstein, Lower Saxony, Hamburg and Bremen as well as surrounding areas of Germany, Denmark and the Netherlands. The spatial resolution of the grid cells areas of $12 \times 12\ km^2$ yields 968 terrestrial grid cells within the study region.

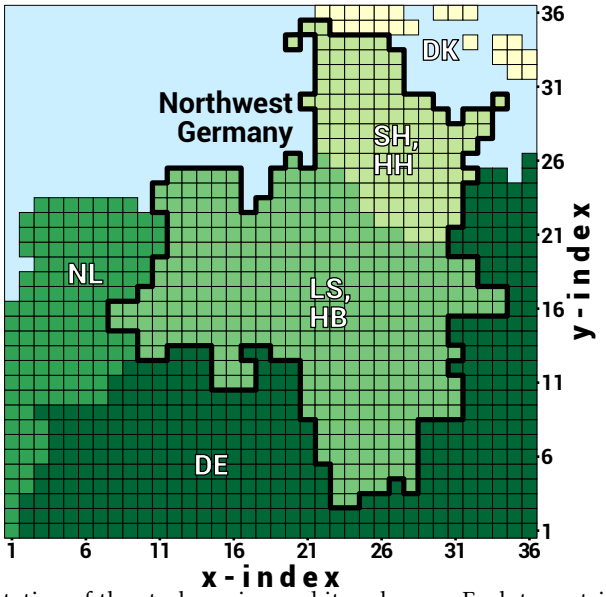

Figure 3.1: Spatial representation of the study region and its subareas. Each terrestrial grid cell (shades of green and yellow) has an area of $12 \times 12\ km^2$. Northwest Germany is highlighted by a thick black outline. Abbreviations: DE=Germany, DK=Denmark, HB=Bremen, HH=Hamburg, LS=Lower Saxony, NL=the Netherlands, SH=Schleswig-Holstein. The blue areas show the North and Baltic Seas.

3.2.2 Target Species

The LMG (*S. grossum*) (Linné 1758) is a well-studied locust species that is widely distributed in Central European grass- and wetlands (Heydenreich, 1999). Though the grasshopper itself tolerates a wide range of temperatures and humidity, the high water demand of its eggs restricts the LMG to wet habitats such as meadows and marshes (Ingrisch & Köhler, 1998; Koschuh, 2004). During a year, it develops through three consecutive life stages (Figure 3.2), which often overlap to some degree within a population: (1) egg / embryo, typical timing between July and June of the following year, below ground; (2) larval, May-October, above ground; (3) imago, July-October, above ground; (Oschmann, 1969; Marshall & Haes, 1988; Köhler & Weipert, 1991; Kleukers et al., 1997; Malkus, 1997; Ingrisch & Köhler, 1998;

Heydenreich, 1999). Stage 1 goes through additional development phases that are included in our model: The embryo development inside the egg is interrupted by a diapause to prevent too early development under rather good conditions, and an extended cold period is needed to break this diapause. Furthermore, for ideal development, the eggs need to be exposed to contact water before and after winter (Ingrisch, 1983), i.e., they must be covered with water or lie in moist soil.

Similar to other locusts, the LMG is regarded as an indicator for the quality of grassland habitats (Báldi & Kisbenedek, 1997; Heydenreich, 1999; Keller et al., 2012; Keßler et al., 2012). It is considered threatened in parts of the study region, e.g., according to the red lists for Schleswig-Holstein (Winkler, 2000) and Germany (Blab et al., 1984; Maas et al., 2002). To our knowledge, more recent lists are not available.

The climate conditions within the LMG's habitat have different implications for population development. Warm temperatures accelerate embryo hatching in spring (Wingerden et al., 1991) and larval development during summer (Uvarov, 1977; Ingrisch & Köhler, 1998). A sustained dry upper soil layer (depth of 2-10 cm) before and after winter causes drought stress during egg / embryo development (Ingrisch, 1983). Considering both factors in terms of climate change, there are two implications for the LMG. On the one hand, increasing temperatures might be beneficial because the accelerated species development could lead to larger population densities and therefore promote dispersal to new habitats (Trautner & Hermann, 2008; Poniatowski et al., 2018a). On the other hand, extended droughts could threaten hygrophilous species like the LMG (Löffler et al., 2019), especially if they occur during spring or autumn, by inhibiting egg and embryo development.

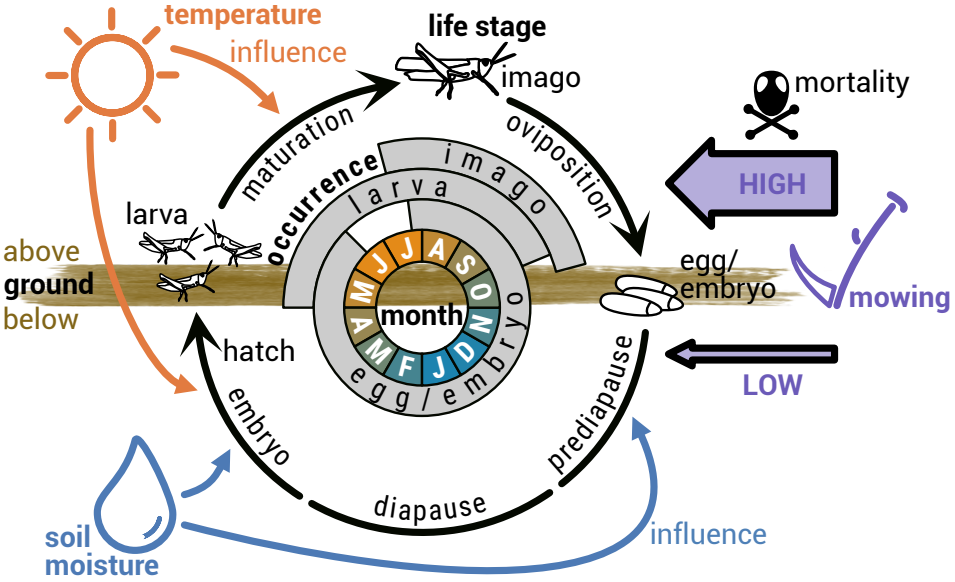

Figure 3.2: Yearly life cycle of the LMG, including the influence of external drivers. Black life stage symbols and circular arrows represent processes between and during life stages, where the life stage egg / embryo is subdivided into three phases (broken arrow). The typical ranges of the life stage occurrences are indicated in gray. The inner circle depicts months, where the color indicates seasonal changes in temperature. The influence of the external drivers of temperature, soil moisture and mowing is shown by colored symbols and arrows. Mowing impact is distinguished into high (aboveground) and low (belowground) mortality.

Mowing is particularly harmful during the aboveground phase, as larvae and imagines can hardly escape the harvesters and are mostly killed (Malkus, 1997; Marzelli, 1997). Eggs and embryos, however, are only mildly affected by the mechanical soil disturbances of harvesters. Therefore, extensive grassland mowing with 1-2 cuts during the belowground phase,

i.e., early or late in the year, is not considered problematic. It can even benefit the LMG by maintaining the grasshopper's favored microclimate in an open and heterogeneous vegetation structure (Malkus, 1997; Sonneck et al., 2008; Miller & Gardiner, 2018). To limit complexity, other factors of grassland suitability, such as vegetation structure or food availability, are not included in this study and are instead considered ideal for LMG development.

3.2.3 Climate Data

The climate data are taken from high-resolution scenario simulations generated by the regional climate model COSMO-CLM[2] (CCLM4-8-17) introduced by Keuler et al. (2016). For our study, this regional model was driven at its lateral boundaries by simulation results of the global model ICHEC[3]-EC-EARTH and three Representative Concentration Pathways (RCPs): RCP2.6, RCP4.5 and RCP8.5. These pathways represent potential climate developments with different global warming rates for the 21st century. The number indicates the equivalent of additional radiative forcing in Wm^{-2} (van Vuuren et al., 2011) of the increasing greenhouse gas concentrations by the year 2100. Hereafter, the climate change scenarios will be distinguished by action taken towards reducing CO_2 emissions: *full force* (*FF*, RCP2.6), *moderate* (*MOD*, RCP4.5) and *business as usual* (*BAU*, RCP8.5). The regional model provides time series of daily climate data values (mean or sum) that are spatially resolved to grid cells of size $12 \times 12\ km^2$. Common in such regional models, these cells are located in a rotated pole grid coordinate system. COSMO-CLM only provides a single climate projection per global model, RCP and grid cell that would have limited HiLEG to deterministic time series within a climate change scenario. To mitigate this limitation for the stochastic model processes (Section 3.2.6), we resampled the climate time series per replicate run by randomly rearranging the years without losing the long-term trend (see Appendix A.2 and Chapter 2, Section 2.5). From the available data, we used time series for the years 1995-2080, with the regional model providing simulated data from 2006 onwards. Only the data before 2006 are readings of actual meteorological values.

We considered three climate parameters relevant for the LMG population dynamics as implemented in our model: *surface temperature* (*ts*) [$°C$], *contact water* (*cw*) [$kg\ m^{-2}$] and *relative humidity-upper ground* (*rhug*) [%]. Parameter *ts* is explicitly calculated by the climate model described below and simply referred to as *temperature* hereafter. The parameters *cw* and *rhug* are deduced from other provided time series (see Appendix A.1). They were established because a sufficient amount of contact water and humidity in the upper soil layer is relevant for the LMG egg development, as described by Ingrisch (1983). Throughout the model, *cw* and *rhug* are used in combination and are therefore referred to by the joint term *humidity* hereafter.

Additionally, we introduced the parameter *relative soil moisture content* (*rsmc*) [%], hereafter referred to as *soil moisture*. It is a representation of the parameter *total soil moisture content* (*mrso*) [$kg\ m^{-2}$] calculated by the climate model divided by its yearly maximum values. *Soil moisture* and *humidity* are correlated parameters, as both depend on *mrso* (see Appendix A.1, Equations A.2, A.7 and A.10). In our analysis, we mainly focus on *soil moisture* for reasons of simplicity. It is closer to parameters considered by stakeholders (e.g., total soil moisture, precipitation) than the more abstract parameter *humidity* (in terms of our model) and is thus easier to comprehend. Together with the parameter *temperature*, projections of *soil moisture*

[2]Consortium for Small-scale Modeling in Climate Mode
[3]Irish Centre for High-End Computing

for the years 2000-2080 are given in Figure 3.3. Their spatial distributions in the study region are shown in Figure 3.5.

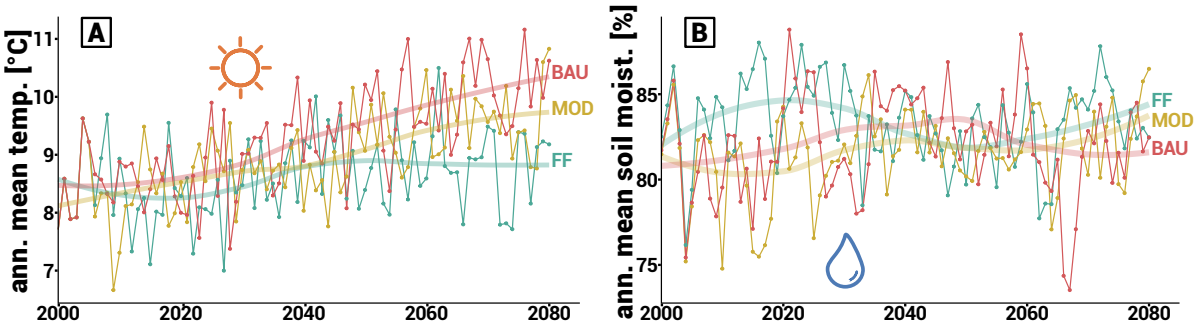

Figure 3.3: Projections of the annual mean values for the climate parameters *temperature* (A) and *soil moisture* (B) for the years 2000-2080. Climate change scenarios *FF*, *MOD* and *BAU* are indicated by colors (and labels). The thin lines show the actual means of the parameter values; the thick lines show the smoothed trends.

3.2.4 Land Use

Anthropogenic influence on the model species is represented by mechanical mowing as a scheduled grassland use measure. It is executed uniformly over the whole study region once per year at the beginning of the same calendar week (mowing day). Within our model, mowing has a solely negative effect on the model species, but with different severities for the below- and aboveground populations. Other indirect effects of mowing are not included in the model (see Section 3.2.2).

3.2.5 Simulation Output

For each simulation scenario, we generated fifty replicate runs (using different random seeds) to account for stochasticity (Section 3.2.6, Table 3.3). To assess and compare the suitability of different regions for population viability under different scenarios, we focused on two output values per grid cell: the mean population density (referred to as 'mean density' hereafter) over the full simulation duration and all replicates and the mean population lifetime (referred to as 'mean lifetime' hereafter) over all replicates.

Note that the maximum duration of simulation runs limits the lifetime to 20 years in our analysis. Values close to 20 years hint at population survival over the whole simulation duration in most (or all) replicates, and, thus, hint at good conditions for longer persistence as well.

3.2.6 Model Description

A full model description following the ODD (Overview, Design concepts, Details) protocol (Grimm et al., 2006; Grimm et al., 2020) is provided in Chapter 2. Here, we provide a 'Summary ODD' (Grimm et al., 2020), which includes the models' overall rationale, an overview of the entities and processes, and verbal descriptions of the key processes. In the following, ODD keywords are in italics and capitals.

The HiLEG model is applied to the life cycle of the LMG, whose life stages are affected by climate and land use. Climate conditions affect development and mortality, while land use (mowing events) induces additional mortality, especially during the aboveground phase. By its present parameterization, the model is nonspatial in the sense that the local LMG populations do not interact with each other. Spatial heterogeneity in land use and biotic variables such as habitat size are ignored. However, the essential climate variables are spatially differentiated to apply the model to spatial gradients in climate change scenarios, covering Northwest Germany and the surrounding regions (Figure 3.1). The *PURPOSE* of the model is to answer the following questions: (1) How do the population density and lifetime shift regionally, given different climate change scenarios? (2) Which mowing schedule has the least negative impact on the overall population density and viability in the study region? (3) Does the mowing impact severity depend on the spatial location (with its specific climate)?

The empirical *PATTERNS* used to ensure that the model is sufficiently realistic for its purpose are the observed features of the life cycle and their sensitivity to environmental conditions, which were taken from the literature. These patterns were used for the model's design. The model output in terms of the population structures, densities and persistence were not compared to other data, as such data are sparse. Therefore, all model predictions are relative, not absolute. The model was implemented in C++. The source code of the model implementation, the executable program and the input files used for the simulations runs are available via a GitLab repository[4].

The model has the following *ENTITIES*: *Grid Cells* (defining environmental conditions), and *Population* per *Grid Cell* comprised of *Life Stages*, which are comprised of age-distinguished *Cohorts*. *Flows* are auxiliary entities that manage the density transfer between *Life Stages* or their loss through mortality. Table 3.1 provides an overview of the model's entities and their *STATE VARIABLES*. The LMG develops through three main *Life Stages* during a year (Section 3.2.2). Following Ingrisch (1983) and Wingerden et al., 1991 , we divided the egg / embryo stage into prediapause, diapause and postdiapause development (called 'embryo' hereafter) to account for the clutch's different susceptibility to climate conditions in autumn, winter and spring.

This subdivision yields five *Life Stages*: (1) prediapause, (2) diapause, (3) embryo, (4) larva, and (5) imago. Stages 1 to 3 occur below ground, and stages 4 and 5 occur above ground. Furthermore, stages 2 and 4 can have multiple *Cohorts* to account for survival over several years in case of conditions during winter that are unsuitable for development and to account for different temperature-driven development speeds depending on the hatching date.

The transition between different *Life Stages* is complex because the development and / or mortality of *Cohorts* and *Life Stages* depends on their previous state and is influenced by climate conditions (*temperature*, *humidity*). *Flows* are therefore used to collect all the contributions of all the *Cohorts* of a certain *Life Stage* that completed development and therefore 'flow' to the next *Life Stage*. In the case of mortality, a *Flow* determines the amount of density lost by a *Life Stage* and its *Cohorts*.

The model uses daily time steps. Here, *SCALE* also reflects the sampling of the climate data. However, the single mowing event per year is considered on a weekly basis (the first day of a calendar week). To account for this weekly frequency, a year has 364 days by definition, resulting in exactly 52 full calendar weeks. Simulations were run for 20 years (7280 time steps) or stopped earlier for a local *Population* in the case of extinction.

[4]HiLEG GitLab repository: `https://git.ufz.de/leins/hileg`

Table 3.1: Overview of the model's life cycle entities (first column) and their state variables (second column). The text in parentheses of columns one and two represents the entity's or state variable's symbol when used, e.g., in equations. The third column gives the (initial) value(s) of the state variables, the fourth column gives their units (if any). In the fifth column, a brief description of the state variable is provided. The indexes for location and time step that distinguish entities and their dynamically changing states are implied and not explicitly specified in the identifier. The parameter $A_{hab} = 62,500\ m^2$ is the habitat size modeled for a Population.

Entity (symbol)	State Variable (symbol)	Value(s)	Unit	Description
Population (P)	coordinate ($coord_{x,y}$)	$x,y \in [1,36]$		Index of rotated pole grid coordinates (see main text)
	set of Life Stages (P^{stages})	$\{S^{pre}, S^{dia}, S^{emb}, S^{lar}, S^{ima}\}$		Distinguished Life Stages of the target species
	density ($dens^P$)	$\sum\{dens^{pre}, dens^{dia}, dens^{emb}, dens^{lar}, dens^{ima}\}$	$ind.\ m^{-2}$	Summed Life Stage densities
	aboveground density ($dens^P_{above}$)	$\sum\{dens^{lar}, dens^{ima}\}$	$ind.\ m^{-2}$	Summed density of the aboveground Life Stages
	minimum density ($dens_{min}$)	$\frac{1}{A_{hab}}$	$ind.\ m^{-2}$	Minimum density of one individual per habit
Life Stage (S^{name})	name	$\in \{pre, dia, emb, lar, ima\}$		Name of the distinguished Life Stages
	set of Cohorts ($S^{name}_{cohorts}$)	$\{C^m, \ldots, C^n\}, \{m,n\} \in \mathbb{N}$		Distinguished Cohorts associated with the Life Stage
	density ($dens^{name}$)	$\sum\{dens^m, \ldots, dens^n\}, \{m,n\} \in \mathbb{N}$	$ind.\ m^{-2}$	Summed densities of the associated Cohorts
	gain ($gain^{name}$)		$ind.\ m^{-2}$	Summed total flow amount of the incoming Flows (see below)
	aboveground flag ($above^{name}$)	$\in \{TRUE, FALSE\}$		Boolean flag defining whether the stage occurs above ground
	maximum age ($dens^{name}_{max}$)	$\in \{210, 1700, 120, 90, 120\}$	days	Maximum age of the associated Cohorts
Cohort (C^{name})	ID	$\in \mathbb{N}$		Unique Cohort identifier
	density ($dens^{ID}$)		$ind.\ m^{-2}$	The Cohort's individual density
	age (age^{ID})		days	Age in days since Cohort creation
	development progress ($prog^{name}_{ID}$)	$\in [0,1]$		The ratio of development compared to full development
	developing flag (dev^{ID})	$\in \{TRUE, FALSE\}$		Boolean flag defining the use of $prog^{ID}$ (see the main text)
Flow (F^{name}_{type})	type	$\in \{trans, repr, mort\}$		Defines how the Flow is processed
	life stage of origin ($orig$)	$\in \{S^{pre}, S^{dia}, S^{emb}, S^{lar}, S^{ima}\}$		Life Stage used to determine the amount of flow
	life stage of destination ($dest$)	$\begin{cases} \text{mort}, & \text{if type=mort} \\ \in \{S^{pre}, S^{dia}, S^{emb}, S^{lar}, S^{ima}\}, & \text{otherwise} \end{cases}$		Life Stage receiving the amount of flow, or the amount of mortality
	set of influences (I^{name}_{type})			Environmental drivers associated with this Flow
	base flow rate ($rate^{name}_{type}$)		day^{-1}	Daily per capita base flow rate
	dynamic flow rate (dyn^{ID}_{type})		day^{-1}	Daily per capita flow rate per Cohort in the life stage of origin
	current flow amount ($amount^{ID}_{type}$)	$dens^{ID} \times dyn^{ID}_{type} \times day$	$ind.\ m^{-2}$	Amount of density flow over one day
	total flow amount ($amount^{name}_{type}$)	$\sum\{amount^m_{type}, \ldots, amount^n_{type}\}, \{m,n\} \in \mathbb{N}$	$ind.\ m^{-2}$	Summed amount (per Cohort) of density flow over one day
Grid Cell (G)	coordinate ($coord_{x,y}$)	$x,y \in [1,36]$		Index of rotated pole grid coordinates (see main text)
	carrying capacity (cap_{above})	25	$ind.\ m^{-2}$	Maximum aboveground density
	temperature (ω_{ts})		°C	Local surface temperature
	humidity (ω_{rhug})		%	Local relative humidity in the upper 2 cm of the ground
	contact water (ω_{cw})		$kg\ m^{-2}$	Amount of water in the upper 2 cm of the ground
	mowing day (t_{mow})	none or $\in \{134, 141, \ldots, 274\}$	day	Day of yearly mowing event

Abbreviations: above=aboveground, C=Cohort, cap=capacity, coord=coordinate, cw=contact water, dens=density, dest=destination, dev=development, dia=diapause, dyn=dynamic, emb=embryo, F=Flow, G=Grid Cell, hab=habitat, ID=Cohort identifier, ima=imago, ind=individuals, kg=kilogram, lar=larva, m=meter, max=maximum, min=minimum, mort=mortality, mow=mowing, orig=origin, P=Population, pre=prediapause, prog=progress, repr=reproduction, rhug=relative humidity upper ground, S=Life Stage, t=time step, temp=temperature, trans=transfer, ts=surface temperature

Table 3.2: List of variables used to initialize a simulation run. The first column is the variable name used in the text. The second column is the variable symbol when used in the model equations. The third column is the initial value(s) / value options used for the simulation runs. The fourth column is a brief description of the variable. The parameters below the double line can vary in principle but are constants in the presented work.

Variable Name	Symbol	Value(s)	Description
starting date	t_{init}	1^{st} Jan. 2000, 2020, 2040, 2060	The date of initial time steps translated to climate data index
mowing day	t_{mow}	none or day 134, 141, ..., 274	The timing of mowing per year
climate change scenario	CCS	FF, MOD or BAU	Representative Concentration Pathways of CO_2 model
duration	t_Δ	$7,280\ days$	Runtime in days
habitat area	A_{hab}	$250 \times 250\ m^2$	Area of grassland plot inside a Grid Cell
initial density	$dens_{init}$	$\frac{\{0,1000,0,0,0\}}{A_{hab}}$	The initial Population density per Life Stage in individuals m^{-2}
carrying capacity	cap_{above}	$25\ individuals\ m^{-2}$	Maximum aboveground density per square meter

FF=full force, MOD=moderate, BAU, business as usual, above=aboveground, cap=capacity, dens=density, hab=habitat, init=initial, mow=mowing, scen=scenario, t=time step

The study region comprises 1296 (36×36) *Grid Cells*, each having an area of 144 km^2 (12 km× 12 km), which corresponds to the resolution of the climate input data (Figure 3.1). In total, 968 *Grid Cells* are terrestrial and therefore belong to the model domain. Within a *Grid Cell*, a single habitat is considered, which represents a virtual grassland plot with a size of 6.25 *ha* (250 $m \times 250\ m$). *Grid Cells* and hence habitats are not connected; i.e., there is no exchange of individuals: if populations become extinct, there is no recolonization.

The model is *INITIALIZED* with a starting date, simulated duration, mowing day and climate change scenario (Table 3.2). Additionally, each *Population* receives an initial density per *Life Stage* (i.e., 1000 eggs in the diapause stage, zero density for the other *Life Stages*). The *carrying capacity* [individuals m^{-2}] for the aboveground population (i.e., the larva and imago *Life Stages* only) is assumed to be identical for all the *Grid Cells* to reduce the number of confounding factors in the model analysis. We used the four 20-year time intervals 2000-2019 (abbreviated to 2000-19 hereafter), 2020-39, 2040-59 and 2060-79 to track changes for past and future climate conditions. Time series of climate data per *Grid Cell* are used as *INPUT DATA*, which drives the model's dynamics.

Table 3.3 provides an overview of the model's *PROCESSES*. Each *Life Stage* has its own set of processes. The basic rationale of the model is to assume a daily base rate for all processes, which represents benign or observed average environmental conditions. This base rate is then modified ('influenced') by environmental drivers. Our model includes predefined functions or equations – called *Influences* – that may be applied under certain environmental conditions. The equations used to represent the *Influences* and their parameterization as applied to the target species are listed in Chapter 2, Tables 2.6 and 2.7. Generally, each Influence provides a factor that can mediate the effect of environmental conditions on the variables *dynamic flow rate* and *development progress* of a *Flow* or *Cohort*, respectively.

In each time step and for every *Grid Cell*, four main blocks of *PROCESSES* are *SCHEDULED*: 'Update environmental drivers', 'Flow update', 'Life Stage update', and 'Cohort update'. The first three blocks are scheduled one after the other, while 'Cohort update' is executed as a submodel of 'Life Stage update'. During 'Flow update', the *Flow*'s state variables (Table 3.1), *total flow amount*, *current flow amount* and *dynamic flow rate* are calculated from the contributions of *Cohorts*' state variables, including the effects of environmental influences.

Table 3.3: Overview of the model processes and their daily rates and equations. Processes (second column) are distinguished by Life Stage (first column) and referenced by their symbol (third column) as used in the model equations. The fourth column defines the equation and environmental drivers (Influences, f-symbols, cf. Table 2.6 of Chapter 2) used for calculating a cohort-specific dynamic rate. Equation segments marked with *s are simplifications of the iterative process of updating the flow rate described in Algorithm 4 of Chapter 2). Superscript letters reference the sources used to parameterize the processes and equations for the LMG (coefficients in Table 2.7 of Chapter 2): [a]Ingrisch (1983), [b]B. Schulz (pers. comm.), [c]Wingerden et al. (1991), [d]Ingrisch & Köhler (1998), [e]Helfert & Sänger (1975), [f]Helfert (1980), [g]Kriegbaum (1988), [h]Waloff (1950).

Life Stage (symbol)	Process	Process symbol	Dynamic rate (daily)	Description
pre-diapause (S^{pre})	mortality	F^{pre}_{mort}	$dyn^{ID}_{mort} = rate^{pre}_{mort} + (1 - rate^{pre}_{mort})^* \times (f^A_{sig} \times f^B_{thd} + f^C_{mow})$	The base mortality rate a increases in two cases: (1) humidity-driven $(f^A_{sig})^a$ if contact water $(f^B_{thd})^a$ is missing; (2) if mowing is scheduled $(f^C_{mow})^b$
	development	$prog^{pre}_{ID}$	$prog^{pre}_{ID} = \begin{cases} prog^{pre}_{ID} + f^D_{thd}, & if\ f^D_{thd} > 0 \\ 0, & \text{otherwise} \end{cases}$	Needs three days below 10 °C in a row $(f^D_{thd})^a$ to fully develop
	transfer	F^{pre}_{trans}	$dyn^{ID}_{trans} = \begin{cases} 1, & if\ prog^{pre}_{ID} = 1 \\ 0, & \text{otherwise} \end{cases}$	Immediately transfers to diapause stage if fully developed
diapause (S^{dia})	mortality	F^{dia}_{mort}	$dyn^{ID}_{mort} = rate^{dia}_{mort} + (1 - rate^{dia}_{mort}) \times f^E_{mow}$	The base mortality rate increases if mowing is scheduled $(f^E_{mow})^b$
	development	$prog^{dia}_{ID}$	$prog^{dia}_{ID} = \begin{cases} prog^{dia}_{ID} + \frac{f^F_{thd}}{2}, & if\ prog^{dia}_{ID} < 0.5, \\ prog^{dia}_{ID} + \frac{f^G_{thd}}{2}, & if\ prog^{dia}_{ID} \geq 0.5 \wedge f^G_{thd} \neq 0, \\ 0.5, & \text{otherwise} \end{cases}$	Needs 61 days below 5 °C to break diapause $(f^F_{thd})^{a,c}$ and afterwards three days above 10 °C in a row $(f^G_{thd})^a$ to fully develop. Temperatures > 5 °C before diapause is broken reverse development
	transfer	F^{pre}_{trans}	$dyn^{ID}_{trans} = \begin{cases} 1, & if\ prog^{dia}_{ID} = 1 \\ 0, & \text{otherwise} \end{cases}$	Immediately transfers to embryo stage if fully developed
embryo (S^{emb})	mortality	F^{emb}_{mort}	$dyn^{ID}_{mort} = rate^{emb}_{mort} + (1 - rate^{emb}_{mort})^* \times (f^H_{exp} + f^I_{sig} \times f^J_{thd} + f^K_{mow})$	The base mortality is defined by the temperature $(f^H_{exp})^c$. It increases in two cases: (1) humidity-driven $(f^I_{sig})^a$ if contact water $(f^J_{thd})^a$ is missing and / or (2) if mowing is scheduled $(f^K_{mow})^b$
	transfer	F^{emb}_{trans}	$dyn^{ID}_{trans} = rate^{emb}_{trans} \times f^L_{bin}(f^M_{exp}, f^N_{exp}, dens^{ID}, prog^{name}_{ID})$	The base transfer rate is multiplied by a temperature- $(f^M_{exp}, f^N_{exp})^c$, progress- and the density-driven hatching probability stemming from a binomial distribution (f^L_{bin})
larva (S^{lar})	mortality	F^{lar}_{mort}	$dyn^{ID}_{mort} = rate^{lar}_{mort} + (1 - rate^{lar}_{mort})^* \times (f^O_{cap} + f^P_{lin} + f^Q_{mow})$	The base mortality $rate^d$ increases with density $(f^O_{cap})^b$ and in two additional cases: (1) the temperature (f^P_{lin}) is below 10 °C and / or (2) if mowing is scheduled $(f^Q_{mow})^b$
	transfer	F^{lar}_{trans}	$dyn^{ID}_{trans} = rate^{lar}_{trans} \times f^R_{bin}(f^S_{lin}, f^T_{lin}, dens^{ID}, prog^{lar}_{ID})$	The base transfer rate is multiplied by a temperature- $(f^S_{lin}, f^T_{lin})^{e,f}$, progress- and density-driven maturation probability stemming from a binomial distribution (f^R_{bin})
imago (S^{ima})	mortality	F^{ima}_{mort}	$dyn^{ID}_{mort} = rate^{ima}_{mort} + (1 - rate^{ima}_{mort})^* \times (f^U_{cap} + f^V_{lin} + f^W_{mow})$	The base mortality $rate^g$ increases with density $(f^U_{cap})^b$ and in two additional cases: (1) the temperature (f^V_{lin}) is below 10 °C and / or (2) if mowing is scheduled $(f^W_{mow})^b$
	reproduction	F^{ima}_{repr}	$dyn^{ID}_{repr} = rate^{ima}_{repr}$	Fixed reproduction $rate^{d,h}$

Abbreviations: bin=binominal, cap=capacity, dens=density, dia=diapause, , emb=embryo, exp=exponential, f=symbol of Influence function, F=Flow, ID=Cohort identifier, ima=imago, lar=larva, lin=linear, mort=mortality, mow=mowing, pre=pre-diapause, prog=progress, repr=reproduction, sig=sigmoid, t=time step, thd=threshold, trans=transfer

The submodel 'Life Stage update' then calculates a *Life Stage*'s *gain* from the incoming transfer *Flow* of its preceding *Life Stage* and its *density* from the *density* of its subordinate *Cohorts*: *gain* is used to determine whether to create a new *Cohort* from it or add it to an existing *Cohort*; densities of the subordinate *Cohorts* are determined by the submodel 'Cohort update' before they are added to the *Life Stage*'s density. Furthermore, *Cohorts* that exceed the maximum age before progressing to the next *Life Stage* or whose density falls below a certain minimum are removed. During 'Cohort update', a *Cohort*'s density is changed by adding the potential *gain* determined by the 'Life Stage update' submodel and subtracting loss through mortality or the outgoing transfer *Flow*. Additionally, some *Cohorts* develop only if environmental conditions are suitable, so their *development progress* is updated accordingly. Figure 3.4 provides an overview of the model's entities, the processes, and their interactions via *Flows* and *Influences*.

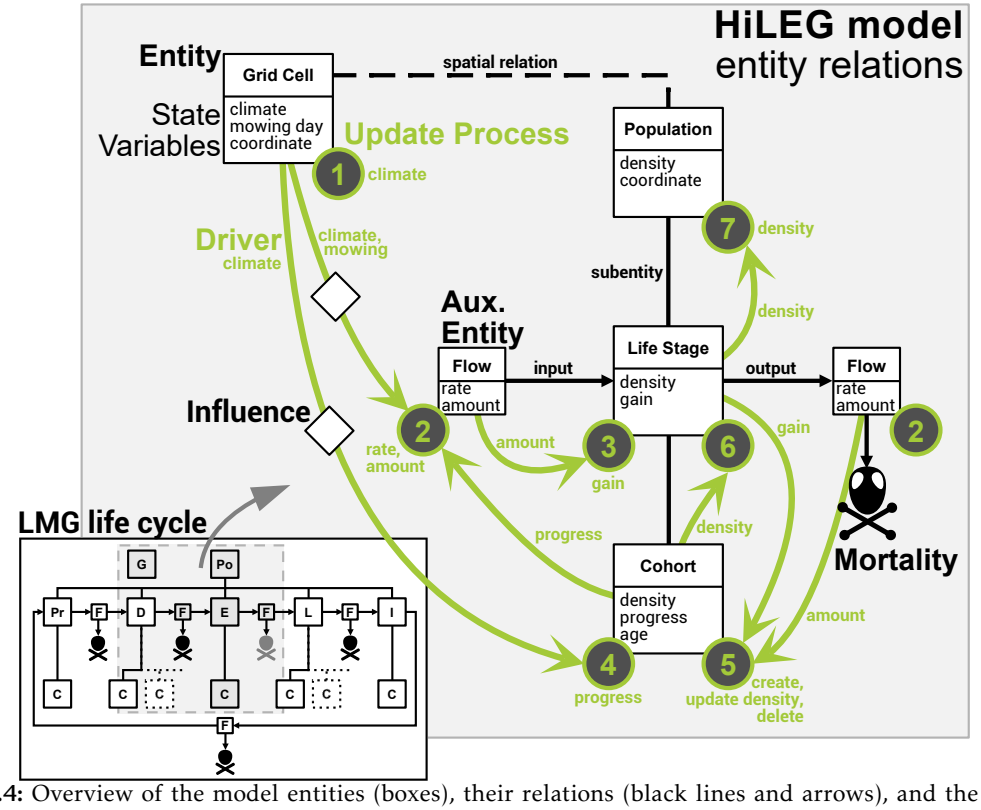

Figure 3.4: Overview of the model entities (boxes), their relations (black lines and arrows), and the order and drivers of the update process (green) for a single grid cell during one time step. The entities are *Grid Cell*, *Population*, *Life Stage*, *Cohort* and *Flow* (an auxiliary entity that uses state variables of the previous time step to manage the density transfer between *Life Stages* and loss through mortality). *Influences* define the impact of environmental conditions on model processes. The white subplot shows entities and their relations as applied to the LMG life cycle. The gray dashed rectangle within the subplot highlights entities used to explain the update process (main plot). The scheduling of the processes is as follows: (1) Update the environmental conditions. (2) Update the flow rates and amounts depending on the climate conditions and mowing while considering the development processes of the associated *Cohorts*. (3) Calculate the gain of the *Life Stage* depending on the input flow amount. (4) Update the development progress of the existing *Cohorts* depending on the climate conditions. (5) Create a new *Cohort*, and update the density of existing *Cohorts* and / or delete *Cohorts* that are of too low density or overaged depending on the *Life Stage*'s gain and output flow amount. (6) Calculate the *Life Stage* density by summing its *Cohorts*' densities. (7) Calculate the *Population* density by summing its *Life Stages*' densities. Symbols: Entities (squares), Influences (diamonds), Processes (circles, text corresponds to modified state variables), Drivers (green arrows, text corresponds to state variable used in target Process), optional *Cohorts* (dotted squares and lines). Abbreviations in the LMG life cycle: C=Cohort, D=diapause, E=embryo, F=Flow, G=Grid Cell, I=imago, L=larva, Po=Population, Pr=prediapause.

3.3 Results

The results presented here are subdivided into three Sections: (1) patterns and trends found in the climate data that are relevant to the LMG (Section 3.3.1); (2) analysis of the HiLEG model output stemming from simulations with climate as only external driver (Section 3.3.2); and (3) analysis of the simulation runs with mowing as an additional anthropogenic impact on the LMG (Section 3.3.3). Since the results are complex, as they cover large environmental gradients and detailed effects of environmental drivers on the study species, in the following, the main results are also directly discussed in terms of the underlying mechanism. Note that the model output occasionally reaches densities close to the population's carrying capacity, which in reality is rarely the case on a large scale. Within the idealized conditions (Section 3.2.2) of our model realization, however, this behavior is expected and can be considered unproblematic for the analysis, because we were focusing on the relative impacts of climate change and land use on population development rather than those of density dependence.

3.3.1 Patterns and Trends in Climate Data

The different climate projections showed spatial patterns and temporal trends for the years 2000 to 2079 in terms of *temperature* and *soil moisture*. Note that for reasons of consistency, even the past time period 2000-19 consists mostly of simulated data (see Section 3.2.3). The coarse spatial patterns for all the climate change scenarios, averaged over 20-year periods, show that temperature increased slightly from north to south, except for two colder mountain regions in the south (Figure 3.5, marks 1-2). Over time, the temperature generally increased similarly in the study region. Overall, the increase was stronger for more severe scenarios with three exceptions. First, during the simulation period 2000-19, temperatures were more or less identical between the scenarios. Second, for the period 2020-39, the temperature increase was slightly higher for scenario *MOD* than for *BAU*. Third, during the late periods 2040-59 and 2060-79, temperature remained almost constant for scenario *FF*.

For *soil moisture*, the patterns were more complex than those of *temperature*. There were four regions of distinctively low soil moisture (Figure 3.5, marks 3-6) because these regions have a soil type that seems to favor drought (K. Keuler, pers. comm., cf. Keuler et al., 2016). During the first period (2000-19), the *MOD* and *BAU* scenarios clearly showed lower soil moisture than the *FF* scenario in almost all the cells and an additional dry region in the southeast (Figure 3.5, mark 6). Over time, however, many of those cells improved for the severe *BAU* scenario while degrading for the *FF* scenario. Nonetheless, the soil moisture for the *BAU* scenario was barely higher than that for the intermediate *MOD* scenario (Figure 3.3).

Overall, the spatial patterns in the soil moisture showed the following temporal trends: The northwestern dry region expanded over time (Figure 3.5, mark 4); some small dry regions appeared in the center of the study region; the moisture of the mountain regions increased less than that of their surroundings; the edges around the central eastern dry region became wetter; and there was a spatial gradient of soil moisture increase in the southeast and decrease in the northwest.

On a monthly basis, the climate parameters generally followed the trends in the yearly averages (cf. Figure 3.3, data not shown). For all the climate change scenarios and time periods, the temperature usually reached its minimum around January and its maximum around July with gradual changes between these months. The soil moisture was lowest in September and

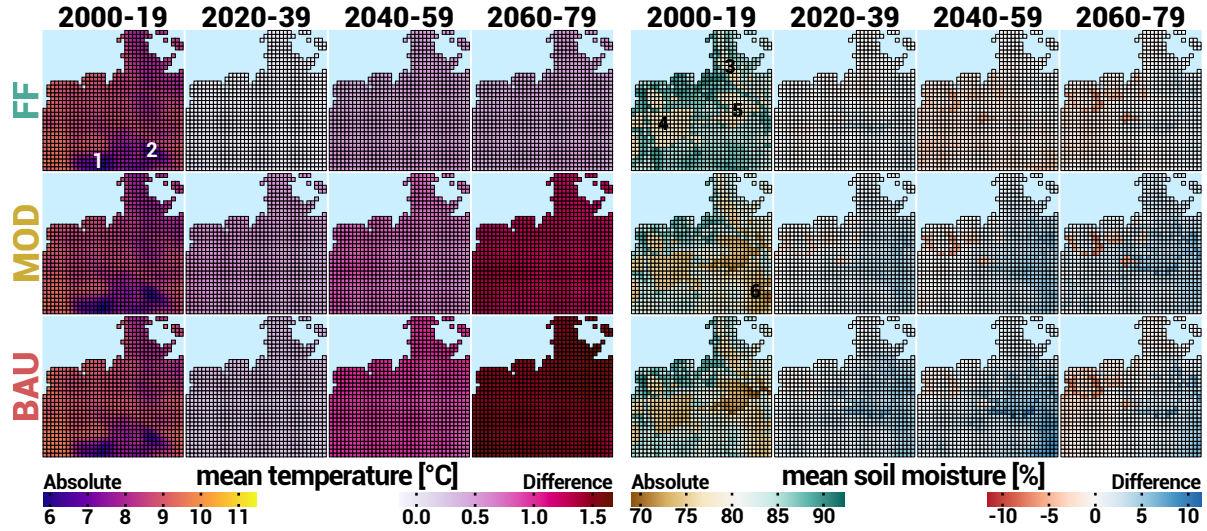

Figure 3.5: Spatial representation of the mean daily climate values *temperature* (LEFT) and *soil moisture* (RIGHT) for the years 2000-2079 in Northwest Germany. Within each plot, the absolute values for the simulation period 2000-19 per climate change scenario are in the first column; differences from the period 2000-19 are in the second (2020-39), third (2040-59) and fourth (2060-79) columns. The *FF* scenario is in the TOP row; the *MOD* scenario is in the MIDDLE row; the *BAU* scenario is in the BOTTOM row. Numbers mark colder mountain areas (1 and 2) and main dry regions (3-6).

gradually increased to its maximum in March before constantly decreasing again. An important exception from this general pattern appeared in the *BAU* scenario during the period 2060-79 (Figure 3.6): the monthly soil moisture values deviated from the yearly trend such that June to October were especially dry, while November to May were wetter than usual. This finding indicates a severe and possibly extended dry season that could not be detected by examining only the yearly mean values.

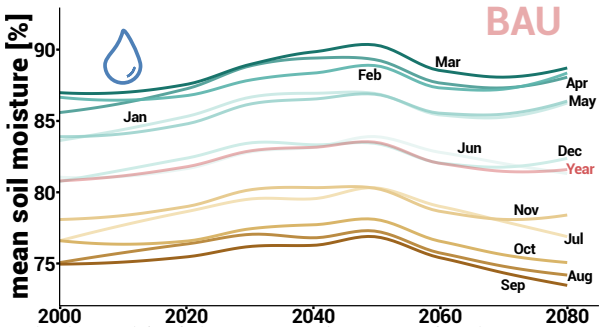

Figure 3.6: Projections (smoothed trends) of the mean *soil moisture* for the years 2000-2080 for the *BAU* climate change scenario distinguished by month and year (with labels).

3.3.2 Climate Change Impact on LMG

The results of the HiLEG model confirm that without direct anthropogenic influence, the LMG mostly benefits from climate change in Northwest Germany. Within each climate change scenario, there was a clear upward trend from 2000 to 2059 for both the mean density and lifetime (Figure 3.7). For the last simulation period (2060-79), there was a saturation yielding results similar to that of 2040-59.

Comparing the climate change scenarios within the same simulation periods, the mean re-

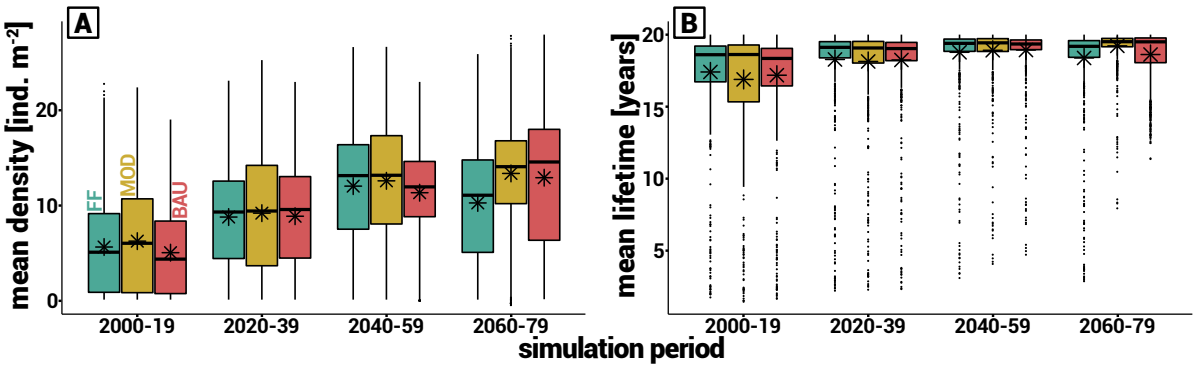

Figure 3.7: Population mean density [individuals m^{-2}] (A) and lifetime [years] (B) per grid cell for the study region distinguished between climate change scenarios *FF*, *MOD* and *BAU* (colored labels) and simulation periods (from left to right: 2000-19, 2020-39, 2040-59, and 2060-79). Asterisks mark the overall mean values.

sults were quite similar except for differences between the *FF* scenario and the other two scenarios in the period 2060-79 (Figure 3.7). The scenarios led to similar spatial patterns in the mean density and lifetime within the same time period but also created certain subtle differences (Figure 3.8).

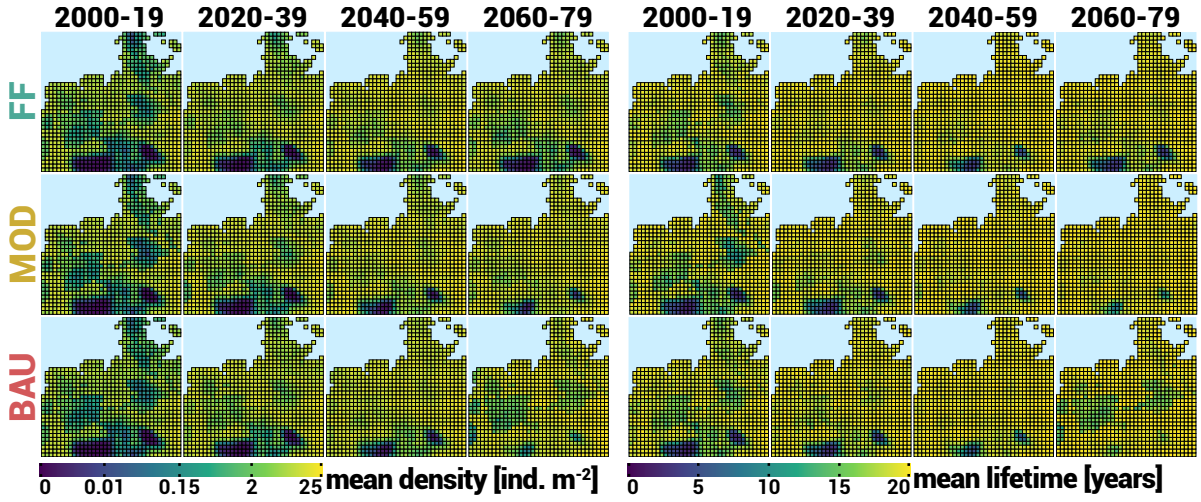

Figure 3.8: Log scaled mean density [individuals m^{-2}] (LEFT) and lifetime [years] (RIGHT). Within each plot the *FF*, *MOD*, *BAU* climate change scenarios are shown in the TOP, MIDDLE, and BOTTOM rows, respectively, and the simulation periods from left to right are 2000-19, 2020-39, 2040-59, and 2060-79.

First, the population conditions improved over time in initially unsuitable areas such as cold mountain regions and dry regions (cf. Figure 3.5, marks 1-5). An exception was 2060-79 when compared to the previous simulation period 2040-59. Here, the *FF* climate change scenario had negative effects on the mean densities and lifetimes in most of the cells. The *MOD* scenario showed almost no changes compared to the previous time period. The *BAU* scenario yielded improvements outside the dry regions but had negative effects within these dry regions.

Comparing these spatially resolved model results to the climate data showed that they reflect the temperature patterns: high temperatures support population development, while colder regions notably reduce the mean density and lifetime (Figure 3.5, marks 1-2). Recurrent significantly colder years (Figure 3.3A, 2060-79, *FF* minima) can inhibit the positive long-term effect of warm temperatures (Figure 3.8, 2060-79, *FF*). The soil moisture patterns, however,

are less perceptible: Though population development was clearly hindered in the main dry regions (Figure 3.5, marks 3-5) during the simulation period 2000-19, the mean lifetime increased significantly starting in 2020. The mean density in these regions, however, remained limited compared to those in the surrounding areas. Another pattern connected to soil moisture is the strong negative effect of an extended dry season (Figure 3.6) on populations in most dry regions during the period 2060-79 for the *BAU* scenario (Figure 3.8, green areas in the bottom-right subplots).

The peaks in the mountain regions remained mostly uninhabitable for the LMG throughout all the simulations, as these areas stayed relatively cold (Figure 3.5, marks 1-2). In these regions, the population declined almost constantly and went extinct after a few years. This phenomenon is due to the impact of the overall lower temperatures on the LMG's development and mortality: First, it slowed down the development of the embryos and larval cohorts; second, the temperature threshold of increased larva and imago mortality occurred earlier in the year; third, the decelerated development additionally shifted larva and imago occurrence to a later, hence even colder, season of the year. Departing from the mountain peaks, the conditions for the LMG gradually improved, allowing a longer lifetime at first and increasing the population density thereafter. The time lag in population development between the warm and cold cells shown in Figure 3.11B (mark a) illustrates such a temperature-induced shift in the life cycle.

Low soil moisture had a negative impact on the LMG if the dry season had already started in late spring or lasted until autumn. In these cases, either the embryos (spring) or the prediapause eggs (autumn) experienced drought stress. Within the study region, extinction by drought was mainly caused by the latter, i.e., if a cell still had dry soil after oviposition (Figure 3.11B, mark b). Increased embryo mortality through drought stress in spring usually did not lead to extinction but minimized the mean density.

The reoccurrence of conditions unfavorable to the LMG in the period 2060-79 for the *BAU* climate change scenario was due to climate projections for this scenario. Though the notably higher temperatures led to favorable conditions in large parts of the study region, a strongly extended dry season in the central areas had considerable negative effects on the mean densities and lifetimes (Figure 3.8, green areas in the bottom-right subplots). As a result, the overall mean density and lifetime increased, while their larger variations (Figure 3.7) reflected the low values in the dry areas.

3.3.3 Impact of Grassland Mowing in Addition to Climate Change

The extent of the negative influence of grassland mowing on the LMG life cycle was highly dependent on the calendar week in which it occurred (Figure 3.9). While mowing during spring and late autumn barely affected the mean lifetime, it severely reduced the mean density if it occurred in summer and early autumn. This result was independent of the climate change scenario and simulation period. However, due to the positive effect of higher temperatures in future scenarios, the time windows of negative impact both shifted and shortened: Late mowing (after week 33) became less detrimental, while early mowing (before week 26) had only a slightly more negative effect (Figure 3.9, *MOD* and *BAU* scenarios).

The spatial distribution of the mowing-dependent mean lifetime revealed regional differences between the effects of mowing timing (Figure 3.10). In particular, the periods of negative mowing impact did not apply to all regions in the same way. Figure 3.10 illustrates these differences using simulation period 2060-79 of the *BAU* climate change scenario as an

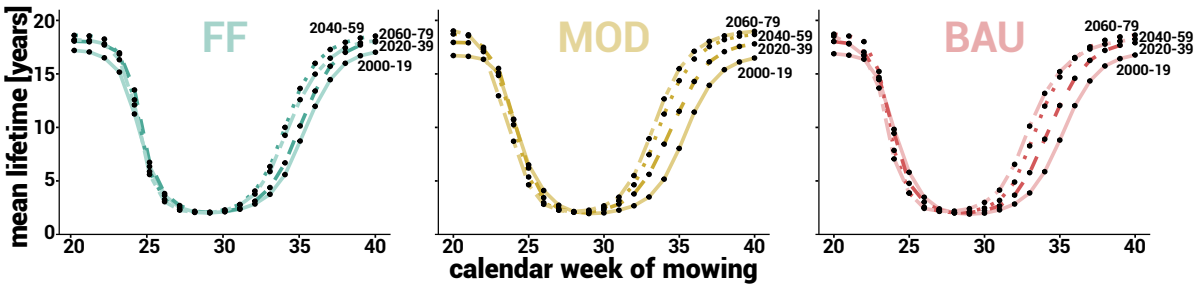

Figure 3.9: Population mean lifetimes averaged over the whole study region (y-axis) depending on the calendar week of grassland mowing (x-axis) for climate change scenarios *FF* (LEFT), *MOD* (MIDDLE), *BAU* (RIGHT) and the simulation periods (different line types, with labels). Mowing events (black dots) occurred on the first day of the same calendar week in each simulation year.

example. Apart from an overall negative effect of mowing on the LMG populations (compare Figure 3.10B-C to Figure 3.10A), conditions for the LMG gradually degraded from north to south when mowing occurred early (Figure 3.10B). Moreover, within the southern mountain regions, the conditions remained relatively stable despite early mowing and stood out compared to their surroundings (Figure 3.10B). However, both patterns were inverted when mowing occurred late (Figure 3.10C). In this case, conditions gradually improved from north to south and were rather unsuitable within the mountain regions. Finally, as a side effect, the negative influence of mowing was generally stronger in the dry regions than in the wet regions, especially for late mowing (Figure 3.10C).

Note that mowing in week 23 fell into the short period of slightly more negative impact under future climate conditions than under current climate conditions (Figure 3.9, *BAU* scenario). Hence, the respective spatial pattern contained many cells of short mean lifetimes (dark green, Figure 3.10B). Nevertheless, the LMG remained rather unaffected by this scenario in the upper north and southern mountain regions. Qualitatively similar patterns were found for mowing weeks 22-26 in all three climate change scenarios and all simulation periods (see Appendix A.3).

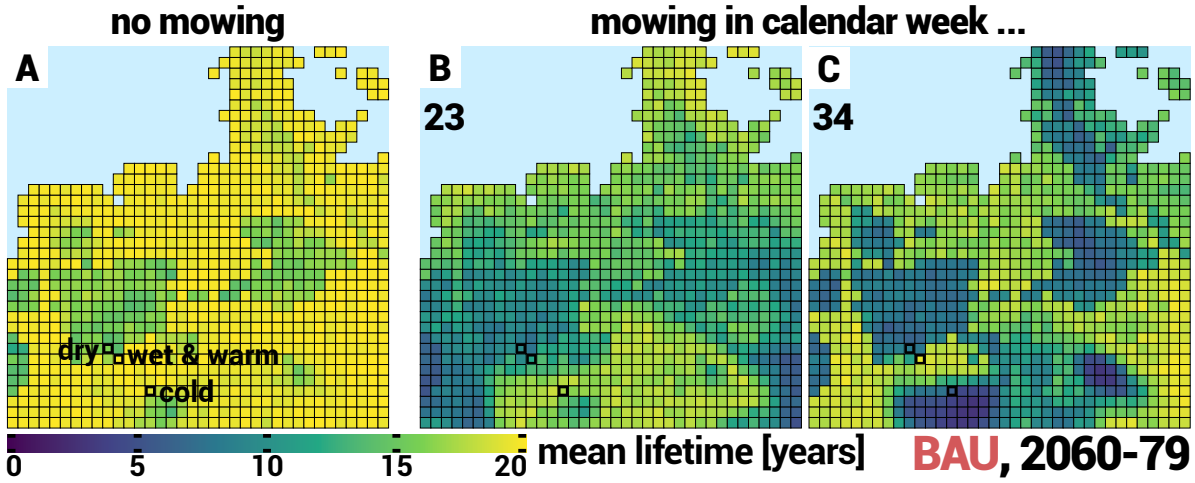

Figure 3.10: Spatial distributions of the mean lifetimes for the *BAU* climate change scenario and simulation period 2060-79; without mowing (A) and with mowing in calendar weeks 23 (B) or 34 (C). Thick black squares mark selected dry, wet & warm and cold cells.

The development of the mean density inside single grid cells showed that the described patterns are mainly determined by three relevant climate categories within the study region:

wet and warm (mostly southern cells outside the dry and mountain regions); cold (mostly northern grid cells and especially mountain regions, Figure 3.5, marks 1-2); and dry (Figure 3.5, marks 3-5). We selected a representative grid cell for each of the climate categories (highlighted in Figure 3.10) to illustrate the characteristic population development (Figure 3.11).

The resulting population development patterns confirm that without mowing, the population eventually reached high densities in all three cell categories (Figure 3.11A-B). The highest values occurred under wet and warm conditions (the maximum density is already achieved in 2070), followed by cold and dry conditions. Early mowing in week 23 favored populations in cold regions but worsened the situation in dry regions; this worsening was even more prominent in wet and warm regions (Figure 3.11C). Late mowing in week 34 hindered population development only slightly under wet and warm conditions but hindered it more severely in dry regions (Figure 3.11D). Under cold conditions, late mowing had a grave impact and often caused premature extinction (Figure 3.11A).

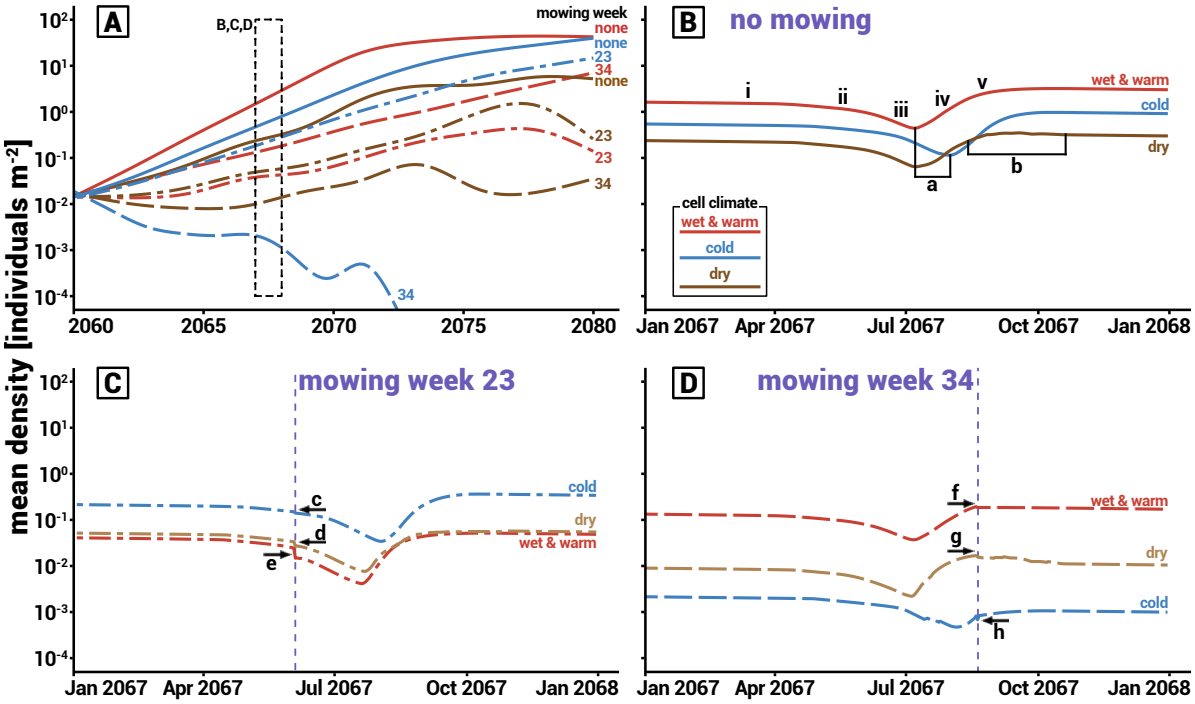

Figure 3.11: Trend in the mean population density (y-axis, logarithmic scale) inside three climatically different grid cells (wet & warm, red lines; cold, blue lines; dry, brown lines) without mowing (B, see also the line labels in A), with mowing in week 23 (C) and with mowing in week 34 (D) for the *BAU* climate change scenario and simulation period 2060-79. Plot A shows the smoothed trend for the whole simulation period (2060-79), and plots B-D show the detailed developments in 2067. Purple vertical lines mark the mowing weeks in C and D. Black lowercase letters (a-h) highlight the following selected events: a) shifts in the development speed, b) period of drought stress in dry cells, c) minor effect of early mowing in cold cells, d) medium effect of early mowing in dry cells, e) major effect of early mowing in wet & warm cells, f) minor effect of late mowing in wet & warm cells, g) medium effect of late mowing concurring with drought stress in dry cells, and h) major effect of late mowing in cold cells. Roman numbers in plot B indicate life stage occurrence on the basis of the development without mowing in the wet & warm cells: i) diapause, ii) embryo, iii) larva, iv) imago, v) prediapause. In plot A, the carrying capacity (25 individuals m^{-2}) is exceeded because it does not apply to the belowground population.

The main driver for the different impacts of mowing was temperature. It shifted the hatching date and altered the duration of the larval life stage. For instance, a development delay of three weeks occurred in cold cells compared to wet and warm cells (Figure 3.11B, mark a). This was advantageous in the case of early mowing in week 23 because – due to the delay

– the population was still in the belowground phase and was thus less affected by mowing (low mortality, Figure 3.11C, mark c). Fast developing populations in warm cells, however, were strongly affected (Figure 3.11C, mark e) because many eggs had already hatched. Thus, most of the aboveground larval population was killed by mowing. In dry cells, the slightly slower population development led to a moderate loss of larvae, which prevented substantial growth (Figure 3.11C, mark d). These different effects of early mowing in the different cell types explain the spatial pattern in the long mean lifetimes in cold (mountain) regions and shorter lifetimes in wet and warm cells and in dry cells (Figure 3.10B).

In contrast, when mowing occurred later in the year, fast population development proved beneficial. In wet and warm cells, oviposition had mostly already taken place, and mowing had only a minor effect on the belowground clutch (Figure 3.11D, mark f). However, slowly developing populations in cold regions were hit in the middle of the aboveground phase and a large number of larvae and imagines were lost (Figure 3.11C, mark h). As a consequence, the small number of eggs placed in the ground resulted in a constant population reduction from year to year (Figure 3.11A). In dry regions, populations were affected by late mowing in week 34 (Figure 3.11D, mark g), which concurred during the drought period. Thus, late mowing in dry cells allowed population survival but prevented further growth (Figure 3.11A).

Notably, the gradients of the mean lifetime from north to south and the differences between the mountain regions and other regions Figure 3.10B-C) did not occur without mowing (Figure 3.10A). This finding indicates that the regionally different, temperature-induced shifts in life stage development do not necessarily have considerable long-term effects on populations without mowing. However, in combination with specific mowing schedules, minor temporal shifts can have major effects on the populations' susceptibility to mowing and, thus, on long-term population development.

3.4 Discussion

The simulation results of the presented HiLEG model provide the following answers to our research questions: (1) outside of dry regions, climate change increases LMG population viability and promotes the species' spatial expansion; (2) grassland mowing is mostly unproblematic during autumn and winter, but highly detrimental in late spring and summer; and (3) regionally different climate conditions affect the mowing impact and should therefore be addressed by adaptive mowing schedules. These findings are discussed in more detail below.

There is basically no regional shift in the LMG distribution but an expansion in the suitable regions in Northwest Germany. The overall increasing temperatures create new potential habitats in regions that are otherwise too cold (mountainous) or too dry. This is caused either by the direct positive influence of warmth or indirectly by accelerating the LMG's development such that it suffers from drought stress less often. In fact, we found that more drastic climate change facilitates the survival and growth of the LMG even more strongly in future scenarios. The positive effects of increasing temperatures on the grasshopper's abundance and distribution visible in our results are in line with the results of Poniatowski et al. (2018a) and Trautner & Hermann (2008). However, extended dry seasons, as projected for the period 2060-79 in the *BAU* climate change scenario (Figure 3.6), could inhibit this beneficial effect by causing drought stress for the LMG clutch. Regions affected by low soil moisture in this way (Figure 3.5, marks 3-5) could become less habitable for the LMG, while nearby wetter regions still benefit from the temperature increase Figures 3.7 and 3.8, *BAU*, 2060-79). It is the duration of the dry season that makes *soil moisture* a crucial factor for the survival

of the LMG. Although our results show that dry regions do not necessarily cause drought stress within the study region, it is likely that such a problematic extension of dry seasons will become more common in the future, especially in regions that are generally drier than Northwest Germany. Hence, at a larger scale, droughts are likely to affect the species' survival and lead to a distribution shift from dryer to wetter regions, if migration is not hindered.

Anthropogenic disturbance through land use was more critical to the viability of the species than expected climate change. The effects of grassland mowing were particularly severe when they occurred during the aboveground phase of the LMG life cycle. Currently, it is common in extensively used grasslands that the mowing season starts before the aboveground phase is reached. For instance, Gerling et al. (2022)[5] show for the federal state of Schleswig-Holstein, a subarea of our study region, that early mowing yields the highest benefit for a farmer. Later mowing, however, has a strong impact on the LMG's development if it occurs during the aboveground phase of the population. Even when considering that imagines can partly escape harvesters (Malkus, 1997) and thus apply lower mowing-induced mortality rates (Marzelli, 1997; Kiel, 1999), the negative effect does not change qualitatively (i.e., when we reduced the imago mortality to 0.5 instead of 0.95 per day, data not shown). Although negative impacts decrease when mowing late, two counterarguments need to be considered: late mowing (after summer) is rather unprofitable for the farmer and hence may not be a feasible land use measure; and the future shift of problematic mowing to a shorter period of time in summer (Figure 3.9) might go along with a similar shift of vegetation growth, thus further reducing the economic profitability of late mowing.

Our simulations with the combined impact of climate change and grassland mowing revealed regional differences that need consideration when choosing a mowing schedule. The date of mowing mainly determines in which parts of the study region the impact on the species is high and where it is low. Mowing dates that are unproblematic in one region can have a highly lethal effect in another region. In most of those cases, if a population is affected by early mowing in a highly negative manner, its development is hardly influenced in simulations with late mowing. In contrast, in other regions, the population is highly disturbed by late mowing but remains mostly unaffected if mowing occurs early in the year. Altogether, the regional impact of the mowing schedule can be subdivided into five phases: (1) in early spring, the populations are largely unaffected in all regions; (2) between late spring and early summer, they are severely affected only in warm regions; (3) during summer, all populations are highly affected, barely allowing survival (Figure 3.9); (4) between late summer and early autumn, they are severely affected in cold regions; and (5) in autumn, populations in all regions are affected equally. The duration and beginning of each phase slightly differ between the climate change scenarios and simulation periods, but overall, they show the same pattern (see Appendix A.3).

Obviously, temperature is the key factor affecting population dynamics. The LMG prefers a warm climate and hardly survives in cold (mountain) areas. That is why the simulated lifetimes are longer and population densities are higher in the more severe climate change scenarios – as long as there are no extended drought events. However, lower, not too low, temperatures can be advantageous for the LMG if early mowing is applied. As shown in Figure 3.11B, population development is slower in such regions, meaning that the aboveground phase, which is highly susceptible to mowing, occurs later and lasts longer. Compared to warmer regions, this finding explains the low impact during late spring and early summer

[5] Study was still in preparation when the original article was published. The reference has been updated here as the study has now been published

(phase 2 of the phases described above) and the high negative impact during late summer and early spring (phase 4, see the examples in Figure 3.10B-C and Figure 3.11C-D)

Based on our results, we can develop some possible management strategies for a species such as the LMG to increase population viability depending on the expected climate conditions in certain regions. Our results suggest that adaptive grassland management that takes into account the local climate conditions with respect to the LMG's life cycle would be the method of choice. In practice, however, it may prove unrealistic to implement such micromanagement. Therefore, we discuss some more generic management strategies in the following.

According to our findings, looking exclusively at climate change, the LMG mostly benefits from the projected temperature increase. Thus, the crucial parameter to consider for management strategies in such a scenario is soil moisture. In regions projected to experience longer dry periods, particularly if they extend into autumn, one could focus on installing, maintaining or expanding measures that keep grasslands from drying up (Miller & Gardiner, 2018), especially if those grasslands are close to streams or other fresh water bodies. Alternatively, one could consider implementing migration corridors and stepping stone biotopes to facilitate dispersal to wetter regions (Kimura & Weiss, 1964; Schumacher & Mathey, 1998). Apart from that, it is important to keep in mind that one or two carefully timed grassland cuts per year can also be considerably beneficial for the development of the LMG (Malkus, 1997). These cuts help maintain a favorable vegetation structure (Sonneck et al., 2008) and can facilitate hatching by allowing more sunlight – and, therefore, warmth – to the upper ground (Miller & Gardiner, 2018).

There are further adaptive management strategies that may allow LMG survival in cultivated grasslands. Our simulations demonstrated that intensive land use with mowing during summer, i.e., the LMG's aboveground phase, can be lethal for a population (Figure 3.9). If the grassland cuts, though, are scheduled either right at the beginning or the end of the aboveground phase (Wingerden et al., 1992) or only every other year, populations can survive the cuts, though likely with low abundance. Figure 3.11A supports the latter suggestion by showing that populations do not immediately become extinct when exposed to a disadvantageous mowing schedule. Another possibility could be to apply different mowing schedules in neighboring grassland plots. In that way – given that individuals may migrate from one plot to another – they might find refuge until vegetation regrows (Malkus, 1997). Although those small-sized plot relations cannot be represented on the current scale of the HiLEG model, the spatial gradient covered by our model (Figure 3.10B-C) gives an idea of the options and necessary regional adjustments. It can make a large difference to have an offset of one or two weeks between mowing in grid cells not too far apart from each other.

In addition to adaptive scheduling, changing either the technique, e.g., inside-out-mowing (Malkus, 1997), or the mown area, e.g., by leaving uncut grass strips (Kiel, 1999; Humbert et al., 2009), could help reduce the fatalities in case the cut cannot be delayed. Uncut grass strips might even facilitate the subsequent development of the LMG because larval instars can make use of vegetation with diverse height profiles (Krause, 1996).

From a methodical point of view, our results highlight that a model's resolution can play a key role in supporting management strategies for a target species. The daily time step allowed us to capture short but distinct weather events and small seasonal shifts in the climate that would have gone unnoticed in monthly or yearly mean values. However, in our simulations, these daily dynamics had a significant impact on both short- and long-term population development. Similarly, the different impacts of environmental conditions (climate and land

use) on the populations' different life stages could not have been discovered without explicitly considering the LMG life cycle and each life stage's specific characteristics. The spatial resolution of our model ($12 \times 12\ km^2\ cell^{-1}$) is quite high compared to that of global climate models[6]. This high resolution allowed us to take into account spatial differences and gradients in neighboring regions, especially with regard to the suitability of mowing schedules. Szewczyk et al. (2019) state that process-based regional-scale models, such as the HiLEG model, could be further downscaled to predict species distribution at a more local or habitat level. An even higher spatial resolution could allow the consideration of additional heterogeneity in the microclimate and grassland composition of potential relevance to species such as the LMG. LMG imagines tend to choose moist locations with patchy vegetation for oviposition (Krause, 1996; Malkus, 1997). Such locations prevent drought stress (Ingrisch, 1983) and promote egg development speed, as they are sunlit (Wingerden et al., 1992). Larvae initially prefer a patchy, low- to medium-height vegetation structure (Malkus, 1997). Older instars and imagines retreat to high, dense vegetation for protection (Wingerden et al., 1992).

In this work, we intentionally consider spatial heterogeneity with regard to only the climate parameters but assume that most of the other characteristics (mowing schedule, carrying capacity, habitat size, base demographic rates) are spatially homogeneous. We make this assumption because the purpose of our analysis is to determine the impact of (spatially heterogeneous) climate change and its interaction with land use. The analysis would have been confounded by other sources of spatial heterogeneity. To deduce specific species conservation plans, it would be desirable and possible to include the spatial heterogeneity of the other mentioned factors as well. Another extension of the model could be to include dispersal between different grassland patches, which would allow for the migration of individuals from less suitable grassland patches to more suitable ones. Additionally, dispersal between metapopulations (Levins, 1969; Hanski, 1999) could partially provide refuge from the negative effects of grassland use through recolonization from other grassland patches (Brown & Kodric-Brown, 1977). However, Bönsel & Sonneck (2011) emphasize that metapopulation dynamics cannot be assumed for low-dispersal species such as the LMG in highly fragmented landscapes. Hence, such rescue effects will just be relevant on small spatial scales and in regions with appropriate habitat connectivity. Large-scale shifts in the spatial distribution of the species will occur only on long time scales.

3.5 Conclusion

We introduced the HiLEG model for the PVA of terrestrial animal species that develop through several life stages and whose development is affected by changing climate conditions and anthropogenic disturbances. The model helps identify potentially suitable regions for the species in a prospectively changing and disturbed environment. Our model can be adapted to the life cycles of different target species by setting the appropriate demographic population parameters, spatially explicit climate data and information about the timing of disturbances. In that way, it can be used as a tool for stakeholders and decision makers in conservation biology for finding strategies to conserve endangered species.

We applied our model to the LMG in Northwest Germany. The analysis showed that the LMG can broadly benefit from climate change, although with some regional variability. More importantly, however, the benefits were often not maintained in combination with land use.

[6] cf. grid resolution of global climate models: `portal.enes.org/data/enes-model-data/cmip5/resolution`

In particular, the timing of grassland mowing turned out to be a crucial factor for population survival. Furthermore, its effect on the species strongly depended on the spatially heterogeneous climate conditions. Our consideration of the different population life stages and the daily resolution of the climate variables was critical for detecting unexpected, strong long-term effects on the LMG's population viability. This observation became even more prominent as the effects differed spatially.

To protect the LMG in cultivated grasslands, we suggest applying adaptive management strategies. Such strategies should consider the regional differences that mainly result from the temperature-driven development speed of LMG populations. They should be updated on a regular basis (depending on the climate change severity) to keep track of possibly changing conditions. Regions projected to experience longer and more severe dry seasons should either supply sufficiently large refugia to maintain local populations or build stepping stone habitats that allow LMG dispersal to more suitable regions. Overall, we showed that conservation of the LMG or other species with similar traits is possible even in cultivated grasslands as long as smart, adaptive and far-sighted management strategies are applied.

Author Contributions

Johannes A. Leins: Conceptualization, Methodology, Software, Formal analysis, Investigation, Resources, Data curation, Writing - original draft, Visualization. **Thomas Banitz**: Conceptualization, Methodology, Writing - review & editing. **Volker Grimm**: Writing - review & editing. **Martin Drechsler**: Conceptualization, Methodology, Formal analysis, Writing - review & editing.

Acknowledgements

This work has been carried out within the project *Ecoclimb*[7], funded by the German Federal Ministry of Education and Research (grant no. 01LA1803B). We are further grateful for discussions with the other project team members and thank particularly Björn Schulz from the *Stiftung Naturschutz Schleswig-Holstein* for providing data and literature about the large marsh grasshopper. Furthermore, we thank three anonymous reviewers for their helpful comments and suggestions.

[7] Website of project *Ecoclimb*: `https://www.b-tu.de/en/ecoclimb/`

4 Large scale PVA modelling of insects in cultivated grasslands: the role of dispersal in mitigating the effects of management schedules under climate change

An article with similar content to this chapter is published as: *Leins, J. A., Grimm, V., & Drechsler, M. (2022). Large scale PVA modelling of insects in cultivated grasslands: the role of dispersal in mitigating the effects of management schedules under climate change. Ecology and Evolution, 2022;12:e9063. DOI: 10.1002/ece3.9063*

Abstract

In many species, dispersal is decisive for survival in a changing climate. Simulation models for population dynamics under climate change thus need to account for this factor. Moreover, large numbers of species inhabiting agricultural landscapes are subject to disturbances induced by human land use. We included dispersal in the HiLEG model that we previously developed to study the interaction between climate change and agricultural land use in single populations. Here, the model was parameterized for the large marsh grasshopper (LMG) in cultivated grasslands of North Germany to analyze (1) the species development and dispersal success depending on severity of climate change in sub regions, (2) the additional effect of grassland cover on dispersal success, and (3) the role of dispersal in compensating for detrimental grassland mowing. Our model simulated population dynamics in 60-year periods (2020-2079) on a fine temporal (daily) and high spatial (250×250 m^2) scale in 107 sub regions, altogether encompassing a range of different grassland cover, climate change projections and mowing schedules. We show that climate change alone would allow the LMG to thrive and expand, while grassland cover played a minor role. Some mowing schedules that were harmful to the LMG nevertheless allowed the species to moderately expand its range. Especially under minor climate change, in many sub regions dispersal allowed for mowing early in the year, which is economically beneficial for farmers. More severe climate change could facilitate LMG expansion to uninhabited regions, but would require suitable mowing schedules along the path. These insights can be transferred to other species, given that the LMG is considered a representative of grassland communities. For more specific predictions on the dynamics of other species affected by climate change and land use, the publicly available HiLEG model can be easily adapted to the characteristics of their life cycle.

Keywords: bilinear interpolation, climate change, dispersal success, land use, large marsh grasshopper, spatially explicit model

4.1 Introduction

The 2021 IPCC assessment report (IPCC, 2021) confirms that climate change poses a great threat to global biodiversity. Distribution of species is expected to change (Van der Putten et al., 2010), potentially leading to increased extinction risk as ranges shrink or species must persist in new communities. Species distribution models (SDMs) are therefore widely used to predict future distributions based on climate, habitat, and occurrence data (Srivastava et al., 2019). However, in fragmented and agricultural landscapes, extinction risk is at the same time severely affected by land use practices (Oliver & Morecroft, 2014). Accounting for these effects with SDMs, which are correlative, is particularly difficult for insects that require a representation of their life cycle on a fine temporal scale. Here, the timing of anthropogenic processes such as management schedules relative to the species life stage can be critical for population viability (Leins et al., 2021).

Population Viability Analyses (PVA) using mechanistic models are an important complement to SDMs for estimating the risk of species loss in changing and disturbed environments (Naujokaitis-Lewis et al., 2013). PVA models describe a species' viability as a function of its life cycle, environmental conditions such as forage supply, and anthropogenic influences such as mechanical disruption of habitats (Coulson et al., 2001; Beissinger & McCullough, 2002).

Incorporating a dispersal process into such model analysis is considered another important factor for predicting both population viability (Driscoll et al., 2014) and species distribution (Bateman et al., 2013). According to metapopulation theory (Levins, 1969; Hanski, 1999), dispersal between habitats in a fragmented landscape can prevent extinction. Moreover, it is critical to the interpretation of SDMs whether and how quickly species can actually reach regions that have been projected to be suitable (Bateman et al., 2013).

In this study, we explore the combined effect of climate change and disturbance through land use on a dispersing species by conducting a PVA of the large marsh grasshopper (*Stethophyma grossum*, hereafter referred to as LMG, Figure 4.1) in cultivated grasslands of North Germany. The LMG, a well-studied species inhabiting wet meadows and marshes, is considered an indicator for the quality of grassland communities, similar to other grasshopper species (Sörens, 1996; Báldi & Kisbenedek, 1997; Keßler et al., 2012). It is a slow, yet fairly good disperser due to its flight ability (Sörens, 1996) and believed to extend its range in response to climate change (Trautner & Hermann, 2008; Poniatowski et al., 2020; Leins et al., 2021). Anthropogenic disturbances, in particular the timing of mowing events, affect the species differently depending on the current stage of the LMG's life cycle. The German federal state of Schleswig-Holstein (SH) serves as study region, for which we extracted a highly resolved map of its grasslands (72,969 plots of roughly 6.25 ha each) using the software DSS-Ecopay (Mewes et al., 2012; Sturm et al., 2018). Three climate change projections of increasing severity up to the year 2080 function as environmental conditions, while mechanical grassland mowing applies as anthropogenic disturbance.

We address the following three research questions regarding the LMG:

(1) Are there (regional) differences in dispersal success depending on climate change scenario?

(2) Is the success of dispersal additionally affected by spatial patterns such as grassland cover?

(3) Can dispersal compensate for otherwise detrimental grassland mowing?

Figure 4.1: A male adult of the large marsh grasshopper, *Stethophyma grossum* (photo: Daniel Konn-Vetterlein)

We used the PVA model HiLEG (*Hi*gh resolution *L*arge *E*nvironmental *G*radient) introduced in Leins et al. (2021) and extended it by two features for the analysis of this study: the actual dispersal process within a predefined neighborhood of species habitats; and bilinear interpolation of the available, spatially coarse climate projections to achieve heterogeneous, gradual values of high spatial resolution throughout the study region. Originally, HiLEG is a spatially differentiated stage- and cohort-based simulation model that can be parameterized to represent the life cycle of terrestrial animal species, particularly insects. The new features together with the high-resolution grassland map render HiLEG from a spatially differentiated to a spatially explicit simulation model.

In Leins et al. (2021), we explored the effects of climate change on the LMG at a rather low spatial ($12 \times 12\ km^2$) but high temporal resolution (daily time steps) while the 21 predefined management schedules were timed in one-week intervals between calendar week 20 and 40. We found that although the LMG mostly benefits from climate change, the timing of land use, i.e., the mowing schedule, is the most critical factor for the species' survival. This is particularly relevant, because the intensification of anthropogenic grassland use in Germany is advancing (Bundesamt für Naturschutz, 2017). Moreover we showed that the high temporal resolution was required to detect long-term impact of management schedules and climate change.

The original model, however, represented isolated local effects on the LMG and ignored dispersal between habitats. Due to the relevance of dispersal effects, we extended HiLEG by the features described above to analyze the implications of external drivers on dispersal success of the LMG. Using the realistic grassland map allows us to additionally consider the interaction between grassland distribution and dispersal at the landscape-scale.

The results of the simulations depend on the relative timing of dispersal and mowing events, but local effects of climate change and management may still dominate. Since high-resolution maps of species occurrence are often not available, a more general question is therefore, what the additive value of introducing higher spatial resolution and dispersal to a large-scale PVA model might be.

4.2 Material and Methods

There are four main elements to our analysis: the study region (German federal state SH), the target species (LMG), climate data (projections from 2020 to 2080) and land use (grassland mowing). The following subsections include a description of these elements. Simulations

for the present study are performed using an extension of the HiLEG model introduced in Leins et al. (2021). Section 4.2.5 includes a description of the model along with the relevant changes made to it for this study.

4.2.1 North German Grasslands

Germany' most northern federal state SH serves as study region. The state's grassland areas, i.e., 72,969 cells of roughly 6.25 ha in size each, were extracted using the Software DSS-Ecopay (Mewes et al., 2012; Sturm et al., 2018) and mapped to 107 climate cells (Figure 4.2) of available climate projections (Section 4.2.3). Appendix B.3 describes the mapping of all cells including their further specifications. Compared to the agricultural area of Germany as a whole (50.6 %), SH is the most intensively farmed federal state with 68.5 % (Statistisches Bundesamt, 2021).

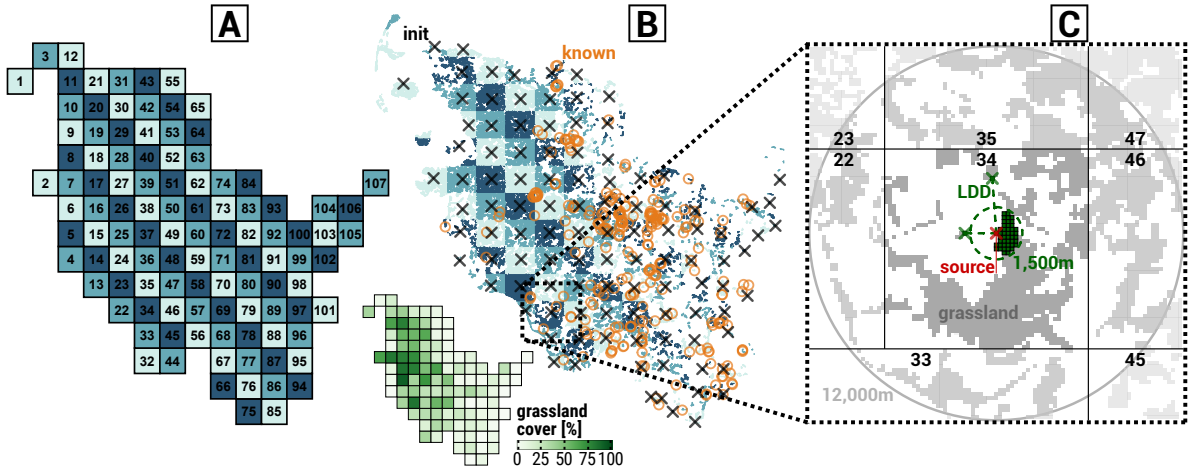

Figure 4.2: Distribution of 107 climate cells (A) and 72,929 grassland cells including *grassland cover* [%] per climate cell (B) in Schleswig-Holstein (SH), and grassland cells within a *dispersal distance* of > 12,000 *m* around the source habitat of a selected initial population (C). The numbers in A assign a unique ID to each climate cell. Turquoise colors in plots A and B are used to highlight mapping of grassland cells to respective climate cells. In plot B, black crosses mark the 107 initial populations that are closest to the respective climate cell's geometric center and orange circles known LMG locations in SH in the years 2000 to 2016. The bottom subplot of B depicts the percental *grassland cover* within 1,500 m of the geometric per climate cell. In plot C, a red cross marks the source habitat of the initial population in climate cell 34. Green colors highlight grassland involved in dispersal: the dashed green circle around the source habitat represents the starting population's dispersal radius of 1,500 *m*; green cells are available grassland within this radius; and the two green crosses connected to the source habitat by dashed lines represent the habitats reached via long distance dispersal (LDD). LDD applies, if there are no cells within the 1,500 *m* range of the source cell in either one of eight cardinal directions (North, Northeast, etc.) to reflect the assumption that nearby grassland, if present, is prioritized for colonization or as stepping stone for farther dispersal. Grey cells depict the remaining grassland that can be reached over time through dispersal from cells other than the source habitat, where the shades of grey from dark to light represent: grassland within the source climate cell 34; grassland outside the source cell but within a 12,000 *m dispersal distance*; and grassland in a *dispersal distance* farther than 12,000 *m*. The four vertical and horizontal black lines delimit the source climate cell from its seven neighbors identified by black numbers. Note: here, there is no neighboring climate cell to the Southwest

4.2.2 The Large Marsh Grasshopper

The well-studied LMG (*Stethophyma grossum*, Linné 1758) is widely distributed in Central European grass- and wetlands (Heydenreich, 1999). Due to the high water requirements of

its eggs, the species is bound to wet habitats such as meadows and marshes, although the grasshopper itself tolerates a wide range of temperatures and humidity (Ingrisch & Köhler, 1998; Koschuh, 2004). It used to be considered threatened in SH state (Winkler, 2000) but was recently given the status of 'least concern' (Winkler & Haacks, 2019). Still, the LMG is regarded an indicator for the quality of grassland biotopes (Sörens, 1996; Keßler et al., 2012), similar to other grasshopper species (Báldi & Kisbenedek, 1997). The annual life cycle of the LMG (Figure 4.3) can be divided into the following five life stages, beginning with the stage after oviposition: (1) prediapause development inside egg, roughly occurring between July and November, below ground; (2) diapause (preventing too early development during mild winter months), November-March, below ground; (3) embryo development before egg hatching, March-June, below ground; (4) larva maturation, May-October, above ground; (5) imago (including oviposition), July-October, above ground; (Oschmann, 1969; Marshall & Haes, 1988; Köhler & Weipert, 1991; Kleukers et al., 1997; Malkus, 1997; Ingrisch & Köhler, 1998; Heydenreich, 1999). Although the majority of an LMG population usually stays within a close range of its hatching location (Malkus, 1997), it has been shown that new populations could establish in habitats several hundred meters from their origin within two years (Marzelli, 1994) while some offspring even reached distances of three or more kilometers (Keller, 2012; Van Strien, 2013). The latter is likely to be facilitated by the LMG's flight ability (Sörens, 1996).

Population development is affected differently by the climate conditions in an LMG habitat. Embryo hatching in spring (Wingerden et al., 1991) and larval development during summer (Uvarov, 1977; Ingrisch & Köhler, 1998) is accelerated by warm temperatures. Eggs / embryos experience stress in the event of a sustained dry soil before and after winter (Ingrisch, 1983). In the face of climate change, increasing temperatures might benefit the species by accelerating its development and expansion (Trautner & Hermann, 2008; Poniatowski et al., 2018a) while extended droughts might prove detrimental for hygrophilous species like the LMG (Löffler et al., 2019).

4.2.3 High-resolution Climate Data

We obtain climate data from high-resolution scenario simulations of the COSMO-CLM[1] regional climate model (CCLM4-8-17) published by Keuler et al. (2016). In our analysis, the lateral boundaries of COSMO-CLM were controlled by simulation results from the global model ICHEC[2]-EC-EARTH and three Representative Concentration Pathways (RCPs) distinguished by action taken towards reducing CO_2 emissions (in parenthesis): RCP2.6 (full force, FF), RCP4.5 (moderate, MOD) and RCP8.5 (business as usual, BAU). Time series of daily climate data (mean or sum) are provided by the regional model, spatially resolved to grid cells of size 12×12 km^2. We used the years 2015-2080 of these time series and resampled them without losing long-term trends by randomly rearranging years within a 20-year time window (see Chapter 2, Section 2.5). This was necessary because the stochastic model processes (Section 4.2.5) would otherwise have been limited by the fact that only a single, deterministic climate projection was available per global model, RCP and grid cell. Three climate parameters were relevant for the LMG population dynamics as implemented in our model: *surface temperature* [°C], *contact water* [$kg\ m^{-2}$] and *relative humidity upper ground* [%].

We applied bilinear interpolation to the climate values of the four adjacent climate cells of each grassland cell to achieve heterogeneous, gradual climate data values of high spatial

[1] Consortium for Small-scale Modeling in Climate Mode
[2] Irish Centre for High-End Computing

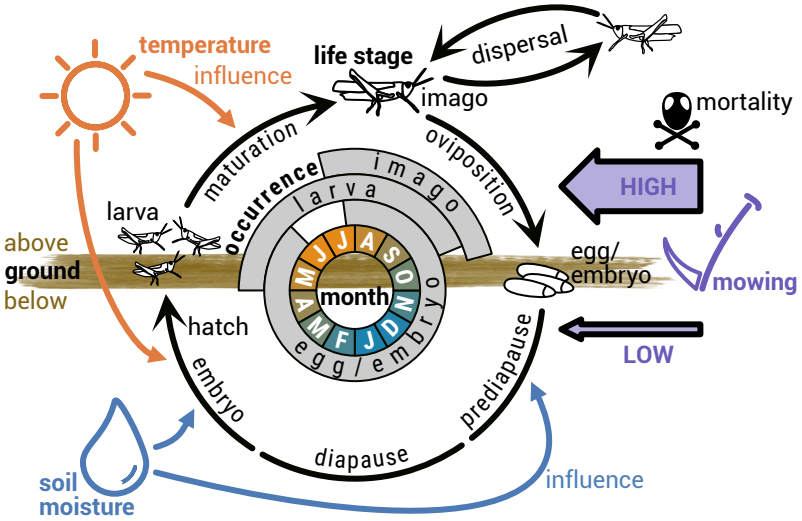

Figure 4.3: Yearly life cycle of the large marsh grasshopper, including the influence of external drivers. Black life stage symbols and arrows represent processes between and during life stages, where the life stage 'egg / embryo' is subdivided into three phases (broken arrow) and the dispersal process is directed to neighboring habitats. The typical ranges of the life stage occurrences are indicated in grey. The inner circle depicts months, where the color indicates seasonal changes in temperature. The influence of the external drivers of temperature, soil moisture and mowing is shown by colored symbols and arrows. Mowing impact is distinguished into high (aboveground) and low (belowground) mortality

resolution throughout the grassland of the study region (Chapter 2, Section 2.7.6, Equations 2.25, 2.26 and 2.27). This was done by weighing the distances from the center of the adjacent climate cells to a grassland cell of interest, multiplying their climate values by the resulting weights and summing up the results (Section 4.2.5). Figure 4.4 illustrates the calculation of the directional weights for a single grassland cell using a simplified geometric example. The calculated values of the weights per grassland cell are referenced in Appendix B.3.

4.2.4 Grassland Mowing

Anthropogenic disturbances to the LMG are represented by mechanical grassland mowing that occurs two to three times per year depending on the mowing schedule (Table 4.1). In terms of our model, the impact of mowing on the model species is exclusively negative, though of different magnitude with respect to the above- and belowground life stages. Indirect effects of mowing, e.g. the observation that an early and / or late cut could maintain a beneficial vegetation structure for the species (Malkus, 1997; Sonneck et al., 2008; Miller & Gardiner, 2018), are not included in the model. However, such low-impact maintenance cuts with only a minor mortality effect on the LMG are accounted for by the base mowing schedule named *M20+00+44* (acronym: *M00*) that stands for an undisturbed environment and always takes effect where no other schedules apply. The first number of the schedule's name stands for early mowing calendar week 20 (day 133) and the last number for late mowing week 44 (day 301). The middle number defines the (additional) mowing weeks 22-38 of more intensive grassland mowing schedules (acronyms: *M22-M38*). If either of the numbers in the schedule name is a double zero, the respective mowing time is omitted, so there are only two mowing events rather than three.

Gerling et al. (2022) gave the main lead for the rationale of these two-cut schedules: they are

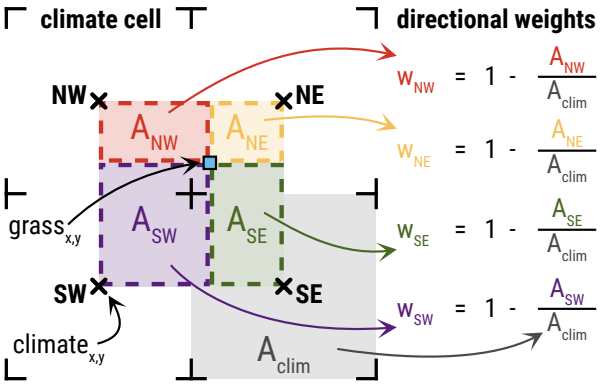

Figure 4.4: Calculation of the weights applied to bilinearly interpolate the climate values of four climate cells (black crosses) to achieve a distinct value for a grassland cell (blue square) that is enclosed by the climate cells. These directional weights are determined using the square area of a climate cell (A_{clim}, grey) and the rectangular directional areas (A_{NW}, red; A_{NE}, yellow; A_{SE}, green; A_{SW}, purple) formed between the grassland cell coordinate and the center of the respective climate cell in secondary cardinal direction (Northwest, NW; Northeast, NE; Southeast, SE; Southwest, SW). Climate cells closer to the grassland cell result in smaller areas while receiving larger directional weights (w_{NW}, w_{NE}, w_{SE}, w_{SW}), which is accounted for by building the inverse of the ratio from directional area to climate cell area

used for (1) the intensive schedules with mowing weeks 22-25 which omit early mowing in week 20, because grassland cuts are usually at least six weeks apart; and (2) the schedules of mowing weeks 35-38 which omit mowing in week 44, because an additional late maintenance cut is neither necessary, because of slowed grassland growth in autumn, nor economically beneficial for farmers.

4.2.5 Extended HiLEG Model

A comprehensive description of the HiLEG model following the delta-ODD (Overview, Design concepts, Details) protocol (Grimm et al., 2006; Grimm et al., 2020) is provided in Chapter 2. Here, we give a 'Summary ODD' (Grimm et al., 2020), which includes a digest of HiLEG's main model description as introduced in Leins et al. (2021) and an overview of the extensions applied to the model for the present study. Unaffected mechanisms and parameters are either briefly described for general understanding or omitted in the main text. ODD keywords are in italics and capital letters hereafter.

We applied the HiLEG model to the LMG's life cycle, with its life stages influenced by climate and land use. Both, the species' development and mortality were affected by climate conditions, while the latter additionally increased during mowing events, especially in the species' aboveground phase (Section 4.2.2). The model extension added a dispersal module rendering HiLEG spatially explicit, thus allowing dispersal between populations within a predefined radius. Essential climate variables were spatially differentiated on a large scale ($12{\times}12\ km^2$) and resolved to a higher scale of 6.25 ha in the model extension through bilinear interpolation (Figure 4.4) to achieve relevant spatial gradients within the grasslands of the North German federal state SH (Figure 4.2B). We ignore other spatial heterogeneity in land use and biotic variables such as vegetation height or habitat size. Hereafter, all descriptions that neither concerned the dispersal process nor bilinear interpolation of the climate data were already included in the original model version.

While the ultimate *PURPOSE* of the HiLEG model is to analyze the regional effects of different climate change scenarios (CCS) and mowing schedules on the population viability of

Table 4.1: Yearly grassland mowing schedules as applied in the simulation runs. First column gives the names of the 18 mowing schedules that encode the calendar weeks of yearly mowing occurrence divided by a plus (+) symbol. An acronym of the schedule name is provided in the second column, encoding the relevant mowing week in its name. The last three columns give the actual yearly mowing days (first day of respective calendar week) per mowing schedule. Schedules that include cells containing a dash (encoded by '00' in the respective name) only have two mowing occurrences per year, all others have three. The first mowing schedule *M20+00+44* represents low-impact mowing, while more intensive mowing schedules follow in the rows below the double line.

Schedule name	Acronym	Mowing days		
M20+00+44	M00	133	-	301
M00+22+44	M22	-	147	301
M00+23+44	M23	-	154	301
M00+24+44	M24	-	161	301
M00+25+44	M25	-	168	301
M20+26+44	M26	133	175	301
M20+27+44	M27	133	182	301
M20+28+44	M28	133	189	301
M20+29+44	M29	133	196	301
M20+30+44	M30	133	203	301
M20+31+44	M31	133	210	301
M20+32+44	M32	133	217	301
M20+33+44	M33	133	224	301
M20+34+44	M34	133	231	301
M20+35+00	M35	133	238	-
M20+36+00	M36	133	245	-
M20+37+00	M37	133	252	-
M20+38+00	M38	133	259	-

species such as the LMG (Leins et al., 2021), we here focus on exploring the potential role of dispersal, which was ignored in the original version of HiLEG. The *PURPOSE* of the extended model is to answer the following questions: (1) Are there (regional) differences in dispersal success depending on climate change scenario? (2) Is the success of dispersal additionally affected by spatial patterns such as grassland cover? (3) Can dispersal compensate for otherwise detrimental grassland mowing?

We have drawn from literature the empirical *PATTERNS* that ensure the model is sufficiently realistic for its purpose, namely the observed characteristics of the species' life cycle with its sensitivity to environmental conditions (Leins et al., 2021) and dispersal metrics (Marzelli, 1994; Griffioen, 1996; Malkus, 1997). The model's design allowed for these empirical patterns to in principle emerge in the model as well ('pattern-oriented modelling', Grimm & Railsback, 2012). In terms of population structure, density, persistence and dispersal, the model output was not compared to other data, since they are scarce. All model predictions are, thus, relative, not absolute. However, 251 known LMG habitats (Figure 4.2B, orange circles) adapted from survey data[3] recorded in the years 2000 to 2016 were used to analyze some implications of regional effects. We used C++ for the implementation of the model's source code. It is available for both, the original model and extensions, via a GitLab repository[4] along with the executable program and the input files used for the simulation runs.

The following *ENTITIES* build the model's core: *Climate Cells* (defining large scale climate conditions in a 12×12 km^2 region), *Grassland Cells* (defining environmental conditions, e.g.

[3]Provided by Landesamt für Landwirtschaft, Umwelt und ländliche Räume via our project partner Stiftung Naturschutz Schleswig-Holstein

[4]HiLEG GitLab repository: `https://git.ufz.de/leins/hileg`

interpolated climate values, on a scale of 250×250 m^2), and per *Grassland Cell* a *Population* comprised of *Life Stages*, which are comprised of age-distinguished *Cohorts*. The most relevant *STATE VARIABLE* for the interpretation of the simulation results is the *density* [in individuals / eggs m^{-2}] of a *Cohort*, *Life Stage* or *Population*. During a year, the LMG develops through five consecutive *Life Stages* (Figure 4.3): (1) prediapause, (2) diapause, (3) embryo, (4) larva, and (5) imago. *Density* is transferred to the next *Life Stage* (life cycle) or neighboring *Populations* (imago dispersal), and lost through *mortality*. The auxiliary *ENTITY Flow* controls the *density* transfer and in this function connects both the stages of the life cycle and habitats within a neighborhood. Environmental conditions such as climate, disturbances and grassland cover influence the amount of transferred / lost *density*. Daily hatching of eggs, maturation from larva to imago as well as *dispersal rate* and *mortality* are stochastically determined by drawing from density dependent binominal distributions. See Chapter 2, Sections 2.2, 2.4 and 2.7 for details on *ENTITIES*, *STATE VARIABLES* and for an overview of all stochastic elements of the model.

The model runs on basis of daily time steps where the *SCALE* corresponds to the sampling of the climate data. By definition, a year has 364 days (52 full calendar weeks) to account for the weekly mowing schedules. A simulation run takes 21,840 time steps (60 years) starting in the beginning of 2020 and terminating by the end of 2079. In the case of premature extinction of all *Populations*, simulations stop earlier. Each *Grassland Cell* in the study region (Section 4.2.1) represents a potential species habitat and is connected to cells within a predefined radius to allow dispersal between habitats.

To be able to better observe dispersal effects and explore the potential role of dispersal for population viability, we chose an artificial *INITIAL* setting for each simulation run in terms of species distribution: a single *Population* was placed at the center of one of the 107 *Climate Cells* (i.e., the *Grassland Cell* closest to the geometric center of the *Climate Cell*, cf. black crosses in Figure 4.2B), while all other *Grassland Cells* initially remained unoccupied. This initial setup was repeated separately for each of the 107 distinct *Climate Cells*. Furthermore, a simulation run was *INITIALIZED* with one out of three CCS (Section 4.2.3) and one of 18 mowing schedules (Table 4.1). The artificial setup with a single starting location per simulation run, thus no initial populations at other locations of the study region, allowed us studying regional dispersal effects independent of potential immigration from other starting locations.

A similar simplification is inherent in the mowing schedules, which were comprised of fixed dates, whereas in reality farmers would to some degree respond to, e.g., an earlier beginning of vegetation growth due to climate change by shifting mowing to earlier dates. However, to account for this would require both a grassland model capable of predicting climate change response and a model of farmer decision making. This would have made our model considerably more complex and uncertain. Instead, we focused on the changing influence of a fixed mowing date on the climate-related shifting life cycle of the grasshopper. While dynamic schedules would likely change the quantitative model results and might shift potential thresholds in output parameters in time, our approach was sufficient for the objective of comparing the qualitative long-term effects on dispersal success between mowing schedules.

The *Population* at a starting location received an *initial density* per *Life Stage* (i.e., 0.725 *eggs* m^{-2} in the diapause stage, zero density for all other *Life Stages*). Independent of the defined mowing schedule, a starting location was only exposed to the low-impact mowing schedule *M20+00+44* by default to serve as rather undisturbed source of dispersal to their close vicinity. *Populations* at non-starting locations were initialized empty and receive

their *density* through potential immigration. All non-starting locations were subject to the initially defined mowing schedule.

For comparability with the original model setup of spatially stationary populations, we additionally ran the simulations with low-impact mowing schedule *M20+00+44* while the dispersal process was disabled. Thereby, the starting population remained confined to its source habitat and was predominantly affected by climate. Comparison with the other mowing schedules was not practical because, as described above, they were not applied to the source habitats in the simulations with dispersal.

Distinct climate data time series were employed as *INPUT DATA* per *Climate Cell* to drive the model dynamics. To have heterogeneous, gradual values at the location of each *Grassland Cell* as well, bilinear interpolation was applied using the climate data of the (up to) four closest adjacent neighbors. This was achieved by weighing the distances from a *Grassland Cell* G_a to the center of the (up to) four *Climate Cells* $\in \{\Omega_{a,NE}, \Omega_{a,SE}, \Omega_{a,SW}, \Omega_{a,NW}\}$ into secondary cardinal directions of G_a. The resulting bilinear weights $w_{bilin}^{a,dir}$ were multiplied with their respective climate values $\omega_{clim}^{a,dir}$ and then summed to achieve the interpolated value ω_{clim}^{a} at G_a.

$$\omega_{clim}^{a} = \sum_{dir \in DIR_{sec}} w_{bilin}^{a,dir} \times \omega_{clim}^{a,dir} \tag{4.1}$$

$$w_{bilin}^{a,dir} = 1 - \frac{(size_{clim} - dist_{a,dir}^{x}) \times (size_{clim} - dist_{a,dir}^{y})}{(size_{clim})^2} \tag{4.2}$$

$$dist_{a,dir}{}^{x}y = |coord_{xy}^{a} - center_{xy}^{a,dir}| \times size_{hab} \tag{4.3}$$

Here, $DIR_{sec} \subset DIR = \{N, NE, E, SE, S, SW, W, NW\}$ are the secondary cardinal directions NE, SE, SW and NW of the cardinal directions North (N), Northeast (NE), East (E), Southeast (SE), South (S), Southwest (SW), West (W) and Northwest (NW) and $\omega_{clim}^{a,dir}$ is the projected value in the *Climate Cell* $\Omega_{a,NE}$ into direction dir of G_a. Size of *Climate Cell* and *Grassland Cell* are given by $size_{clim}$ and $size_{hab}$ (Table 4.2). The value $dist_{a,dir}^{xy}$ for the distances in x- and y-direction was calculated using the geometric center of a *Climate Cell* ($center_{xy}^{a,dir}$).

Six main *PROCESSES* are included in the model: 'Update environmental drivers', 'Flow update', 'Life Stage update', 'Cohort update', 'Bilinear climate interpolation' and 'Dispersal setup'. Their scheduling is described in Algorithm 1 of Chapter 2, Section sec:21processes. The first three of these processes are *SCHEDULED* for every inhabited *Grassland Cell* and during each time step of a simulation run. 'Cohort update' and 'Bilinear climate interpolation' are submodels of 'Life Stage update' and 'Update environmental drivers', respectively, and thus *SCHEDULED* every time step, as well. 'Dispersal setup' is only *SCHEDULED* in the event of an empty *Grassland Cell* becoming inhabited. Additionally, five types of sub *PROCESSES* can be associated with a *Life Stage* that apply depending on parametrization: (1) mortality (all stages), (2) development (prediapause, diapause), (3) transfer (all except imago), (4) reproduction (imago only), and (5) dispersal (imago only). For all sub processes, a daily *base rate* representing benign or observed average environmental conditions is assumed. Environmental drivers can modify ('influence') these *base rates* of the processes using predefined functions called *Influences* (Chapter 2, Section 2.7.1).

Table 4.2: Simulation parameters as used for the model extension and dispersal process of the large marsh grasshopper (LMG). The first column gives the parameter name and the respective symbol applied in equations. Second and third column contain the parameter's value and unit (if any). The fourth column gives a more detailed description of the parameter.

Parameter / State Variable (symbol)	Value	Unit	Description
Dispersal radius (rad_{disp})	1,500	m	Home range of the LMG given by the maximum covered distance of an individual (Griffioen, 1996)
Base dispersal rate ($rate^{ima}_{disp}$)	0.00595	day^{-1}	Daily dispersal rate of the LMG determined by the farthest disperser found in a 'mark and recapture' study (Malkus, 1997)
Dispersal preference ($pref^{near}$)	1.0		Preference of selecting a neighbor during the dispersal process, where higher values result in selection of closer neighbors
Sight $sight_{disp}$	0.5		Ability to find a selected neighbor during a dispersal process
Decay rate (dec_{disp})	0.04		Distance dependent probability to survive the dispersal process
Climate Cell size ($size_{clim}$)	12,000 m		The size (width / height) of a square *Climate Cell*
Habitat size ($size_{hab}$)	250 m		The size (width / height) of a square *Grassland Cell* (habitat)

Abbreviations: clim=climate, dec=decay, disp=dispersal, hab=habitat, ima=imago,pref=preference, rad=radius

While the first four above sub-processes were already part of the original model, bilinear climate interpolation (see above) and the dispersal process are introduced in the present version. Figure 4.2C depicts the relevant grassland cells included for calculating the dispersal from an exemplary source population inside the climate cell with ID 34 to the neighborhood in reach as it was applied for the LMG. Cells belonging to this neighborhood are either within a predefined radius rad_{disp} (Table 4.2) from the source population in question; or the closest (if any) grassland cells in each of the eight cardinal directions DIR (see above) that have no neighbors within the predefined radius. The latter is called long distance dispersal (LDD, see Chapter 2, Sections 2.7.1.7 and 2.7.5) and is included to account for the LMG's flight ability (Sörens, 1996) that is especially relevant in otherwise isolated habitats. Figure 4.5 illustrates how and in which cases grassland cells are selected for the LDD process.

The *dispersal rate* (Eqn. 4.4) between any population P_a and a neighbor P_b within the neighborhood N_a is stochastically determined each time step using the *base dispersal rate* defined for the *Life Stage* of interest (here, $rate^{ima}_{disp}$ for the LMG's imago stage) and a dispersal probability $p^{disp}_{a,b}$ (Eqn. 4.5):

$$rate^{ima}_{disp}(a,b) = rate^{ima}_{disp} \times p^{disp}_{a,b} \tag{4.4}$$

$$p^{disp}_{a,b} = pref_{a,b} \times p^{find}_{a,b} \times p^{surv}_{a,b} \tag{4.5}$$

The dispersal probability itself is calculated using a preference factor ($pref_{a,b}$) to select nearby target populations depending on the distance to all neighbors, a probability ($p^{find}_{a,b}$) to find the selected neighbor during the dispersal process and a probability ($p^{surv}_{a,b}$) to survive the dispersal, where both latter probabilities depend on *grassland cover*. Parameters applied to adjust the three factors / probabilities are given in Table 4.2. Furthermore, the dispersers are subject to *dispersal mortality* which is the difference of the sum of all the dispersal probabilities

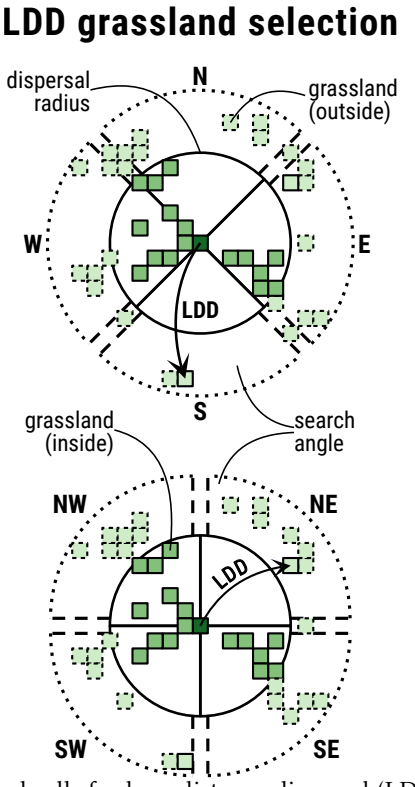

Figure 4.5: Determination of grassland cells for long distance dispersal (LDD) in cardinal (TOP) and secondary cardinal direction (BOTTOM) of a source habitat (dark green). The solid black circle encompasses grassland cells (medium green) within a defined dispersal radius. Light green cells represent grassland outside of the dispersal radius, where dashed cells are unreachable from the source habitat and solid cells are selected for LDD. Each two of the dashed black lines in the outer ring of the plot, which are approximately perpendicular to each other, enclose the angle at which cells for LDD are searched in that direction. Longer distances than indicated here are possible. Cells for LDD are only searched in case no grassland is found within the dispersal radius of either one of the directions to reflect the assumption that nearby grassland, if present, is prioritized for colonization or as stepping stone for farther dispersal. Cells in straight secondary cardinal or cardinal direction (spaces between parallel dashed lines in the outer ring) are ignored for the search in cardinal or straight cardinal direction, respectively.

multiplied by the base dispersal rate:

$$mort_{disp}^{ima} = \left(1 - \sum_{P_n \in N_a} p_{a,n}^{disp}\right) \times rate_{disp}^{ima} \tag{4.6}$$

Table 4.2 gives an overview of the simulation parameters additionally defined model extension. We followed the maximum covered distance of 1,500 m described by Griffioen (1996) for the LMG's dispersal radius and defined the individuals that traveled the largest distance during one day (1 out of 168) in a 'mark and recapture' study by Malkus (1997) as dispersers to determine the daily *base dispersal rate*. The remaining dispersal parameters were approximated using initial test simulations and their usage is explained in more detail in Chapter 2, Section 2.7.5.

The model output was *DESIGNED* in such a way that different aspects of a population development and dispersal success could be *OBSERVED* or rather analyzed with respect to the study's *PURPOSE*. This data is distinguished into direct parameters produced for each inhabited cell during the simulation runs of the model itself, and indirect parameters calculated for a region's whole population in the post-processing of the direct output. Relevant evaluation

parameters of the first category are the daily *life stage densities* given in $individuals\,/\,eggsm^{-2}$ depending on the respective stage. They allow *OBSERVING* the actual dispersal process over time. The indirect evaluation parameters, used to facilitate the *OBSERVATION* of a population's dispersal success, are the following four: (1) the *dispersal distance* in meters from a source habitat to an occupied habitat, (2) the *established distance* in meters from a source habitat to a habitat with *imago density* $\geq 0.002\ individualsm^{-2}$ during a year, (3) the *population size* in total number of individuals / eggs in all established habitats, and (4) the *population density* in individuals / eggs m^{-2} for all established habitats. For the analysis, it was convenient to consider parameters (1) and (2) on the basis of their maximum value, i.e., the habitat farthest from the source, to compare dispersal success. All parameters were determined only using inhabited cells at the end of a simulation year to match values in the same life stage (typically diapause) and after mowing schedules had been fulfilled. In the following, *population size* and *density* are thus given in *eggs*, because populations are usually in the diapause life stage by the end of the year.

4.3 Results

We added a representation of dispersal to the model of Leins et al. (2021). To make sure to achieve a realistic representation, despite sparse quantitative data on dispersal of LMG, we compared *dispersal distances* in the model to the findings of Marzelli (1994). The author found that in a natural and anthropogenically undisturbed grassland environment new LMG populations could establish in a distance of 400 m from an existing population within two years. Considering the defined measure for *established distance* (Section 4.2.5) our model confirmed these findings: within an environment of moderate grassland mowing (Table 4.1, *M20+00+44*) the LMG on average established in distances of about 14,000 m in 60 years (i.e., roughly 467 m every two years).

With this model version, we obtained the following key results: (1) qualitative patterns of dispersal success are similar in the study region independent of CCS, but there are regions that allow more successful dispersal depending on severity of climate change; (2) spatial patterns have an effect on foremost *population size* (high *grassland cover*) and *dispersal distance* (low *grassland cover*); and (3) mowing schedules that might seem problematic when looking at an isolated habitat could still allow (slowed) dispersal outside of a population's home range. These results are described in more detailed in the following.

The dispersal success of the LMG differed depending on region, CCS and mowing schedule. Figure 4.6 depicts different outcomes of the dispersal process exemplary for an initial population in the center of climate cell 34 (black arrow in top left subplot). The first two rows of Figure 4.6 show the distribution of LMG populations chronologically in 15-year-steps in an undisturbed (first row) and disturbed environment (second row) using the MOD scenario: Under ideal conditions with low-impact mowing, the LMG continuously spread out until it occupied grasslands in a distance > 20,500 meters and established in grasslands in a distance > 12,500 meters in the year 2079 (Figure 4.6, first row). The dispersal process became significantly slowed down (10,250 / 8,000 m) when a mowing schedule with a deviating early cut in calendar week 23 (*M00+23+44*) was applied (Figure 4.6, second row).

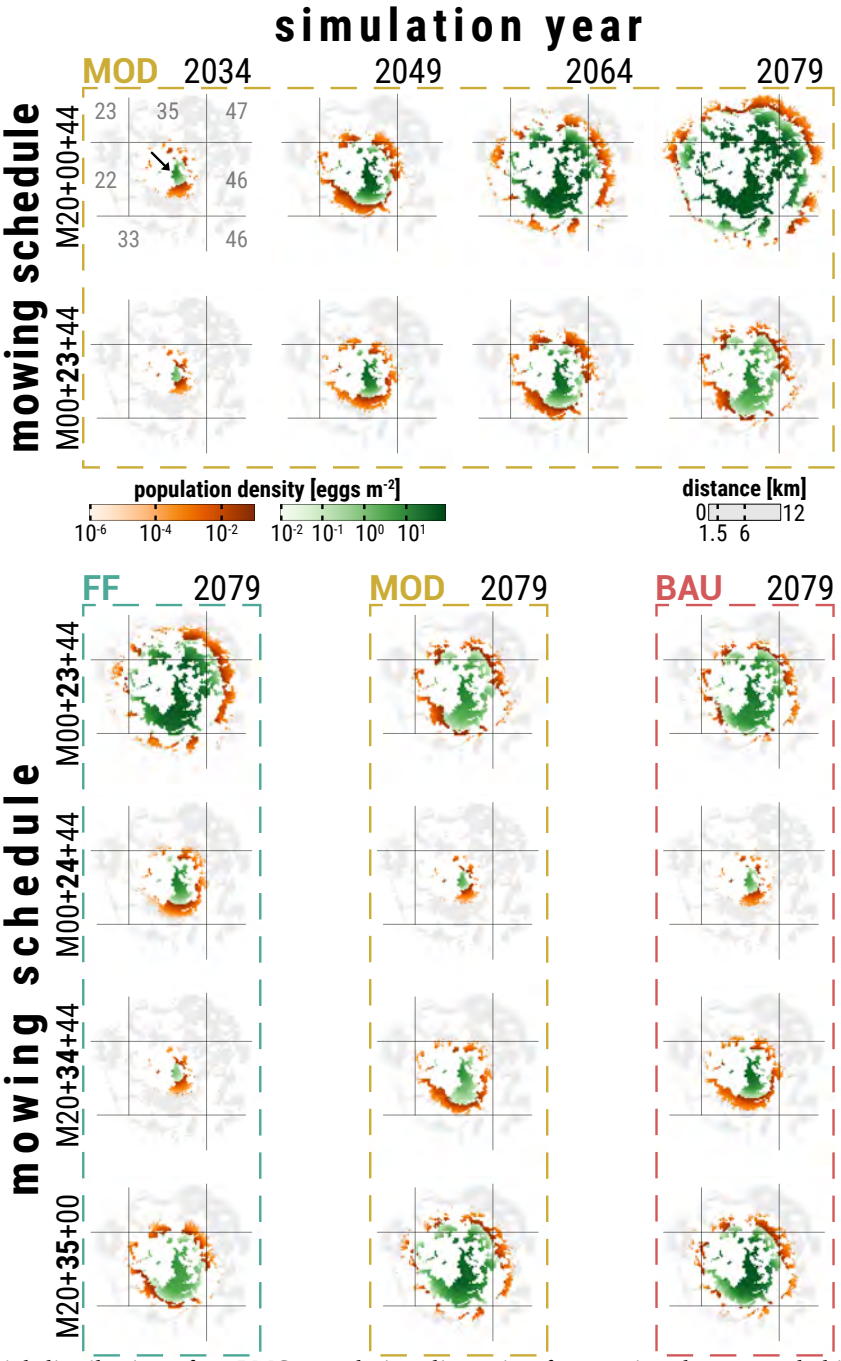

Figure 4.6: Spatial distribution of an LMG population dispersing from a singular source habitat in the center (black arrow in top left subplot) of climate cell 34. Each colored cell within the 20 subplots represents the *population density* in eggs m^{-2} (mean over 10 replicates) in a 6.25 ha grassland habitat inside a 16 km radius of the source habitat at the end of a simulation year. GREEN cells are considered habitats with an established LMG population, i.e., an imago *life stage density* ≥ 0.002 *individuals* m^{-2} during a simulation year; ORANGE cells represent unestablished populations at the cutting edge of the dispersal process, i.e., a imago *life stage density* $< 0.002 individuals m^{-2}$; GREY cells are habitats that are reachable at the end of the 60 year simulation time in case of ideal conditions with minimal disturbances (cf. top right subplot); WHITE areas were either unreachable or do not qualify as grassland. The grey grid lines delineate the climate cells from each other, where the grey numbers in the top left plot label the ID of the respective climate cell. The top two rows show – from left to right – the chronological LMG distribution progress after 15, 30, 45 and 60 simulation years exemplary for the MOD climate change scenario (CCS), where the first row is the progress under ideal conditions (low-impact mowing) and the second row in an environment disturbed by mowing schedule *M00+23+44* (mowing in calendar week 23 instead of 20). Each of the 12 plots in the three bottom columns depict the LMG distribution at the end of the final simulation year 2079 depending on the CCS FF (first column), MOD (second) and BAU (third) as well as the applied mowing schedules *M00+23+44* (first row), *M00+24+44* (second), *M20+34+44* (third) and *M20+35+44* (last)

The three bottom columns of Figure 4.6 compare the final dispersal success in the year 2079 between simulation scenarios. It became evident that the mowing schedule had a different impact on the dispersal success depending on which CCS occurred: Deviating early mowing in, for instance, week 23 (Figure 4.6, third row, *M00+23+44*) still allowed substantial dispersal success for the LMG in the event of the less severe FF scenario (Figure 4.6, first bottom column), while it already became quite inhibited for both other scenarios (Figure 4.6, second / third bottom column), especially MOD. Mowing just one week later (Figure 4.6, *M00+24+44*) already had a great negative impact on the dispersal success in all three CCS, allowing population establishment only in close vicinity of < 5,000 m for the FF scenario while restricting it to grassland roughly within the dispersal radius of 1,500 m from the source habitat for MOD and BAU. The strong negative impact in climate cell 34 continued for several weeks and the dispersal success afterwards became more inhibited for the FF scenario, shown on the example of additional mowing in calendar week 34 (Figure 4.6, *M20+34+44*). Later schedules starting with additional mowing in calendar week 35 (Figure 4.6, *M20+35+00*) allowed for gradual improvement in dispersal success. In these cases, the dispersal process became slightly more successful in the MOD than in the BAU scenario and remained restricted the most for the FF scenario.

Figure 4.7 provides an overview of the dispersal success in terms of *maximum established distance* at the end of a simulation run depending on CCS, mowing schedule and source habitat. In an undisturbed environment (*M00*), established populations on average reached distances of roughly 14,000 m and at most up to 40,000 m. More importantly the figure highlights, in which simulations population establishment basically remained restricted to the dispersal radius of the source habitat (Figure 4.7, dots below black horizontal dashed line). This was the case for virtually all of the regions (or rather source habitats) when mowing schedules *M20+26+44* (*M26*) to *M20+31+44* (*M31*) were applied. Only outside of this time window, i.e., early mowing before calendar week 26 or late mowing after week 31, dispersal could be successful to some extent, depending on region and CCS. As described above on the example of climate cell 34, early mowing schedules were in favor of the FF scenario while late mowing was in favor of MOD and especially BAU.

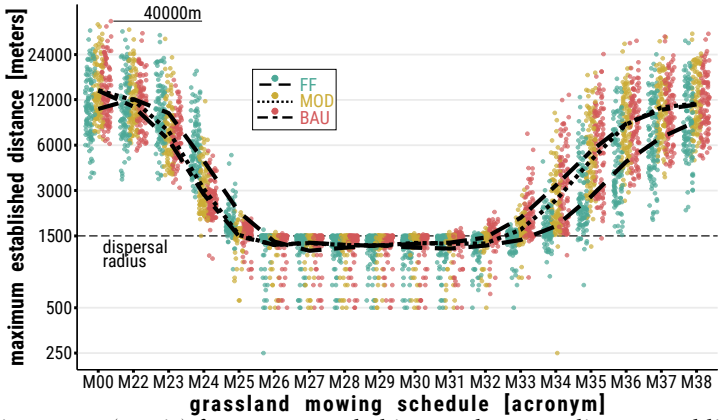

Figure 4.7: Distance in meters (y-axis) from a source habitat to the most distant established population in its neighborhood by the end of a simulation run in 2079 depending on mowing schedule (x-axis) and climate change scenario (CCS; green=FF, brown=MOD, pink=BAU). Each colored dot represents this distance value for either one of the 107 initial populations (or climate cells) averaged over ten replicates. The trend lines are distinguished by CCS and follow the mean for the distance value over the 107 cells in the study region depending on the applied mowing schedule. The horizontal black dashed line marks a distance of 1,500 *m*. Populations established directly through (LDD) from the source habitat were omitted in the calculating to avoid misleading maxima outside the dispersal radius

Figure 4.8A depicts the spatial distribution of results on the example of the *maximum es-*

tablished distance by the end of simulation runs for scenario FF and a low-impact mowing schedule. We compared the spatial results of evaluation parameters *population size*, *population density* and *maximum established distance* for all three CCS and a low-impact mowing schedule to (a) the *population density* of simulations without dispersal and (b) the grassland cover within dispersal radius (1,500 m) of the initial populations. Table 4.3 provides the 18 corresponding correlation coefficients (ρ). Please refer to Appendix B.1 for illustrations of spatial simulation results of the evaluation parameters used in Figure 4.8 and Table 4.3 depending on CCS, and to Appendix B.4 for scatter plots depicting the parameter correlation resulting in the coefficients of Table 4.3.

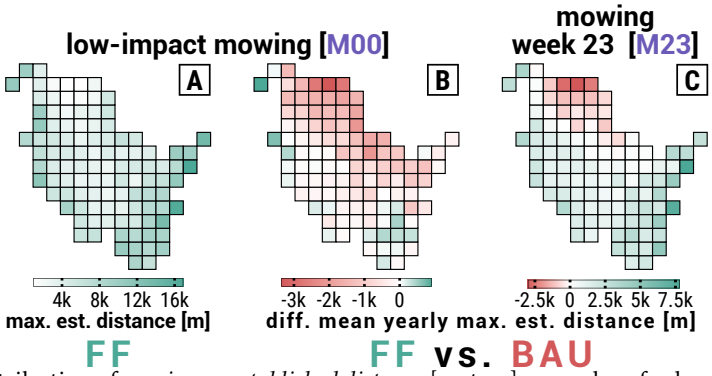

Figure 4.8: Spatial distribution of *maximum established distance* [meters] exemplary for low-impact mowing [*M00*] and climate change scenario (CCS) FF (subplot A), and difference (delta) in dispersal success in terms of mean yearly maximum establishment distance [meters] between CCS FF and BAU exemplary for (B) low-impact mowing [*M00*] and (C) mowing in week 23 [*M23*]. See Table 1 for detailed timing of mowing schedules. Each of the 107 cells per subplot represent INDEPENDENT simulation runs, or rather their mean over 10 replicate runs, and depict the results of the dispersal process from a SINGLE initial population in the center of a cell. In subplots B and C, values were determined per replicate by subtracting the yearly *established distance* of the CCS mentioned second from the CCS mentioned first in the header and then calculating the replicate mean of absolute delta. Further, the cells' background colors highlight which of the respective CCS on average shows the higher differences during the 60 simulation years, where a LIGHTER color represents lower average difference. GREEN cells are in favor of FF and PINK cells in favor of BAU. Please refer to Appendices B.1 and B.2 for distribution maps of all CCS and mowing schedules

We found that the *population density* resulting from simulations without dispersal is positively correlated with all evaluation parameters coming from simulations with dispersal, yet to different extents. There was a high correlation between the two *population densities* and the expected *maximum established distance* could be estimated reasonably well from simulations without dispersal, but *population size* could only be derived moderately. Generally speaking, the correlation was always higher for less severe CCS.

Regarding the effect of spatial patterns on the dispersal success, there were only correlations expectable within the domain of the HiLEG model: independent of the CCS and mowing schedule, *grassland cover* positively correlated with *population size* but did not correlate with *population density*; due to the LDD process, large *maximum established distances* were achieved in regions with low grassland cover, resulting in a moderate negative correlation.

Though the correlation with grassland cover was similar for all CCS, there are regional patterns in SH that only became apparent when looking at the difference (delta) of dispersal success between CCS depending on the considered mowing schedule. Figures 4.8B-C show the difference in *maximum established distance* averaged over the whole simulation run exemplary for the delta between FF and BAU in scenarios of low-impact mowing (Figure 4.8B) and mowing in week 23 (Figure 4.8C). The examples highlight, on the one hand, that there are in fact regions better suited under less severe climate change and others better suited under

more severe climate change. On the other hand, they show that the suitability can spatially shift depending on the mowing schedule.

Table 4.3: Coefficients ρ (last column) from correlation of evaluation parameters A (first column) and B (second column) dependent on climate change scenario (third column). Correlated values stem from summarized results of 107 regionally different and independent simulations (with and without dispersal), each with 10 replicate runs (5 without dispersal), and data of *grassland cover* around the initial population within the respective region.

Correlated evaluation parameters		**Climate change scenario (CCS)**	**Corr. coeff.** ρ $(A \sim B)$
A	B **(with dispersal)**		
population density $[eggs\ m^{-2}]$ (without dispersal)	population size $[\sum\ eggs]$	FF (RCP2.6)	0.4
		MOD (RCP4.5)	0.35
		BAU (RCP8.5)	0.24
	population density $[eggs\ m^{-2}]$	FF (RCP2.6)	0.87
		MOD (RCP4.5)	0.85
		BAU (RCP8.5)	0.74
	max. established distance $[meters]$	FF (RCP2.6)	0.71
		MOD (RCP4.5)	0.68
		BAU (RCP8.5)	0.56
grassland cover [%] within $1,500\ m$	population size $[\sum\ eggs]$	FF (RCP2.6)	0.63
		MOD (RCP4.5)	0.67
		BAU (RCP8.5)	0.68
	population density $[eggs\ m^{-2}]$	FF (RCP2.6)	0.06
		MOD (RCP4.5)	0.11
		BAU (RCP8.5)	0.04
	max. established distance $[meters]$	FF (RCP2.6)	−0.45
		MOD (RCP4.5)	−0.48
		BAU (RCP8.5)	−0.52

There are other regional patterns in SH that occurred repeatedly when comparing the delta of simulation results between climate scenarios (see Appendix B.2 for comprehensive illustration). The state was divided into two parts by a virtual diagonal line running from the Northwest to the Southeast. Regions in the Northeast usually allowed a greater dispersal success for more severe CCS with occasional exceptions in the eastern part. Southwest regions tended to allow more successful dispersal for less severe CCS. Low-impact and late season mowing resulted in the MOD scenario allowing higher dispersal success than the FF scenario throughout all regions. Overall the largest deltas in dispersal success occurred in the upper Northeast, along most of the west coast and in the southeastern regions.

Please note again that the regional deltas depicted in Figures 4.8B-C and Appendix B.2 represent the mean deltas over the full simulation runs and thereby do not capture variations in deltas during the simulations. Therefore, mean deltas can be low although there is in fact a clear difference between the CCS in many years. Since the same CCS does not always lead to larger dispersal success, these differences may, however, cancel each other out. Furthermore, the mean deltas can be different from the final deltas at the end of the simulation runs, but as time series of deltas are affected by many peculiarities, discussing them in detail would not easily lead to general insights. Overall, we found the mean deltas displayed in Figures 4.8B-C and Appendix B.2 to be good indicators for identifying the CCS allowing for better dispersal success, and chose them deliberately to avoid focusing only on the final dispersal success.

4.4 Discussion

The implications of the findings described in Section 4.3 that we obtained by extending the HiLEG model by a dispersal process will be discussed below.

4.4.1 LMG is a Fairly Good but Slow Disperser

We found that in the simulations, the average distance for establishing new populations was roughly 467 m within two years, which is comparable to the dispersal distances of 400 m within two years reported by Marzelli (1994). The difference between model and empirical observation may have several reasons. In our simulations, the conditions were considered ideal other than in the natural environment of the field study. Also, the simulated grassland plots had a fixed size thus dispersal steps were restricted to a minimum distance of 250 m; excluding shorter distances certainly shifted the mean *dispersal distance* to larger values.

Regarding the applied dispersal radius, a 'mark and recapture' study by Malkus (1997) only found specimens in a maximum distance of 624 m. Other studies using genetic markers, however, estimated maximum dispersal distances of 3,000 m (Van Strien, 2013) or calculated a connection distance between two populations of up to 3,264 m (Keller, 2012). The value of 1,500 m we adapted from (Griffioen, 1996) thus appears to be plausibly middle ground, at least in an environment of high *grassland cover*.

In a more fragmented landscape, mobility of the LMG must be considered in a different light. Bönsel & Sonneck (2011) conducted a triannual 'mark and recapture' study for an isolated, yet stable habitat and found that none of the LMG specimens migrated to either one of the four suitable 1,500 to 9,000 m distant study sites, concluding a low dispersal activity in a highly fragmented environment. Marzelli (1994) observed, on the other hand, that the LMG is able to cross unsuitable areas of 300 m, allowing dispersal at least in a slightly fragmented landscape. Regarding the LDD process there is no quantification of its parameters in the literature but evidence that it occurs at least occasionally: individuals of the LMG were found on an island 10 km offshore with the next known onshore population about 16 km away (Oppel, 2005) while flight was observed where individuals ascended more than 20 meters into the air and out of sight (Trautner & Hermann, 2008).

With this knowledge we implemented LDD using the values of regular dispersal, because it already includes parameters that reduce dispersal probability with distance between grassland plots. We restricted LDD to landscapes where the distance between grassland plots is larger than 1,500 m (see Section 4.2.5) to reflect the assumption that nearby grassland, if present, is prioritized for colonization or as stepping stone for farther dispersal. The effects on LMG dispersal by potentially unbridgeable barriers such as highways or forests and climate conditions such as wind direction were ignored in our simulations, as we focused on studying the interplay of climate change relevant parameters and mowing schedules. However, we increased *dispersal mortality* with decreasing *grassland cover* (Section 4.2.5) to account for unsuitable conditions in fragmented landscapes.

The fact that the dispersal success remained within reasonable bounds despite the applied simplifications and estimations provides the confidence to consider our simulation results of applied mowing schedules valid as well. More importantly, the rather short projected *dispersal distances*, especially in a disturbed environment, reinforce the choice for our approach to study the development of individual populations at regional or even local level.

4.4.2 Climate Change Facilitates the Expansion in North SH State

The regional patterns of dispersal success in an undisturbed environment for each CCS separately are qualitatively very similar to each other. Some of the patterns even follow climatic conditions already largely found in simulations without dispersal that will be discussed later. Comparing the deltas between evaluation parameters of the three CCS pairs (FF vs. MOD, FF vs. BAU, MOD vs. BAU), however, revealed regional differences (Figures 4.8B-C, Appendix B.2) with possible implications for climate dependent management strategies.

With some exceptions in the Southwest, the LMG widely benefits from climate change in SH. This again confirms our previous findings (Leins et al., 2021) as well as the results from similar studies (Trautner & Hermann, 2008; Poniatowski et al., 2018a). A moderate climate change (MOD) would be beneficial for the LMG in the whole study region. In case of severe climate change (BAU) only the western coastal regions would be worse off but the conditions running from North to East of the study region would improve the most in this scenario. The latter is relevant for two reasons.

First, the northeastern interior of SH is the region where currently most of the inhabited LMG habitats are located (Figure 4.2B, orange circles). With climate change in mind, conditions would thus improve the most particularly for these existing populations. Second, the northern regions are currently the most difficult terrain for the LMG, where hardly any populations are found. Although it is going to remain the least suitable region climatically (Figure 4.8A, Appendix B.1), it would improve the most in the more severe CCS (Figures 4.8B-C, Appendix B.2) and as a result could facilitate LMG expansion to the North. Poniatowski et al. (2020) already found that many grasshopper species including the LMG expand their range due to global warming. Especially a climate change driven northern range shift is often discussed for – among other species (Van der Putten, 2012) – insects as well (Stange & Ayres, 2010) and was particularly shown for several grasshopper species (Poniatowski et al., 2018a).

4.4.3 Higher Grassland Cover Allows Larger Population Size

The second region currently scarcely populated by the LMG is the west coast of SH and its interior. Only in the southern and central parts along the coast, a few populations are found. This is despite the fact of it having a high grassland cover (Figure 4.2B) and that our simulations showed suitable conditions of potentially high *population density* throughout the region (Appendix B.2) even with mild climate change (FF). Especially on the central west coast with highest grassland cover (Figure 4.2B) that is notably correlated with high *population size* (Table 4.3, ρ between 0.63 and 0.68) there are currently no known LMG populations (Figure 4.2B, missing orange circles).

Even though it is reasonable that the higher availability of grassland allows a larger number of populations – and thus higher overall *population size*, the reason for the sparse presence of the LMG is apparently neither the climatic nor the biotic conditions but likely the fact that the northwestern region of SH has the state's highest percentage of agricultural land, with more than 74 % (Statistisches Amt für Hamburg und Schleswig-Holstein, 2021).

The negative correlation of *grassland cover* with *maximum established distance* (Table 4.3, $\rho = -0.45$ to -0.52), on the other hand, can be ignored within the domain of the model. It is due to the fact that especially in fragmented landscapes the LDD process applies, allowing for above-average *dispersal distances*.

The main problem for all of the currently (mostly) uninhabited regions, especially in the Northwest of the study region, is the relatively large distance to the closest established LMG populations (Figure 4.2B, orange circles). Measures to assist the LMG to migrate to these regions are likely to depend on local constraints and can only be partly derived from the results of the present study. We will nevertheless address potential management strategies later in the discussion.

4.4.4 Mowing Slows Down Dispersal but still Allows it up to a Threshold

The key to all above considerations is the right timing of grassland mowing because it is one of the critical factors for the dispersal success (Figure 4.7) and survival of LMG populations. In our preceding study, it was unclear how to interpret the diminishing effect of mowing on the LMG's lifetime during summer and early autumn (Leins et al., 2021, Figure 9). From the results of the present study we learn that, while population development might become increasingly restricted when mowing up to calendar week 25 and down to calendar week 32 (Figure 4.7), it still allows (slower) dispersal and establishment outside of a source habitat's dispersal radius (Figure 4.6).

It is important to bear in mind that there is a spillover effect within the dispersal radius due to the unrealistically undisturbed source habitats and that the mowing dates should be interpreted in relative, not absolute terms (Section 4.2.5). Yet, the resulting dates provide valuable insight for potential management strategies in agricultural grasslands, because it means that there are ways of supporting LMG establishment and dispersal while allowing economically beneficial land use. Especially the early mowing weeks of late spring and early summer are of relevance here, because they were found to be most cost-effective (Gerling et al., 2022).

Furthermore, with a minor climate change (FF) mowing is even less problematic for a longer period of time before summer in most parts of SH than it would be with the more severe scenarios MOD and BAU (Figure 4.8C, Appendix B.2). Such a longer period of unproblematic mowing with the Clim-FF scenario could be highly relevant when considering the implications of climate change for the species. Yet, this assessment is only valid under the assumption that beginning and duration of vegetation growth does not shift in the same way as the life cycle development of the LMG. In order to examine this hypothesis, dynamic models of grassland growth and management decisions would indeed be useful.

We discussed above that from climate change alone the LMG would benefit in all (MOD) or most (BAU) parts of the study region. However, SH is with an agricultural area of 68.5 % (Statistisches Bundesamt, 2021) the most intensively farmed state in Germany (50.6 %). In such an environment, the LMG would thus be better off in case of minor climate change or none at all. It would still require measures reducing intensive grassland use to allow the LMG to thrive and expand.

4.4.5 Spatially Stationary Simulations as Indicator for Suitable Regions

As pointed out above, simulations without dispersal could already help identifying regions that in principle support LMG development and highlight the general implications of disturbances such as mowing on LMG populations. Depending on the evaluation parameter of simulations with dispersal, we found correlations of different extent with the *population*

density stemming from the spatially stationary simulations (Table 4.3, top rows): Less surprisingly, the *population density* of established habitats within a region highly correlated (ρ = 0.74–0.87), because it is mainly driven by regional climate conditions. Furthermore, there is only little correlation (ρ = 0.24–0.4) with the *population size* as it depends more on *grassland cover* (see above).

Interestingly, however, there is a noticeable positive correlation (ρ = 0.56–0.71) with the *established distance*, especially for the less severe CCS. Therefore, results from simulations of stationary populations could already be a good indicator for the development – and even the general ability to disperse – of species such as the LMG in a regional context. Within the domain of our model, high spatial resolution thus is not the key factor for broadly identifying (climatically) suitable regions. This is a useful insight, especially because simulations without dispersal require less information about a target species and have a much shorter runtime.

The actual development and distribution of a dispersing population could, however, change both qualitatively and quantitatively depending on the spatial patterns and climatic gradients within a region. Particularly in combination with disturbances, the introduction of the dispersal process delivered valuable information: First, mowing schedules that seemed highly problematic in spatially stationary simulations could still allow (reduced) dispersal success. Second, the grassland cover could change the implications of a region's general suitability, because it might either hinder dispersal in fragmented landscapes of otherwise suitable conditions (Bönsel & Sonneck, 2011) or improve population establishment with high cover (Table 4.3, bottom rows) and thus a larger number of refuges.

The relevance of a dispersal process and spatial patterns might increase further if other factors are additionally considered. A mechanistic dispersal process (Vinatier et al., 2011) instead of the present statistical approach could, for instance, result in a more directed preference for neighboring habitats. This effect would especially apply, if (micro) climate was more heterogeneous or less gradually distributed in a study region. Similarly, a more realistic distribution of varying land use (timing) or other detrimental / beneficial environmental conditions could hinder / promote regional dispersal attempts. Furthermore, considering the effects of spatial patterns such as fragmentation on, for example, *dispersal* and *mortality rates* or extinction events might further change species distribution. Ways of including some of these mechanisms into the model to analyze the dispersal success in more detail are addressed at the end of the discussion.

4.4.6 Management Decisions Require Expertise on a Regional Level

Overall our results showed that there is no universal formula for protecting and supporting LMG populations in cultivated grasslands of North Germany, just a tendency in the implications of (future) climate change and a coarse window of unsuitable mowing schedules. Though a broad approach of rather low-impact land use could be applied using our results, it would probably not be feasible on a large spatial scale, because such measures of poor spatial targeting have proven to be less effective (Meyer et al., 2015). At the same time, the uncertainty of climate change makes robust and cost-effective conservation policies necessary (Drechsler et al., 2021). Therefore, management decisions require expertise on a regional or even local level and should remain flexible, especially in grasslands (Joyce et al., 2016), to be able to react to the severity of climate change (Hulme, 2005). As mentioned above, our approach regarding management strategies is too broad to recommend specific local measures

of LMG conservation, but we want to discuss below some suggestions that can nevertheless be derived from our results. We focus mainly on such suggestions, which could also be addressed with the HiLEG model using an adapted simulation setup in a follow-up study.

Heller & Zavaleta (2009) compiled a ranked list of recommendations for management strategies and conservation planning in the face of climate change. The authors recommended the integration of climate change monitoring into conservation planning, particularly in terms of management schedules. We can follow this recommendation because our results show, even for a small state like SH, that regional differences occur due to timing of mowing and severity of climate change (Figures 4.7 and 4.8). Coupling the mowing schedules to local climate conditions in some grassland plots could be one way to simulate such monitoring and help clarify its effect on the species dispersal success, especially if the coupled schedule falls outside the unsuitable time window. Additionally simulating aggregated grassland plots of suitable timing could help analyzing the effect of creating refuges of larger size, which is another recommendation stemming from the ranked list.

Our results and data further suggest that, despite the regional differences already discussed above, there are other factors worth considering for the allocation of conservation planning. Obviously, conservation measures should be focused on regions where the target species is already present, at least if the objective is not its reintroduction. In case of the LMG in SH (Figure 4.2B, orange circles), this does not necessarily match the regions suited best for the species, as discussed in Sections 4.4.2 and 4.4.3 regarding varying climate conditions and grassland cover. The spatial maps of dispersal success we compiled for this study (Figure 4.8, Appendices B.1 and B.2) give a first idea of both, potentially promising regions and others that would require precaution in management.

Along with the occurrence data, the spatial maps also highlight potential dilemmas for conservation planning, namely that the regions whose suitability would likely develop the most are sparsely inhabited, and that the most populated regions also have fragmented grasslands. While developing uninhabited, yet connected grasslands for species such as the LMG might be a long-term management objective, the species' low dispersal speed could prove problematic for conservation planning in fragmented landscapes. Creating undisturbed satellite habitats in terms of metapopulation theory (Levins, 1969; Hanski, 1999) would in theory promote occasional (long distance) dispersal and compensate for local extinction, but the benefits of such metapopulation dynamics in fragmented landscapes for slowly dispersing species are controversial (Bönsel & Sonneck, 2011).

Altogether, simulating and exploring the prospects of different measures in different regions before actually implementing them is advisable. Such simulations could easily be conducted with only minor modifications to the HiLEG model and deliver valuable insights to conservation agencies for the protection of local LMG populations. With the right set of parameters, the model could additionally be adjusted for the life cycle of other species to achieve a broader picture of the implications for disturbed grassland communities in the face of climate change. However, as grasshopper species like the LMG are considered indicators for the quality of grassland biotopes (Sörens, 1996; Báldi & Kisbenedek, 1997; Keßler et al., 2012), the analysis of single species already gives a good idea of the implications for such a community.

4.5 Conclusion

The introduction of dispersal into the highly resolved, yet formerly non-spatially-explicit HiLEG model provided valuable insights regarding the implications of anthropogenic disturbances for the large marsh grasshopper (LMG) under different climate change scenarios. Our study reconfirmed that the LMG in principle benefits from a moderate climate change in temperate regions and was also helpful in unraveling the impact of grassland mowing schedules that were previously unclear. Namely that some of the schedules, despite inhibiting population development, could still allow species dispersal to some extent. It depends on the regional conditions and severity of climate change which mowing schedules this mainly involves.

A milder climate change permits a longer mowing period in the beginning of the season and is more beneficial in the southwestern parts of Schleswig-Holstein (SH). This is an important observation, because early mowing provides the highest yields for farmers. More severe climate change, on the other hand, allows for earlier resumption of mowing after summer, especially outside the western interior of the state. Grassland cover only plays a minor role in the development of the LMG, though a high cover facilitates population establishment within a region.

However, many of the regions that might either improve the most under climate change (North SH) or offer high grassland cover (West SH) are currently scarcely populated by the LMG. Assisting the grasshopper in migrating to those regions will require flexible management decisions on a local level, especially because the key factors hindering the LMG from thriving are anthropogenic (thus controllable) disturbances such as grassland mowing. Improving these practices might benefit other (insect) species as well, because of the LMG's role as indicator for the quality of grasslands. However, this would need to be tested as the life cycles and their most sensitive phases can vary widely between species. HiLEG was designed to be adaptable for other grassland insect species as well (Leins et al., 2021).

In the above discussion, we identified four factors that we recommend to consider for such regional management decisions: (1) the development of climate conditions (when and in which region to apply measures); (2) the grassland cover (size, number and distribution of refuges); (3) the existence of LMG populations (habitats prioritized for protection); and (4) the use of simulation models (identifying suitable measures before implementing them).

The results from both the present and previous study, with and without consideration of dispersal, provided a number of key indicators for potential management strategies in cultivated landscapes. With their input alone, a reasonable protection of grassland (insect) species such as the LMG can be achieved. To further assist stakeholders on a regional level in their decision for viable management strategies, a more realistic or rather heterogeneous integration of disturbances could be of relevance. Such a follow-up study can easily be performed with only minor modifications to the HiLEG model along with the matching set of parameters – eligible for other target species as well.

Author Contributions

Johannes A. Leins: concept, design and implementation of the model; acquisition and processing of input data; analysis and interpretation of the simulation output; drafting and visualization of the article. **Volker Grimm**: data interpretation; drafting and editing of the review. **Martin Drechsler**: model concept; data interpretation; review and editing of the article.

Acknowledgements

This work has been carried out within the project *Ecoclimb*[5], funded by the German Federal Ministry of Education and Research (grant no. 01LA1803B). We especially thank Björn Schulz from the *Stiftung Naturschutz Schleswig-Holstein* for providing further expertise and literature about the dispersal behavior of the large marsh grasshopper. Furthermore, we thank two anonymous reviewers for their helpful comments and suggestions.

Data Accessibility Statement

Open access model code, executables and required input data are available via GitLab[6]. Output data generated by the HiLEG simulation runs for this study[7], the aggregated data used for analysis and illustration with dispersal[8] and without dispersal[9], and a representation of the data used for mapping and weighing climate and grassland cells for bilinear interpolation[10] are available online. The model release version used to run the simulations for this study is also available via GitLab[11] along with detailed descriptions of the input data and simulation parameters.

[5] Website of project *Ecoclimb*: https://www.b-tu.de/en/ecoclimb/
[6] HiLEG GitLab repository: https://git.ufz.de/leins/hileg
[7] Generated output data: https://www.ufz.de/record/dmp/archive/11898/en/
[8] Data used for illustration (with dispersal): https://www.ufz.de/record/dmp/archive/11896/en/
[9] Data used for illustration (without dispersal): https://www.ufz.de/record/dmp/archive/11899/en
[10] Bilinear interpolation mapping data: https://www.ufz.de/record/dmp/archive/11900/en/
[11] HiLEG release version v1.4: https://git.ufz.de/leins/hileg/-/tree/v1.4

5 Finding the right balance of conservation effort in cultivated grasslands: A modelling study on protecting dispersers in a climatically changing and anthropogenically disturbed environment

An article with similar content to this chapter is ready for submission to *Conservation Biology* as: *Leins, J. A. & Drechsler, M. Finding the right balance of conservation effort in cultivated grasslands: A modelling study on protecting dispersers in a climatically changing and anthropogenically disturbed environment*

Abstract

Managing cultivated grasslands in a sustainable way is controversial, because it often goes along with economical loss and additional effort for local farmers. On the plus side, such a management could permit inhabiting species not only to survive but to thrive and expand their range. In order to satisfy both aspects, it can be helpful to minimize conservation effort to a degree that is still ecologically beneficial but intervenes as little as possible with regional land-use customs. Computer simulations are a useful tool to find such compromises prior to implementing management strategies. We simulated the population development of the large marsh grasshopper, a grassland species with limited dispersal abilities, in a disturbed and climatically changing environment of Germany up to the year 2080. Our results show that - in a spatially aggregated landscape - adapting the harvesting schedule in a relatively low number $\leq$ 7 % of (in)directly connected yet otherwise intensively managed grasslands suffices for species preservation and even expansion to some extent. The effect on dispersal success of additional conservation effort above this 7 % threshold is significantly lower than it is below the threshold. In terms of population size, however, every additional refuge benefits the grasshopper. Climate change enhances the positive effects on the target species even further. A higher level of fragmentation, however, requires a substantially larger conservation effort in terms of protected grassland proportion. Therefore, it is recommended and more effective to focus on the implementation of protected areas within spatially aggregated grasslands. Stakeholders should additionally be aware of the fact that it can take several years for a conservation effort to become apparent and measurable, especially if the goal is to support an isolated or reintroduced species in expanding into unpopulated territories.

5.1 Introduction

Unsuitable land use practices can amplify the negative impact of global warming or constrain the adaptive capacities of endemic species (Oliver & Morecroft, 2014). In fact, there are instances of formerly endangered species benefiting from climate change in theory that could still be prevented from thriving by regional land use practices (Leins et al., 2021; Leins et al.,

2022; Poniatowski et al., 2018a). From a perspective of conservation planning, it is imperative to identify measures that support target species or ecological communities on a long run before implementing them, especially in cultivated landscapes.

In such regions, it is impossible to implement comprehensive measures at will to achieve a conservation goal, as land is often in private ownership or other interests are of (higher) relevance. Rather, it is necessary to take focused and metered conservation measures that allow target species to thrive and, ideally, expand their range despite the disturbed environment. With the respective knowledge it can be easier to either find the land owners' acceptance towards conservation measures or intervene with their land use practices as little as possible (Moloney et al., 2018; Will et al., 2021; Nguyen et al., 2022). As thoroughly discussed in our previous studies (Leins et al., 2021; Leins et al., 2022), simulation models together with population viability analysis (PVA) are a valuable tool to aid stakeholders in their effort of identifying such suitable measures. We showed furthermore that suitably managing smaller grassland plots can suffice to support populations locally and that even less suitable, homogeneously distributed management plans can allow moderate dispersal of a species.

However, both natural and cultivated environments are usually more heterogeneous in terms of composition and usage. Projecting required connectivity between suitable habitats to allow successful dispersal in an otherwise disturbed environment is more challenging. There are different concepts on assessing connectivity in randomly distributed environments. In percolation theory (Stauffer & Aharony, 1994), a critical probability threshold is determined above which the general connectivity of an (infinite) environment is assured. On basis of this theory, With (2002) suggested a proportion threshold level ≥ 50 % of connected replicate landscapes (generated using the same probability value) as a more reasonable measure for applied movement ecology to assess likely connectivity in finite landscapes. Another approach extends the binary definition of suitable and unsuitable habitats to include habitats of intermediate suitability (Wiegand et al., 2005; Wiegand et al., 1999). These so-called poor-quality habitats could function as stepping stones between suitable habitats that are otherwise (too) far apart, and in this way achieve connectivity way below the thresholds mentioned before.

All above concepts are considered for the analysis and setup of the present study using another extension of the HiLEG model (Chapter 2). The study explores the effects of applying conservation effort of increasing extent (number of protected habitats) on the population development and dispersal success of the large marsh grasshopper (LMG, *Stethophyma grossum*) in cultivated grasslands of different fragmentation levels. More precisely, the analysis aims at identifying the effort required to support an established LMG population at the edge of uninhabited territory in dispersing into new habitats of North Germany depending on projected climate change scenarios (CCS) of increasing severity. We addressed this issue with the following research questions:

(1) How does the relative effort in conservation-oriented grassland management affect the population development of a species with limited dispersal ability?

(2) Are there time-critical factors that are worth considering for conservation planning in a climatically changing environment?

(3) Does the conservation effort required to meet a conservation target differ depending on the spatial landscape structure?

The formerly endangered (Winkler & Haacks, 2019; Winkler, 2000) LMG is a species well suited for such an analysis. It is native to wet grasslands (Heydenreich, 1999) and is affected differently by external factors such as climatic conditions (Wingerden et al., 1991; Ingrisch,

1983) and land use (Leins et al., 2021) during its annual life cycle. Studies confirm that in theory it is benefiting from global warming (Leins et al., 2021; Poniatowski et al., 2018a; Trautner & Hermann, 2008), but at the same time its range could mostly remain restricted by land use practices (Löffler et al., 2019; Poniatowski et al., 2018a; Leins et al., 2022). It occasionally traverses greater distances, but its basic dispersal ability is rather low rendering it vulnerable to local disturbances. Mowing schedules that could allow reasonable regional development of the species exist (Leins et al., 2021; Marzelli, 1997), yet, the broad implementation of such schedules could prove difficult due to their reduced cost-effectiveness (Gerling et al., 2022).

Particularly regarding the latter difficulty, the present study intends to evaluate a limiting configuration of regional land use schedules. That is, a simulation setup in which single protected refuges are randomly distributed (with varying probability) in an intensively managed environment, i.e., a limited number of refuges in cultivated grasslands of high yield. Local populations must therefore cope in an environment that is suitable in principle, but for the most part highly disturbed. Taking into account two spatial configurations of a landscape, the grasslands surrounding an initially isolated population is either aggregated with a high number of (suitable) habitats, or fragmented with a low number of respective habitats. Both the spatial configuration and the location of the initial populations are obtained from realistic data and surveys of North German grasslands. As another factor affecting the LMG's life cycle, three CCS of increasing severity were applied during simulation runs.

Overall, the simulation results are expected to clarify, if and to what extent configurations of minimal heterogeneity (high number of intensively managed grassland versus varying, yet low number of refuges) already suffice to achieve a regionally sustained or expanding LMG population.

5.2 Material and Methods

The experimental setup (Section 5.2.1) and evaluation parameters (Section 5.2.2) used for the present study are described in the following. Table 5.1 gives and overview of the relevant parameters for initialization and evaluation of the simulation runs. The simulations were run using the most recent version of the HiLEG model[1] and the output data[2,3] as well as calculated evaluation data[4] are available online. For a detailed description of the implementation and parameterization of the HiLEG model, please refer to Chapter 2.

5.2.1 Experimental Setup

We used the stage- and cohort-based, spatially explicit HiLEG model to simulate the development of an LMG population dispersing from one out of two known grassland habitats on the edge of grasslands in the German federal state of Schleswig-Holstein (SH) (Fig. 5.2A-B) that are currently uninhabited by the LMG. Following Griffioen (1996) the LMG's maximum dispersal radius (potentially connecting two habitats) was defined as $rad_{disp} = 1{,}500\ m$ and the occasional long distance dispersal (Oppel, 2005) due to its principle flight ability (Sörens,

[1] GitLab repository of HiLEG release version v1.5: https://git.ufz.de/leins/hileg/-/tree/v1.5
[2] Output data (spatially aggregated region): https://www.ufz.de/record/dmp/archive/12742/en/
[3] Output data (spatially fragmented region): https://www.ufz.de/record/dmp/archive/12741/en/
[4] Evaluation data: https://www.ufz.de/record/dmp/archive/12743/en/

1996) was ignored for the present analysis. Existing grasslands were subdivided into habitat plots with an area of $A_{hab} = 250 \times 250\ m^2$ each. The first known habitat (in the upper center of the state) is located in a landscape of spatially rather aggregated grasslands, while the surroundings of the second known habitat (on the northern border of the state) are highly fragmented, yet still within dispersal range of the target species. For reasons of comparability, only one of these habitats is initially considered populated in a single simulation run. This originating habitat is defined as protected, i.e., biotic and abiotic conditions (despite climate) are considered ideal, and only low-impact grassland mowing at the start and end of the vegetation period (cf. Table 5.1, T_{prot}) is applied to account for management required to maintain a favorable vegetation structure for the LMG (Marzelli, 1997). Apart from that, mowing has a solely lethal impact on the population, but to a significantly different extent depending on the species' life stage (Leins et al., 2021). Surrounding grasslands are either exposed to a conventional mowing schedule with five cuts per year (cf. Table 5.1, T_{conv}), or randomly selected to function as protected habitat similar to the habitats of origin. The probability p_{prot} to be selected as protected habitat is defined at simulation start, where possible values are $p_{prot} \in \{0.01, 0.02, \ldots, 0.2, 1.0\}$. Here, a simulation with $p_{prot} = 1.0$ functions as control or benchmark and represents a scenario where all habitats are defined as protected.

The timing of grassland mowing is coupled to the start of the vegetation period t_{veg}. Following Gerling et al. (2020), this period starts when the yearly temperature sum surpasses 200.0 °C. Adapting their calculation to the surface temperature ω_{ts} used in the present study gives the following equation:

$$
\begin{aligned}
sum_{ts} &= \sum_{i=1}^{I} (x \times \omega_{ts}^{i}) \forall I \in \{1, 2, \ldots, 364\}\ until\ sum_{ts} \geq 200.0°C, \\
x &= \begin{cases} 0.5, & if\ 1 \leq i \leq 31 \\ 0.75, & if\ 32 \leq i \leq 59 \\ 1.0 & if\ i \geq 60 \end{cases}, \\
\omega_{ts}^{i} &= \begin{cases} 0, & if\ \omega_{ts}^{i} < 0 \\ \omega_{ts}^{i}, & \text{otherwise} \end{cases}
\end{aligned}
\tag{5.1}
$$

Here, sum_{ts} is the summed surface temperature, ω_{ts}^{i} is the mean surface temperature (ignoring negative values) on day i of a year, and x is a weight including the temperature values of January and February with only 50 % and 75 % of their extent. The value of t_{veg} equals the day i where t_{sum} reaches 200.0 °C.

Simulations run for 60 years on the basis of a daily time step starting January 2020 and ending December 2079. One out of three CCS is applied at simulation start. Below, these scenarios will be distinguished by action taken towards reducing CO_2 emissions: full force (FF, RCP2.6), moderate (MOD, RCP4.5) and business as usual (BAU, RCP8.5), where RCP stands for *Representative Concentration Pathways of* CO_2. The projected climate parameters of daily resolution have a different effect on the processes of population dynamics depending on the current life stage (e.g. Wingerden et al., 1991; Ingrisch, 1983) and define the start of the vegetation period as described above. They also differ on the spatial scale and at least slightly per habitat.

For each combination of the above simulation parameters, 100 replicates were created, with each of them using a unique random seed. Per replicate, or rather random seed, this leads to a different distribution of protected habitats, time series of climate projections and changes the outcome of stochastic processes on a cohort-level.

Table 5.1: Selection of parameters used to initialize a simulation run (above double line) and to evaluate simulation results (below). First column: parameter name used in text. Second column: mathematical parameter symbol. Third column: valid parameter value(s) and their units (if applicable). Fourth column: brief description of parameter.

Parameter Name	Symbol	Value(s) / Unit	Description
starting date	t_{init}	01 January 2020	The date of initial time steps translated to climate data index
duration	t_Δ	$21,840\ days$	Runtime in days resp. time steps
habitat area	A_{hab}	$250 \times 250\ m^2$	Area of a grassland habitat
initial region	reg_{init}	$\in \{aggr, frag\}$	Definition of originating habitat (region in terms of spatial configuration of grassland surrounding it, where aggr=aggregated and frag=fragmented
climate change scenario	CCS	$\in \{FF, MOD, BAU\}$	Representative Concentration Pathways of CO_2 model
start of vegetation period	t_{veg}	day	Day on which the yearly sum of surface temperature ω_{ts} reaches 200.0°C (see Eqn. 5.1)
mowing schedule	T_{mow}	$\in \{T_{conv}, T_{prot}\}$	Applied set of yearly mowing events at a distinct grassland habitat
conventional mowing schedule	T_{conv}	$= \{42, 84, 126, 168, 210\}$	Yearly timing (days after t_{veg}) of mowing events in conventional managed grasslands
protective mowing schedule	T_{prot}	$= \{49, 217\}$	Yearly timing (days after t_{veg}) of mowing events in protected habitats
protected grassland probability	p_{prot}	$\in \{0.01, 0.02, \ldots, 0.2, 1.0\}$	Probability of grassland to be defined as protected habitat ($T_{mow} = T_{prot}$) at simulation start
dispersal radius	rad_{disp}	$1,500\ m$	Maximum distance covered by an individual (Griffioen, 1996)
inhabited status	$stat_{inh}$	$\in \{occ, est, res\}$	The inhabited status of a grassland habitat, where occ=occupied, est=established, res=residential
potential range	rng_{pot}	m	The distance in meters from habitat of origin to farthest habitat (in)directly connected by rad_{disp}
realized (inhabited) range	rng_{inh}, $inh \in stat_{inh}$	m	The distance in meters from habitat of origin to farthest occupied / established / residential habitat
number of changing habitats	Δn_{inh}, $inh \in stat_{inh}$	$\in \mathbb{N}$	Yearly number of habitats changing their inhabited status to occupied / established / residential
population density	$dens_{occ}$	$ind.\ m^2$	Population density in $individuals\ m^2$ considering all occupied habitats in the region

Abbreviations: aggr=aggregated, BAU=business as usual, CCS=climate change scenario, conv=conventional, dens=density, disp=dispersal, est=established, FF=full force, frag=fragmented, hab=habitat, inh=inhabited, init=initial, m=meters, MOD=moderate, mow=mowing, occ=occupied, pot=potential, prot=protective / protected, rad=radius, reg=region, res=residential, rng=range, scen=scenario, stat=status, t=time step, veg=vegetation

5.2.2 Evaluation Parameters

To determine dispersal success and population development depending on simulation setup, we calculated or extracted several evaluation parameters from the simulation output and grouped them by the initialization parameters (Table 5.1) $reg_{init} \in \{aggr, frag\}$ (initial region containing the habitat of origin), $T_{mow} \in \{T_{conv}, T_{prot}\}$ (conventional / protective mowing schedule), $CCS \in \{FF, MOD, BAU\}$ (climate change scenario) and $p_{prot} \in \{0.01, 0.02, \ldots, 0.2, 1.0\}$ (protected grassland probability). The results were further accumulated by simulation year and spatially distinguished by two states of a grassland habitat: (1) the mowing schedule randomly determined at simulation start ($T_{mow} \in \{T_{conv}, T_{prot}\}$),

where conventional usage (T_{conv}) represents a five-cut mowing schedule and protective usage (T_{prot}) defines a species' *refuge* with two cuts at start and end of the vegetation period (cf. Table 5.1 for definition of mowing days); and (2) the inhabited status during a simulation year ($stat_{inh} \in \{occ, est, res\}$), i.e., whether a habitat was *occ*upied at all, at some point contained a large enough population to be considered *est*ablished when monitored ($imago\ density \geq 0.002\ individuals\ m^{-2}$, including immigrants), or at some point contained a large enough *res*idential population (hatched from eggs laid in preceding year, i.e., $imago\ density \geq 0.002\ individuals\ m^{-2}$, excluding immigrants). Figure 5.1 illustrates the inhabited status of a hypothetical grassland cell using a stylized representation of imago density development within three years. The distinction between the inhabited status is crucial for the interpretation of the results: a habitat may become randomly occupied for a brief period, but never develop a substantial population size; locally measuring a large enough (thus theoretically established) population can be due to a high number of immigrants from nearby (protected) habitats; considering a population residential highlights a locally uninterrupted life cycle, but as a measure it masks the presence of smaller populations.

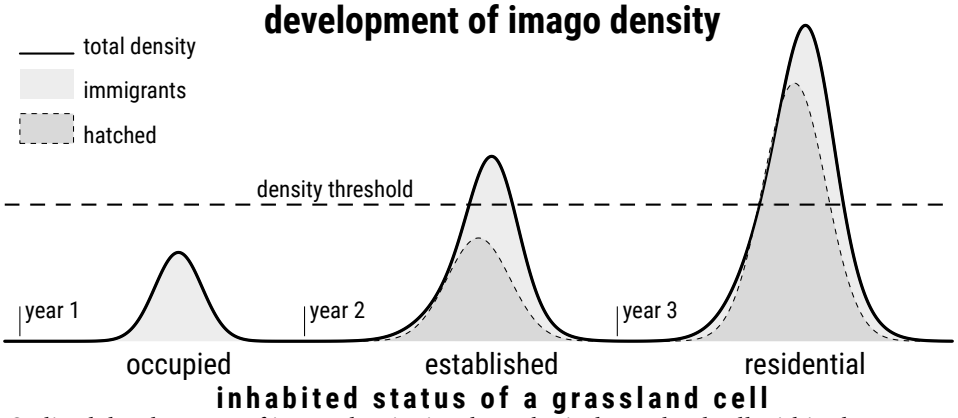

Figure 5.1: Stylized development of imago density in a hypothetical grassland cell within three years to illustrate the local inhabited status. The solid line represents the current total imago density, the light grey areas the density share of immigrants, and the dark grey areas, framed by a dashed line, the density share originating from eggs hatched in the cell itself. The dashed horizontal line marks the density threshold responsible for a change in inhabited status: if a total density > 0 remains below the threshold, the cell is considered *occupied*; if total density exceeds the threshold, the status changes to *established*; if, in addition, the density share of hatched eggs exceeds the threshold, the local population is considered *residential*

The evaluation parameters used in the analysis have two levels. One is the spatial configuration that arises from the random distribution of protected habitats. Here, two protected habitats are defined as directly connected if the distance between them is not greater than the LMG's dispersal radius ($rad_{disp} = 1,500\ m$). If there is a connection through other directly connected protected habitats, the two habitats in question are considered to be indirectly connected. All protected habitats (in)directly connected to the habitat of origin are considered the *protected network*. The straight distance [meters] from the originating habitat to the farthest habitat in the protected network will be called *potential range* ($range_{pot}$). When ignoring the habitats' land use type ($type_{use}$), all grasslands (in)directly connected to the originating habitat are considered the *functional network* and described as *functionally connected*.

The second level of evaluation parameters is the realized distribution and development of an LMG population depending on the categories and spatial configuration described above: (1) the straight distance [meters] from the habitat containing the initial population to the farthest occupied habitat (*realized occupied range*, $range_{occ}$), established habitat (*realized established range*, $range_{est}$) or residential habitat (*realized residential range*, $range_{res}$); (2) the yearly number of habitats changing their inhabited status to occupied (Δn_{occ}), established (Δn_{est}) or

residential (Δn_{res}) for the first time; and (3) the mean population density [$individuals\ m^2$] of all occupied habitats ($dens_{occ}$).

5.3 Results

Benchmark for the analysis are the replicate(s) that yielded the most optimistic results by the end of the simulation in 2079. These were the ones parameterized with ideal (yet unrealistic) conditions of 100 % protected grasslands ($p_{prot} = 1.0$) in the most severe scenario BAU, as the LMG benefits from global warming (Leins et al., 2021). Here, the grasshopper managed to occupy habitats in distances of up to 13,313 m (aggregated region) and 8,139 m (fragmented region). The resulting distribution under ideal conditions is depicted in Figure 5.2B (black dots).

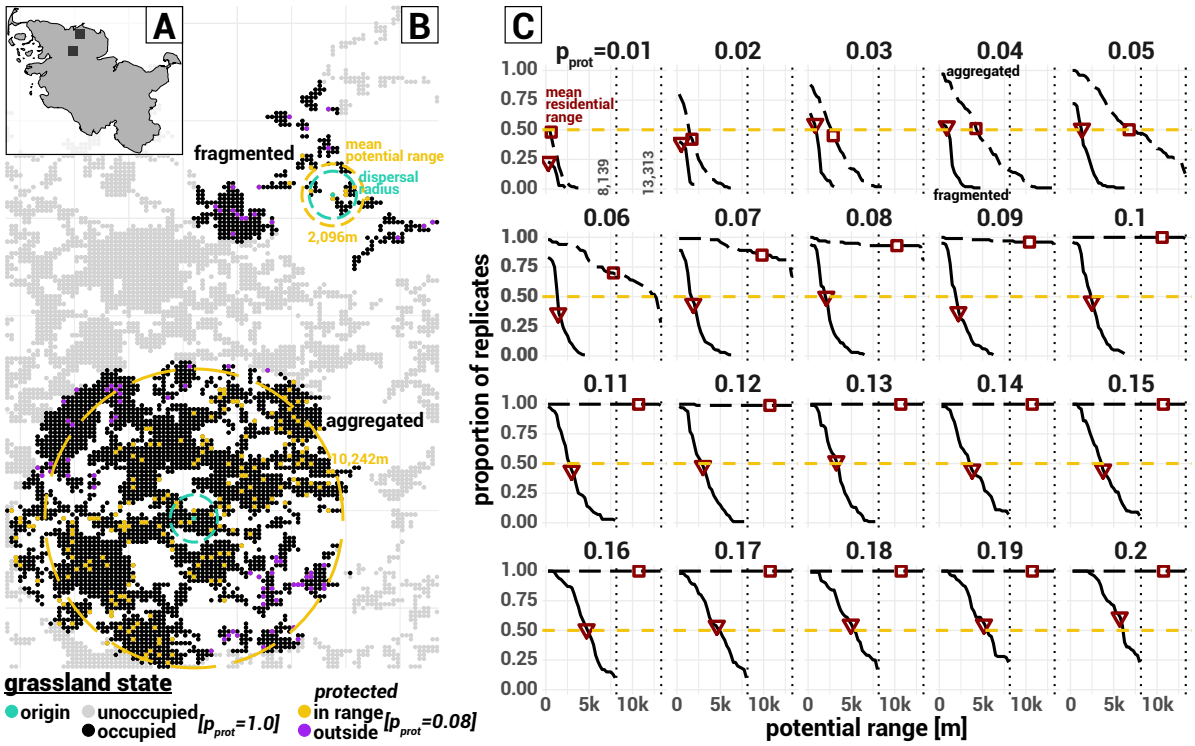

Figure 5.2: Outline map of the federal state Schleswig-Holstein (A), with the black rectangles marking both study regions containing the habitats of origin. Distribution of grasslands (grey dots) in the study region (B) and habitats occupied at simulation end (black dots) under ideal conditions ($p_{prot} = 1.0$, RCP8.5) in at least 1 out of 100 replicates. Eeach dot represents a grassland plot with an area of 62,500 m^2. The green dots mark the habitats of origin in the fragmented and aggregated landscape, and the green circle their dispersal radius. Other colored dots highlight the distribution of protected grasslands for one realization of $p_{prot} = 0.08$, where the orange dots mark refuges belonging to the protected network of either of the originating habitats, and the purple dots the ones outside the network. The orange circles depict the potential ranges of the same p_{prot} value depending on region (fragmented: 2,096 m; aggregated: 10,242 m). Proportion of replicates (y-axis) having a respective minimum potential range (x-axis) from the originating habitat's perspective (C) in the fragmented (solid black lines) or aggregated region (dashed black lines) depending on the protected grassland probability p_{prot} ranging from 0.01 to 0.2 (subplots). The horizontal orange dashed line marks a proportion of 0.5. Red marks highlight the mean realized residential range at simulation end depending on region (triangle: fragmented; square: aggregated)

The potential range (cf. Section 5.2.2) is different depending on initial region. Figure 5.2B (colored dots) shows the distribution of protected habitats exemplary for one realization (or

replicate) of $p_{prot} = 0.08$, where the orange dots represent habitats belonging to the *protected network* (orange dots) in either one of the initial regions. In general, the proportion of replicates having protected habitats within a certain *potential range* greatly differs between regions (Figure 5.2C). While for the aggregated grasslands and $p_{prot} > 0.06$ in more than 50 % of the cases (cf. *threshold level* in With, 2002) the potential range reaches as far as the realized occupied range under ideal conditions (Figure 5.2C, black dashed lines above purple horizontal line), this is only true for a small percentage $\ll$ 50 % of replicates for $p_{prot} > 0.13$ of the fragmented landscape (Figure 5.2C, black solid lines).

Contrary, the proportion (or number) of replicates having certain realized (residential) ranges (Figure 5.3, Table 5.2A-C) does not match the potential range. The LMG's residential range is usually below or occasionally equal to the determined potential range of protected grasslands (Figures 5.3C and F, Table 5.2A). In none of the simulations (protected) grasslands outside the protected network received sufficient immigration to allow an established or residential population (Figures 5.3B-C and E-F, purple line). This is despite the observation that there are a occasions during the simulation runs where grasshoppers occupy grasslands outside the reach of the closest refuge (Figures 5.3A and D, dots above purple line; Table 5.2C), but in numbers too low to survive without repeated additional immigration. Thus, the functional connectivity of grasslands (independent of their inhabited status) did not result in realized (residential) ranges outside the protected network.

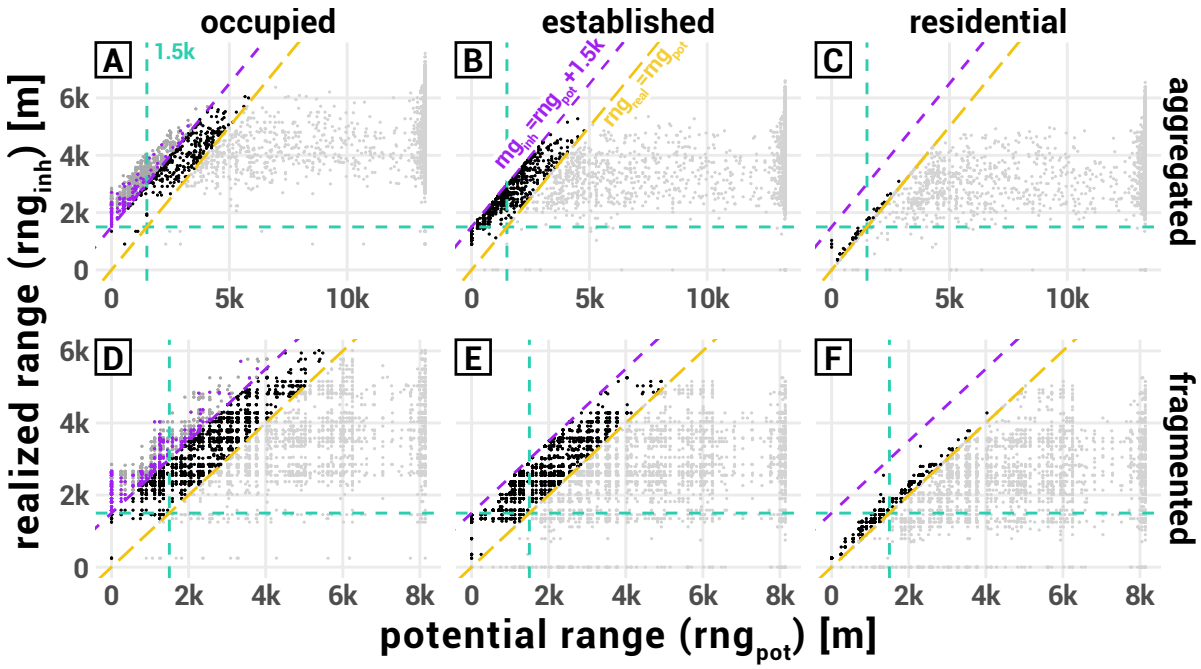

Figure 5.3: Potential range (r_{pot}) in meters (x-axis) versus realized range (r_{rel}) in terms of farthest occupied (A, D), established (B, E) or residential (C, F) habitat during a 60 year simulation run in the aggregated (TOP) or fragmented (BOTTOM) landscape (note different scales in subplots). Each dot represents one replicate run (N=6,000), while the shade of a dot highlights whether r_{real} remained below (light grey) or within 1,500 m (black) of r_{pot}, or exceeded it further (dark grey). The diagonal dashed lines mark the respective thresholds (ORANGE: $r_{real} = r_{pot}$, PURPLE: $r_{real} = r_{pot} + 1{,}500\ m$). Purple dots additionally mark (occupied) refuges outside the latter threshold. Vertical and horizontal dashed green lines mark the 1,500 m dispersal radius around the habitat of origin. The potential range was only calculated up to respective range under ideal conditions ($p_{prot} = 1.0$, RCP8.5), thus the clustering of points at the maximum values of the x-axis.

Table 5.2: Simulation replicate stats grouped by: (second column) constraint regarding inhabited status dependent range rng_{inh} compared to potential range rng_{pot}; (third) inhabited status; and (last six) region and climate change scenario. Upper rows (ID A-C) contain proportion and number of replicates achieving habitats of an inhabited status of certain constraint during simulation run, e.g. with rng_{inh} remaining within rng_{pot} (first three rows). Bottom rows (ID D) contain R-squared values for rng_{inh} dependent on rng_{prot}

	replicate subsetting		**aggregated**			**fragmented**		
ID	**constraint**	**inh. status**	**FF**	**MOD**	**BAU**	**FF**	**MOD**	**BAU**
			proportion (number) of replicates					
A	$rng_{inh} \leq rng_{pot}$	occupied	0.83 (n=1663)	0.83 (n=1651)	0.8 (n=1597)	0.43 (n=864)	0.33 (n=662)	0.24 (n=487)
		established	0.87 (n=1730)	0.85 (n=1706)	0.83 (n=1651)	0.6 (n=1207)	0.45 (n=900)	0.31 (n=619)
		residential	0.99 (n=1990)	0.99 (n=1988)	0.98 (n=1967)	0.97 (n=1933)	0.9 (n=1802)	0.72 (n=1438)
B	$rng_{inh} > rng_{pot} \wedge rng_{inh} \leq rng_{pot} + 1{,}500\ m$	occupied	0.07 (n=131)	0.05 (n=103)	0.05 (n=100)	0.36 (n=718)	0.36 (n=723)	0.28 (n=552)
		established	0.14 (n=270)	0.15 (n=294)	0.17 (n=349)	0.4 (n=793)	0.55 (n=1100)	0.69 (n=1381)
		residential	0.01 (n=10)	0.01 (n=12)	0.02 (n=33)	0.03 (n=67)	0.1 (n=198)	0.28 (n=562)
C	$rng_{inh} > rng_{pot} + 1{,}500\ m$	occupied	0.1 (n=206)	0.12 (n=246)	0.15 (n=303)	0.21 (n=418)	0.31 (n=615)	0.48 (n=961)
		occupied refuge	0.02 (n=35)	0.02 (n=36)	0.03 (n=54)	0.03 (n=52)	0.05 (n=98)	0.11 (n=228)
			R-squared					
D	$rng_{pot} \sim rng_{inh}$	occupied	0.36	0.4	0.7	0.14	0.35	0.65
		established	0.34	0.37	0.68	0.11	0.33	0.64
		residential	0.51	0.55	0.77	0.33	0.53	0.74

However, the share of protected grasslands influences the pace of the dispersal process within the protected network after a settling phase of five to nine years (Figures 5.4A-B), depending on region and protected grassland probability. Differences in the residential range depending on the probability of protected habitats slowly become apparent afterwards and grow more significant with advanced simulation time. In the aggregated landscape, it takes on average 29-42 years to find residential habitats outside the dispersal radius of the originating habitat while LMG residents remain within this radius for $p_{prot} \in \{0.01, 0.02\}$ (fragmented: 39-59 years, $p_{prot} \in \{0.01, \ldots, 0.06\}$).

The initial delay in achieving residential habitats is explained by the (decreasing number of) newly occupied grasslands during the first years (Figures 5.4C-D): Singular source of colonization is the population in the originating habitat (thus the decreasing number of new habitats) up to the point where occupied (protected) habitats have grown a large enough population themselves to breed a substantial number of emigrants (Figures 5.4E-F). Only after that, the maximum residential range is constantly increasing; or diverging for some of the lower p_{prot} values. The number of grasslands changing their inhabited status enters a fading 'occupied-residential' cycle of different extent and slope depending on p_{prot} and grassland configuration around the habitat of origin (Figures 5.4C-F). In the fragmented landscape, the rate of yearly occupation-residence remains low for all values of p_{prot} and never reaches the level of the initial exodus (Figure 5.4D). This proves to be different in the aggregated landscape, where both rates keep increasing for most of the p_{prot} values (Figure 5.4C).

Increasing conservation effort (in terms of p_{prot}) continuously leads to an extended (residential) range by the end of the simulation in the aggregated landscape (Figure 5.5, TOP), but the

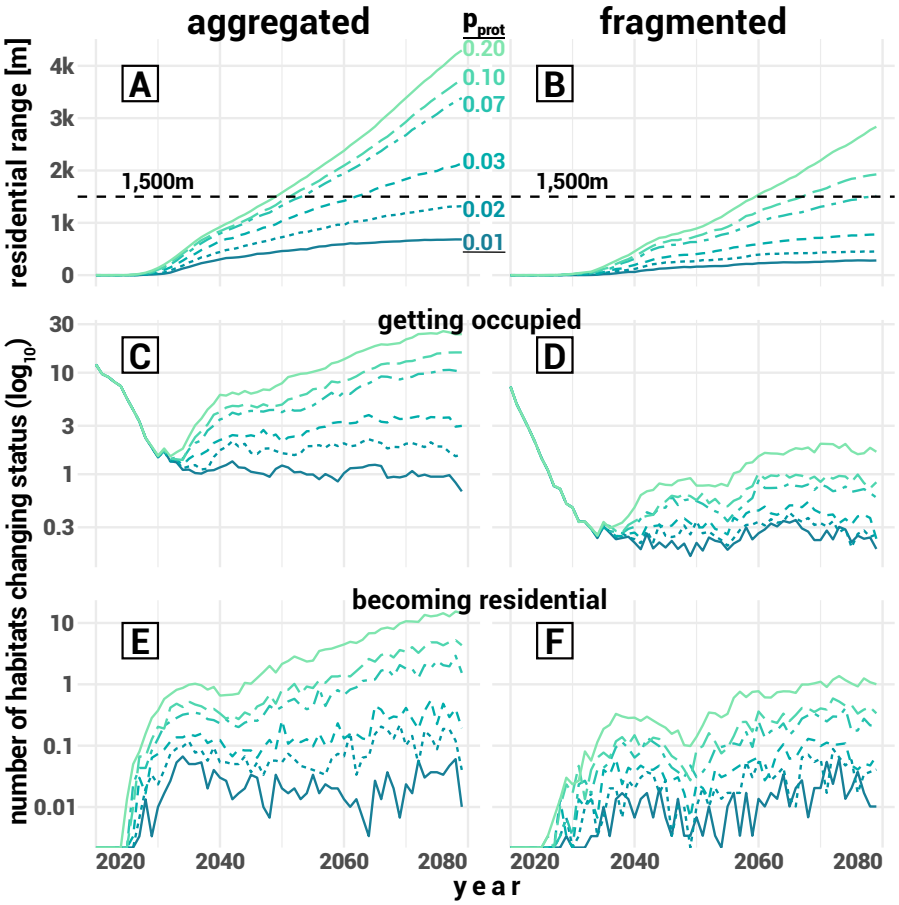

Figure 5.4: Yearly development (x-axis) of evaluation parameters (y-axis, mean over replicates and climate change scenarios, n=300) by initial region (LEFT: aggregated, RIGHT: fragmented) and (for clarity) selected protected grassland probabilities p_{prot} (line types and colors). A, B: residential range in meters. C, D: log_{10}-scaled number of habitats getting occupied for the first time. E, F: log_{10}-scaled number of habitats becoming residential for the first time. The dashed horizontal line in A and B marks the 1,500 m dispersal radius of the originating location.

rate of range expansion declines with each additional effort. While for values of $p_{prot} \leq 0.07$ (threshold depending on CCS), every additional percentage point significantly extends the range, above this threshold constantly more effort is required to achieve substantial range expansion. Independent of the CCS, a 3-4 % share of protected grasslands suffices to allow the LMG to become residential in habitats outside the dispersal radius of the originating habitat.

These patterns are different in the fragmented landscape (Figure 5.5, BOTTOM). Though also here every increase in conservation effort promotes the LMG's dispersal success to some extent, a share of 7-11 % of protected grasslands (depending on CCS) is required to leave the sphere of the originating habitat after 60 years. Even with higher efforts, the realized residential range remains rather low under mild or moderate climate change. Only under severe climate conditions a high conservation effort allows a substantial dispersal success.

Looking at the population density, there is a highly positive correlation with the value of p_{prot} (Figure 5.6). Every additional protected habitat (within potential range of the LMG) aids the species in regionally extending its population. There is only a slightly more significant effect when increasing small p_{prot} values compared to higher values, but a substantial gain in population density remains when increasing higher values as well.

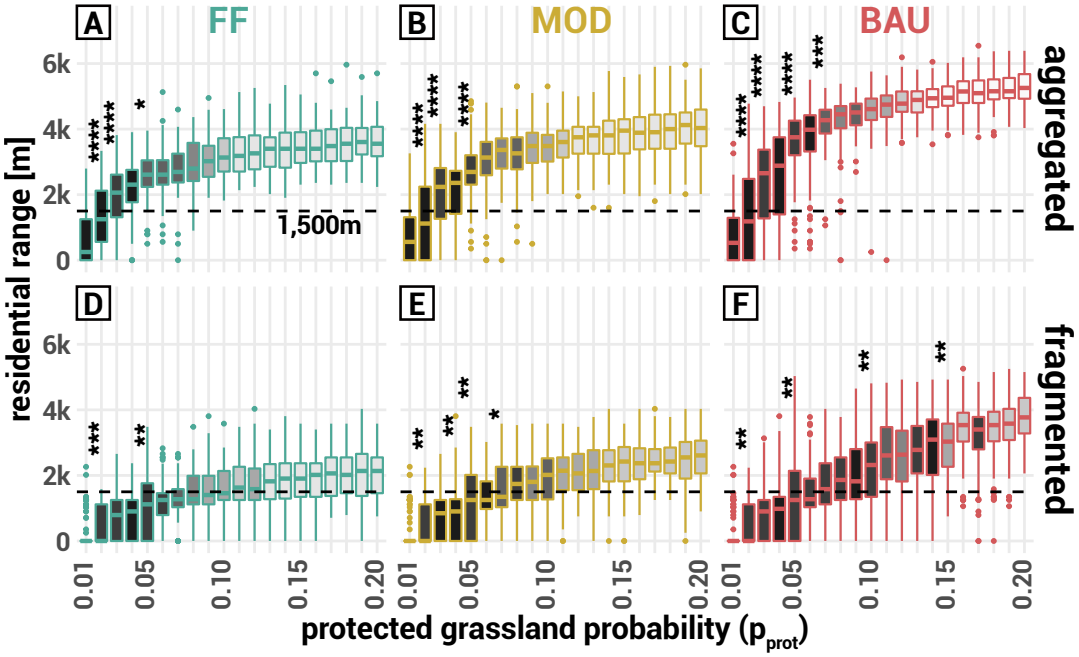

Figure 5.5: Residential range in meters (y-axis) by the end of the simulation run (2079) in the aggregated (TOP) and fragmented (BOTTOM) landscape depending on protected grassland probability p_{prot} (x-axis) and CCS (green: FF, RCP2.6; brown: MOD, RCP4.5; pink=BAU, RCP8.5). Grey-scale fill highlights the additional conservation effort (p_{prot}) required to significantly increase the range, where the darkest grey stands for $p_{prot} + 0.01$ and the lightest for $p_{prot} + 0.08$ and above. Asterisks mark the P-Value of groups that achieve a significant increase in distance with an additional conservation effort of only 1 % values: $**** = P \leq 0.0001$, $*** = 0.0001 < P \leq 0.001$, $** = 0.001 < P \leq 0.01$, $* = 0.01 < P \leq 0.01$

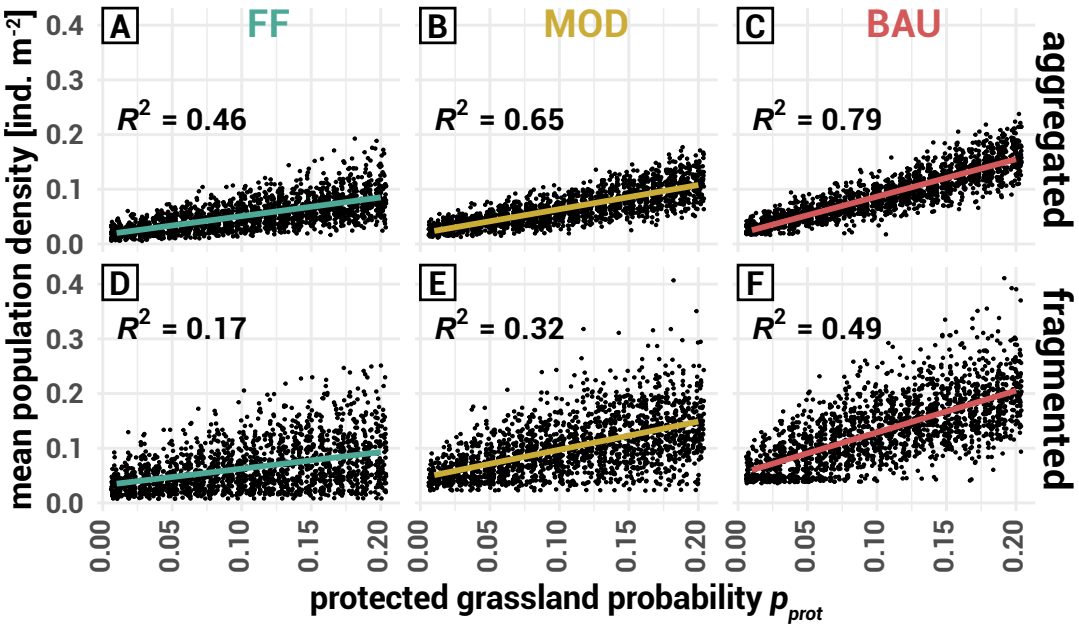

Figure 5.6: Regional mean population density $[ind.\ m^{-2}]$ (y-axis) by p_{prot} (x-axis) at the end of the simulation run in the aggregated (TOP) and fragmented (BOTTOM) landscape distinguished by climate change scenario (COLUMNS, green: FF, RCP2.6, brown: MOD, RCP4.5, pink: BAU, RCP8.5). Colors highlight the linear trend lines and correlation coefficients.

5.4 Discussion

The following sections discuss the implications for species such as the LMG regarding the effect of poor-quality habitats on weak dispersers (Section 5.4.1), the relevance of lags in population development for conservation planning (Section 5.4.2), the increased conservation effort for fragmented landscapes (Section 5.4.3), and the positive long-term influence limited efforts can have on species development (Section 5.4.4). Note again the meaning of the inhabited status, as it is important for the interpretation of the results: (1) an *occupied* habitat had an arbitrary small imago density during a year; (2) in an *established* habitat, the overall imago density surpassed a defined threshold but could exclusively consist of immigration; and (3) for determining a residential habitat, immigration is ignored but the density hatched from eggs laid in the preceding year must surpass the same threshold.

5.4.1 Highly Disturbed Habitats Insufficient for Transit of Weak Dispersers

In metapopulation theory (Hanski & Gilpin, 1997), landscapes are usually binary distinguished into terrain suitable and unsuitable for a species. Accounting for a more natural environment, areas that are accessible by a species yet unfavorable for colonization can be considered an additional category of terrain (Wiegand et al., 1999). These so-called poor-quality habitats could facilitate reaching suitable terrain outside the potential dispersal range of a migrating or roving species (Wiegand et al., 2005). At first glance, this facilitation also applies to the results of the present study.

The potential range of the protected network exceeded the dispersal radius of the target species' originating habitats when protecting only a low percentage of grasslands both in the aggregated and fragmented landscape (Figure 5.2B-C) Especially in the fragmented landscape, the realized occupied range of the LMG often exceeded the potential range (Table 5.2C), occasionally with even the closest neighboring refuges outside the species' dispersal radius (Figure 5.3, purple dots). The latter clearly indicates that the LMG utilized the whole functional network (of unprotected habitats) during its dispersal process, i.e., passed through poor-quality habitats to reach refuges outside the protected network.

Upon closer evaluation, though, the results indicate that utilizing poor-quality habitats in a highly disturbed environment might not work for species with a short (annual) life cycle and limited dispersal abilities such as the LMG. In contrast to the occasionally clearly exceeding *occupied* range, the realized *established* range always remained within dispersal radius of the closest refuge (Figures 5.3B and E, black dots) and the *residential* range rarely exceeded the potential range by a few hundred meters (Figures 5.3C and F, black dots). Especially in the fragmented landscapes, residential populations rather 'pooled' on the edge of the potential range (Figure 5.3F, black dots) suggesting that the environment lacked the means (i.e., habitats suitable enough) for further dispersal.

In most of the cases, the residential range remained well below the potential range during the 60 years (Figure 5.2C, red marks; Figures 5.3C and F, light grey dots below orange line; Table 5.2), although both ranges might eventually align with prolonged simulation time. This alignment is also supported by two factors connected to increasing severity of climate change: (1) more established / residential populations are found outside the potential range (Table 5.2B), especially in the fragmented landscape; and (2) the correlation between potential range and realized ranges (cf. R-squared values in Table 5.2D) becomes more pronounced. Thus,

an environment better suited for the development of the LMG (i.e., its benefit from climate change, cf. Section 5.1) promotes realized ranges closer to the potential range.

The observation that grasslands and refuges outside the protected network were occupied but could not sustain an established or residential population indicates that species such as the LMG require a frequent amount of immigration during the initial colonization of a new habitat. Apparently, the connection between refuges via highly disturbed poor-quality habitats of the present simulation setup is insufficient to substantially provide this influx. This observation is in line with the findings of Poniatowski et al. (2018b) that habitat quality is more important for grassland insects (including grasshoppers) than (functional) connectivity between them. Though it is possible that with with increasing number of replicates a remote residential population might occasionally develop, the high number of simulations where the realized residential range remained well below (aggregated) or 'pooled' on the edge (fragmented) of the potential range rather suggests that the distance between refuges allowing smooth dispersal lies below the theoretical dispersal radius of the LMG.

This presumed link between refuge distance and smoothness of dispersal is supported by the maximal realized ranges depending on the value of p_{prot}: In more than 50 % of the cases, relatively low p_{prot} values build a protected network up to distances unreachable during simulation time (Figure 5.2C), especially in the aggregated landscape. At the same time, dispersal success further increased (significantly) despite of a relevant increase in potential range (Figures 5.4, 5.5, 5.6). Thus, a higher probability of having (additional) refuges within dispersal radius of other refuges, and therefore reduced distances between them, aids the LMG in occupying more distant refuges within the protected network.

Note that the simulation setup depicts a rather extreme scenario in a landscape of overall highly intensive land use with limited numbers of ideally managed refuges (cf. p_{prot}). This setup was chosen on purpose to analyze whether it makes sense to implement a (even low-level) diversification of management schedules. As shown in Chapters 3 and 4, there are management schedules that would support dispersal success and allow reasonable yields at the same time. Applying a heterogeneous (less extreme) setup of management schedules likely could lift the LMG's restriction on the functional network.

5.4.2 Delay in Establishment Must be Accounted for in the Evaluation of the Conservation Effort

The simulation results show that there is an initial delay in observing established or residential populations aside from the habitat of origin (Figure 5.4, TOP). With advanced simulation time, observing newly occupied / residential habitats settles into a colonization-residence cycle (Figure 5.4, MIDDLE / BOTTOM). Hence, the dispersal dynamics of the present model do not follow a continuous diffusion process as postulated in Fick's laws (Fick, 1855). Foremost the initial lag is a familiar concept in invasion biology (Shigesada & Kawasaki, 1997), and two of its main localized causes, inherent population growth and environmental conditions (Crooks & Soulé, 1999), are also included in the present model. In conservation biology, however, the concept of dispersal lag is, as far as known, not discussed. This is despite the fact that already in classical metapopulation theory (Hanski & Gilpin, 1997), time scales of both local and regional dynamics (e.g. population growth and dispersal processes) are applied and often considered to be interrelated (Drechsler & Wissel, 1997), so that the local dynamics drive the regional dynamics. It has further been reported that in a dynamic landscape, both population growth below a certain threshold and local environmental conditions alter

the persistence of a metapopulation compared to the classical theory (Johst et al., 2002a). Both the interrelation as well as the altered persistence could possibly result in a delayed dispersal process similar to the present simulation results.

In the dispersal analysis of a range-expanding species, on the other hand, ignoring the effect of local dynamics could result in a qualitative overestimation of dispersal speed, as indicated by the delayed residential range. Therefore, it may be worthwhile for stakeholders in conservation biology to consider the (initial) lag in dispersal during their planning, albeit to enable a species rather than controlling it as intended in invasion biology. Especially for smaller species that are difficult to monitor, such as the LMG, the effect of (initial) lagging phases could be an important factor when assessing newly implemented conservation measures, because their effectiveness might only emerge after a prolonged period of time. While the present study represents a specific case with a singular source of emigration (similar to a species' reintroduction), the cyclic trend of habitat establishment (Figure 5.4, BOTTOM) shows that such a delay remains even with advanced simulation time.

The development seen in Figure 5.4 suggests that newly occupied grasslands require (1) a persistent influx from already established / residential habitats, (2) time to become residential themselves, and (3) a large enough population to be substantial source of emigration. Though in a highly disturbed landscape, as applied in the present study, such a development only works within a network of potentially connected refuges (Figure 5.4.1), this network does not need to be implemented all at once as indicated by the delayed dispersal process. Depending on the identified species-specific dispersal / establishment rate, conservation planners could initially set up (temporary) refuges within a reasonable radius around known established populations, reevaluate regularly and consecutively add more distant refuges based on the evaluation. Including processes of learning and adapting into conservation planning was suggested before (Grantham et al., 2010) and simulation models such as HiLEG can supply a conceptual basis to support stakeholders in their practical planning.

Achieving the above requirements in a fragmented landscape is much more difficult because of the lower number of available grassland. Even with a high conservation effort there is rarely a single habitat becoming residential per year (Figure 5.4F), while in an aggregated landscape this is already the case with relatively low effort (Figure 5.4E).

5.4.3 Required Conservation Effort Significantly Higher for Fragmented Landscapes and Minor Climate Change

In general, the simulation results indicate that, for a species benefiting from climate change such as the LMG, required conservation effort would be the lowest under severe climate conditions and in an aggregated landscape (Figures 5.4, 5.5, 5.6). While the positive response of the LMG regarding climate change was already shown in previous studies (Leins et al., 2021; Poniatowski et al., 2018a; Trautner & Hermann, 2008), it is reasonable to focus conservation planning on conditions more challenging for the species. First, because the United Nations remains committed to achieving the 1.5 °C goal (Paris Agreement, 2016), i.e., a less beneficial scenario for the LMG. Second, because the effect of measures can only be observed after some years (cf. Chapter 5.4.2), focusing a broader conservation effort on short-term gain could be convenient (Wilson et al., 2006).

However, it is questionable, whether it makes sense to expend any effort on protecting grasslands in a fragmented landscape. Allowing the LMG to achieve self-sustaining populations in distances rather close to the origin might already take decades and require a high number of

protected grasslands (Figures 5.4B), especially under less severe climate conditions (Figures 5.5D-E).

Even when considering the trend that every additionally protected grassland helps increasing the population density (Figure 5.6), it does not necessarily apply to the less severe climate conditions in the fragmented landscape. The correlation between the protected grassland probability p_{prot} and population density is weak under minor climate conditions (Figure 5.6D, $R^2 = 0.17$) and low under medium conditions (Figure 5.6E, $R^2 = 0.32$), so it is not guarantied that implementing additional protected grasslands would have a substantial effect.

In scenarios of the aggregated landscape, the effect of conservation effort on population development is higher. Increasing the probability of protected grassland quickly reflects in success of occupying, establishing or residing in more distant habitats (Figures 5.4A, 5.5A-C) and correlates better with population density (Figures 5.6A-C), especially in the more severe CCS. Focusing conservation planning on LMG populations present in aggregated landscapes might thus prove more sustainable and effective.

5.4.4 Slightly Increasing Low Conservation Effort Can Have Positive Long-term Effect

In cultivated grasslands, it might prove difficult to provide incentives for farmers or other stakeholders in order to implement suitable measures. A recent review by Nguyen et al. (2022) highlights, for instance, that despite the general recognition to preferably apply conservation measures at a landscape-scale, there are few real-world examples of such implementations.

However, as discussed before, every additional effort in protecting grasslands could support the population development of the LMG, especially in the aggregated landscape (Figures 5.5, 5.6, TOP). Here, the simulation results show that protecting a low percentage of 1 – 3 % of grasslands already has a notable effect on the dispersal success or rather allows self-sustaining populations aside from the habitat of origin (Figures 5.5A-C). More importantly, each additional percentage point in the low single digits allows a significant expansion of the realized residential range by the end of the simulation run (cf. black boxes marked with asterisks in Figure 5.5).

While increasing the conservation effort further still has an effect on both realized ranges and - as discussed before - the population density (Figure 5.6), it requires a constantly larger effort to achieve a significant response in range (cf. grey scale of boxes in Figure 5.5). Therefore, it can be sufficient to achieve a small number (1 – 3 %) of protected grasslands (in vicinity of an already protected population) and smartly increasing the number over time (cf. 5.4.2) up to a reasonable threshold (5 – 8 %). Above this threshold, additional effort would not be in vain, but no longer have a strong effect.

Regarding the review mentioned above, the present simulation results offer the prospect that for species such as the LMG, even localized measures could have a positive effect, although coordinated conservation effort at the landscape-scale would be more beneficial on the long run.

5.5 Conclusion

In a highly disturbed or intensively managed environment, protected grasslands might only have a limited positive effect on species with low dispersal ability and a rather short life cycle such as the large marsh grasshopper (LMG). On a regional scale, a population remains restricted to refuges within its (in)direct dispersal range and cannot make use of intensively managed grassland as transit habitats to sustainably establish in refuges outside a network of protected habitats that are (in)directly connected by the species' maximum dispersal radius. Within a reasonable period of time, populations might in fact often only establish in distances well below the potential range of this protected network. Placing refuges closer together as required by a species' dispersal radius can notably aid it in dispersing farther and establish a robust core population. This positive effect is particularly evident when, in terms of dispersal radius, larger distances between refuges are reduced and becomes less striking when refuges were already closer together. Therefore, it can be more beneficial to create some (additional) neighboring refuges in an area with none or few protected grasslands than to do so in an area with already nearby refuges.

When implementing such refuges, it can be of importance to consider the potential delay in local population development of species with similar traits as the LMG. It can take several years to have a visible effect of the conservation effort. First, it may require some time for a species to find a suitable habitat, and second, the species needs to develop a population size large enough to measure during a survey. Such a delay on the spatial edge of a range-expanding dispersal process can lead to a cyclic colonization behavior that can easily be overlooked. Stakeholders should keep the delay in mind when assessing the effectiveness of their conservation measures for species difficult to monitor.

Focusing the conservation efforts on an aggregated landscape is much more promising than on a fragmented environment. The probability of achieving a protected habitat in range of another is higher within an agglomeration of grasslands. Furthermore, despite the fact that the intensively managed grasslands do not aid in dispersing to refuges outside the protected network, they could still function as temporary habitats and thus contribute to the overall population development. This is rarely the case in a fragmented environment.

In general, the results show that even in a rather extreme setup of a intensively managed environment with the occasional refuge, species of limited dispersal ability could establish to some extent and range. Implementing a more heterogeneous setup of land use management (i.e., schedules with different levels of negative impact on a target species' development) should allow a species to expand even outside the range of locations considered protected habitats. Previous studies showed that such intermediate schedules exist. HiLEG can be used to explore such a heterogeneous setup to identify management schedules that promote a target (grassland) species in thriving regionally.

Part III

Synthesis

6 General Discussion

This work had two main objectives, namely to introduce a simulation model for projecting population dynamics and viability in a changing and disturbed environment, foremost for grassland insects, and to demonstrate the model's capabilities using three studies of the large marsh grasshopper (LMG). The spatially explicit model extrapolates high-resolution processes to spatially and temporally large scales, where many existing models that address population viability (Chaudhary & Oli, 2020) either have low process resolution, are small-scale, or even combine both levels of coarseness. Overcoming these limitations in resolution and scale, however, can be decisive to project a species' response to climate and land-use change (Radchuk et al., 2013; Driscoll et al., 2014; Radchuk et al., 2014). Therefore, this thesis addresses the relevance of such an approach through the case studies of a specific species.

In this final chapter, I briefly summarize the key results of the thesis (Section 6.1), discuss their implications (Sections 6.2, 6.3 and 6.4) and value in terms of simulation models (Section 6.5) as well as the limitations of this work (Section 6.6), and wrap up in a conclusion about the findings of this study (Section 6.7).

6.1 Key Results

The key results of this thesis can be classified into model-related and conservation-related findings.

On the model-related side, it was shown that the resolution and detail of simulation parameters and processes can make a difference: (1) the inclusion of multiple high-resolution parameters in a model implementation allows their potentially relevant combined effects to emerge; (2) the effect of short-term responses to changes in environmental conditions can change simulation results substantially on the long-run, e.g. the probability of population survival; and (3) increasing the spatial resolution can affect the quantitative results connected to spatial processes such as dispersal success.

On the conservation-related side, the following findings are relevant for management in general: (1) regional targeting of conservation measures is more effective than spatially uniform approaches; (2) case-specific and controlled increase of conservation effort and adaptable measures are recommended; and (3) getting stakeholders involved is essential and requires detailed system knowledge.

Moreover, there are key findings for the LMG in particular: (1) it benefits from climate change but its adaptation is restrained by unsuitable land use; (2) suitable mowing schedules exist that allow local development and range expansion; and (3) careful consideration of life cycle characteristics can ensure conservation even in a highly disturbed environment.

6.2 Small-scale Ecological Mechanisms Provide Long-term Insights

With the implementation and application of the simulation model HiLEG (*Hi*gh resolution *L*arge *E*nvironmental *G*radient), I showed that it can be worthwhile not only to understand small-scale or high-resolution ecological and biological processes, but also to integrate them into large-scale simulation models. In Chapter 3, I highlighted that incorporating the detailed stages of a species' life cycle, together with the daily resolution of external conditions, can capture relevant long-term effects that likely would have gone unnoticed with a coarser representation of the system's mechanisms. Though other studies also emphasize the relevance of scale for individual factors, such as a detailed life cycle (Radchuk et al., 2013) or high resolution of climate data (Radchuk et al., 2014), the key here was the combined effect of high-resolution conditions and processes. For instance, when temperature-driven population development speed determined whether grassland mowing occurred during a vulnerable stage of the life cycle, the three factors *climate data*, *disturbances timing* and *detailed species characteristics* interacted with each other.

The potentially combined effects became additionally pronounced by increasing spatial resolution and activating species dispersal, as discussed in Chapter 4. Although the evaluation of local conditions already allows general conclusions to be drawn for regional viability and can even be used to estimate, e.g., qualitative dispersal success, projecting a species' quantitative distribution requires finer spatial resolution and detailed knowledge of a species' dispersal mechanisms. Furthermore, disturbances that are problematic when considered individually may have less negative impact if they can be avoided by dispersing between habitats. While in particular the latter idea of avoiding disturbances seems straightforward, its detailed spatial implications can only become apparent if it is explicitly included into model predictions. This is even more so if the implications can change depending on other environmental conditions. For example, Driscoll et al. (2014) emphasized the importance of including a dispersal process for predicting population viability, as did Bateman et al. (2013) for species distribution.

In Chapter 5, I showed that increasing spatial and temporal heterogeneity through the random distribution of differently scheduled disturbances amplifies the combined effects described above. The spatial composition of a disturbed landscape, for instance, can play a vital role in assessing how the proportion of undisturbed sites affects the development of a species. Again, it is the combination of external factors that can have a relevant effect. In this case, it was the interplay between the landscape composition and spatiotemporal occurrence of disturbances leading to the conclusion that it is preferable to allocate sites of suitably timed disturbances in a spatially aggregated environment. Foregoing this kind of heterogeneity in the model implementation or simulation setup would have led to a different conclusion.

Altogether, from a modelling perspective, one should carefully consider which system processes to exclude if the objective is to realistically project long-term effects (Topping et al., 2015). In the three studies presented here, the scale and resolution of several parameters and processes were gradually increased. Among these processes, I want to emphasize the importance of detail regarding a species' life cycle. To my knowledge, this approach is too rarely taken in modelling studies. Given the potential long-term effects of disturbances on a single life stage, especially in combination with high-resolution or large-scale data, using such an approach should be more common.

6.3 Flexibility of Measures and Heterogeneity of Landscapes

The application of the HiLEG model in the three studies discussed here led to several insights regarding conservation planning in general, despite being designed for the LMG in particular.

Foremost, the spatially homogeneous application of conservation measures is not the most feasible approach, as thoroughly discussed in Chapter 4, even though a positive effect may occur on average . Chapter 3 showed that gradual differences or regional thresholds in environmental conditions can substantially alter the effect of a measure. In fact, there is evidence in the literature that poor spatial targeting of conservation measures reduces their effectiveness (Meyer et al., 2015).

Mapping a more heterogeneous environment in terms of land use practices can be a first step towards a more targeted approach to conservation planning. In Chapters 3 and 4 measures were applied homogeneously and in this way helped to identify thresholds in management timing. The approach in Chapter 5 instead implemented more spatially heterogeneous grassland management schedules. Although the heterogeneity of this approach with randomly distributed refuges in a highly disturbed environment was minimal, it could support regional population development at least to some extent. Together with the findings from Chapters 3 and 4 that there are thresholds for long-term viability in terms of mowing weeks, it becomes clear that greater spatial heterogeneity of management schedules (i.e., additionally applying less disruptive schedules) would enhance the positive effect.

The relevance of additionally designing conservation measures more flexibly was discussed in Chapter 4, and there are also studies that recommend such adaptive management strategies in a changing climate (Heller & Zavaleta, 2009). Especially in a changing environment, it is vital that such measures are both robust (Drechsler et al., 2021) and reactive (Hulme, 2005). In Chapters 3 and 5, I showed that such robust and reactive measures can be of relevance for species with shifting and shortening life cycles, and with developmental delays affecting their range expansion. Examples of environmental challenges that require such flexibility in measures include the likely prolonged droughts in yet unknown locations described in Chapter 3, or the unclear adaption of established refuges discussed in Chapter 5, and the uncertainty of future climate conditions in general.

To be successful with the implementation of heterogeneous and flexible measures, clear conservation goals, focused regional targeting and regular reevaluation of the achievements are required, as for instance suggested by Grantham et al. (2010). Species that, e.g., are expanding their range could thereby be supported with relatively little conservation effort, which is also discussed in Chapter 5.

In case that the opportunities for implementing conservation measures are limited, there are different approaches outlined in the present studies. On the one hand, it can make sense to focus on measures with higher success rates and short-term gain (Wilson et al., 2006) as described in Chapter 5 for landscapes with spatially aggregated grasslands. On the other hand, it makes sense to be prepared for more challenging scenarios such as uncertain climate change. In Chapters 4 and 5, I discussed that priority should be given to preserving existing populations rather than enabling their dispersal, especially when the scope of a project is in a fragmented landscape and restoring its spatial structure is not an option. This priority is particularly relevant because the success of rather weak dispersers in such fragmented landscapes is controversial (Bönsel & Sonneck, 2011).

6.4 Land use Hinders Species Adaptation to Global Change

In the specific case study of the LMG in grasslands of Northwest Germany, which has to adapt to global change and cope with a disturbed environment, there are different implications regarding climate conditions, timing and allocation of land use, spatial landscape composition, individual population development and dispersal success. The most striking insight discussed in all three present studies (Chapters 3, 4, 5) is that despite the LMG's prospect of benefiting from climate change, which was also projected by other studies (Trautner & Hermann, 2008; Poniatowski et al., 2018a), it is human land use that could still hinder its adaptation and expansion (Poniatowski et al., 2018a; Löffler et al., 2019).

From a strictly climatic perspective, the LMG could mostly both increase its population size and expand its range under more severe climate change, unlike many other species that need to shift their range to respond to changing climate gradients (Parmesan et al., 1999; Chen et al., 2011; Van der Putten, 2012). There are some exceptions to this trend for the LMG, such as the risk of droughts being detrimental to the species' clutch, which is lower under minor climate change, as shown in Chapter 3, and regional characteristics that are not in favor of the most severe *business as usual* scenario, as discussed in Chapter 4. Overall, moderate climate change offers the most robust prospects for LMG development and expansion, and even the desirable minor climate change (cf. 1.5 °C goal of Paris Agreement, 2016) will not prevent the LMG from thriving in theory.

In practice, however, the timing of land use in cultivated grasslands could counteract the positive climate effects, especially if, e.g., mowing occurs during the vulnerable larva and imago life stages, which is quite common in conventional land use (Johst et al., 2002b). While early mowing before the beginning of these stages or late mowing after their occurrence is favorable and in fact beneficial for the LMG (Malkus, 1997; Sonneck et al., 2008), with the early cut even providing high yields for farmers, it is questionable whether additional cuts during the vulnerable stages can be sufficiently prevented with existing incentives for stakeholders (Kleijn et al., 2011). Alternatives include adapted land use techniques (Malkus, 1997; Kiel, 1999; Humbert et al., 2009) and carefully timed schedules with multiple mowing dates, which were presented in Chapter 4. However, due to regional differences and a changing climate, such timing would require good knowledge of local species and / or careful monitoring of these species, as mentioned in the previous Section 6.3 regarding adaptive measures. The dispersal ability of the LMG, despite its limitations, could prove beneficial in identifying suitable timing, because some mowing dates found to be problematic for isolated populations in Chapter 3 allowed for regional development to some extent when incorporated into schedules of the dispersal analysis in Chapter 4.

Another approach studied in Chapter 5 to support population development and expansion of the LMG was to randomly place refuges with favorable mowing in a highly disturbed grassland environment with conventional mowing, rather than overall adapting the mowing schedules and thereby focus on timing alone. As discussed in the previous Section 6.3, already an approach of minimal heterogeneity demonstrated the positive effect increasing diversity of land use practices could have on species such as the LMG. The LMG could expand its range to habitats that were (in)directly connected by its dispersal radius, but could not make substantial use of poor-quality sites (conventional mowing) to reach unconnected refuges. Obviously, frequent immigration from nearby established populations is required. However, according to the findings in Chapters 3 and 4, additionally adapting the schedules in at least some of the conventional sites could tilt the effect towards farther range expansion. A similar effect was shown of Chapter 5, where placing sites of favorable mowing closer

together than suggested by the dispersal radius of the LMG allowed for higher dispersal success. This confirms the findings that a sufficiently large number of high-quality habitats is more relevant than theoretical connectivity (Poniatowski et al., 2018b).

The observation of 'quality before connectivity' further explains the reduced dispersal success in a fragmented landscape, even when occasional long-distance dispersal is taken into account. Chapter 5 showed that high conservation effort is required to assist the LMG range expansion in such a landscape, while the effort is relatively low in an environment with spatially aggregated grasslands. The intensity of climate change essentially affected the prospect of dispersal success only quantitatively. Spatial composition played a negligible role in the development of individual populations, while each suitably managed site contributed to stabilizing the overall LMG population within a region.

Finally, for practical conservation planning regarding the LMG, but also for other (similar) species in general, it is advisable to have good knowledge of the life cycle specifics and its environmental requirements. Regarding the LMG in particular, Chapter 3 showed the long-term relevance of temperature and soil moisture for development speed and dehydration of the clutch, Chapters 3 and 4 highlighted the effect of land use on the survival and expansion of the aboveground population, and Chapter 5 indicated the implications that an intrinsic development delay can have on the evaluation of applied measures.

The latter delay, or lag in particular, is a well-known concept in invasion biology (Shigesada & Kawasaki, 1997), which to the best of my knowledge has not yet been widely used in conservation biology. Yet, for the assistance of slowly developing species with limited dispersal ability, it is helpful to be aware of such processes so that conservation measures can be successful, even more so in an otherwise highly disturbed environment. For example, an initially isolated population of the LMG in a mostly cultivated landscape may take a few decades to expand its range in terms of establishing robust sub-populations outside the dispersal radius. Newly inhabited sites may need several years to develop a population large enough to contribute substantially to dispersal. That is, if environmental conditions on site are favorable and / or suitable measures have been implemented at a number of sites in vicinity of the initial population. Ignoring potential lags or relying on individual surveys, e.g. the LMG's success in occupying a new site observed by Marzelli (1994), could lead to overestimating the dispersal ability of a species and thus, in the worst case, incorrectly assessing a measure as unsuccessful. Careful monitoring of newly established refuges in proximity of an existing population could help avoid such misconceptions, as discussed in Chapter 5, and is in line with the recommendation of Grantham et al. (2010) to incorporate learning and adaptation processes into conservation planning.

6.5 Models as Tools for Acceptance of Conservation Planning

HiLEG is a simulation model designed for exploring the long-term effects for species that are differently affected by external conditions during different stages of their life cycle. While the model only represents a specific species in this work, its overall rationale can be used more generally. Due to its extensive parameterizability described in Chapter 2, a user can adjust the level of detail and resolution depending on the approach of a study. In this way, HiLEG can help determine the population viability and distribution of a target species in a disturbed and changing environment, and is used to explore how adaptation of anthropogenic disturbances could improve both the viability and dispersal success of a species.

Such information on the potential of adaptive land use may be promising in theory, but can only be effective in the practice of cultivated landscapes if stakeholders are involved and convinced of the benefits, which is often not the case. Nguyen et al. (2022) recently pointed out that despite the general recognition of their merits, there are few real-world examples of landscape-scale conservation measures. In this context, I emphasized in Chapter 5 that simulation models such as HiLEG can help raising acceptance by identifying in advance ecologically suitable measures of reasonable agricultural scheduling or minimal interference.

In case of the LMG in particular, HiLEG and its applications presented in this thesis have proven to be helpful in identifying such conservation-related details. The model in its current version could be used to explore the more heterogeneous scheduling mentioned above. With a modification of the parameterization it could further be utilized in exploring additional species to get a broader picture of the prospects of grassland communities in the study region.

6.6 Limitations

The HiLEG model allows a detailed simulation of a species' population dynamics and environmental processes. However, it is also subject to a number of limitations that may have reduced the accuracy of some results, although they were not decisive for the general conclusion of this work.

A key constraint that concerns HiLEG as well as other PVA studies is its implementation as a single-species model. Some community effects could be represented using the model's function of *Influences* (Section 2.7.1), but there is no option in the parameterization to directly incorporate the population dynamics of additional species. While the focus of the study was indeed to show the effects of a changing and repeatedly disturbed environment on the development of a particular species, considering the interactions of species within an ecosystem could alter the viability prospects (Redford et al., 2011). Similar limitations relate to the absence of dynamic habitat conditions such as vegetation structure, forage availability or microclimate, and consideration of farmers' behavior or decisions. These limitations could be overcome, e.g., by including modules for vegetation or forage growth, adding a high-resolution topographical layer that transforms coarse climate data to a finer scale, or interfacing with an external model of stakeholder decision, such as an agent based model. Yet, including these dynamics would render the model considerably more complex without necessarily allowing for more detailed insights.

At the spatial level, the rather simplified representation of the dispersal process and the lack of site characteristics are the main limitations. For studying a species such as the LMG, it was sufficient in principle to stochastically determine dispersal based only on distance and grassland availability, and to distinguish the landscape only by grassland and unsuitable sites. In their review, Bowler & Benton (2005) compiled a fairly extensive list of factors that potentially influence more informed dispersal of other species. Some of these factors could, with the proper configuration (e.g. density dependence), also be applied in the current version of HiLEG. Others would require an extension of the model implementation (e.g. habitat variability) or are impractical with the population-based approach used here (e.g. individual dispersal propensity).

A drawback in the analysis of the simulations was the limited possibility to validate the results, since empirical data was either not available or not sampled frequently enough. Therefore, only the comparison with results from laboratory experiments or single spatially limited

field studies (cf. Table 2.5) and the previously mentioned infrequent data surveys (cf. Section 2.1) was feasible.

With regard to climate input data, the HiLEG model is currently restricted to NetCDF[1] data files in the same format as the files provided in the model repository[2]. Although the available climate projections are very comprehensive and could thus also be used in studies of other species, they remain spatially limited to Northwest Germany and the open source model code would need to be revised for the use of other climate data.

6.7 Conclusions

It is a major effort to develop comprehensive ecological models, which include a detailed representation of a species' life stages, their distinct sensitivity to environmental conditions and disturbances, as well as high-resolution submodels at large spatial and temporal scales. I could show with the implementation of the HiLEG model, and the case studies conducted with it, that this effort is justified, because it can make all the difference when assessing the long-term effects of high-resolution processes. Especially for conservation planning of species coping with a disturbed and changing environment, it can be vital to draw a detailed picture of the species' prospects rather than relying on coarse data or assumptions.

In general, my case studies illustrated the positive implications high-resolution simulations can have for projecting long-term viability by gradually adding levels of detail to the analyses. The effect external conditions have on individual life stages and the longevity of a species already emerged for isolated populations. Incorporating a dispersal process, thus rendering a model spatially explicit, illustrated that considering dispersal between populations alters viability analyses, because it can partially compensate for negative local conditions. Accounting for spatial characteristics within a landscape, such as the degree of fragmentation or the heterogeneity in land use practices and schedules, further refines an analysis regarding the prospects of regional population development and dispersal success.

For the large marsh grasshopper (LMG) in particular, the studies confirmed that the species in principle benefits from moderate climate change in the temperate study region, yet remains constrained by regional land use practices such as grassland mowing. In contrast, mild climate change could allow for a better interaction between high-yield agriculture and the survival of the species. Dispersal between habitats slightly offset potentially negative effects of external conditions, especially in heterogeneously farmed regions of less fragmented grasslands.

In the face of global change, the most essential recommendation regarding conservation management is to act with foresight and keep measures adaptable, both in space and time, wherever possible. Thorough system knowledge and regular reassessment are other advisable assets to properly project the prospects of a species and involve stakeholders to achieve the right spatial targeting of measures. Such efforts could also benefit other species, entire ecological communities and biodiversity in general. The case of the LMG further demonstrated that the most climatically suitable regions are not necessarily those that require the least conservation effort.

[1] Network Common Data Form (NetCDF) library documentation: `www.unidata.ucar.edu/software/netcdf/`
[2] HiLEG GitLab repository: `https://git.ufz.de/leins/hileg`

To conclude, the HiLEG simulation model can be a valuable tool for conservation biologists to identify current and future requirements not only for the LMG in particular, but also for similar species or ecological communities in general. It can be used to explore scenarios of different dimensions, with the level of detail depending on the user and the objective in question. Applying HiLEG to analyze the suitability of isolated habitats, the distribution of species, or the viability of cross-regional populations can provide important insights for conservation planning, stakeholder exchange and the actual decision-making for implementing conservation measures.

Although the HiLEG model has been deliberately designed to be adaptable and scalable, it remains confined to a limited domain of ecological modelling. However, it is also with intention to distribute HiLEG as an open-access and open-source application. I encourage everyone not only to improve or modify HiLEG for their own purposes, but more importantly to take the same approach to their own simulation models, regardless of potential flaws and drawbacks. It is my understanding that open and transparent provision of scientific data and results is the basis for good research. This openness should apply to simulation models and their implementation details as well.

Bibliography

Addison, P. F. E., Rumpff, L., Bau, S. S., Carey, J. M., Chee, Y. E., Jarrad, F. C., McBride, M. F. & Burgman, M. A. (2013). Practical solutions for making models indispensable in conservation decision-making. *Diversity and Distributions* 19(5), 490–502.

Báldi, A. & Kisbenedek, T. (1997). Orthopteran assemblages as indicators of grassland naturalness in Hungary. *Agriculture, Ecosystems & Environment* 66(2), 121–129.

Bateman, B. L., Murphy, H. T., Reside, A. E., Mokany, K. & VanDerWal, J. (2013). Appropriateness of full-, partial- and no-dispersal scenarios in climate change impact modelling. *Diversity and Distributions* 19(10), 1224–1234.

Beissinger, S. R. & McCullough, D. R. (2002). Population Viability Analysis. University of Chicago Press. 594 pp.

Benton, T. G., Vickery, J. A. & Wilson, J. D. (2003). Farmland biodiversity: is habitat heterogeneity the key? *Trends in Ecology & Evolution* 18(4), 182–188.

Blab, J., Nowak, E., Trautmann, W. & Sukopp, H. (1984). Rote Liste der gefährdeten Tiere und Pflanzen in der BRD, erweiterte Neubearbeitung. *Kilda, Greven (Reihe Naturschutz aktuell 1)* 4.

Bonnot, T. W. (2016). Novel approaches to conserving the viability of regional wildlife populations in response to landscape and climate change. PhD thesis. University of Missouri–Columbia.

Bönsel, A. B. & Sonneck, A.-G. (2011). Habitat use and dispersal characteristic by Stethophyma grossum: the role of habitat isolation and stable habitat conditions towards low dispersal. *Journal of Insect Conservation* 15(3), 455–463.

Bowler, D. E. & Benton, T. G. (2005). Causes and consequences of animal dispersal strategies: relating individual behaviour to spatial dynamics. *Biological Reviews* 80(2), 205–225.

Bridle, J. R., Buckley, J., Bodsworth, E. J. & Thomas, C. D. (2014). Evolution on the move: specialization on widespread resources associated with rapid range expansion in response to climate change. *Proceedings of the Royal Society B: Biological Sciences* 281(1776), 20131800.

Brown, J. H. & Kodric-Brown, A. (1977). Turnover Rates in Insular Biogeography: Effect of Immigration on Extinction. *Ecology* 58(2), 445–449.

Brussaard, L., Caron, P., Campbell, B., Lipper, L., Mainka, S., Rabbinge, R., Babin, D. & Pulleman, M. (2010). Reconciling biodiversity conservation and food security: scientific challenges for a new agriculture. *Current Opinion in Environmental Sustainability* 2(1), 34–42.

Bundesamt für Naturschutz (2017). Agrar-Report 2017 - Biologische Vielfalt in der Agrarlandschaft. Bonn: BfN / Bundesamt für Naturschutz (Hrsg.)

Carpenter, S. R., Mooney, H. A., Agard, J., Capistrano, D., DeFries, R. S., Díaz, S., Dietz, T., Duraiappah, A. K., Oteng-Yeboah, A., Pereira, H. M., Perrings, C., Reid, W. V., Sarukhan, J., Scholes, R. J. & Whyte, A. (2009). Science for managing ecosystem services: Beyond the Millennium Ecosystem Assessment. *Proceedings of the National Academy of Sciences* 106(5), 1305–1312.

Chaudhary, V. & Oli, M. K. (2020). A critical appraisal of population viability analysis. *Conservation Biology* 34(1), 26–40.

Chen, I.-C., Hill, J. K., Ohlemüller, R., Roy, D. B. & Thomas, C. D. (2011). Rapid Range Shifts of Species Associated with High Levels of Climate Warming. *Science* 333(6045), 1024–1026.

Cordes, L. S., Blumstein, D. T., Armitage, K. B., CaraDonna, P. J., Childs, D. Z., Gerber, B. D., Martin, J. G. A., Oli, M. K. & Ozgul, A. (2020). Contrasting effects of climate change on seasonal survival of a hibernating mammal. *Proceedings of the National Academy of Sciences* 117(30), 18119–18126.

Coulson, T., Mace, G. M., Hudson, E. & Possingham, H. (2001). The use and abuse of population viability analysis. *Trends in Ecology & Evolution* 16(5), 219–221.

Cowan, M. A., Callan, M. N., Watson, M. J., Watson, D. M., Doherty, T. S., Michael, D. R., Dunlop, J. A., Turner, J. M., Moore, H. A., Watchorn, D. J. & Nimmo, D. G. (2021). Artificial refuges for wildlife conservation: what is the state of the science? *Biological Reviews* 96(6), 2735–2754.

Crooks, J. A. & Soulé, M. E. (1999). Lag Times in Population Explosions of Invasive Species: Causes and Implications. In *Invasive Species and Biodiversity Management*. Dordrecht: Springer Netherlands, pp. 103–125.

Dahm, J. (2022). Germany split over ramping up food production. www.euractiv.com. URL: https://www.euractiv.com/section/agriculture-food/news/germany-split-over-ramping-up-food-production/ (visited on 25/05/2022).

Drechsler, M., Frank, K., Hanski, I., O'Hara, R. B. & Wissel, C. (2003). Ranking Metapopulation Extinction Risk: From Patterns in Data to Conservation Management Decisions. *Ecological Applications* 13(4), 990–998.

Drechsler, M., Gerling, C., Keuler, K., Leins, J., Sturm, A. & Wätzold, F. (2021). A quantitative approach for the design of robust and cost-effective conservation policies under uncertain climate change: The case of grasshopper conservation in Schleswig-Holstein, Germany. *Journal of Environmental Management* 296, 113201.

Drechsler, M. & Wissel, C. (1997). Separability of Local and Regional Dynamics in Metapopulations. *Theoretical Population Biology* 51(1), 9–21.

Driscoll, D. A., Banks, S. C., Barton, P. S., Ikin, K., Lentini, P., Lindenmayer, D. B., Smith, A. L., Berry, L. E., Burns, E. L., Edworthy, A., Evans, M. J., Gibson, R., Heinsohn, R., Howland, B., Kay, G., Munro, N., Scheele, B. C., Stirnemann, I., Stojanovic, D., Sweaney, N., Villaseñor, N. R. & Westgate, M. J. (2014). The Trajectory of Dispersal Research in Conservation Biology. Systematic Review. *PLOS ONE* 9(4), e95053.

Fick, A. (1855). Ueber Diffusion. *Annalen der Physik* 170(1), 59–86.

Franco, J., Levidow, L., Fig, D., Goldfarb, L., Hönicke, M. & Luisa Mendonça, M. (2010). Assumptions in the European Union biofuels policy: frictions with experiences in Germany, Brazil and Mozambique. *The Journal of Peasant Studies* 37(4), 661–698.

Gerling, C., Drechsler, M., Keuler, K., Leins, J. A., Radtke, K., Schulz, B., Sturm, A. & Wätzold, F. (2022). Climate–ecological–economic modelling for the cost-effective spatiotemporal allocation of conservation measures in cultural landscapes facing climate change. *Q Open* 2(1), qoac004.

Gerling, C., Strum, A. & Wätzold, F. (2020). The impact of climate change on the profit-maximising timing of grassland use and conservation costs. URL: https://mpra.ub.uni-muenchen.de/105597/ (visited on 03/06/2022).

Grantham, H. S., Bode, M., McDonald-Madden, E., Game, E. T., Knight, A. T. & Possingham, H. P. (2010). Effective conservation planning requires learning and adaptation. *Frontiers in Ecology and the Environment* 8(8), 431–437.

Green, T. W., Slone, D. H., Swain, E. D., Cherkiss, M. S., Lohmann, M., Mazzotti, F. J. & Rice, K. G. (2014). Evaluating Effects of Everglades Restoration on American Crocodile Populations in South Florida Using a Spatially-Explicit, Stage-Based Population Model. *Wetlands* 34 (S1), 213–224.

Griffioen, R. (1996). Over het dispersievermogen van de Moerassprinkhaan. *Nieuwsbrief Saltabel* 15(1), 39–41.

Grimm, V. & Railsback, S. F. (2012). Pattern-oriented modelling: a 'multi-scope' for predictive systems ecology. *Philosophical Transactions of the Royal Society B: Biological Sciences* 367(1586), 298–310.

Grimm, V., Berger, U., Bastiansen, F., Eliassen, S., Ginot, V., Giske, J., Goss-Custard, J., Grand, T., Heinz, S. K., Huse, G., Huth, A., Jepsen, J. U., Jørgensen, C., Mooij, W. M., Müller, B., Pe'er, G., Piou, C., Railsback, S. F., Robbins, A. M., Robbins, M. M., Rossmanith, E., Rüger, N., Strand, E., Souissi, S., Stillman, R. A., Vabø, R., Visser, U. & DeAngelis, D. L. (2006). A standard protocol for describing individual-based and agent-based models. *Ecological Modelling* 198(1), 115–126.

Grimm, V., Railsback, S. F., Vincenot, C. E., Berger, U., Gallagher, C., DeAngelis, D. L., Edmonds, B., Ge, J., Giske, J., Groeneveld, J., Johnston, A. S. A., Milles, A., Nabe-Nielsen, J., Polhill, J. G., Radchuk, V., Rohwäder, M.-S., Stillman, R. A., Thiele, J. C. & Ayllón, D. (2020). The ODD Protocol for Describing Agent-Based and Other Simulation Models: A Second Update to Improve Clarity, Replication, and Structural Realism. *Journal of Artificial Societies and Social Simulation* 23(2), 7.

Hanski, I. (1999). Metapopulation ecology. Oxford University Press.

Hanski, I. A. & Gilpin, M. E. (Eds.) (1997). Metapopulation biology: ecology, genetics, and evolution. San Diego, CA: Academic Press.

Helfert, B. & Sänger, K. (1975). Haltung und Zucht europäischer Heuschrecken (Orthoptera: Saltatoria) im Labor. *Zeitschrift fur angewandte Zoologie*.

Helfert, B. (1980). The regulatory effect of photoperiod and temperature on the life-cycle of ecologically different tettigoniid-species (Orthoptera, Saltatoria). Part 1: Larval development, reproduction and life-span of the parental generation. *Zoologische Jahrbücher, Abteilung für Systematik, Ökologie und Geographie der Tiere* 107(2), 159–182.

Heller, N. E. & Zavaleta, E. S. (2009). Biodiversity management in the face of climate change: A review of 22 years of recommendations. *Biological Conservation* 142(1), 14–32.

Heydenreich, M. (1999). Die Bedeutung der Heuschreckenart Stethophyma grossum L., 1758 (Caelifera: Acrididae) als Bestandteil eines Zielartensystems für das Management von Niedermooren. PhD thesis.

Hulme, P. E. (2005). Adapting to climate change: is there scope for ecological management in the face of a global threat? *Journal of Applied Ecology* 42(5), 784–794.

Humbert, J.-Y., Ghazoul, J. & Walter, T. (2009). Meadow harvesting techniques and their impacts on field fauna. *Agriculture, Ecosystems & Environment* 130(1), 1–8.

Ingrisch, S. (1983). Zum Einfluß der Feuchte auf die Schlupfrate und Entwicklungsdauer der Eier mitteleuropäischer Feldheuschrecken (Orthoptera, Acrididae). *Deutsche Entomologische Zeitschrift* 30(1), 1–15.

Ingrisch, S. & Köhler, G. (1998). Die Heuschrecken Mitteleuropas. Die Neue Brehm-Bücherei Bd. 629. Magdeburg: Westarp Wissenschaften. 460 pp.

IPCC (2021). IPCC, 2021: Climate Change 2021: The Physical Science Basis. Contribution of Working Group I to the Sixth Assessment Report of the Intergovernmental Panel on Climate Change. Cambridge University Press.

IPCC (2022). IPCC, 2022: Climate Change 2022: Impacts, Adaptation, and Vulnerability. Contribution of Working Group II to the Sixth Assessment Report of the Intergovernmental Panel on Climate Change. Cambridge University Press.

Johst, K., Brandl, R. & Eber, S. (2002a). Metapopulation persistence in dynamic landscapes: the role of dispersal distance. *Oikos* 98(2), 263–270.

Johst, K., Drechsler, M. & Wätzold, F. (2002b). An ecological-economic modelling procedure to design compensation payments for the efficient spatio-temporal allocation of species protection measures. *Ecological Economics* 41(1), 37–49.

Joyce, C. B., Simpson, M. & Casanova, M. (2016). Future wet grasslands: ecological implications of climate change. *Ecosystem Health and Sustainability* 2(9), e01240.

Keller, D. (2012). Insect dispersal in fragmented agricultural landscapes. PhD thesis. ETH Zurich.

Keller, D., Jung, E. & Holderegger, R. (2012). Development of microsatellite markers for the wetland grasshopper Stethophyma grossum. *Conservation Genetics Resources* 4(2), 507–509.

Keßler, T., Cierjacks, A., Ernst, R. & Dziock, F. (2012). Direct and indirect effects of ski run management on alpine Orthoptera. *Biodiversity and Conservation* 21(1), 281–296.

Keuler, K., Radtke, K., Kotlarski, S. & Lüthi, D. (2016). Regional climate change over Europe in COSMO-CLM: Influence of emission scenario and driving global model. *Meteorologische Zeitschrift* 25(2), 121–136.

Kiel, E.-F. (1999). Heuschrecken und Mahd. Empfehlungen für das Pflegemanagement in Feuchtwiesenschutzgebieten. *LÖBF-Mitteilungen* 24, 63–66.

Kimura, M. & Weiss, G. H. (1964). The stepping stone model of population structure and the decrease of genetic correlation with distance. *Genetics* 49, 561–567.

Kleijn, D., Rundlöf, M., Scheper, J., Smith, H. G. & Tscharntke, T. (2011). Does conservation on farmland contribute to halting the biodiversity decline? *Trends in Ecology & Evolution* 26(9), 474–481.

Kleukers, R., Van Nieukerken, E., Odé, B., Willemse, L. & Van Wingerden, W. (1997). De sprinkhanen en krekels van Nederland (Orthoptera). *Nationaal Natuurhistorisch Museum [etc.]*

Köhler, G. & Weipert, J. (1991). Beiträge zur Faunistik und Ökologie des Naturschutzgebietes 'Apfelstädter Ried', Kr Erfurt-Land Teil IV Orthoptera: Saltatoria. *Arch. Nat. Landschaftforschung* 31, 181–195.

Koschuh, A. (2004). Verbreitung, Lebensräume und Gefährdung der Sumpfschrecke Stethophyma grossum (L., 1758) (Saltatoria) in der Steiermark. *Joannea Zoologie* 6, 223–246.

Krause, S. (1996). Populationsstruktur, Habitatbindung und Mobilität der Larven von Stethophyma grossum (Linné, 1758). *Articulata* 11(2), 77–89.

Kriegbaum, H. (1988). Untersuchungen zur Lebensgeschichte von Feldheuschrecken (Orthoptera: Gomphocerinae): Fortpflanzungsverhalten und Fortpflanzungserfolg im natürlichen Habitat. PhD thesis. Universität Erlangen-Nürnberg.

Leins, J. A., Banitz, T., Grimm, V. & Drechsler, M. (2021). High-resolution PVA along large environmental gradients to model the combined effects of climate change and land use timing: lessons from the large marsh grasshopper. *Ecological Modelling* 440, 109355.

Leins, J. A., Grimm, V. & Drechsler, M. (2022). Large-scale PVA modeling of insects in cultivated grasslands: The role of dispersal in mitigating the effects of management schedules under climate change. *Ecology and Evolution* 12(7), e9063.

Levins, R. (1969). Some Demographic and Genetic Consequences of Environmental Heterogeneity for Biological Control. *Bulletin of the Entomological Society of America* 15(3), 237–240.

Levy, O., Buckley, L. B., Keitt, T. H., Smith, C. D., Boateng, K. O., Kumar, D. S. & Angilletta, M. J. (2015). Resolving the life cycle alters expected impacts of climate change. *Proceedings of the Royal Society B* 282, 20150837.

Löffler, F., Poniatowski, D. & Fartmann, T. (2019). Orthoptera community shifts in response to land-use and climate change – Lessons from a long-term study across different grassland habitats. *Biological Conservation* 236, 315–323.

Ma, G., Hoffmann, A. A. & Ma, C.-S. (2015). Daily temperature extremes play an important role in predicting thermal effects. *Journal of Experimental Biology* 218(14), 2289–2296.

Maas, S., Detzel, P. & Staudt, A. (2002). Gefährdungsanalyse der Heuschrecken Deutschlands: Verbreitungsatlas, Gefährdungseinstufung und Schutzkonzepte. Bonn, Germany: Bundesamt für Naturschutz.

Malkus, J. (1997). Habitatpräferenzen und Mobilität der Sumpfschrecke (Stethophyma grossum L. 1758) unter besonderer Berücksichtigung der Mahd. *Articulata* 12(1), 1–18.

Marshall, J. A. & Haes, E. C. M. (1988). Grasshoppers and allied insects of Great Britain and Ireland. Harley Books. Colchester.

Marzelli, M. (1994). Ausbreitung von Mecostethus grossus auf einer Ausgleichs-und Renaturierungsfläche. *Articulata* 9(1), 25–32.

Marzelli, M. (1997). Untersuchungen zu den Habitatansprüchen der Sumpfschrecke (Stethophyma grossum) und ihre Bedeutung für das Habitatmanagement. *Articulata* 12(2), 107–121.

Mawdsley, J. R., O'malley, R. & Ojima, D. S. (2009). A Review of Climate-Change Adaptation Strategies for Wildlife Management and Biodiversity Conservation. *Conservation Biology* 23(5), 1080–1089.

McCarthy, M. A. & Possingham, H. P. (2014). Population Viability Analysis. In *Encyclopedia of environmetrics*. Chichester: John Wiley & Sons, pp. 2016–2020.

Mewes, M., Sturm, A., Johst, K., Drechsler, M. & Wätzold, F. (2012). Handbuch der Software Ecopay zur Bestimmung kosteneffizienter Ausgleichszahlungen für Maßnahmen zum Schutz gefährdeter Arten und Lebensraumtypen im Grünland. UFZ-Bericht 01/2012.

Meyer, C., Reutter, M., Matzdorf, B., Sattler, C. & Schomers, S. (2015). Design rules for successful governmental payments for ecosystem services: Taking agri-environmental measures in Germany as an example. *Journal of Environmental Management* 157, 146–159.

Millennium Ecosystem Assessment (2005). Ecosystems and Human Well-being: Biodiversity Synthesis. *World Resources Institute*, *Washington*, *DC*, 100.

Miller, J. & Gardiner, T. (2018). The effects of grazing and mowing on large marsh grasshopper, Stethophyma grossum (Orthoptera: Acrididae), populations in Western Europe: a review. *Journal of Orthoptera Research* 27(1), 91–96.

Moloney, S., Fünfgeld, H. & Granberg, M. (2018). Climate change responses from the global to local scale: An overview. In *Local Action on Climate Change: opportunities and constraints*. New York: Routledge.

Mottet, A., de Haan, C., Falcucci, A., Tempio, G., Opio, C. & Gerber, P. (2017). Livestock: On our plates or eating at our table? A new analysis of the feed/food debate. *Global Food Security* 14, 1–8.

Munns Jr., W. R. (2006). Assessing Risks to Wildlife Populations from Multiple Stressors: Overview of the Problem and Research Needs. *Ecology and Society* 11(1), 23.

Naujokaitis-Lewis, I. R., Curtis, J. M. R., Tischendorf, L., Badzinski, D., Lindsay, K. & Fortin, M.-J. (2013). Uncertainties in coupled species distribution–metapopulation dynamics models for risk assessments under climate change. *Diversity and Distributions* 19(5), 541–554.

Nguyen, C., Latacz-Lohmann, U., Hanley, N., Schilizzi, S. & Iftekhar, S. (2022). Spatial Coordination Incentives for landscape-scale environmental management: A systematic review. *Land Use Policy* 114, 105936.

Oliver, T. H. & Morecroft, M. D. (2014). Interactions between climate change and land use change on biodiversity: attribution problems, risks, and opportunities. *WIREs Climate Change* 5(3), 317–335.

Oppel, S. (2005). Die Heuschreckenfauna der jungen Düneninsel Trischen im schleswig-holsteinischen Wattenmeer (Insecta: Saltatoria). *DROSERA-Naturkundliche Mitteilungen aus Norddeutschland*, 1–6.

Oschmann, M. (1969). Faunistisch-ökologische Untersuchungen an Orthopteren im Raum von Gotha. *Hercynia* 6(2), 115–168.

Parmesan, C., Ryrholm, N., Stefanescu, C., Hill, J. K., Thomas, C. D., Descimon, H., Huntley, B., Kaila, L., Kullberg, J., Tammaru, T., Tennent, W. J., Thomas, J. A. & Warren, M. (1999). Poleward shifts in geographical ranges of butterfly species associated with regional warming. *Nature* 399(6736), 579–583.

Pe'er, G., Matsinos, Y. G., Johst, K., Franz, K. W., Turlure, C., Radchuk, V., Malinowska, A. H., Curtis, J. M. R., Naujokaitis-Lewis, I., Wintle, B. A. & Henle, K. (2013). A Protocol for Better Design, Application, and Communication of Population Viability Analyses. *Conservation Biology* 27(4), 644–656.

Poniatowski, D., Beckmann, C., Löffler, F., Münsch, T., Helbing, F., Samways, M. J. & Fartmann, T. (2020). Relative impacts of land-use and climate change on grasshopper range shifts have changed over time. *Global Ecology and Biogeography* 29(12), 2190–2202.

Poniatowski, D., Münsch, T., Bianchi, F. & Fartmann, T. (2018a). Arealveränderungen mitteleuropäischer Heuschrecken als Folge des Klimawandels. *Natur und Landschaft* (12), 553–561.

Poniatowski, D., Stuhldreher, G., Löffler, F. & Fartmann, T. (2018b). Patch occupancy of grassland specialists: Habitat quality matters more than habitat connectivity. *Biological Conservation* 225, 237–244.

Poore, J. & Nemecek, T. (2018). Reducing food's environmental impacts through producers and consumers. *Science* 360(6392), 987–992.

Radchuk, V., Johst, K., Groeneveld, J., Turlure, C., Grimm, V. & Schtickzelle, N. (2014). Appropriate resolution in time and model structure for population viability analysis: Insights from a butterfly metapopulation. *Biological Conservation* 169, 345–354.

Radchuk, V., Turlure, C. & Schtickzelle, N. (2013). Each life stage matters: the importance of assessing the response to climate change over the complete life cycle in butterflies. *Journal of Animal Ecology* 82(1), 275–285.

Redford, K. H., Amato, G., Baillie, J., Beldomenico, P., Bennett, E. L., Clum, N., Cook, R., Fonseca, G., Hedges, S., Launay, F., Lieberman, S., Mace, G. M., Murayama, A., Putnam, A., Robinson, J. G., Rosenbaum, H., Sanderson, E. W., Stuart, S. N., Thomas, P. & Thorbjarnarson, J. (2011). What Does It Mean to Successfully Conserve a (Vertebrate) Species? *BioScience* 61(1), 39–48.

Robillard, C. M., Coristine, L. E., Soares, R. N. & Kerr, J. T. (2015). Facilitating climate-change-induced range shifts across continental land-use barriers: Conserving Habitat for Range Shifts. *Conservation Biology* 29(6), 1586–1595.

Rounsevell, M., Berry, P. & Harrison, P. (2006). Future environmental change impacts on rural land use and biodiversity: a synthesis of the ACCELERATES project. *Environmental Science & Policy* 9(2), 93–100.

Schmidt, N. & Zinkernagel, J. (2017). Model and Growth Stage Based Variability of the Irrigation Demand of Onion Crops with Predicted Climate Change. *Water* 9(9), 693.

Schumacher, U. & Mathey, J. (1998). Zur Analyse der Lebensräume von Heuschrecken mit Methoden der Geoinformatik-dargestellt am Beispiel der Riesaer Elberegion. *Angewandte geographische Informationsverarbeitung. Beiträge zum AGIT-Symposium Salzburg*. Vol. 98.

Shigesada, N. & Kawasaki, K. (1997). Biological invasions: theory and practice. Oxford University Press, UK.

Sonneck, A.-G., Bönsel, A. & Matthes, J. (2008). Der Einfluss von Landnutzung auf die Habitate von Stethophyma grossum (Linnaeus, 1758) an Beispielen aus Mecklenburg-Vorpommern. *Articulata* 23, 15–30.

Sörens, A. (1996). Zur Populationsstruktur, Mobilität und dem Eiablageverhalten der Sumpfschrecke (Stethophyma grossum) und der Kurzflügeligen Schwertschrecke (Conocephalus dorsalis). *Articulata* 11(1), 37–48.

Srivastava, V., Lafond, V. & Griess, V. C. (2019). Species distribution models (SDM): applications, benefits and challenges in invasive species management. *CAB Reviews: Perspectives in Agriculture, Veterinary Science, Nutrition and Natural Resources* 14(20).

Stange, E. E. & Ayres, M. P. (2010). Climate Change Impacts: Insects. In *Encyclopedia of Life Sciences (ELS)*. Chichester, UK: John Wiley & Sons, Ltd.

Statistisches Amt für Hamburg und Schleswig-Holstein (2021). Bodenflächen in Schleswig-Holstein am 31.12.2020 nach Art der tatsächlichen Nutzung. Hamburg: Statistisches Amt für Hamburg und Schleswig-Holstein.

Statistisches Bundesamt (2021). Land- und Forstwirtschaft, Fischerei - Bodenfläche nach Art der tatsächlichen Nutzung. Wiesbaden: Statistisches Bundesamt (Destatis).

Stauffer, D. & Aharony, A. (1994). Introduction To Percolation Theory: Second Edition. 2nd ed. London: Taylor & Francis. 192 pp.

Stephens, P. (2016). Population viability analysis. In *Oxford bibliographies. Ecology*. Oxford: Oxford University Press.

Sturm, A., Drechsler, M., Johst, K., Mewes, M. & Wätzold, F. (2018). DSS-Ecopay – A decision support software for designing ecologically effective and cost-effective agri-environment schemes to conserve endangered grassland biodiversity. *Agricultural Systems* 161, 113–116.

Szewczyk, T. M., Lee, T., Ducey, M. J., Aiello-Lammens, M. E., Bibaud, H. & Allen, J. M. (2019). Local management in a regional context: Simulations with process-based species distribution models. *Ecological Modelling* 413, 108827.

Thompson, L. C., Escobar, M. I., Mosser, C. M., Purkey, D. R., Yates, D. & Moyle, P. B. (2012). Water Management Adaptations to Prevent Loss of Spring-Run Chinook Salmon in California under Climate Change. *Journal of Water Resources Planning and Management* 138(5), 465–478.

Topping, C. J., Alrøe, H. F., Farrell, K. N. & Grimm, V. (2015). Per Aspera ad Astra: Through Complex Population Modeling to Predictive Theory. *The American Naturalist* 186(5), 669–674.

Trautner, J. & Hermann, G. (2008). Die Sumpfschrecke (Stethophyma grossum L., 1758) im Aufwind-Erkenntnisse aus dem zentralen Baden-Württemberg. *Articulata* 23(2), 37–52.

UNFCCC (2016). Decision 1/CP. 21. *Paris Agreement. United Nations Framework Convention on Climate Change, Bonn, Germany*.

Uvarov, B. (1977). Grasshoppers and locusts. A handbook of general acridology Vol. 2. Behaviour, ecology, biogeography, population dynamics. London: Centre for Overseas Pest Research. 622 pp.

Van der Putten, W. H. (2012). Climate Change, Aboveground-Belowground Interactions, and Species' Range Shifts. *Annual Review of Ecology, Evolution, and Systematics* 43(1), 365–383.

Van der Putten, W. H., Macel, M. & Visser, M. E. (2010). Predicting species distribution and abundance responses to climate change: why it is essential to include biotic interactions across trophic levels. *Philosophical Transactions of the Royal Society B: Biological Sciences* 365(1549), 2025–2034.

Van Strien, M. J. (2013). Advances in landscape genetic methods and theory: lessons learnt from insects in agricultural landscapes. PhD thesis. ETH Zurich.

van Vuuren, D. P., Edmonds, J., Kainuma, M., Riahi, K., Thomson, A., Hibbard, K., Hurtt, G. C., Kram, T., Krey, V., Lamarque, J.-F., Masui, T., Meinshausen, M., Nakicenovic, N., Smith, S. J. & Rose, S. K. (2011). The representative concentration pathways: an overview. *Climatic Change* 109(1), 5–31.

Vinatier, F., Tixier, P., Duyck, P.-F. & Lescourret, F. (2011). Factors and mechanisms explaining spatial heterogeneity: a review of methods for insect populations. *Methods in Ecology and Evolution* 2(1), 11–22.

Waloff, N. (1950). The egg pods of british short-horned grasshoppers (acrididae). *Proceedings of the Royal Entomological Society of London. Series A, General Entomology* 25, 115–126.

Wiegand, T., Moloney, K. A., Naves, J. & Knauer, F. (1999). Finding the Missing Link between Landscape Structure and Population Dynamics: A Spatially Explicit Perspective. *The American Naturalist* 154(6), 605–627.

Wiegand, T., Revilla, E. & Moloney, K. A. (2005). Effects of Habitat Loss and Fragmentation on Population Dynamics. *Conservation Biology* 19(1), 108–121.

Will, M., Dressler, G., Kreuer, D., Thulke, H.-H., Grêt-Regamey, A. & Müller, B. (2021). How to make socio-environmental modelling more useful to support policy and management? *People and Nature* 3(3), 560–572.

Wilson, K. A., McBride, M. F., Bode, M. & Possingham, H. P. (2006). Prioritizing global conservation efforts. *Nature* 440(7082), 337–340.

Wingerden, W. K. R. E. v., Musters, J. C. M. & Maaskamp, F. I. M. (1991). The influence of temperature on the duration of egg development in West European grasshoppers (Orthoptera: Acrididae). *Oecologia* 87(3), 417–423.

Wingerden, W. K. R. E. v., Musters, J. C., Cannemeijer, F. & Bongers, W. (1992). Simulation of hatching date in three Chorthippus species (Orthoptera arcrididae) in unfertilized and lightly fertilized grasslands. Proc. Exper. & Appl. Entomol. N.E.v. Amsterdam 3, pp. 86–93.

Winkler, C. (2000). Die Heuschrecken Schleswig-Holsteins - Rote Liste. In collab. with L. für Natur und Umwelt des Landes Schleswig-Holstein. Rote Liste [Schleswig-Holstein] 12. Flintbek: Eigenverl. 52 pp.

Winkler, C. & Haacks, M. (2019). Die Heuschrecken Schleswig-Holsteins. In collab. with Schleswig-Holstein. 4. Fassung, Stand der Daten: Dezember 2017. Schriftenreihe: LLUR SH - Natur - RL 27. Kiel: Landesamt für Landwirtschaft, Umwelt und Ländliche Räume. 85 pp.

With, K. A. (2002). Using Percolation Theory to Assess Landscape Connectivity and Effects of Habitat Fragmentation. In *Applying Landscape Ecology in Biological Conservation*. New York: Springer New York, pp. 105–130.

Appendices

A Appendix to Chapter 3

A.1 Climate Parameters

Per grid cell, four climate parameters of daily resolution were available and used in the model: mean surface temperature (ω_{ts}) in °C, summed precipitation (ω_{pr}) in $kg\ m^{-2}$, total soil moisture content (ω_{mrso}) of soil layers 1–8 in $kg\ m^{-2}$, summed sinks of minus tendency of soil moisture content (ω_{smt}) in $kg\ m^{-2}$. From the parameters ω_{mrso}, ω_{pr} and ω_{smt} five additional parameters were deduced: relative soil moisture content (ω_{rsmc}) using ω_{mrso}; relative soil moisture content upper ground (ω_{rmug}) using ω_{rsmc}; relative humidity upper ground (ω_{rhug}) ω_{rmug}; net positive influx (ω_{npi}) in in $kg\ m^{-2}$ using ω_{pr} and ω_{smt}; and summed contact water (ω_{cw}) in $kg\ m^{-2}$ using ω_{npi}. To calculate ω_{rsmc}, first the maximum of ω_{mrso} value was determined using the mean of its yearly maxima:

$$max_{mrso} = \frac{1}{111} \sum_{year=1970}^{2080} max_{mrso}(year) \tag{A.1}$$

On that basis, the overall relative soil moisture content for the whole soil column of depth d_{tot} [in cm] and, without loss of generality, width B_0 (Figure A.1) was calculated:

$$\omega_{rsmc} = \frac{\omega_{mrso}}{max_{mrso}} \tag{A.2}$$

Depending on the value of ω_{rsmc}, we applied one of three different simple two-dimensional geometric soil moisture models (Figure A.1) to calculate ω_{rmug} for the upper soil layer of depth d_{lay} [in cm]. All of them assumed that soil moisture decreases uniformly from top to bottom.

(1) If $\omega_{rsmc} = 0.5$ (Figure A.1A), we assumed that soil water is distributed triangularly with the basis of the triangle being B_0 and the height being the column depth d_{tot}. Here and throughout all following calculations, the relative soil moisture content is represented by the proportion of the blue area in the considered portion of the soil column (Figure A.1). Using the intercept theorem, the relative soil moisture content in the upper soil layer of depth d_{lay} is then given by

$$\omega_{rmug} = \omega_{rmug}\left(d_{tot}, d_{lay}\right) = \frac{d_{lay}}{2 \times d_{tot}} \tag{A.3}$$

(2) To consider a decreased $\omega_{rsmc} < 0.5$ (Figure A.1B), we used the same triangular model but reduced basis of the triangle to $B = 2 \times \omega_{rsmc} \times B_0$ which yields

$$\omega_{rmug} = \omega_{rmug}\left(d_{tot}, d_{lay}\right) = \frac{\omega_{rsmc} \times d_{lay}}{d_{tot}} \tag{A.4}$$

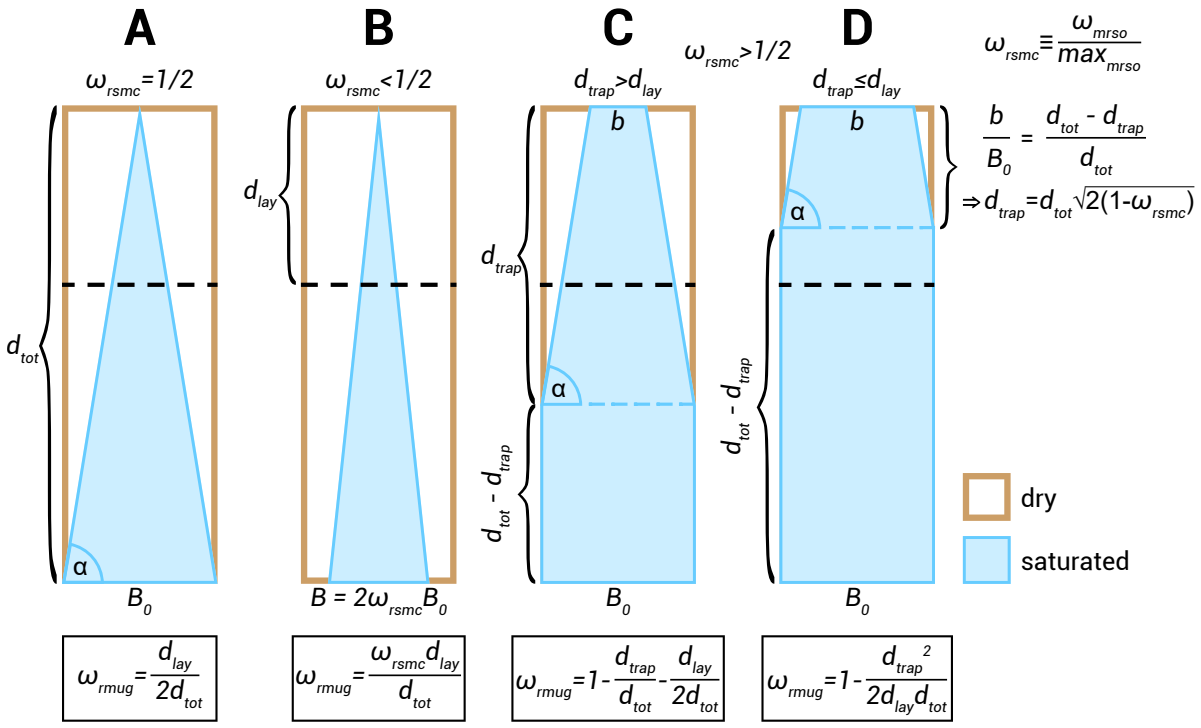

Figure A.1: Graphical representation of a two-dimensional geometric model used to calculate relative soil moisture content in the upper ground (ω_{rmug}) in the upper soil layer with depth d_{lay} (dashed black line) of a soil column of depth d_{tot}. The value of ω_{rmug} is the size of the blue area above the dashed black line divided by the area of the brown rectangle above this line. Four cases are considered depending on saturation ω_{rsmc} of the total soil column: (A) triangular model with base B_0 if 50 % saturated, (B) triangular model with decreased base B if saturated < 50 %, (C) trapezoid model using (the top of) the trapeze, if saturated > 50 % and depth dtrap of saturation-dependent trapeze is greater than d_{lay}, (D) trapezoid model using the full trapeze and (part of) the rectangle on bottom if saturated > 50 % and $d_{trap} \leq d_{lay}$.

(3) If $\omega_{rsmc} > 0.5$ (Figure A.1C-D), we applied a trapezoid soil moisture model by shifting the triangle upwards and clipping it at the surface, obtaining a trapeze on top of the soil column with height d_{trap} [in cm], bottom width B_0 and top width b (Figure A.1). At the fully saturated bottom of the soil column, we kept the rectangle with height $d_{tot} - d_{trap}$. Using the intercept theorem again and assuming that ω_{rsmc} is represented by the proportion of the blue area, we obtained $\frac{b}{B_0} = \frac{d_{tot} - d_{trap}}{d_{tot}}$ and deduced the height of the trapeze:

$$d_{trap} = d_{tot}\sqrt{2\,(1 - \omega_{rsmc})} \tag{A.5}$$

To calculate ω_{rmug} in the upper soil layer, d_{lay} must be compared to d_{trap}:

$$\omega_{rmug} = \omega_{rmug}\left(d_{tot}, d_{lay}\right) = \begin{cases} 1, & \text{if } d_{trap} = 0, \\ 1 - \frac{d_{trap}}{d_{tot}} + \frac{d_{lay}}{2 \times d_{tot}}, & \text{if } d_{trap} > d_{lay}, \\ 1 - \frac{\left[d_{trap}\right]^2}{2 \times d_{lay} \times d_{tot}}, & \text{otherwise} \end{cases} \tag{A.6}$$

In the first case, the height of the trapeze is zero because the soil is fully sated. The second case applies, if the height of the trapeze is greater than the depth of the upper soil layer. Only (the top of) the trapeze is used to calculate ω_{rmug} (Figure A.1C). In the third case, the soil is saturated as much that the upper layer partly reaches into the fully sated bottom of the soil column (Figure A.1D).

In this study, we calculated ω_{rmug} in the upper two centimeters of the full soil column (d_{tot} = 390 cm, d_{lay} = 2 cm) and used it to determine the relative humidity in that soil layer. For this, we additionally assumed a saturation threshold thd_{rmug} = 0.26 to apply reasonable humidity values that influence clutch development according to Ingrisch (1983):

$$\omega_{rhug} = \omega_{rhug}\left(d_{tot}, d_{lay}\right) = \frac{\omega_{rmug}\left(d_{tot}, d_{lay}\right)}{thd_{rmug}} \tag{A.7}$$

The net positive influx ω_{npi} was calculated using only positive values of the net influx

$$\omega_{ni} = max\left(\omega_{pr} - \omega_{smt}, 0\right) \tag{A.8}$$

and a weighted average over the past week (including the current day), where more recent values contribute more to the influx than earlier values:

$$\omega_{npi} = \omega_{npi}(t) = \omega_{ni}(t) + \sum_{\Delta t=1}^{6} \frac{4 \times \omega_{ni}(t - \Delta t)}{3 \times [\Delta t + 1] \times \sum_{n=1}^{6} \frac{2}{n+1}} \tag{A.9}$$

Lastly, the amount of potential contact water ω_{cw} was calculated:

$$\omega_{cw} = \begin{cases} \omega_{npi}, & \text{if } \omega_{npi} \geq thd_{cw}, \\ 0, & \text{otherwise} \end{cases} \tag{A.10}$$

Where the threshold thd_{cw} [in $kg\ m^{-2}$] defining contact water (i.e., eggs of model species covered with water or located in moist soil) was calculated following the minimum contact water determined for the model species by Ingrisch (1983). The authors added 0.5 ml of water per week to a petri dish with a diameter of θ_{out} = 93 mm covered with blotting paper. In the middle of that petri dish, they put another dish with a diameter of θ_{in} = 35 mm. Assuming that 1 milliliter equals 1 gram, the amount of water is equally distributed over a week, a blotting paper height of 0.25 mm, and considering only the outer ring area of the outer petri dish we determined the following contact water threshold in the upper soil layer d_{lay}:

$$thd_{cw} = \frac{0.0005\ kg \times d_{lay} \times day}{\pi \times \left(\left[\frac{\theta_{out}}{2}\right]^2 - \left[\frac{\theta_{in}}{2}\right]^2\right) \times 0.25\ mm \times 7\ days} = 0.98\ kgm^{-2} \tag{A.11}$$

A.2 Resampled Climate Data

The following tables show the resampled climate data time series, i.e., the applied reordering of years by sampling with replacement depending on random seed.

Table A.1: Order of years that is used to read climate data depending on random seed 1-25

Sim. year	Resampled year using random seed x																								
	1	2	3	4	5	6	7	8	9	10	11	12	13	14	15	16	17	18	19	20	21	22	23	24	25
2000	2007	2008	2011	2024	2001	2021	1997	2021	1995	2018	2000	1999	2018	2010	2020	2001	2003	2014	1997	2012	1996	2001	2010	2023	2021
2001	2024	2000	1997	2022	1996	2023	2001	1995	2005	2003	1997	2008	2013	2022	2019	2004	2000	1997	2007	2021	2018	2016	2015	2003	2015
2002	2016	1995	2016	2011	2021	2004	2018	2024	2010	1995	1995	2017	2002	2018	2000	2010	2010	2010	2017	2021	2003	2009	2023	2015	2012
2003	2022	2022	2020	2000	2019	2001	2004	2002	2009	2009	2014	2021	2020	2014	2012	1996	2020	2007	2007	2023	2015	2016	2000	1996	2007
2004	1995	2011	2003	2024	2001	2019	2008	2021	2009	2014	2008	2002	2019	2021	1996	2011	2000	2021	2002	2021	2016	2007	2017	2024	2003
2005	1998	2023	1998	2020	2005	1996	2024	2006	1995	2008	2000	1997	2021	2005	1998	2004	2021	2002	2016	2023	1996	2014	2018	2004	1997
2006	2004	2008	2010	2016	2022	1996	2016	2010	1999	2017	2016	2011	2023	1995	2005	1996	1997	2000	1999	2019	1995	2020	2003	2001	2000
2007	2024	2009	2012	2013	2024	2006	2008	2019	2004	2019	2022	2016	2000	1999	2019	1999	2019	2022	2002	2013	2023	2018	2012	2024	2000
2008	1999	2007	2021	2015	2009	1998	2024	2001	1999	2009	2007	1995	2024	2004	2003	2005	2018	2020	2004	1996	2001	2000	2001	2005	2007
2009	2002	2004	2008	2012	1997	2024	2004	2007	1995	2012	1998	2005	2017	2001	2022	2016	2007	2001	2015	2014	2015	2020	2008	2010	1999
2010	1997	2004	2021	2001	2013	2012	2011	1995	2001	2001	2009	2022	2008	2023	2010	2001	2014	2017	1997	2015	1996	2005	2015	2017	1998
2011	2006	1999	1995	1999	2006	1997	2002	2013	2021	1995	2001	1996	2017	2001	1995	1999	1998	1995	1996	2023	1999	2021	2000	2018	2002
2012	2000	2001	1998	2024	2017	2010	2010	2007	2007	2000	1995	2022	2013	2010	2004	2015	2014	2014	2015	2006	2004	2003	2000	2024	2015
2013	2006	2015	1996	2001	2005	2013	1997	2017	1999	2016	2021	2003	2013	2004	2019	2014	2001	2007	1998	2015	2020	2002	1997	2009	2013
2014	2005	2013	2001	1995	2010	2007	1997	2007	2002	2017	2009	1996	2018	2004	2004	1999	2012	2024	2019	2010	2014	2015	2006	2004	2008
2015	2015	1998	2002	2015	2009	2010	2007	2007	1999	2002	2019	1997	2018	2005	2016	2020	2013	2012	1995	1996	2005	1995	2001	2013	2000
2016	2006	2003	1996	2002	2003	2005	2003	2010	1997	2000	2023	2023	2014	2011	1998	1997	1996	2002	2024	2014	2004	2001	2013	1999	2011
2017	2023	2009	1997	2022	2024	2009	1995	2021	2006	2002	1997	2016	2006	2011	2001	2020	2020	2020	2024	2020	2019	2008	2020	2003	2003
2018	2011	2003	2008	2008	2000	2013	2009	2009	2005	1997	2020	1999	2016	2001	2002	2023	2005	1995	2014	2000	2012	2019	2007	2006	2006
2019	2020	2013	2015	2013	2019	2019	2010	2022	2009	1999	2021	2006	2005	2015	2021	2015	1996	2024	2013	2019	2000	2019	2007	2011	2017
2020	2027	2028	2031	2044	2021	2041	2017	2041	2015	2038	2020	2019	2038	2030	2040	2021	2023	2034	2017	2032	2016	2021	2030	2043	2041
2021	2044	2020	2017	2042	2016	2043	2021	2015	2025	2023	2017	2028	2033	2042	2039	2024	2020	2017	2027	2041	2038	2036	2035	2023	2035
2022	2036	2015	2036	2031	2041	2024	2038	2044	2030	2015	2015	2037	2022	2038	2020	2030	2030	2030	2037	2041	2023	2029	2043	2035	2032
2023	2042	2042	2040	2020	2039	2021	2024	2022	2029	2029	2034	2041	2040	2034	2032	2016	2040	2027	2027	2043	2035	2036	2020	2016	2027
2024	2015	2031	2023	2044	2021	2039	2028	2041	2029	2034	2028	2022	2039	2041	2016	2031	2020	2041	2022	2041	2036	2027	2037	2044	2023
2025	2018	2043	2018	2040	2025	2016	2044	2026	2015	2028	2020	2017	2041	2025	2018	2024	2041	2022	2036	2043	2016	2034	2038	2024	2017
2026	2024	2028	2030	2036	2042	2016	2036	2030	2019	2037	2036	2031	2043	2015	2025	2016	2017	2020	2019	2039	2015	2040	2023	2021	2020
2027	2044	2029	2032	2033	2044	2026	2028	2039	2024	2039	2042	2036	2020	2019	2039	2019	2039	2042	2022	2033	2043	2038	2032	2044	2020
2028	2019	2027	2041	2035	2029	2018	2044	2021	2019	2029	2027	2015	2044	2024	2023	2025	2038	2040	2024	2016	2021	2020	2021	2025	2027
2029	2022	2024	2028	2032	2017	2044	2024	2027	2015	2032	2018	2025	2037	2021	2042	2036	2027	2021	2035	2034	2035	2040	2028	2030	2019
2030	2017	2024	2041	2021	2033	2032	2031	2015	2021	2021	2029	2042	2028	2043	2030	2021	2034	2037	2017	2035	2016	2025	2035	2037	2018
2031	2026	2019	2015	2019	2026	2017	2022	2033	2041	2015	2021	2016	2037	2021	2015	2019	2018	2015	2016	2043	2019	2041	2020	2038	2022
2032	2020	2021	2018	2044	2037	2030	2030	2027	2027	2020	2015	2042	2033	2030	2024	2035	2034	2034	2035	2026	2024	2023	2020	2044	2035
2033	2026	2035	2016	2021	2025	2033	2017	2037	2019	2036	2041	2023	2033	2024	2039	2034	2021	2027	2018	2035	2040	2022	2017	2029	2033
2034	2025	2033	2021	2015	2030	2027	2017	2027	2022	2037	2029	2016	2038	2024	2024	2019	2032	2044	2039	2030	2034	2035	2026	2024	2028
2035	2035	2018	2022	2035	2029	2030	2027	2027	2019	2022	2039	2017	2038	2025	2036	2040	2033	2032	2015	2016	2025	2015	2021	2033	2020
2036	2026	2023	2016	2022	2023	2025	2023	2030	2017	2020	2043	2043	2034	2031	2018	2017	2016	2022	2044	2034	2024	2021	2033	2019	2031
2037	2043	2029	2017	2042	2044	2029	2015	2041	2026	2022	2017	2036	2026	2031	2021	2040	2040	2040	2044	2040	2039	2028	2040	2023	2023
2038	2031	2023	2028	2028	2020	2033	2029	2029	2025	2017	2040	2019	2036	2021	2022	2043	2025	2015	2034	2020	2032	2039	2027	2026	2026
2039	2040	2033	2035	2033	2039	2039	2030	2042	2029	2019	2041	2026	2025	2035	2041	2035	2016	2044	2033	2039	2020	2039	2027	2031	2037
2040	2047	2048	2051	2064	2041	2061	2037	2061	2035	2058	2040	2039	2058	2050	2060	2041	2043	2054	2037	2052	2036	2041	2050	2063	2061
2041	2064	2040	2037	2062	2036	2063	2041	2035	2045	2043	2037	2048	2053	2062	2059	2044	2040	2037	2047	2061	2058	2056	2055	2043	2055
2042	2056	2035	2056	2051	2061	2044	2058	2064	2050	2035	2035	2057	2042	2058	2040	2050	2050	2050	2057	2061	2043	2049	2063	2055	2052
2043	2062	2062	2060	2040	2059	2041	2044	2042	2049	2049	2054	2061	2060	2054	2052	2036	2060	2047	2047	2063	2055	2056	2040	2036	2047
2044	2035	2051	2043	2064	2041	2059	2048	2061	2049	2054	2048	2042	2059	2061	2036	2051	2040	2061	2042	2061	2056	2047	2057	2064	2043
2045	2038	2063	2038	2060	2045	2036	2064	2046	2035	2048	2040	2037	2061	2045	2038	2044	2061	2042	2056	2063	2036	2054	2058	2044	2037
2046	2044	2048	2050	2056	2062	2036	2056	2050	2039	2057	2056	2051	2063	2035	2045	2036	2037	2040	2039	2059	2035	2060	2043	2041	2040
2047	2064	2049	2052	2053	2064	2046	2048	2059	2044	2059	2062	2056	2040	2039	2059	2039	2059	2062	2042	2053	2063	2058	2052	2064	2040
2048	2039	2047	2061	2055	2049	2038	2064	2041	2039	2049	2047	2035	2064	2044	2043	2045	2058	2060	2044	2036	2041	2040	2041	2045	2047
2049	2042	2044	2048	2052	2037	2064	2044	2047	2035	2052	2038	2045	2057	2041	2062	2056	2047	2041	2055	2054	2055	2060	2048	2050	2039
2050	2037	2044	2061	2041	2053	2052	2051	2035	2041	2041	2049	2062	2048	2063	2050	2041	2054	2057	2037	2055	2036	2045	2055	2057	2038
2051	2046	2039	2035	2039	2046	2037	2042	2053	2061	2035	2041	2036	2057	2041	2035	2039	2038	2035	2036	2063	2039	2061	2040	2058	2042
2052	2040	2041	2038	2064	2057	2050	2050	2047	2047	2040	2035	2062	2053	2050	2044	2055	2054	2054	2055	2046	2044	2043	2040	2064	2055
2053	2046	2055	2036	2041	2045	2053	2037	2057	2039	2056	2061	2043	2053	2044	2059	2054	2041	2047	2038	2055	2060	2042	2037	2049	2053
2054	2045	2053	2041	2035	2050	2047	2037	2047	2042	2057	2049	2036	2058	2044	2044	2039	2052	2064	2059	2050	2054	2055	2046	2044	2048
2055	2055	2038	2042	2055	2049	2050	2047	2047	2039	2042	2059	2037	2058	2045	2056	2060	2053	2052	2035	2036	2045	2035	2041	2053	2040
2056	2046	2043	2036	2042	2043	2045	2043	2050	2037	2040	2063	2063	2054	2051	2038	2037	2036	2042	2064	2054	2044	2041	2053	2039	2051
2057	2063	2049	2037	2062	2064	2049	2035	2061	2046	2042	2037	2056	2046	2051	2041	2060	2060	2060	2064	2060	2059	2048	2060	2043	2043
2058	2051	2043	2048	2048	2040	2053	2049	2049	2045	2037	2060	2039	2056	2041	2042	2063	2045	2035	2054	2040	2052	2059	2047	2046	2046
2059	2060	2053	2055	2053	2059	2059	2050	2062	2049	2039	2061	2046	2045	2055	2061	2055	2036	2064	2053	2059	2040	2059	2047	2051	2057
2060	2066	2066	2069	2081	2060	2079	2057	2078	2055	2075	2059	2059	2075	2068	2077	2061	2062	2072	2057	2070	2056	2060	2068	2080	2078
2061	2081	2059	2056	2079	2056	2080	2061	2055	2064	2063	2056	2067	2071	2079	2076	2063	2059	2057	2066	2078	2076	2073	2073	2062	2073
2062	2074	2055	2074	2069	2078	2063	2076	2081	2068	2055	2055	2074	2061	2075	2059	2069	2069	2068	2075	2079	2062	2068	2080	2073	2070
2063	2080	2080	2077	2059	2077	2060	2063	2061	2068	2068	2072	2078	2078	2072	2070	2056	2077	2066	2066	2080	2073	2074	2059	2056	2066
2064	2055	2069	2062	2081	2060	2077	2066	2078	2068	2072	2067	2062	2077	2078	2056	2069	2060	2078	2061	2079	2074	2066	2075	2081	2062
2065	2058	2080	2058	2078	2064	2056	2081	2065	2055	2066	2060	2057	2079	2064	2057	2063	2078	2061	2074	2080	2055	2072	2076	2063	2057
2066	2063	2066	2068	2074	2079	2056	2074	2069	2058	2075	2074	2069	2081	2055	2064	2056	2056	2059	2058	2077	2055	2078	2062	2060	2060
2067	2081	2068	2070	2071	2081	2064	2067	2077	2063	2077	2080	2074	2059	2059	2077	2058	2076	2079	2061	2071	2080	2076	2070	2081	2059
2068	2058	2066	2079	2073	2068	2057	2081	2061	2058	2068	2066	2055	2081	2063	2062	2064	2076	2078	2063	2055	2060	2059	2060	2064	2066
2069	2061	2063	2066	2071	2057	2081	2063	2066	2055	2070	2057	2064	2075	2060	2080	2074	2066	2060	2073	2072	2073	2077	2066	2068	2059
2070	2057	2063	2079	2060	2071	2071	2069	2055	2060	2061	2068	2079	2067	2080	2069	2061	2072	2075	2057	2073	2056	2064	2073	2074	2058
2071	2065	2059	2055	2058	2065	2057	2062	2071	2078	2055	2061	2055	2075	2060	2055	2059	2057	2055	2056	2080	2059	2079	2059	2076	2061
2072	2060	2060	2058	2081	2075	2069	2068	2066	2066	2060	2055	2079	2071	2068	2063	2073	2072	2072	2073	2065	2063	2062	2059	2081	2073
2073	2065	2073	2056	2061	2064	2071	2057	2075	2058	2074	2079	2062	2071	2063	2077	2072	2060	2066	2058	2073	2077	2061	2057	2067	2071
2074	2064	2071	2060	2055	2068	2066	2056	2065	2061	2075	2068	2055	2075	2063	2063	2059	2070	2081	2076	2068	2072	2073	2065	2063	2066
2075	2073	2058	2061	2073	2068	2069	2066	2065	2058	2062	2077	2057	2076	2064	2074	2078	2072	2070	2055	2056	2064	2055	2060	2071	2059
2076	2065	2063	2056	2061	2063	2064	2062	2069	2057	2059	2080	2080	2072	2069	2058	2056	2056	2061	2081	2072	2063	2060	2071	2058	2070
2077	2080	2068	2057	2079	2081	2068	2055	2078	2065	2062	2057	2074	2065	2069	2060	2077	2078	2077	2081	2077	2077	2067	2077	2062	2062
2078	2069	2062	2066	2066	2060	2071	2068	2067	2064	2057	2077	2058	2074	2060	2061	2080	2064	2055	2072	2060	2070	2076	2066	2065	2064
2079	2077	2072	2073	2072	2076	2077	2069	2080	2068	2059	2079	2065	2064	2073	2078	2073	2056	2081	2071	2077	2059	2076	2066	2070	2075

Table A.2: Order of years that is used to read climate data depending on random seed 26-50

Sim. year	Resampled year using random seed x																								
	26	27	28	29	30	31	32	33	34	35	36	37	38	39	40	41	42	43	44	45	46	47	48	49	50
2000	2004	2007	2016	2020	2014	2003	2020	2002	1996	2008	2016	2023	2006	2011	2007	2002	2006	1998	2020	2024	2018	1998	1995	2004	2009
2001	2016	2009	2000	2019	2022	1995	1996	2015	2000	2008	1997	1999	2021	1995	2014	2015	2018	2009	2007	2004	2002	2020	2007	2009	1998
2002	2010	2019	2011	2003	2006	2023	2006	2008	2018	2004	2013	2008	2020	2018	1996	1996	2023	2013	1998	2011	2014	2024	2021	2002	2001
2003	2003	2022	2003	2005	2001	2004	2007	2015	2007	2015	2016	2010	2022	2019	1998	2004	2000	1998	1995	2015	2015	2022	2002	2017	1997
2004	2018	2017	1998	1997	2014	2018	2011	2007	1997	2001	2023	2000	2023	2019	2018	2015	2016	1999	2017	2003	2002	2016	2003	2022	2002
2005	2011	2009	1999	2024	2007	2013	2004	2022	2007	2002	2019	2017	2021	2006	2016	1999	2018	1999	2013	2007	2022	2019	2015	2000	2013
2006	2018	2021	2006	2017	1999	2024	2023	2002	2013	2003	1999	2012	2016	1998	2003	1996	2012	2002	2005	1997	2017	2005	2003	2021	2006
2007	1997	2006	2006	2009	2014	2014	2017	1998	2008	1995	2020	2004	2007	2019	1999	2013	2012	2000	2000	2023	2001	2006	1998	2017	1995
2008	2021	2006	2018	2008	2023	2001	2017	2021	1995	2019	2019	2013	2014	2013	2008	1998	1999	2004	2005	2008	2004	2016	2018	2015	2006
2009	1998	2003	2004	2004	2016	2005	2016	2017	1998	2015	1997	2020	2022	2013	2012	2022	2008	2019	2003	2022	2024	2024	2023	2004	1999
2010	2000	2024	2010	2011	2005	1999	2019	2000	2023	1998	2005	2015	2013	2010	2004	2013	1999	2020	2013	2009	2023	2018	2004	2012	2024
2011	2001	2020	1995	2004	2013	2001	2005	2013	2017	2010	2022	1997	2010	2007	1999	2018	1997	1997	2002	2009	2016	2022	2006	1996	2023
2012	2003	2021	2000	2016	2024	2022	1998	1995	2007	2013	2000	1998	2001	2008	2010	2000	1996	2014	2006	1996	1996	2014	2020	2011	2007
2013	2017	2021	2009	2020	2022	2022	2008	2020	2005	2013	2009	2013	1999	2001	2000	2017	2008	1996	2015	2016	1997	2006	2009	2017	2019
2014	2009	2001	2020	2020	2002	1997	2022	2023	2002	2003	2002	2017	2006	2009	2013	2015	2020	2011	2007	1999	2008	2007	2008	2001	2018
2015	2019	2013	2023	2019	2015	2023	2003	2021	2007	2003	2007	2013	1999	2015	2022	2016	2005	2013	2003	2005	2006	2004	2017	2000	2002
2016	2017	2017	2023	2018	2012	1997	2013	2015	2000	2015	2013	2003	2002	2013	2018	2022	2013	1995	2010	1998	2022	2016	2011	2018	2017
2017	2013	2007	2019	2015	1995	2020	2017	1995	2019	2021	2019	1998	2019	2002	1998	2020	1999	2012	2022	1996	1996	2001	2008	2020	2004
2018	2000	2014	2024	2016	2007	2011	2012	2009	2007	2015	1995	2017	1997	2022	2015	2007	2016	2017	2016	2013	2008	2002	2005	2021	2004
2019	2006	2013	2012	2020	2008	1998	2019	2019	2017	2024	2022	2004	2019	2022	2010	2019	2014	2002	2001	2001	2001	2014	2014	2022	2008
2020	2024	2027	2036	2040	2034	2023	2040	2022	2016	2028	2036	2043	2026	2031	2027	2022	2026	2018	2040	2044	2038	2018	2015	2024	2029
2021	2036	2029	2020	2039	2042	2015	2016	2035	2020	2028	2017	2019	2041	2015	2034	2035	2038	2029	2027	2024	2022	2040	2027	2029	2018
2022	2030	2039	2031	2023	2026	2043	2026	2028	2038	2024	2033	2028	2040	2038	2016	2016	2043	2033	2018	2031	2034	2044	2041	2022	2021
2023	2023	2042	2023	2025	2021	2024	2027	2035	2027	2035	2036	2030	2042	2039	2018	2024	2020	2018	2015	2035	2035	2042	2022	2037	2017
2024	2038	2037	2018	2017	2034	2038	2031	2027	2017	2021	2043	2020	2043	2039	2038	2035	2036	2019	2037	2023	2022	2036	2023	2042	2022
2025	2031	2029	2019	2044	2027	2033	2024	2042	2027	2022	2039	2037	2041	2026	2036	2019	2038	2019	2033	2027	2042	2039	2035	2020	2033
2026	2038	2041	2026	2037	2019	2044	2043	2022	2033	2023	2019	2032	2036	2018	2023	2016	2032	2022	2025	2017	2037	2025	2023	2041	2026
2027	2017	2026	2026	2029	2034	2034	2037	2018	2028	2015	2040	2024	2027	2039	2019	2033	2032	2020	2020	2043	2021	2026	2018	2037	2015
2028	2041	2026	2038	2028	2043	2021	2037	2041	2015	2039	2039	2033	2034	2033	2028	2018	2019	2024	2025	2028	2024	2036	2038	2035	2026
2029	2018	2023	2024	2024	2036	2025	2036	2037	2018	2035	2017	2040	2042	2033	2032	2042	2028	2039	2023	2042	2044	2044	2043	2024	2019
2030	2020	2044	2030	2031	2025	2019	2039	2020	2043	2018	2025	2035	2033	2030	2024	2033	2019	2040	2033	2029	2043	2038	2024	2032	2044
2031	2021	2040	2015	2024	2033	2021	2025	2033	2037	2030	2042	2017	2030	2027	2019	2038	2017	2017	2022	2029	2036	2042	2026	2016	2043
2032	2023	2041	2020	2036	2044	2042	2018	2015	2027	2033	2020	2018	2021	2028	2030	2020	2016	2034	2026	2016	2016	2034	2040	2031	2027
2033	2037	2041	2029	2040	2042	2042	2028	2040	2025	2033	2029	2033	2019	2021	2020	2037	2028	2016	2035	2036	2017	2026	2029	2037	2039
2034	2029	2021	2040	2040	2022	2017	2042	2043	2022	2023	2022	2037	2026	2029	2033	2035	2040	2031	2027	2019	2028	2027	2028	2021	2038
2035	2039	2033	2043	2039	2035	2043	2023	2041	2027	2023	2027	2033	2019	2035	2042	2036	2025	2033	2023	2025	2026	2024	2037	2020	2022
2036	2037	2037	2043	2038	2032	2017	2033	2035	2020	2035	2033	2023	2022	2033	2038	2042	2033	2015	2030	2018	2042	2036	2031	2038	2037
2037	2033	2027	2039	2035	2015	2040	2037	2015	2039	2041	2039	2018	2039	2022	2018	2040	2019	2032	2042	2016	2016	2021	2028	2040	2024
2038	2020	2034	2044	2036	2027	2031	2032	2029	2027	2035	2015	2037	2017	2042	2035	2027	2036	2037	2036	2033	2028	2022	2025	2041	2024
2039	2026	2033	2032	2040	2028	2018	2039	2039	2037	2044	2042	2024	2039	2042	2030	2039	2034	2022	2021	2021	2021	2034	2034	2042	2028
2040	2044	2047	2056	2060	2054	2043	2060	2042	2036	2048	2056	2063	2046	2051	2047	2042	2046	2038	2060	2064	2058	2038	2035	2044	2049
2041	2056	2049	2040	2059	2062	2035	2036	2055	2040	2048	2037	2039	2061	2035	2054	2055	2058	2049	2047	2044	2042	2060	2047	2049	2038
2042	2050	2059	2051	2043	2046	2063	2046	2048	2058	2044	2053	2048	2060	2058	2036	2036	2063	2053	2038	2051	2054	2064	2061	2042	2041
2043	2043	2062	2043	2045	2041	2044	2047	2055	2047	2055	2056	2050	2062	2059	2038	2044	2040	2038	2035	2055	2055	2062	2042	2057	2037
2044	2058	2057	2038	2037	2054	2058	2051	2047	2037	2041	2063	2040	2063	2059	2058	2055	2056	2039	2057	2043	2042	2056	2043	2062	2042
2045	2051	2049	2039	2064	2047	2053	2044	2062	2047	2042	2059	2057	2061	2046	2056	2039	2058	2039	2053	2047	2062	2059	2055	2040	2053
2046	2058	2061	2046	2057	2039	2064	2063	2042	2053	2043	2039	2052	2056	2038	2043	2036	2052	2042	2045	2037	2057	2045	2043	2061	2046
2047	2037	2046	2046	2049	2054	2054	2057	2038	2048	2035	2060	2044	2047	2059	2039	2053	2052	2040	2040	2063	2041	2046	2038	2057	2035
2048	2061	2046	2058	2048	2063	2041	2057	2061	2035	2059	2059	2053	2054	2053	2048	2038	2039	2044	2045	2048	2044	2056	2058	2055	2046
2049	2038	2043	2044	2044	2056	2045	2056	2057	2038	2055	2037	2060	2062	2053	2052	2062	2048	2059	2043	2062	2064	2064	2063	2044	2039
2050	2040	2064	2050	2051	2045	2039	2059	2040	2063	2038	2045	2055	2053	2050	2044	2053	2039	2060	2053	2049	2063	2058	2044	2052	2064
2051	2041	2060	2035	2044	2053	2041	2045	2053	2057	2050	2062	2037	2050	2047	2039	2058	2037	2037	2042	2049	2056	2062	2046	2036	2063
2052	2043	2061	2040	2056	2064	2062	2038	2035	2047	2053	2040	2038	2041	2048	2050	2040	2036	2054	2046	2036	2036	2054	2060	2051	2047
2053	2057	2061	2049	2060	2062	2062	2048	2060	2045	2053	2049	2053	2039	2041	2040	2057	2048	2036	2055	2056	2037	2046	2049	2057	2059
2054	2049	2041	2060	2060	2042	2037	2062	2063	2042	2043	2042	2057	2046	2049	2053	2055	2060	2051	2047	2039	2048	2047	2048	2041	2058
2055	2059	2053	2063	2059	2055	2063	2043	2061	2047	2043	2047	2053	2039	2055	2062	2056	2045	2053	2043	2045	2046	2044	2057	2040	2042
2056	2057	2057	2063	2058	2052	2037	2053	2055	2040	2055	2053	2043	2042	2053	2058	2062	2053	2035	2050	2038	2062	2056	2051	2058	2057
2057	2053	2047	2059	2055	2035	2060	2057	2035	2059	2061	2059	2038	2059	2042	2038	2060	2039	2052	2062	2036	2036	2041	2048	2060	2044
2058	2040	2054	2064	2056	2047	2051	2052	2049	2047	2055	2035	2057	2037	2062	2055	2047	2056	2057	2056	2053	2048	2042	2045	2061	2044
2059	2046	2053	2052	2060	2048	2038	2059	2059	2057	2064	2062	2044	2059	2062	2050	2059	2054	2042	2041	2041	2041	2054	2054	2062	2048
2060	2063	2066	2074	2078	2072	2062	2078	2061	2056	2067	2074	2080	2065	2069	2066	2061	2065	2058	2077	2081	2076	2058	2055	2063	2068
2061	2074	2067	2059	2076	2079	2055	2056	2073	2060	2067	2057	2058	2079	2055	2072	2073	2076	2068	2066	2063	2061	2077	2066	2067	2058
2062	2069	2076	2070	2062	2065	2080	2065	2067	2076	2063	2071	2067	2078	2076	2056	2056	2080	2071	2057	2069	2072	2081	2079	2061	2061
2063	2062	2079	2062	2064	2060	2063	2066	2073	2066	2073	2074	2069	2079	2076	2058	2063	2059	2057	2055	2073	2073	2079	2062	2075	2057
2064	2075	2074	2058	2056	2072	2075	2069	2066	2057	2061	2080	2060	2080	2077	2076	2073	2074	2058	2075	2062	2061	2074	2062	2080	2061
2065	2070	2067	2059	2081	2066	2071	2063	2079	2066	2061	2077	2075	2079	2064	2074	2059	2076	2059	2071	2066	2079	2077	2073	2060	2071
2066	2076	2078	2065	2075	2059	2081	2080	2062	2072	2062	2058	2070	2073	2058	2062	2056	2071	2061	2064	2057	2075	2064	2063	2079	2065
2067	2057	2065	2065	2068	2072	2072	2075	2057	2067	2055	2078	2063	2065	2077	2058	2071	2071	2059	2059	2080	2060	2065	2057	2075	2055
2068	2078	2065	2076	2067	2080	2060	2074	2078	2055	2077	2076	2071	2072	2071	2067	2058	2059	2063	2064	2067	2063	2074	2076	2073	2065
2069	2057	2062	2063	2063	2074	2064	2074	2075	2057	2073	2057	2078	2079	2071	2070	2079	2067	2076	2063	2079	2081	2081	2081	2063	2059
2070	2060	2081	2068	2069	2064	2058	2077	2059	2080	2058	2064	2073	2071	2069	2063	2071	2059	2078	2071	2067	2080	2076	2063	2070	2081
2071	2061	2077	2055	2063	2071	2060	2064	2071	2075	2068	2079	2056	2069	2066	2058	2076	2057	2057	2061	2067	2074	2080	2065	2055	2080
2072	2062	2079	2059	2074	2081	2079	2057	2055	2066	2071	2060	2057	2060	2067	2069	2060	2056	2072	2065	2056	2056	2072	2078	2069	2066
2073	2075	2078	2068	2078	2080	2079	2067	2077	2064	2071	2068	2071	2059	2061	2059	2075	2067	2056	2073	2074	2057	2065	2067	2074	2076
2074	2068	2060	2078	2077	2061	2056	2080	2080	2061	2062	2061	2075	2065	2067	2071	2073	2078	2069	2066	2059	2066	2066	2067	2060	2075
2075	2077	2071	2080	2077	2073	2080	2062	2078	2066	2062	2066	2072	2058	2073	2079	2073	2064	2071	2062	2064	2065	2063	2075	2059	2061
2076	2074	2075	2080	2075	2070	2057	2071	2073	2060	2073	2072	2062	2061	2072	2075	2079	2071	2055	2068	2058	2079	2074	2069	2075	2075
2077	2071	2065	2077	2073	2055	2077	2075	2055	2076	2078	2076	2058	2077	2061	2057	2077	2058	2071	2079	2056	2056	2061	2067	2077	2063
2078	2060	2072	2081	2074	2065	2069	2071	2068	2066	2073	2055	2075	2057	2079	2073	2066	2074	2074	2074	2071	2067	2061	2064	2079	2063
2079	2065	2072	2070	2077	2066	2058	2077	2077	2075	2081	2079	2063	2076	2080	2068	2076	2072	2061	2060	2060	2061	2072	2072	2079	2066

A.3 Population Persistence

The following figure shows the spatial distribution of population mean lifetime [years] distinguished by climate change scenarios FF (RCP2.6, green), MOD (RCP4.5, yellow) and BAU (RCP8.5, pink) simulation periods (2000-19, 2020-39, 2040-59, 2060-79 and calendar week of mowing (none or 20-40).

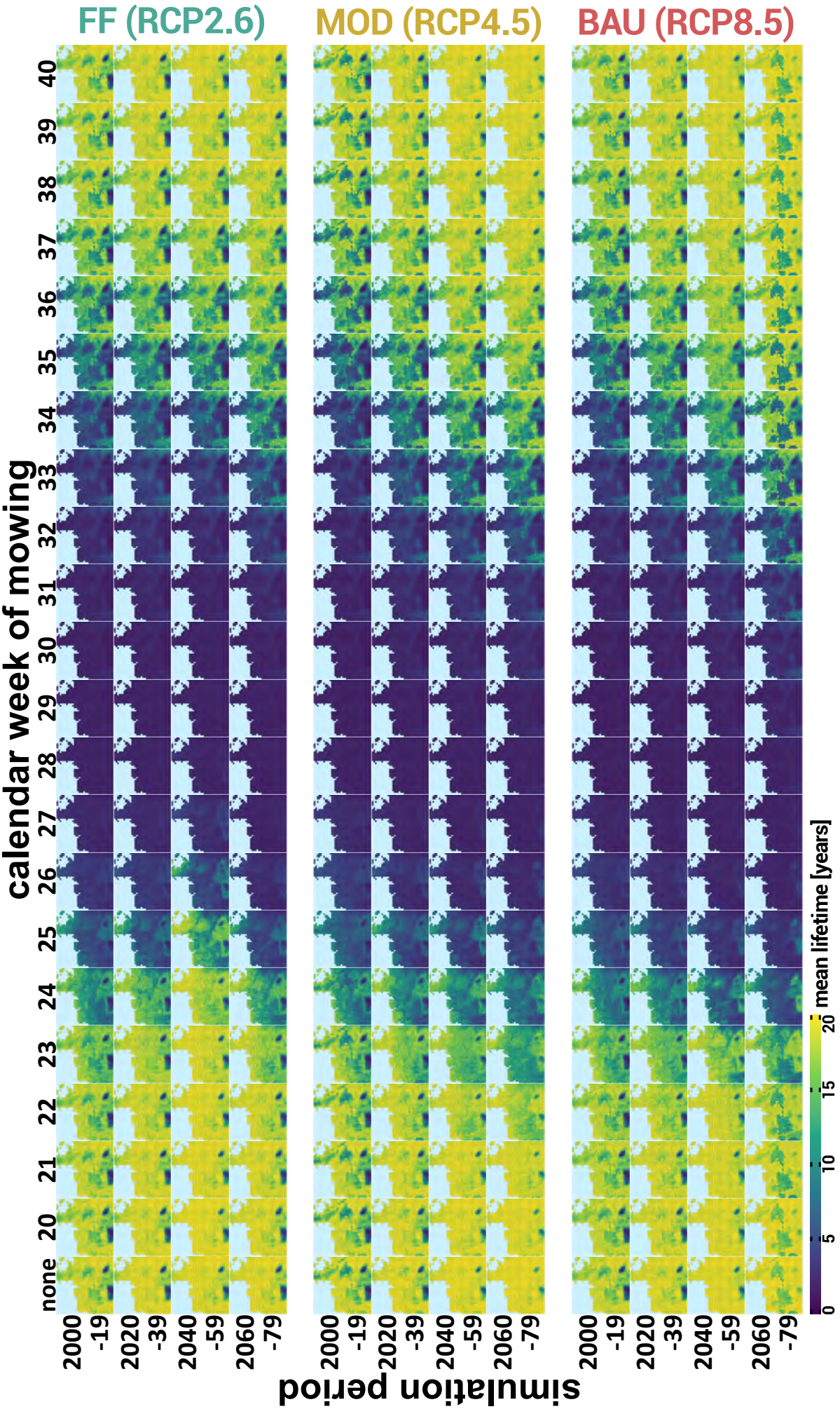

Figure A.2: Spatial distribution of population mean lifetime by climate change scenario, period and mowing week

B Appendix to Chapter 4

B.1 Illustration of Dispersal Success

This section contains illustrations for dispersal success of the large marsh grasshopper (LMG) per climate change scenarios (CCS) depending on source habitat and mowing schedule in terms of three evaluation parameters: (Section B.1.1) the maximum established distance in meters from a source habitat to a habitat with imago density $\geq 0.002\ individuals\ m^{-2}$ during a year, (Section B.1.2) the population size in total number of eggs in all established habitats by the end of a simulation year, and (Section B.1.3) the population density in $eggs\ m^{-2}$ for all established habitats by the end of a simulation year. The title of each Figure indicates, which evaluation parameter, CCS (FF, MOD or BAU) and mowing schedule (cf. Chapter 4, Table 4.1) applies. Each of the 107 subplots in every Figure represents INDEPENDENT simulation runs, or rather their mean over 10 replicate runs, and depicts the results of the dispersal process from a SINGLE initial population in the center of a cell. Inside each subplot, dots are the log-scaled yearly means of the respective value, solid black lines represents their smoothed trends using a generalized additive model and dashed horizontal grey lines mark the mean of the yearly values during the 60 simulation years. The background color of the subplots (FF=green, MOD=brown, BAU=pink) highlights the latter mean value in comparison to other subplots, where a LIGHTER color represents a lower mean, and reflects in the bottom legend.

B.1.1 Illustration of *Maximum Established Distance*

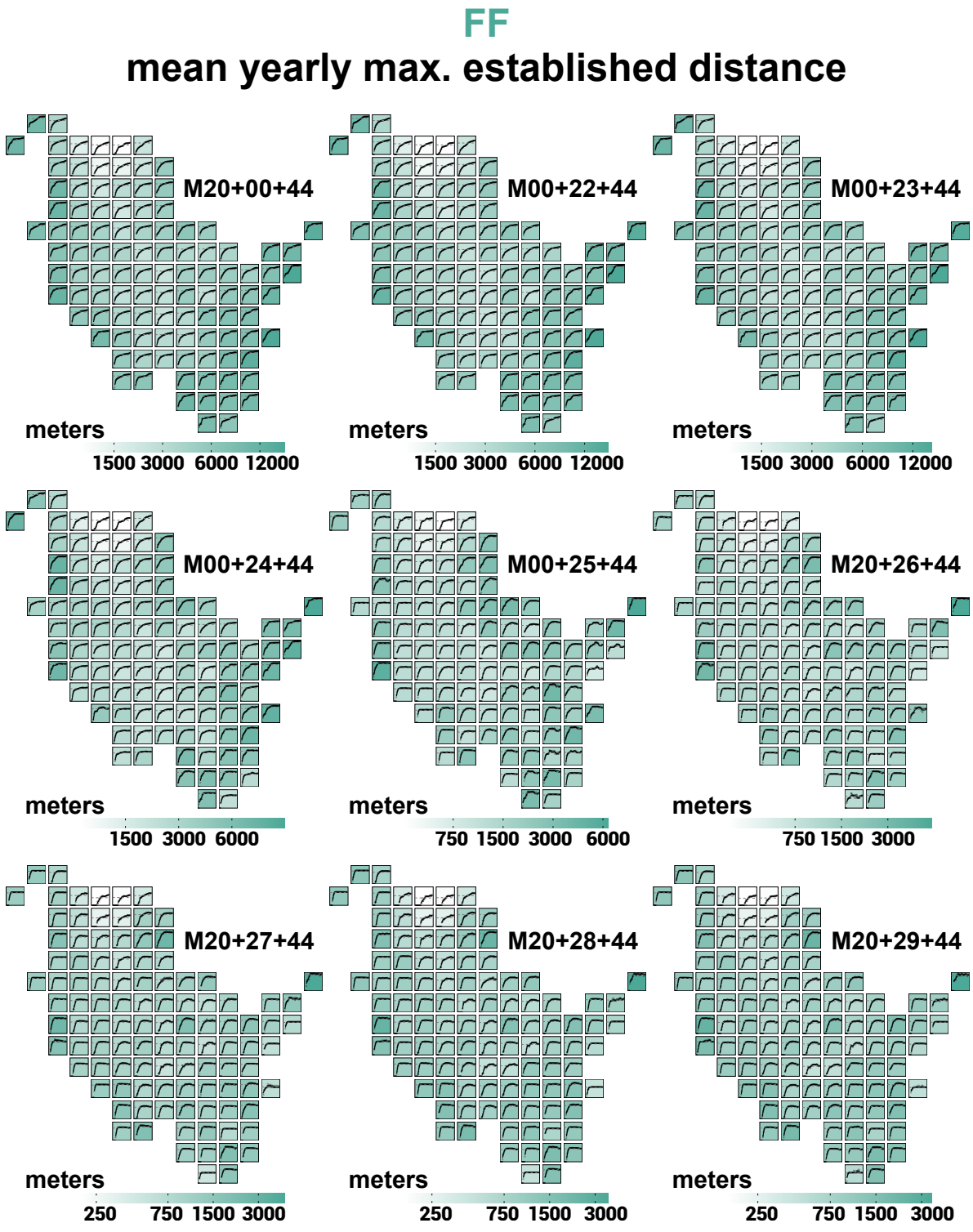

Figure B.1: Map of maximum established distance for scenario FF and mowing schedules M00 and M22-M29

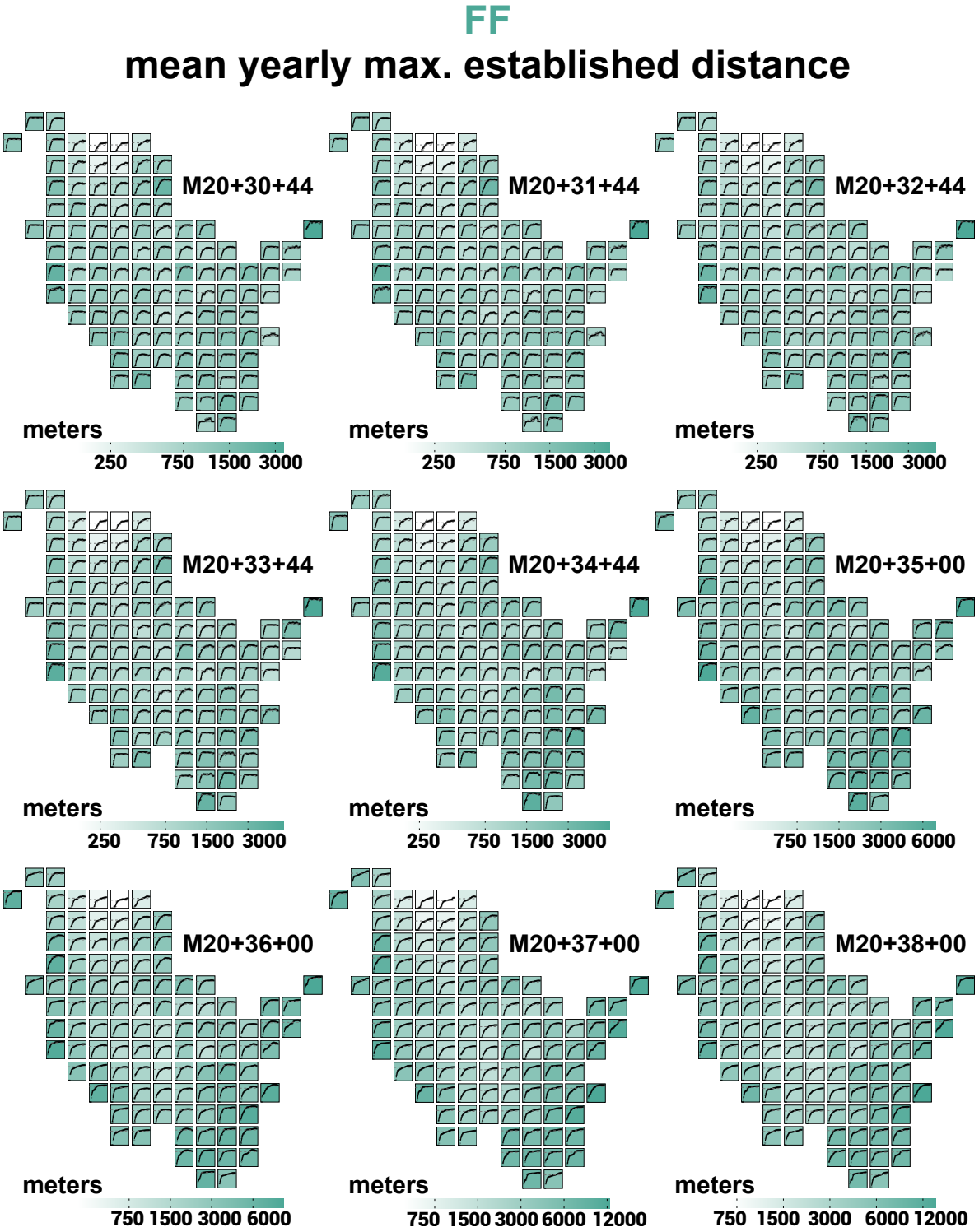

Figure B.2: Map of maximum established distance for scenario FF and mowing schedules M30-M38

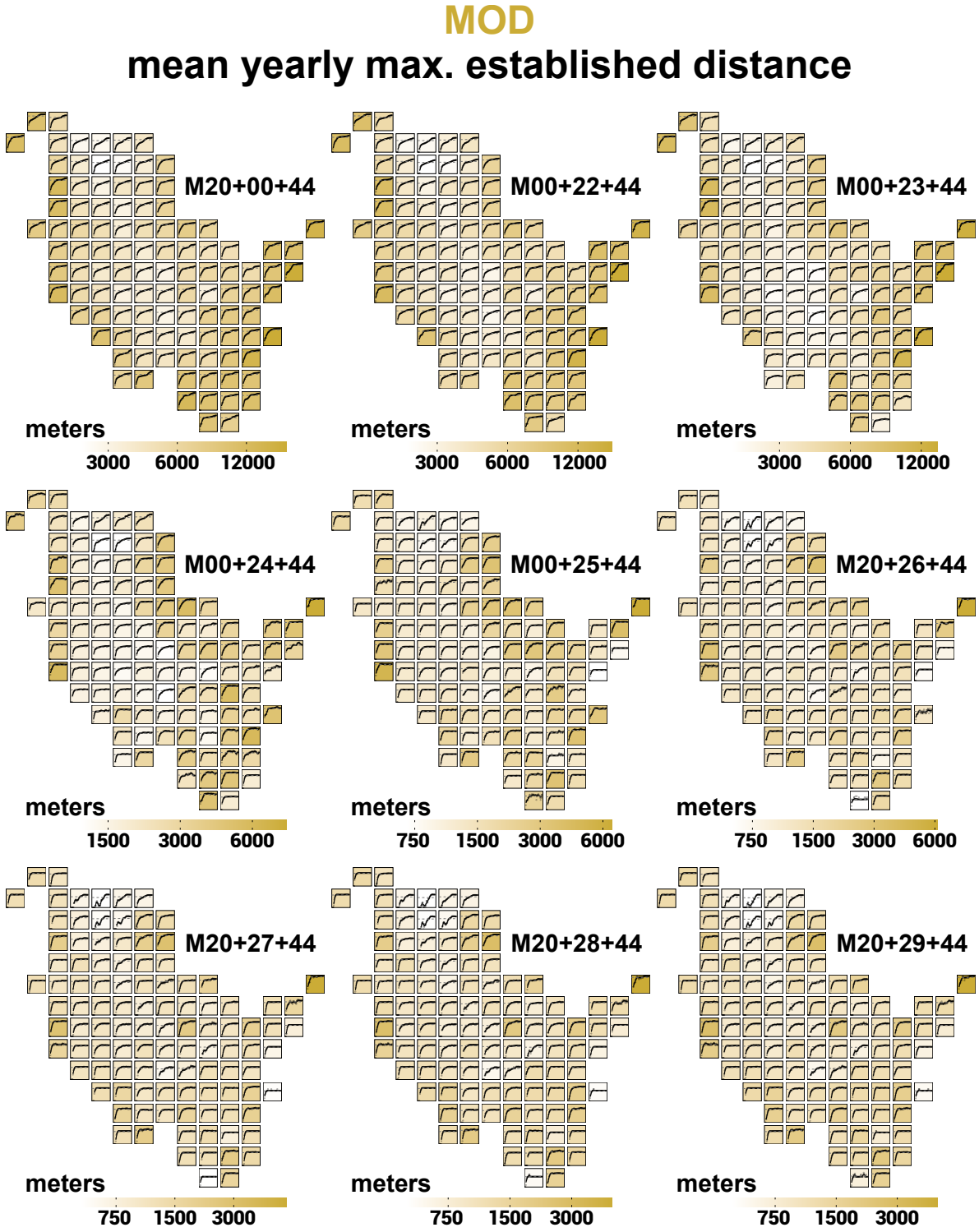

Figure B.3: Map of maximum established distance for scenario MOD and mowing schedules M00 and M22-M29

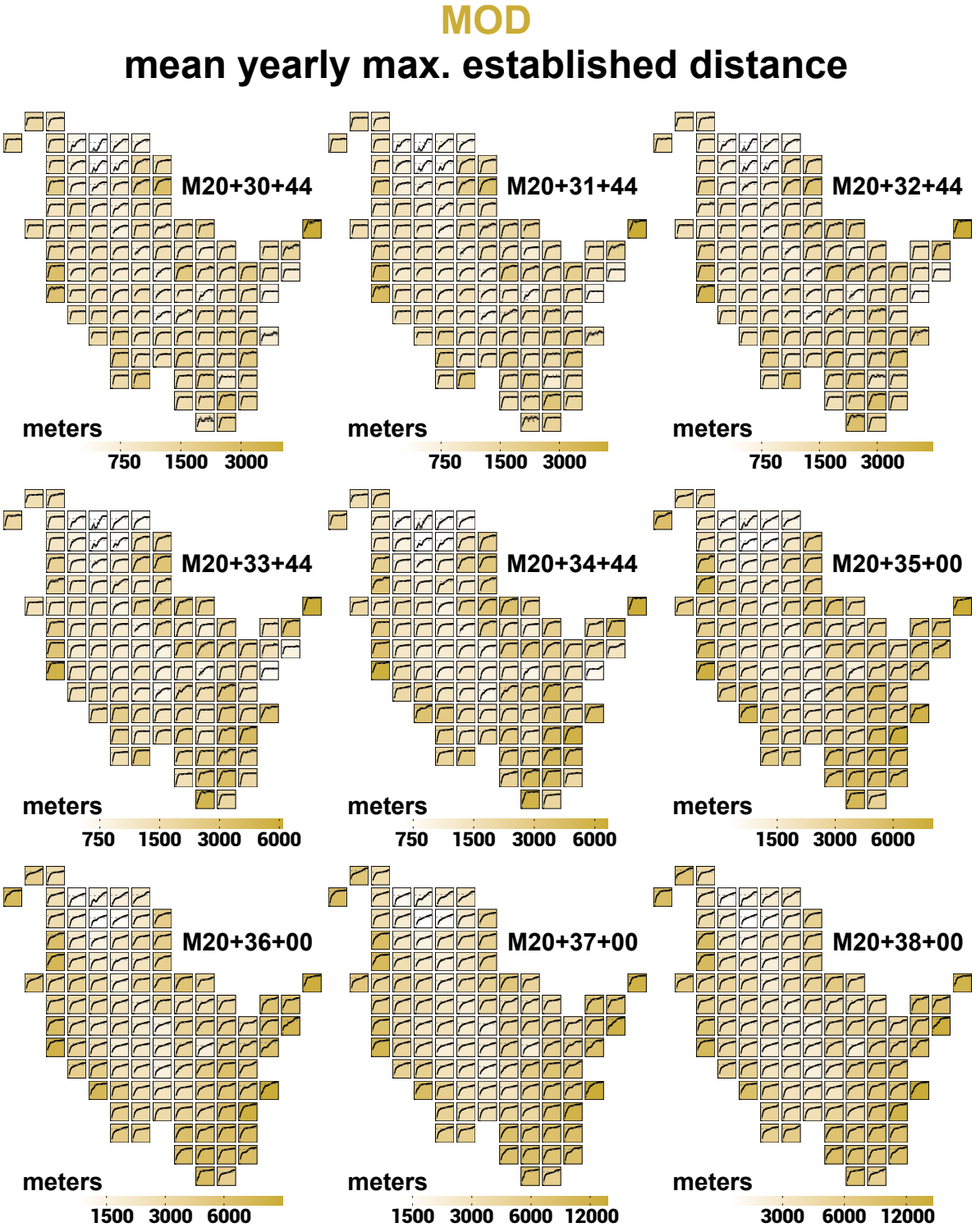

Figure B.4: Map of maximum established distance for scenario MOD and mowing schedules M30-M38

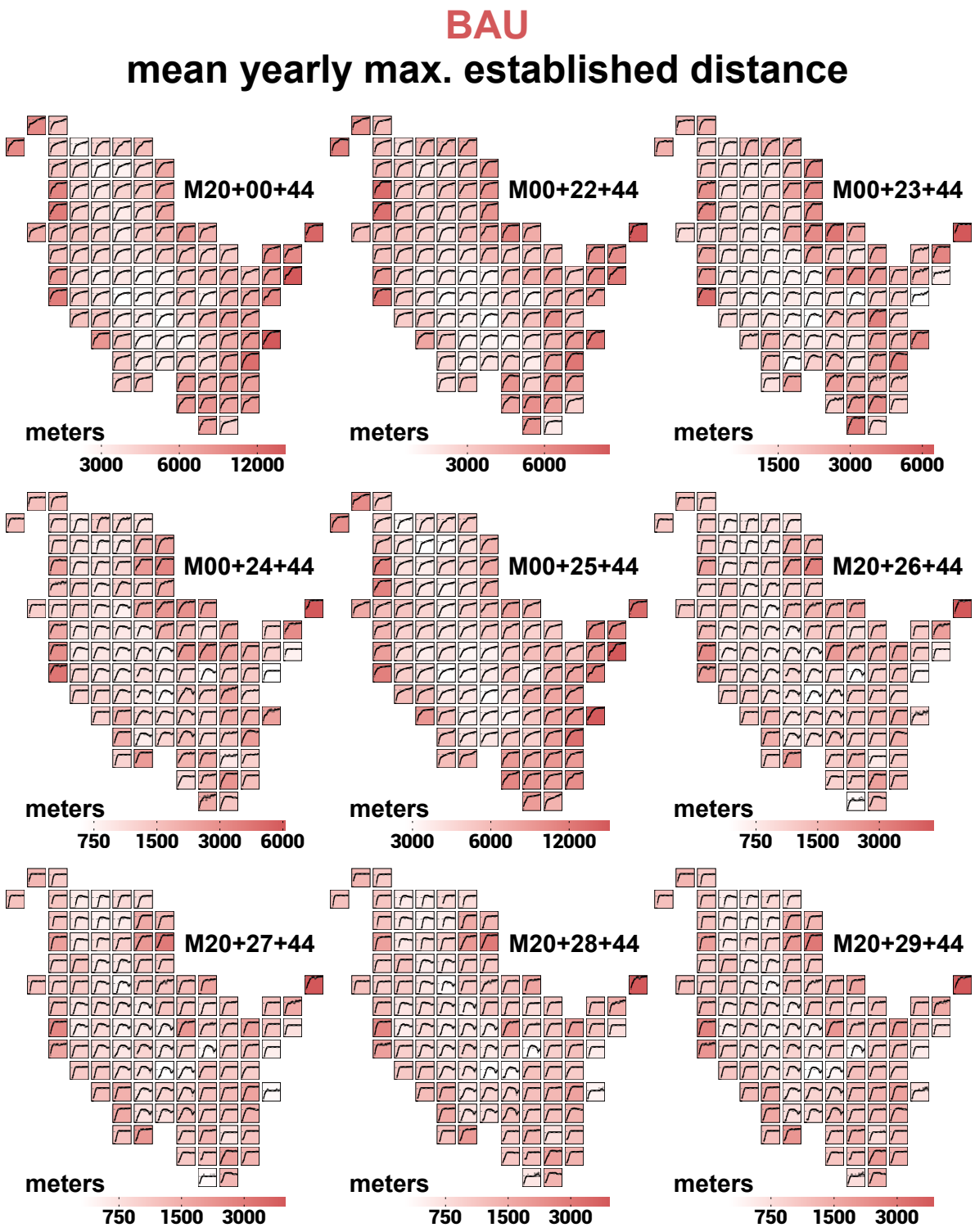

Figure B.5: Map of maximum established distance for scenario BAU and mowing schedules M00 and M22-M29

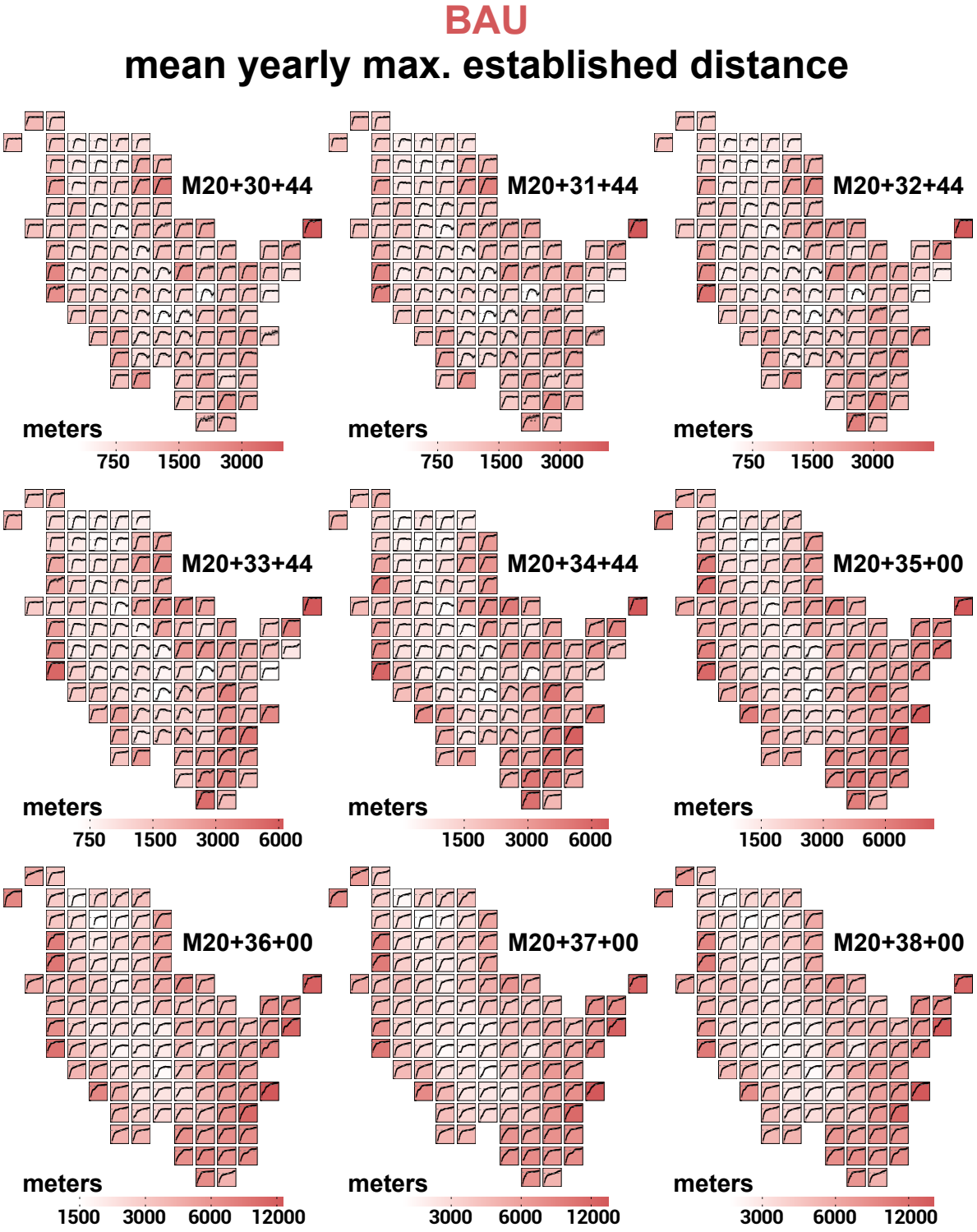

Figure B.6: Map of maximum established distance for scenario BAU and mowing schedules M30-M38

B.1.2 Illustration of *Population Size*

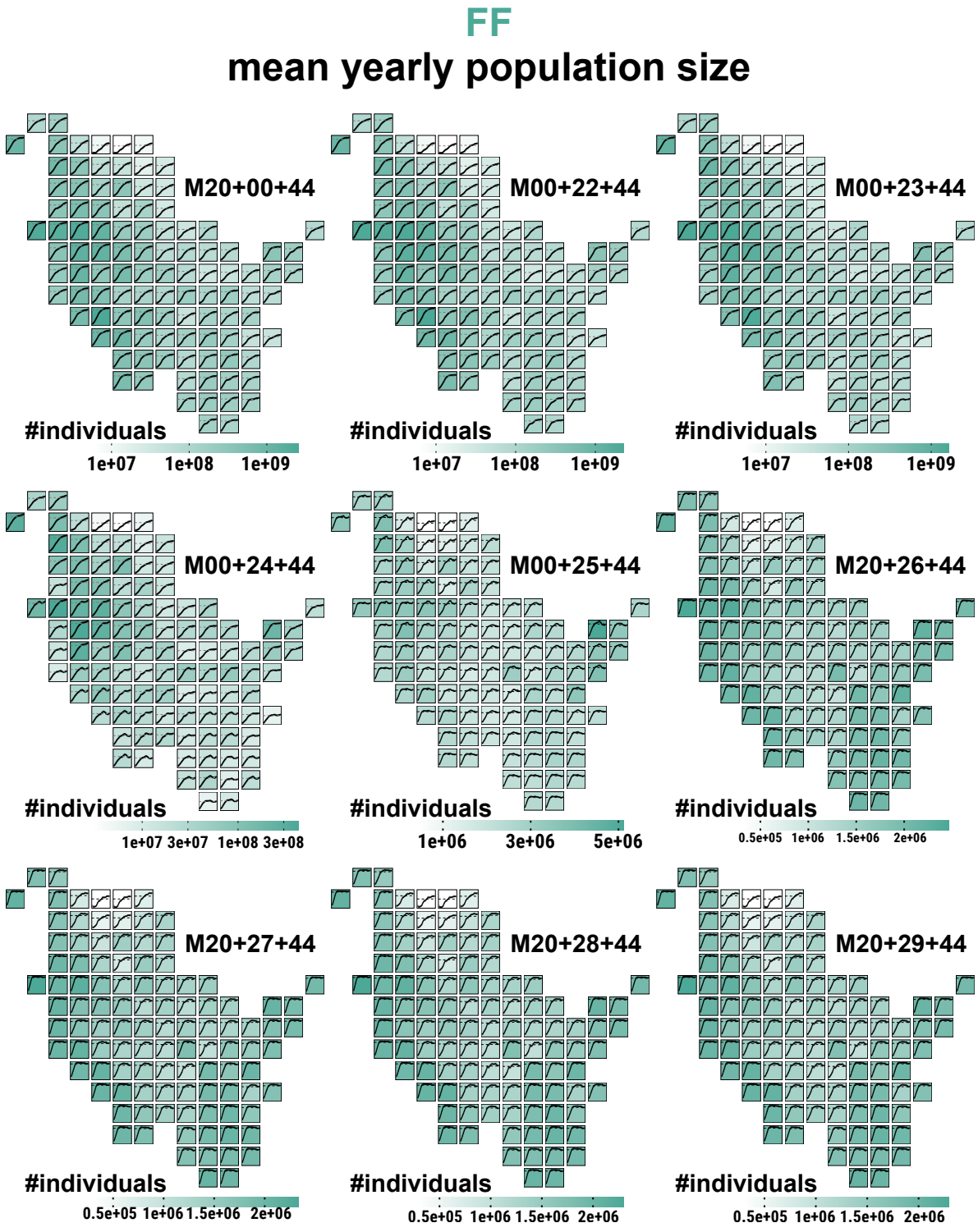

Figure B.7: Map of final population size for scenario FF and mowing schedules M00 and M22-M29

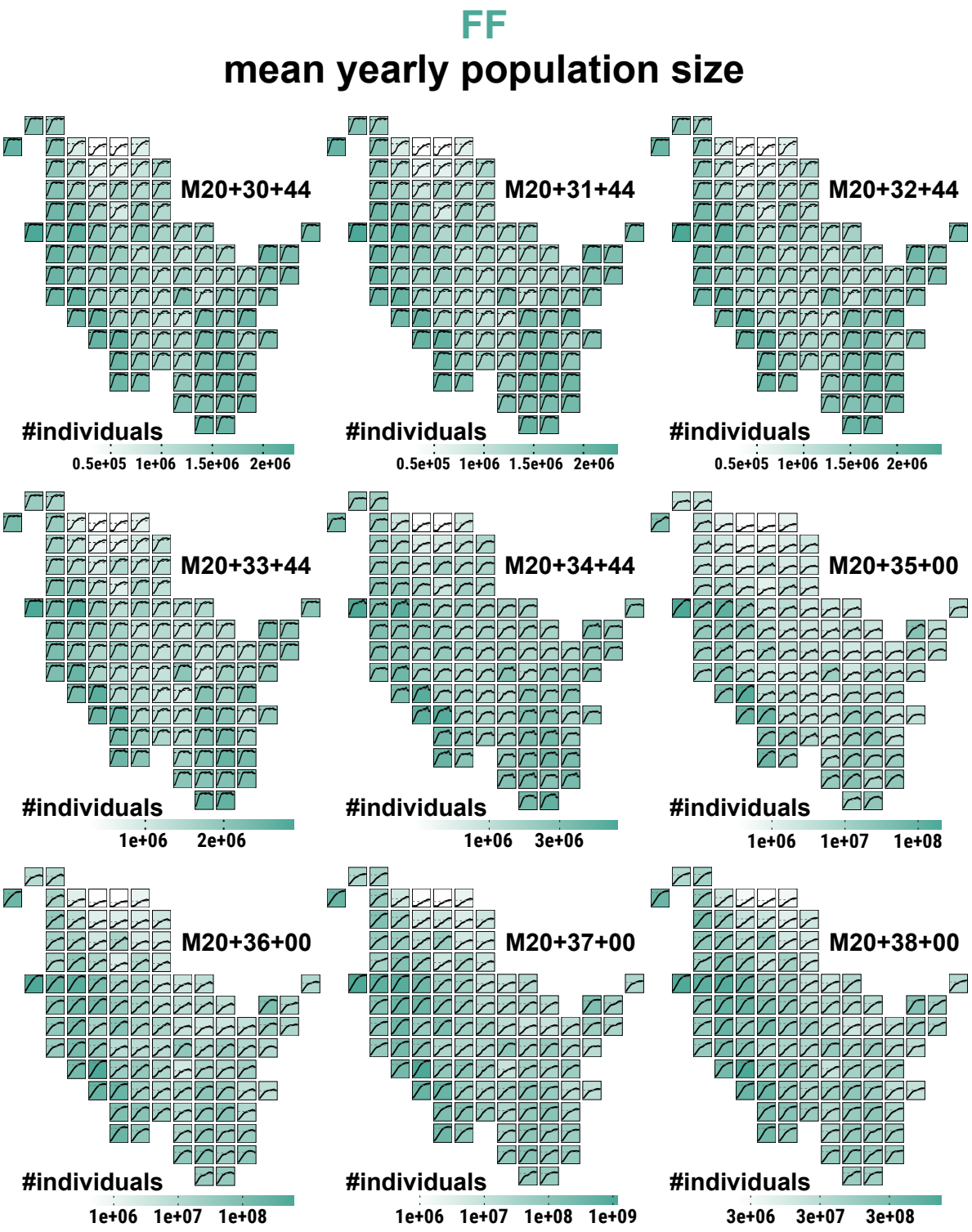

Figure B.8: Map of final population size for scenario FF and mowing schedules M30-M38

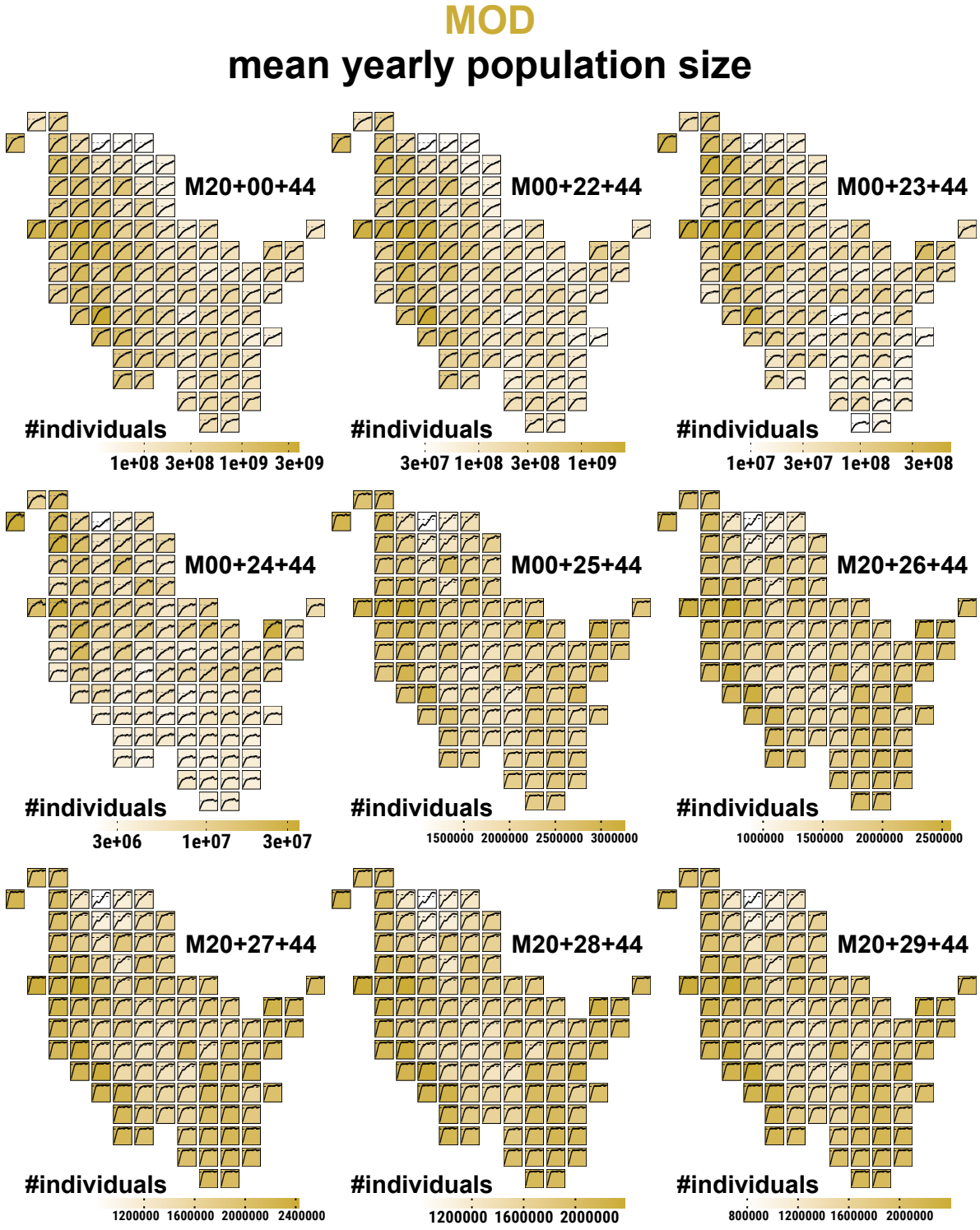

Figure B.9: Map of final population size for scenario MOD and mowing schedules M00 and M22-M29

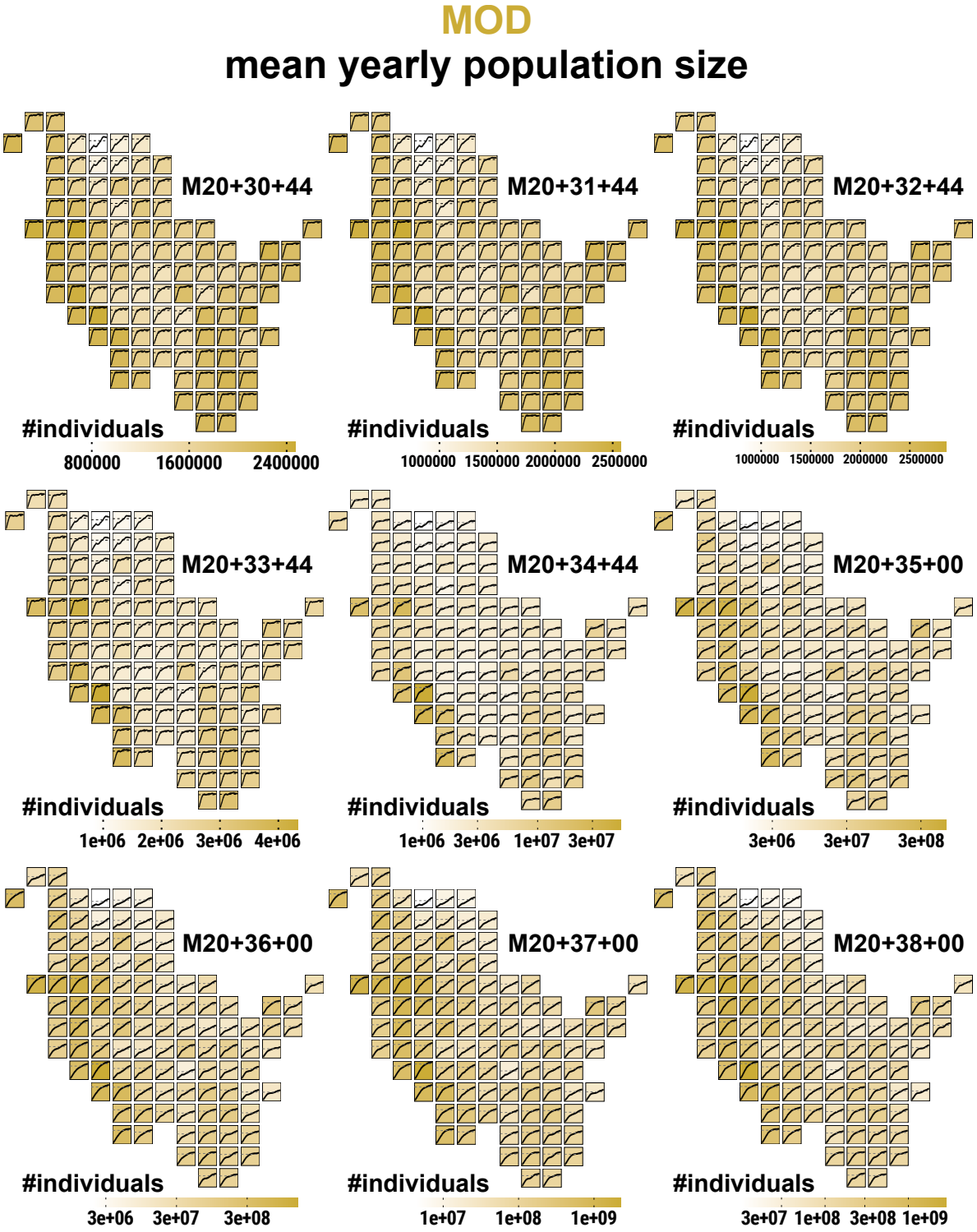

Figure B.10: Map of final population size for scenario MOD and mowing schedules M30-M38

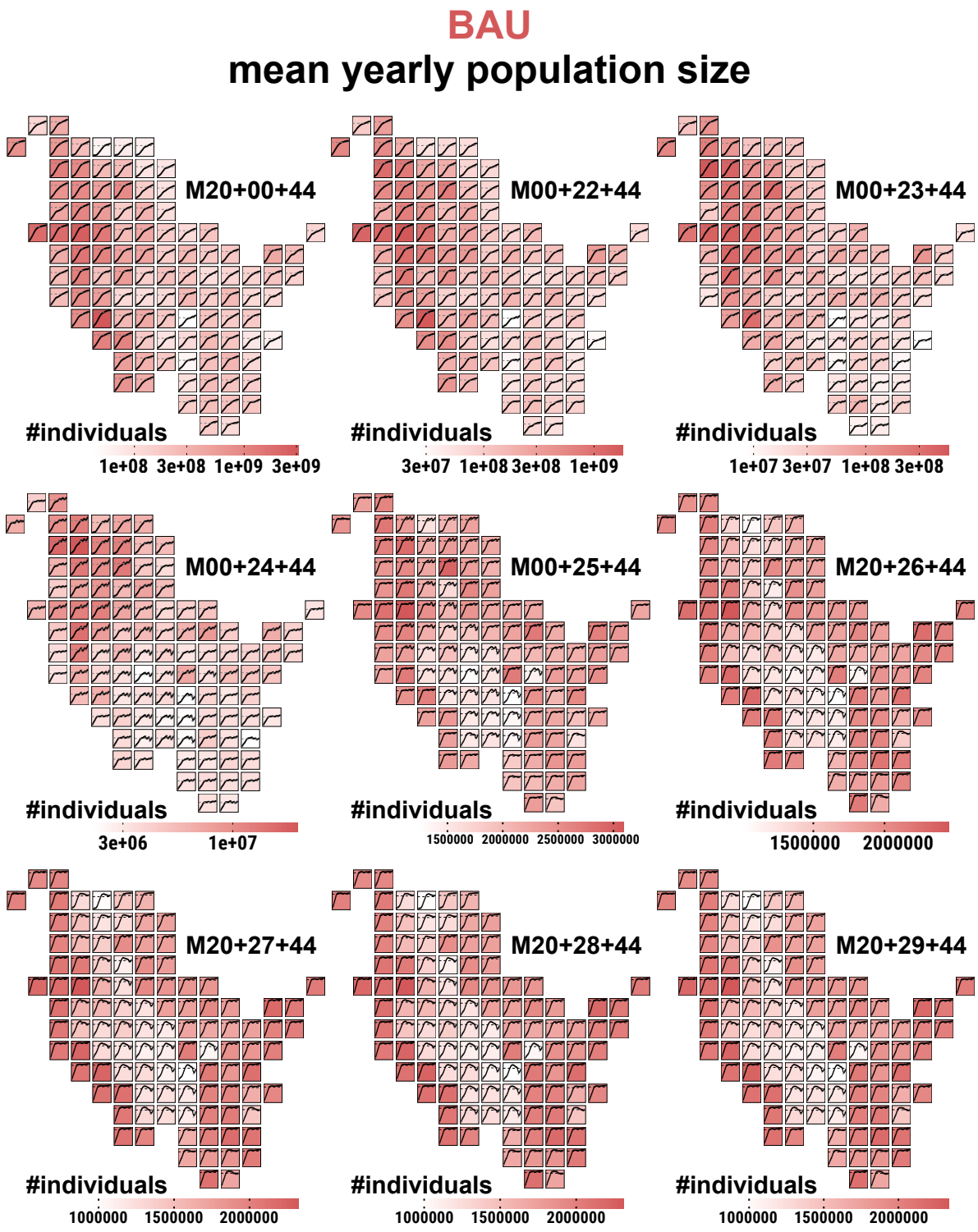

Figure B.11: Map of final population size for scenario BAU and mowing schedules M00 and M22-M29

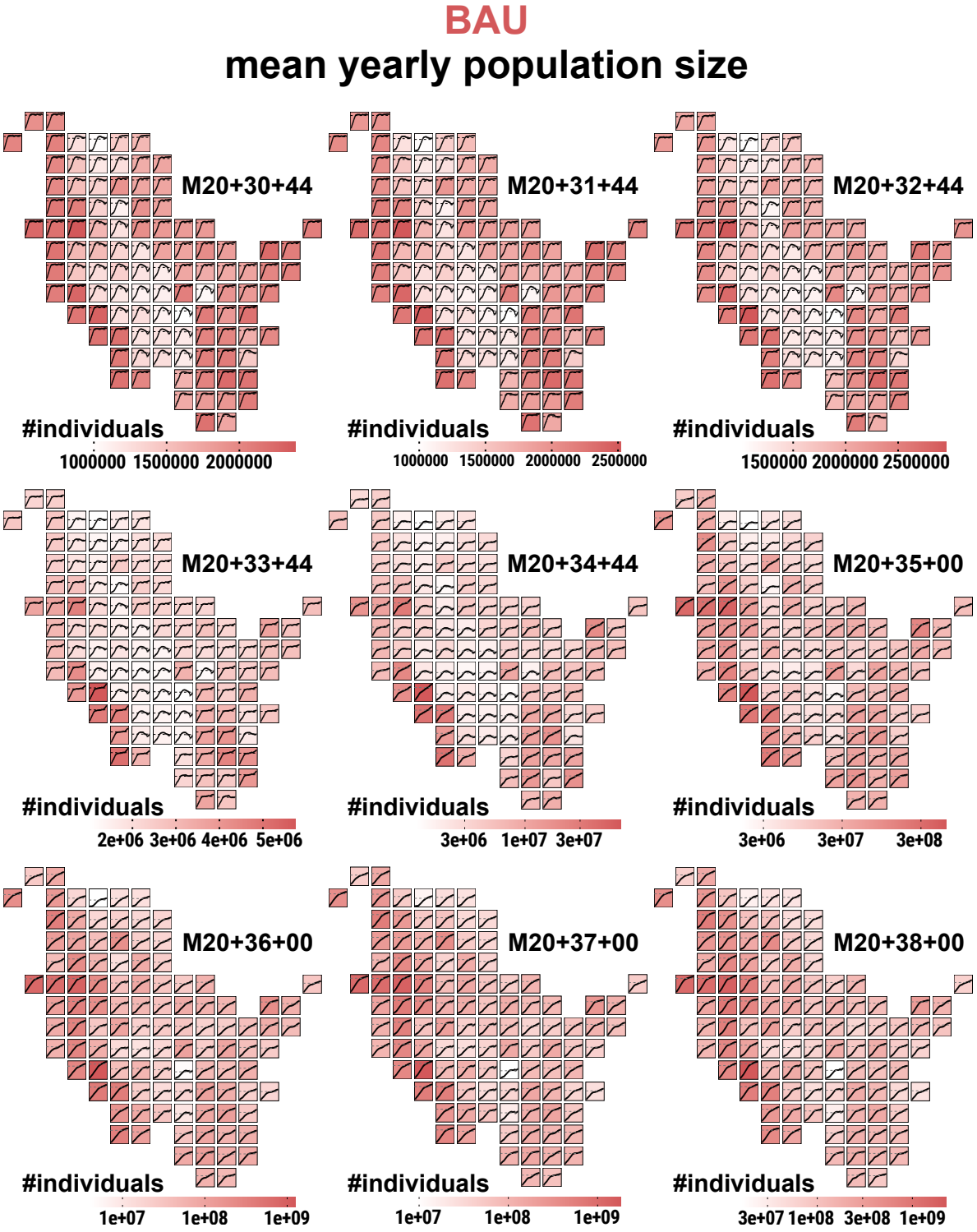

Figure B.12: Map of final population size for scenario BAU and mowing schedules M30-M38

B.1.3 Illustration of *Population Density*

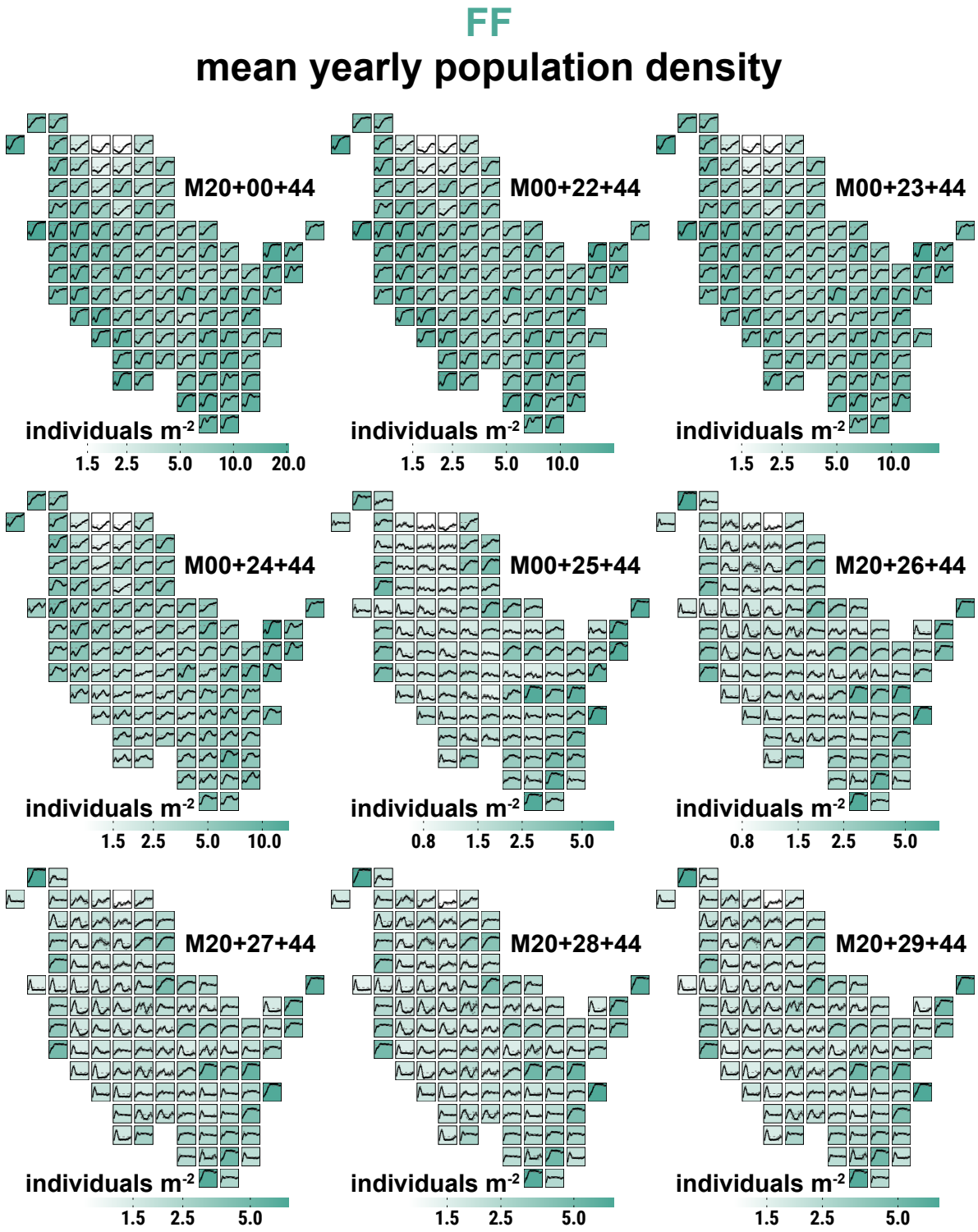

Figure B.13: Map of final population density for scenario FF and mowing schedules M00 and M22-M29

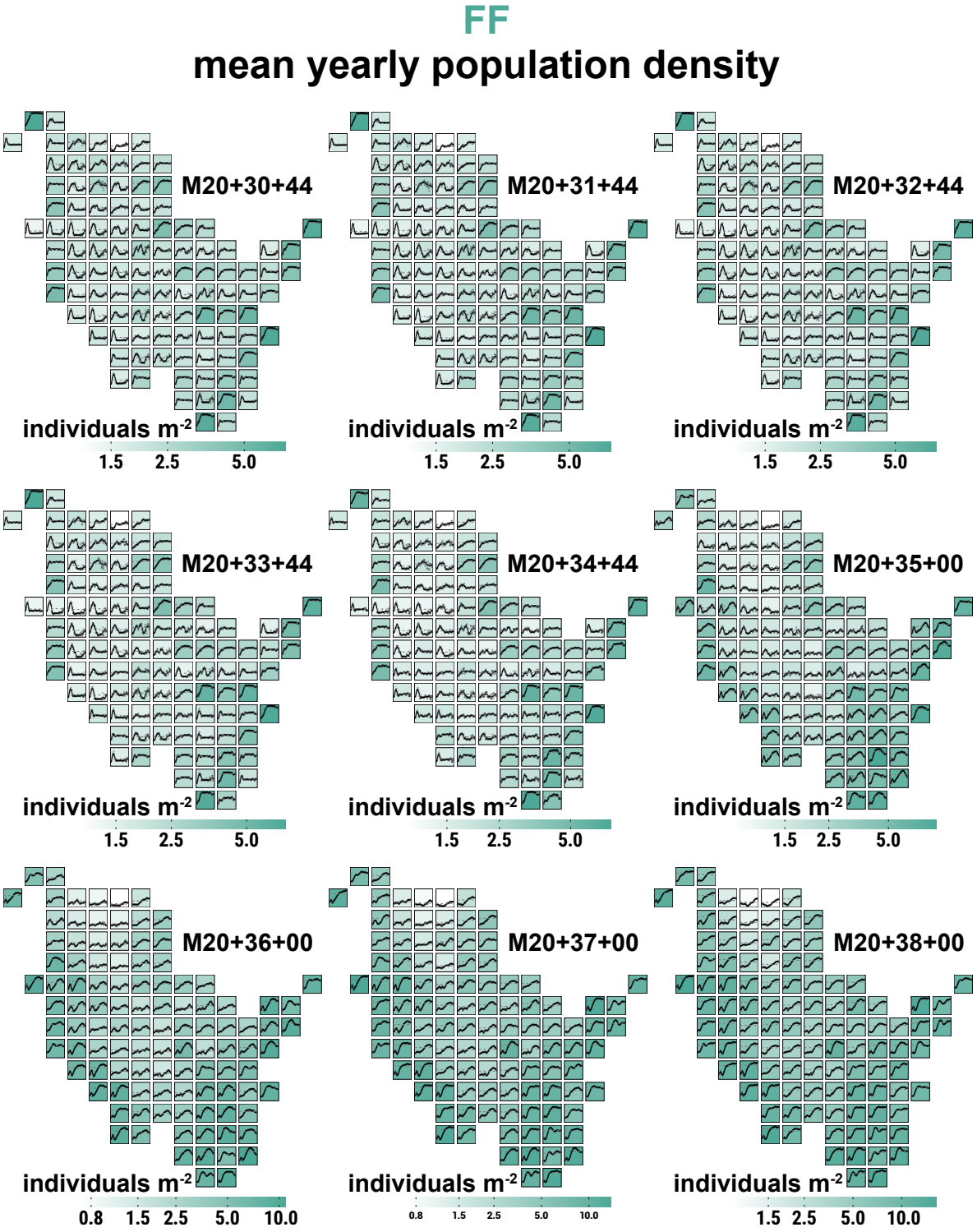

Figure B.14: Map of final population density for scenario FF and mowing schedules M30-M38

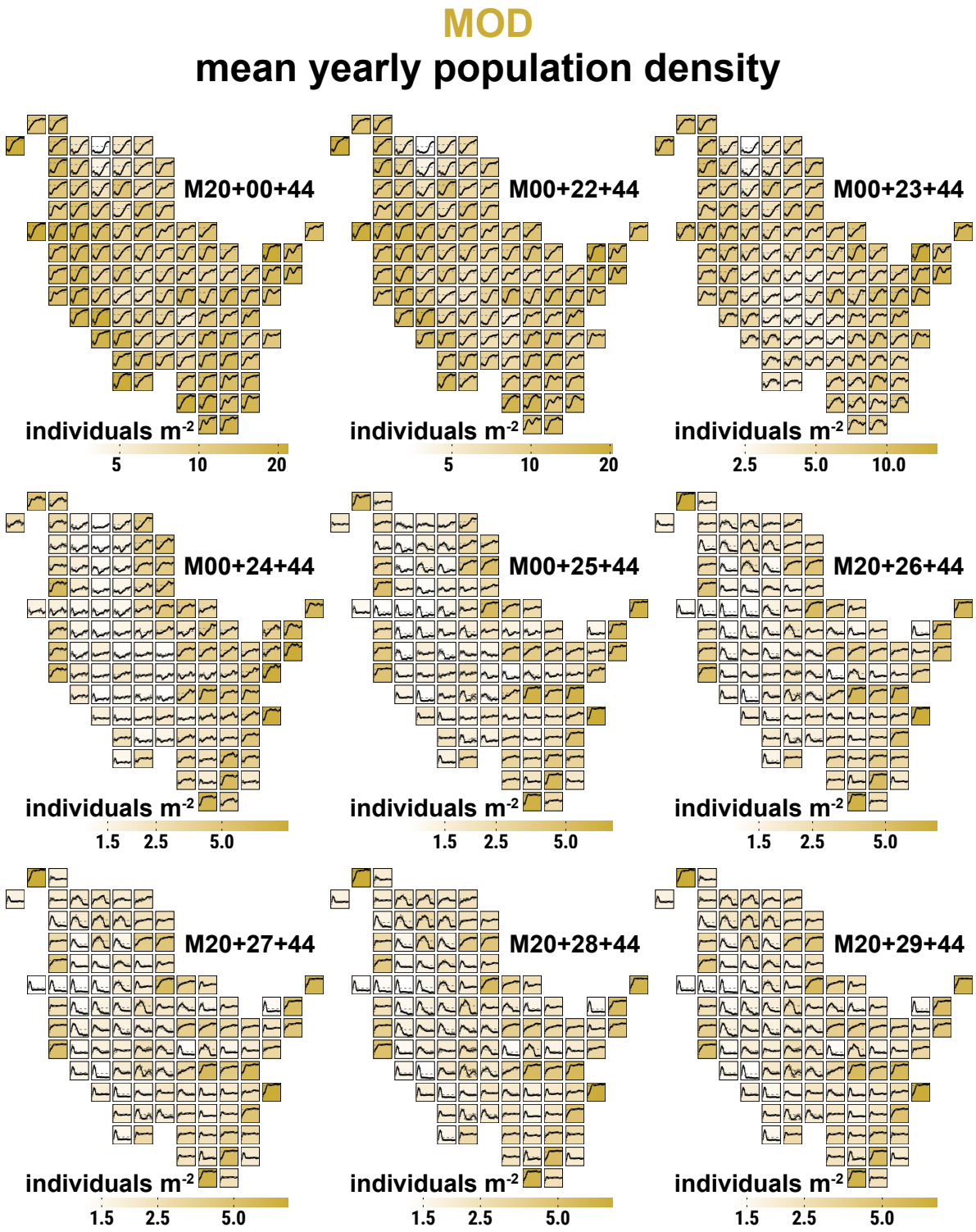

Figure B.15: Map of final population density for scenario MOD and mowing schedules M00 and M22-M29

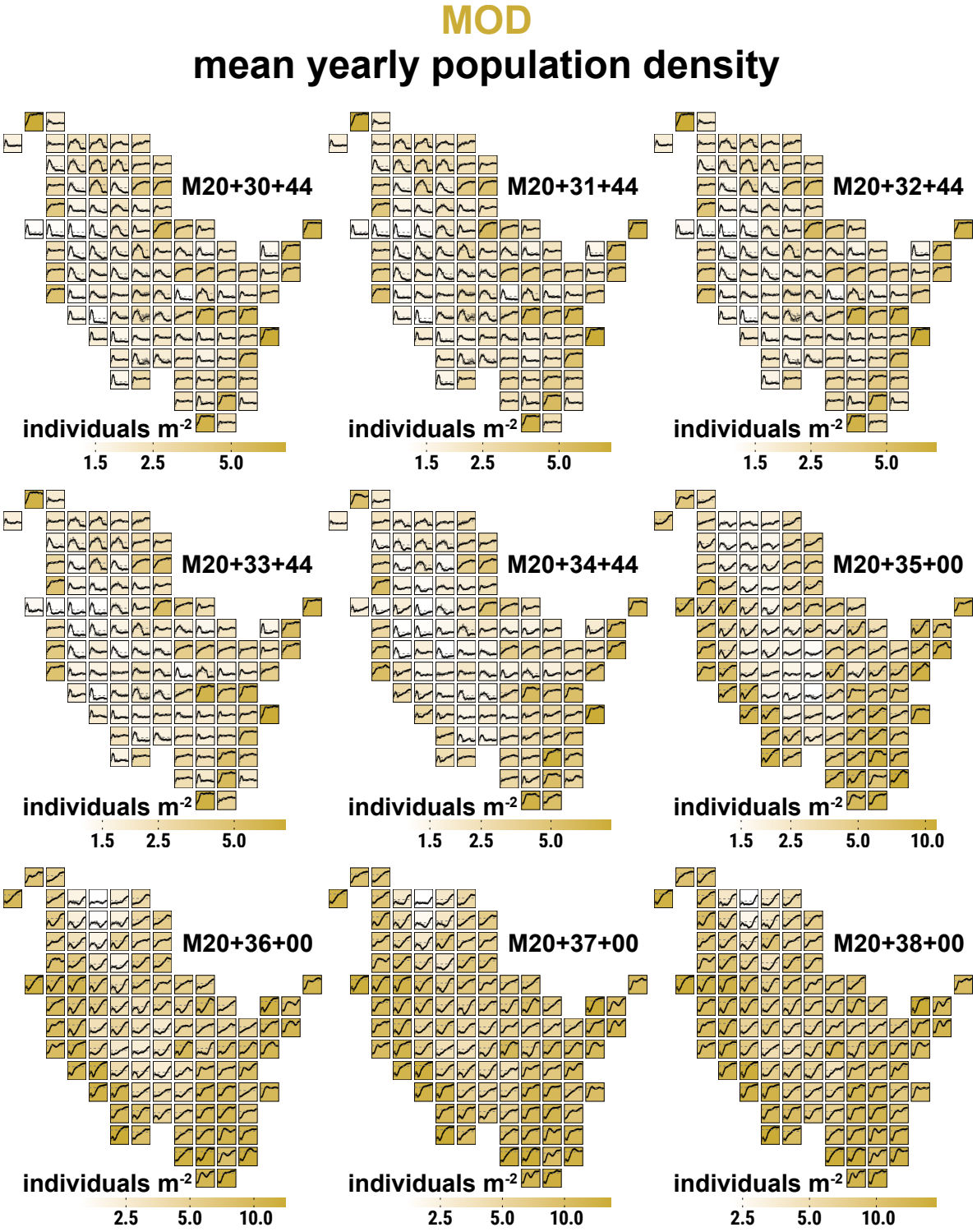

Figure B.16: Map of final population density for scenario MOD and mowing schedules M30-M38

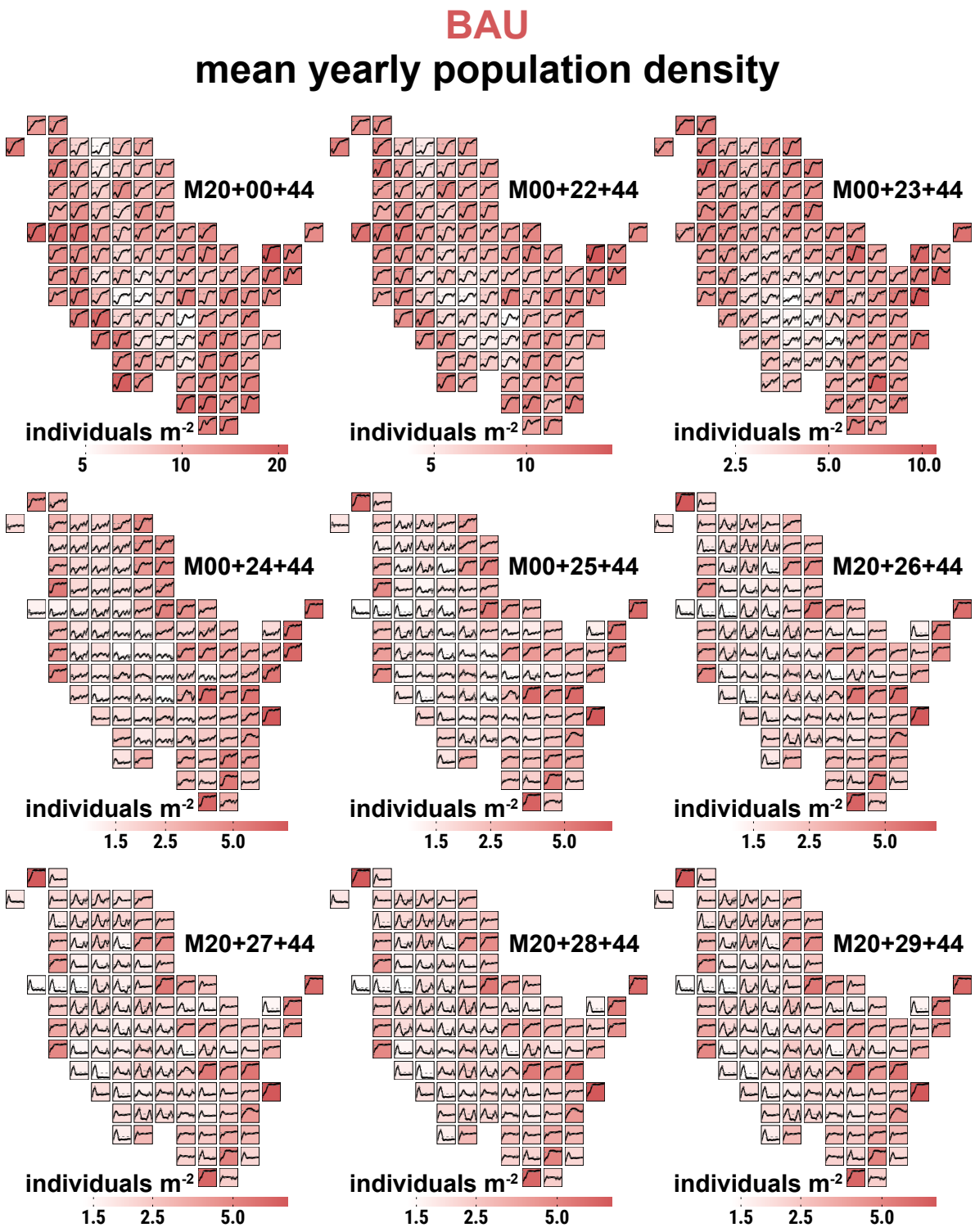

Figure B.17: Map of final population density for scenario BAU and mowing schedules M00 and M22-M29

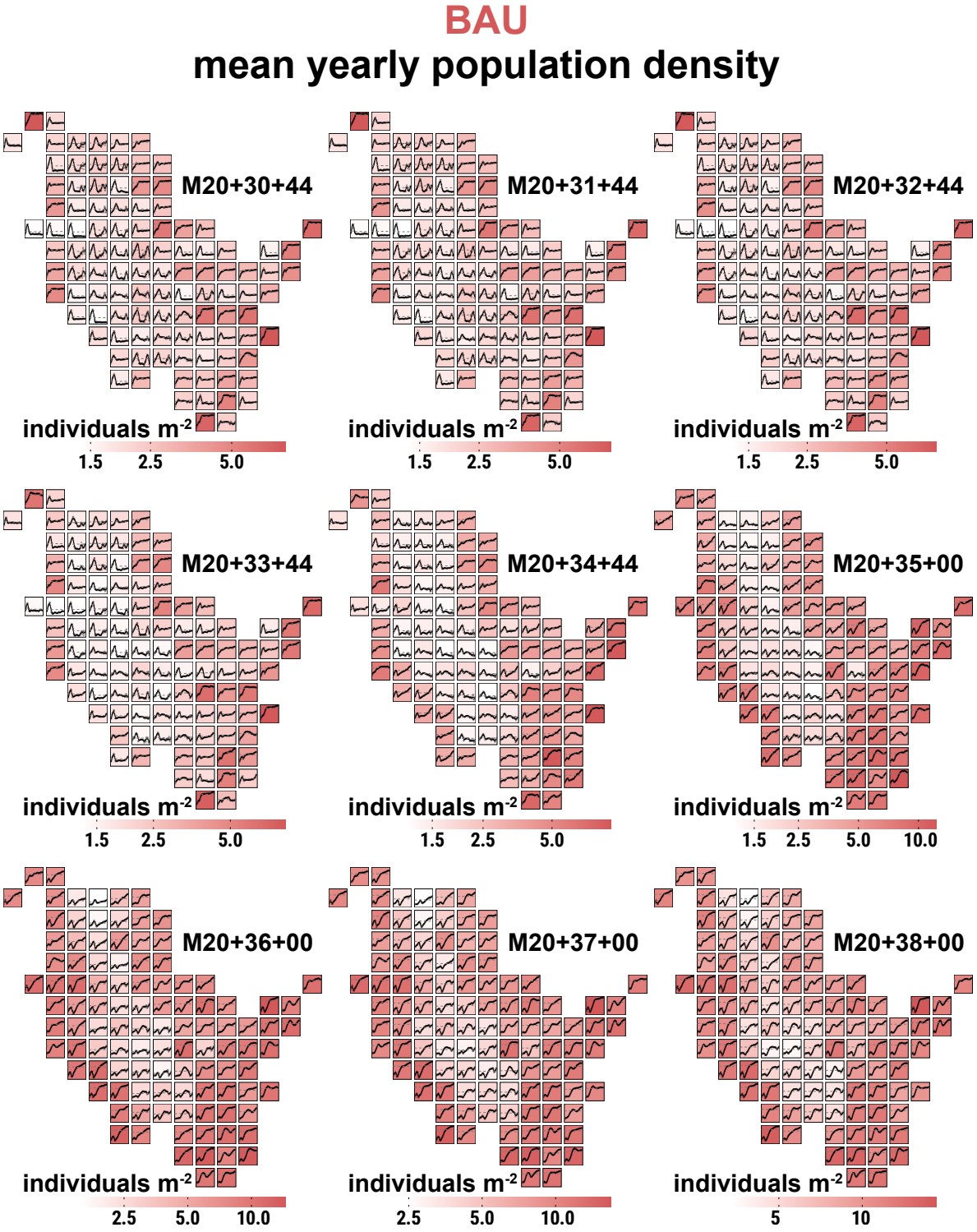

Figure B.18: Map of final population density for scenario BAU and mowing schedules M30-M38

B.2 Illustration of Differences in Dispersal Success

This section contains illustrations of the difference (delta) in dispersal success of the large marsh grasshopper (LMG) between climate change scenarios (CCS) depending on source habitat and mowing schedule in terms of four evaluation parameters: (Section B.2.1) the maximum established distance in meters from a source habitat to a habitat with imago density $\geq 0.002\ individuals\ m^{-2}$ during a year, (Section B.2.2) the population size in total number of eggs in all established habitats at the end of a simulation year, and (Section B.2.3) the population density in $eggs\ m^{-2}$ for all established habitats at the end of a simulation year. The title of each Figure indicates, which evaluation parameter, CCS delta (FF vs. MOD, FF vs. BAU or MOD vs. BAU) and mowing schedule (cf. Chapter 4, Table 4.1) applies. Values were determined per replicate by subtracting the yearly parameter values of the CCS mentioned second from the CCS mentioned first in the title and then calculating the replicate mean of the delta. Each of the 107 subplots in every Figure represents INDEPENDENT simulation runs, or rather their mean over 10 replicate runs, and depicts the results of the dispersal process from a SINGLE initial population in the center of a cell. Inside each subplot, dots are the log-scaled yearly means of the differences, solid black lines represents their smoothed trends using a generalized additive model, solid horizontal grey lines mark zero and dashed horizontal grey lines mark the mean of the yearly values during the 60 simulation years. The background color of the subplots highlight which of the respective CCS on average shows the higher differences during the 60 simulation years, where a LIGHTER color represents lower average difference. GREEN cells are in favor of FF, BROWN cells in favor of MOD and PINK cells in favor of BAU. These colors reflect in the bottom legend.

B.2.1 Illustration of Difference in *Maximum Established Distance*

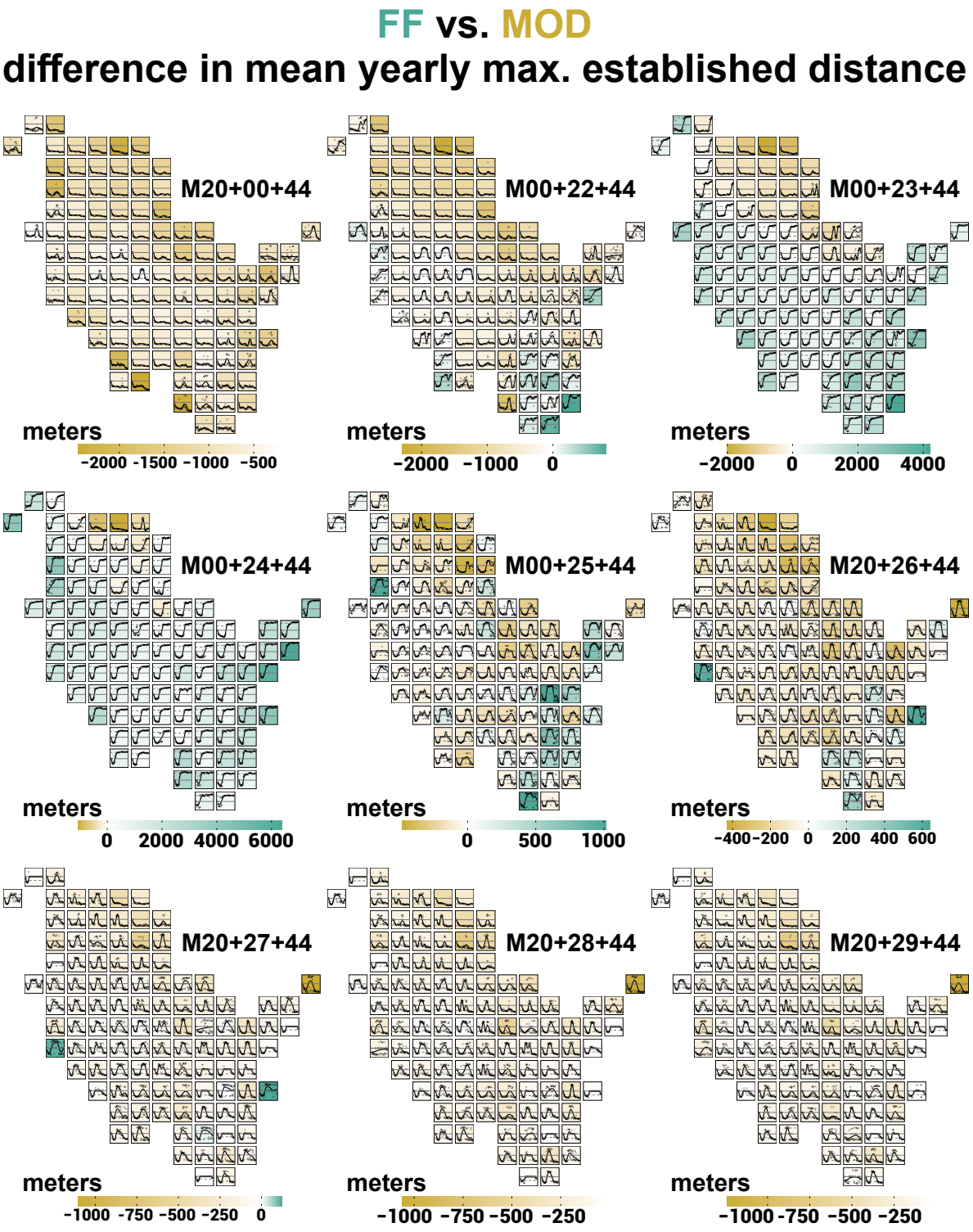

Figure B.19: Map of difference in maximum established distance between scenarios FF and MOD, and mowing schedules M00 and M22-M29

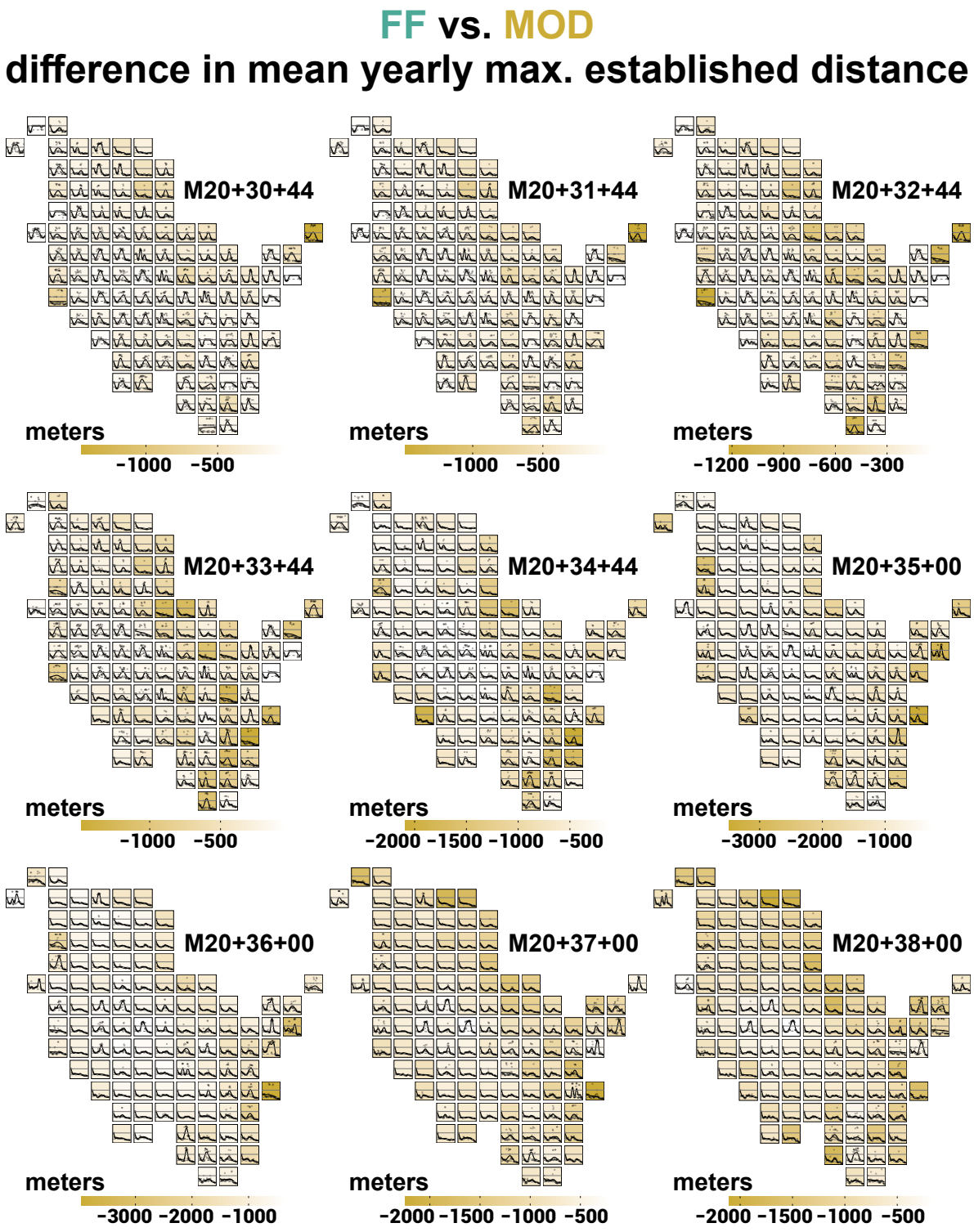

Figure B.20: Map of difference in maximum established distance between scenarios FF and MOD, and mowing schedules M30-M38

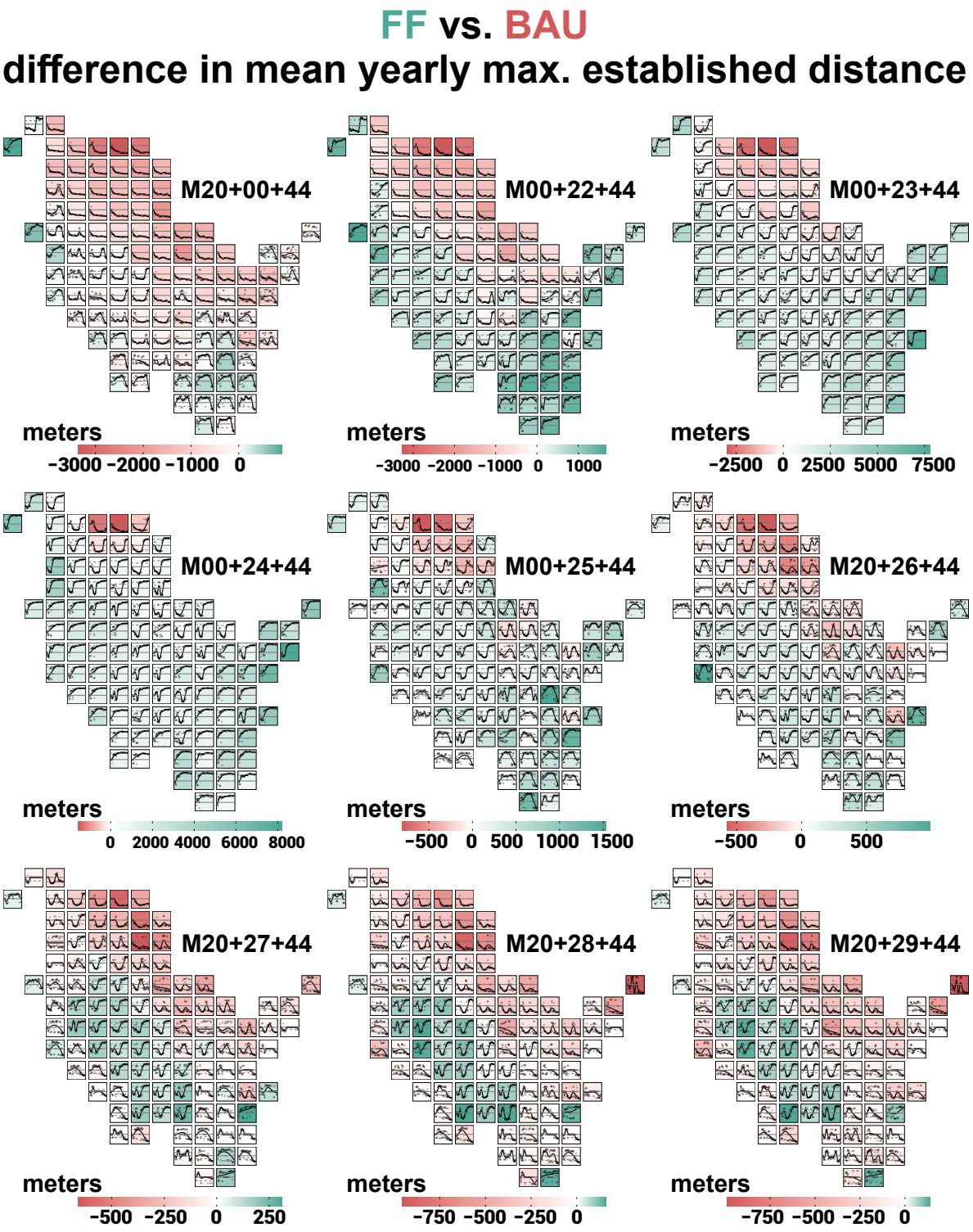

Figure B.21: Map of difference in maximum established distance between scenarios FF and BAU, and mowing schedules M00 and M22-M29

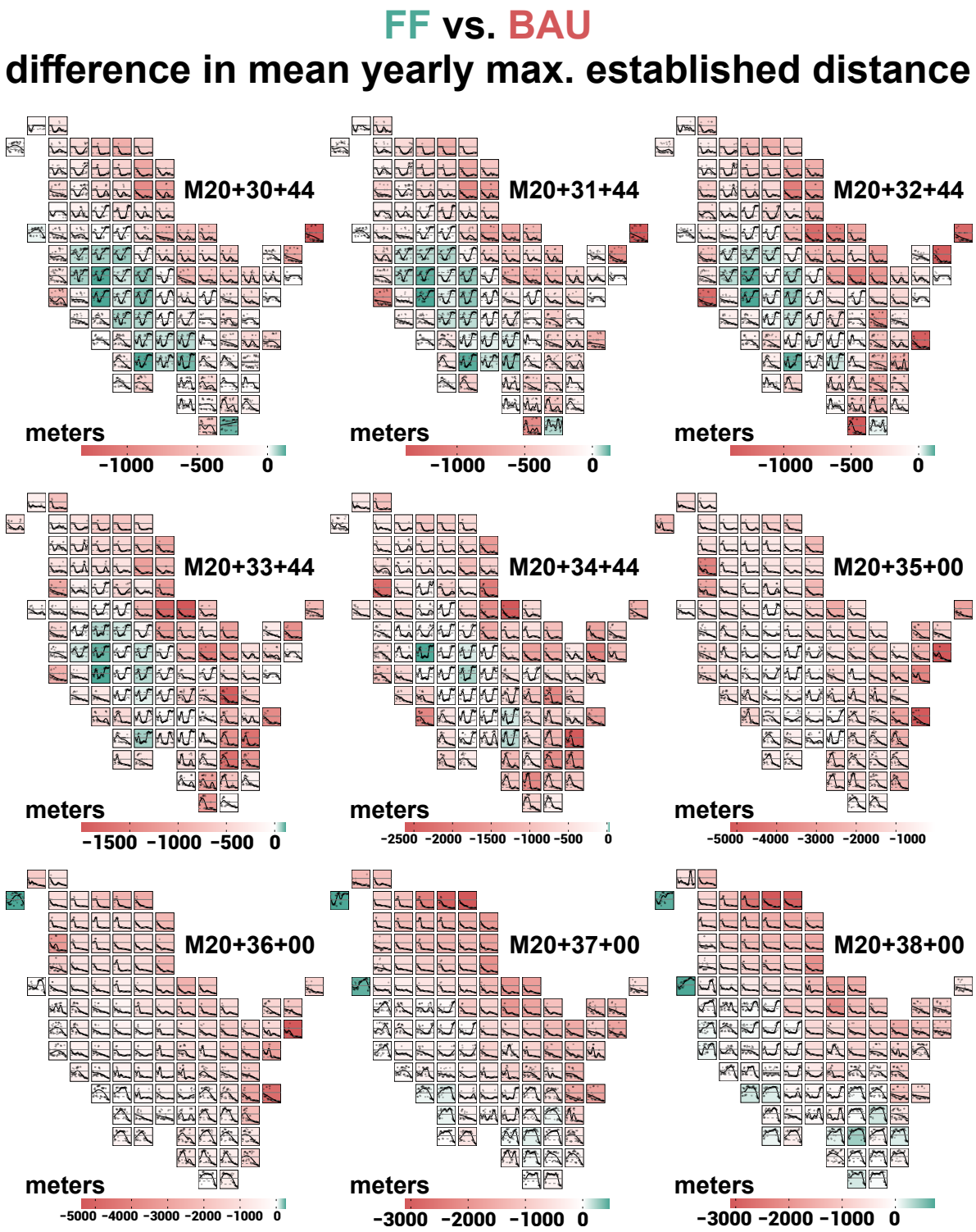

Figure B.22: Map of difference in maximum established distance between scenarios FF and BAU, and mowing schedules M30-M38

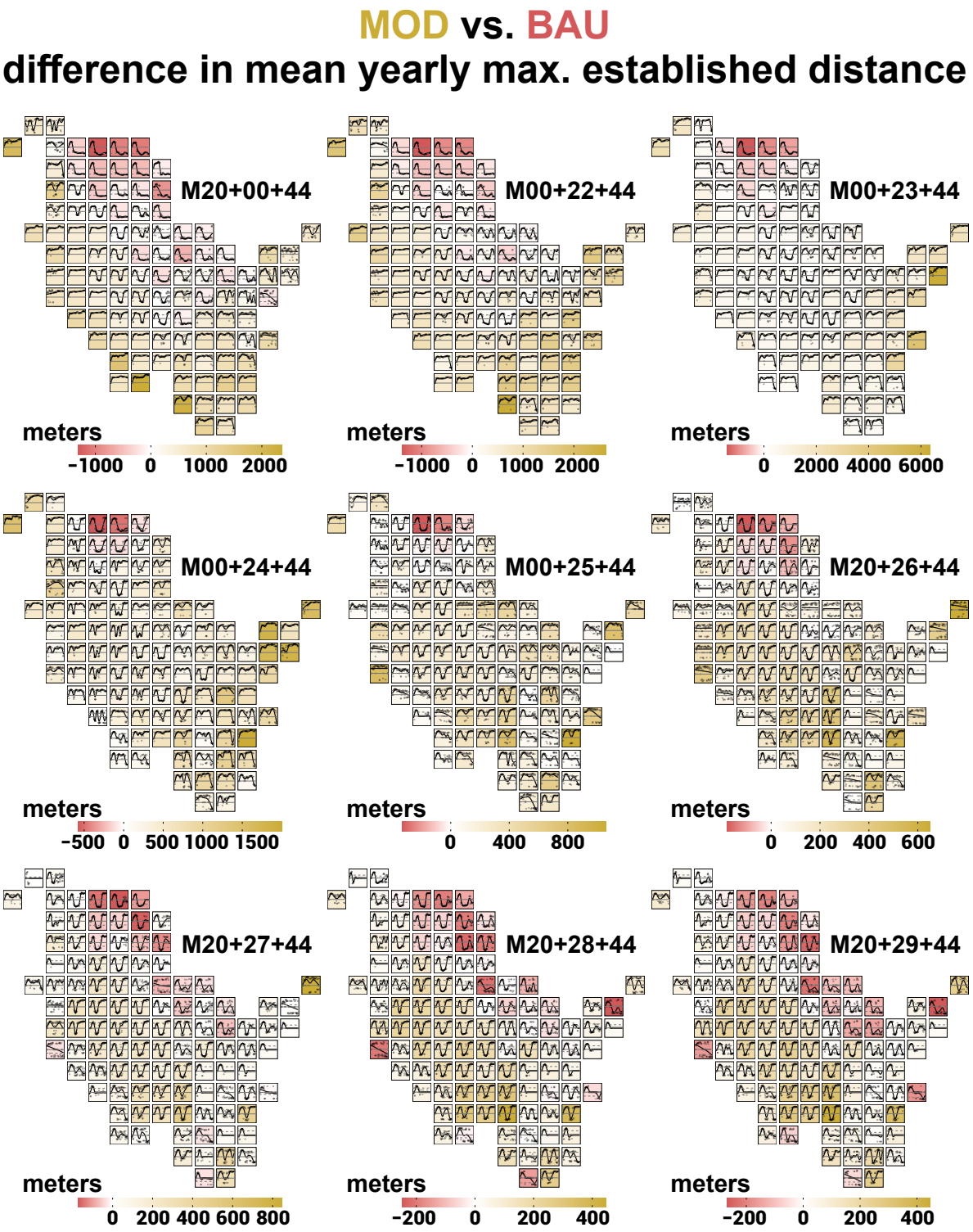

Figure B.23: Map of difference in maximum established distance between scenarios MOD and BAU, and mowing schedules M00 and M22-M29

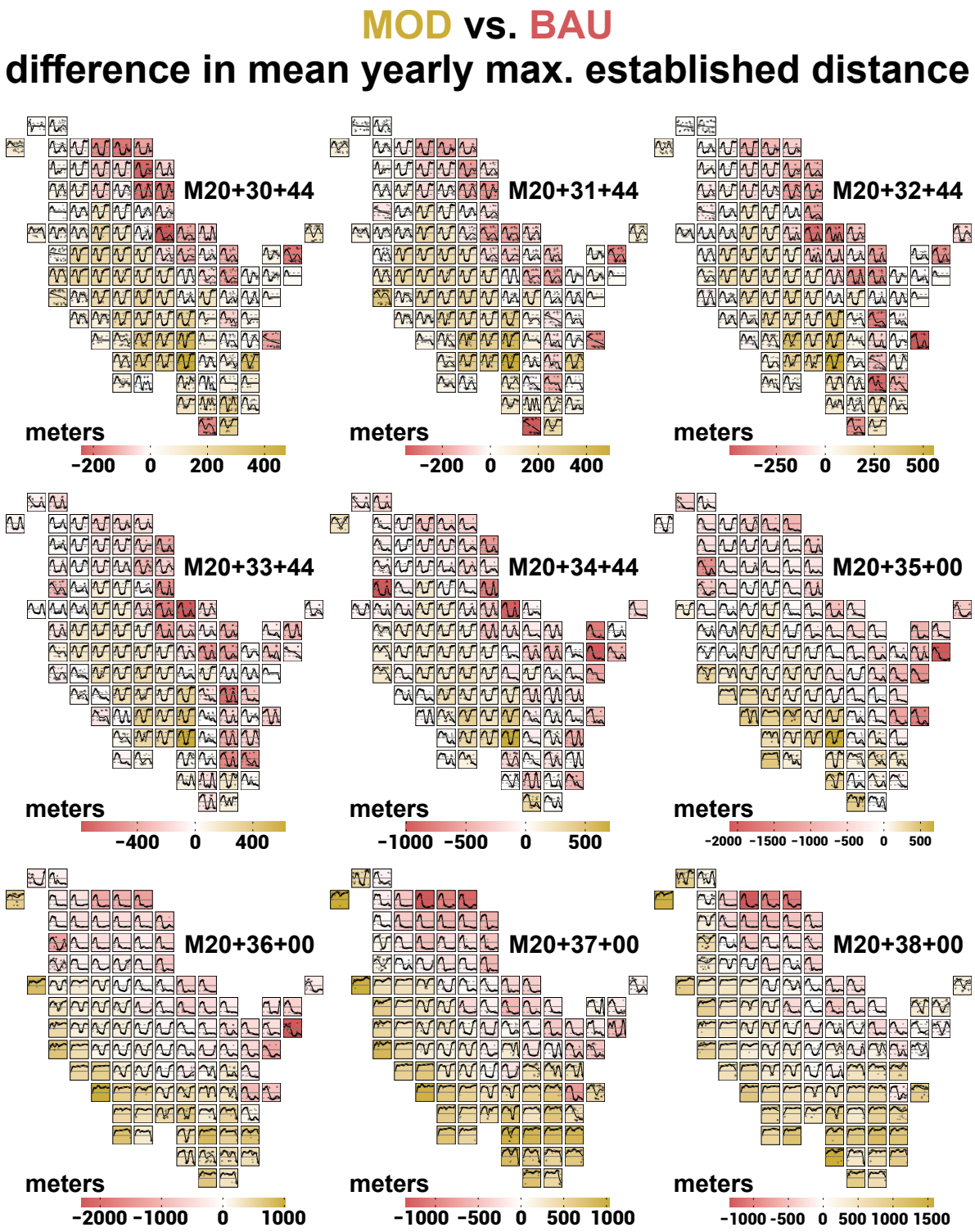

Figure B.24: Map of difference in maximum established distance between scenarios MOD and BAU, and mowing schedules M30-M38

B.2.2 Illustration of Difference in *Population Size*

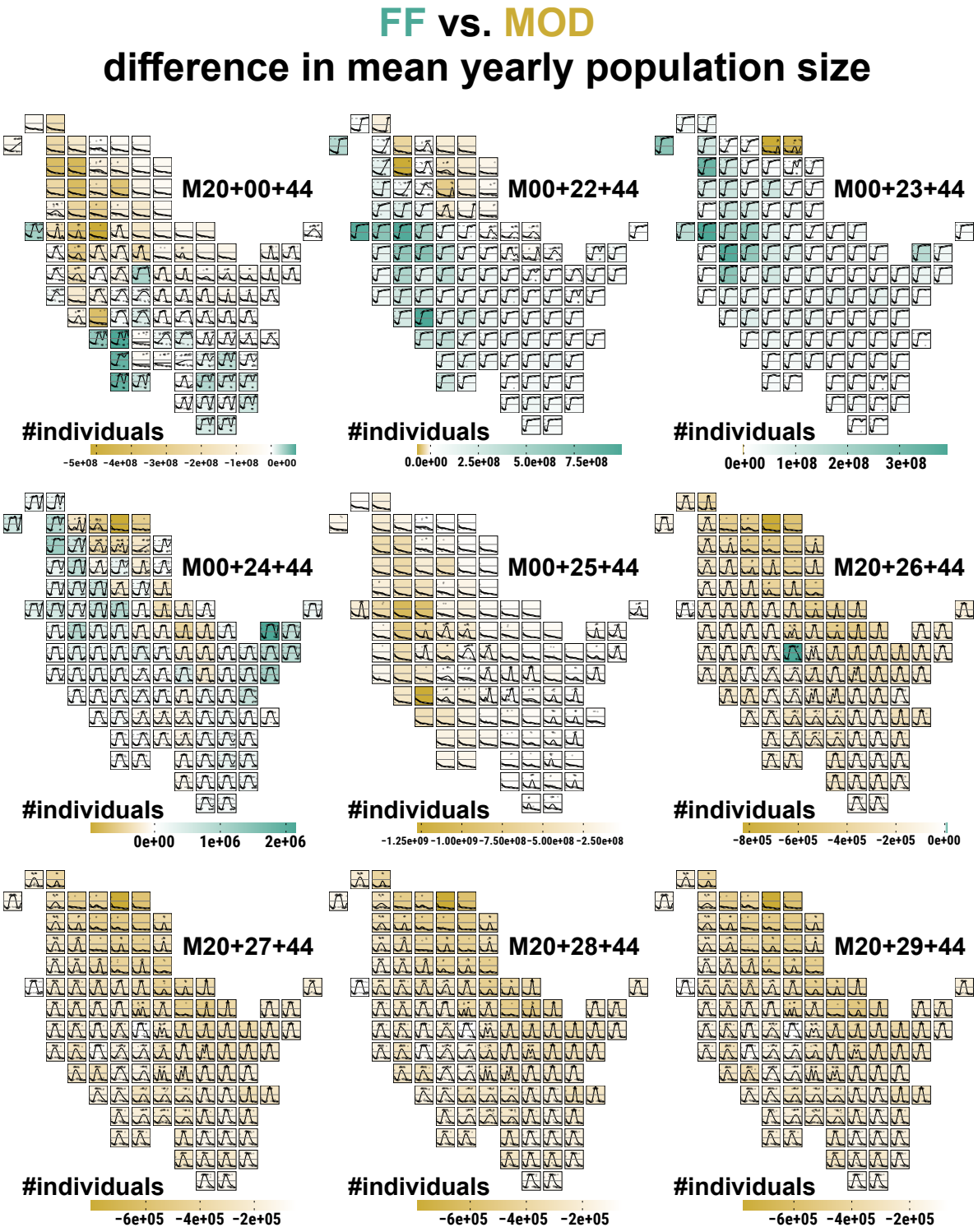

Figure B.25: Map of difference in final population size between scenarios FF and MOD, and mowing schedules M00 and M22-M29

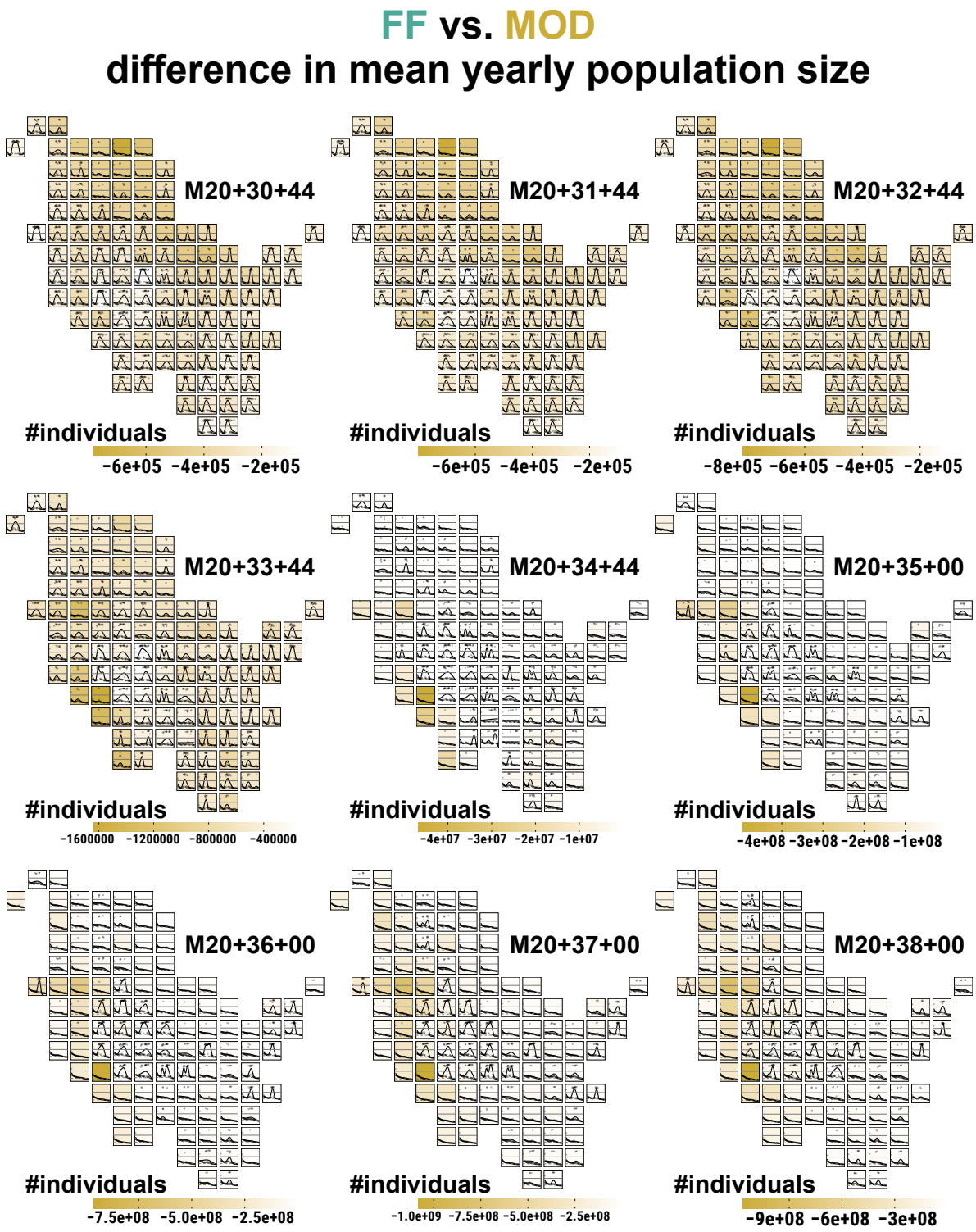

Figure B.26: Map of difference in final population size between scenarios FF and MOD, and mowing schedules M30-M38

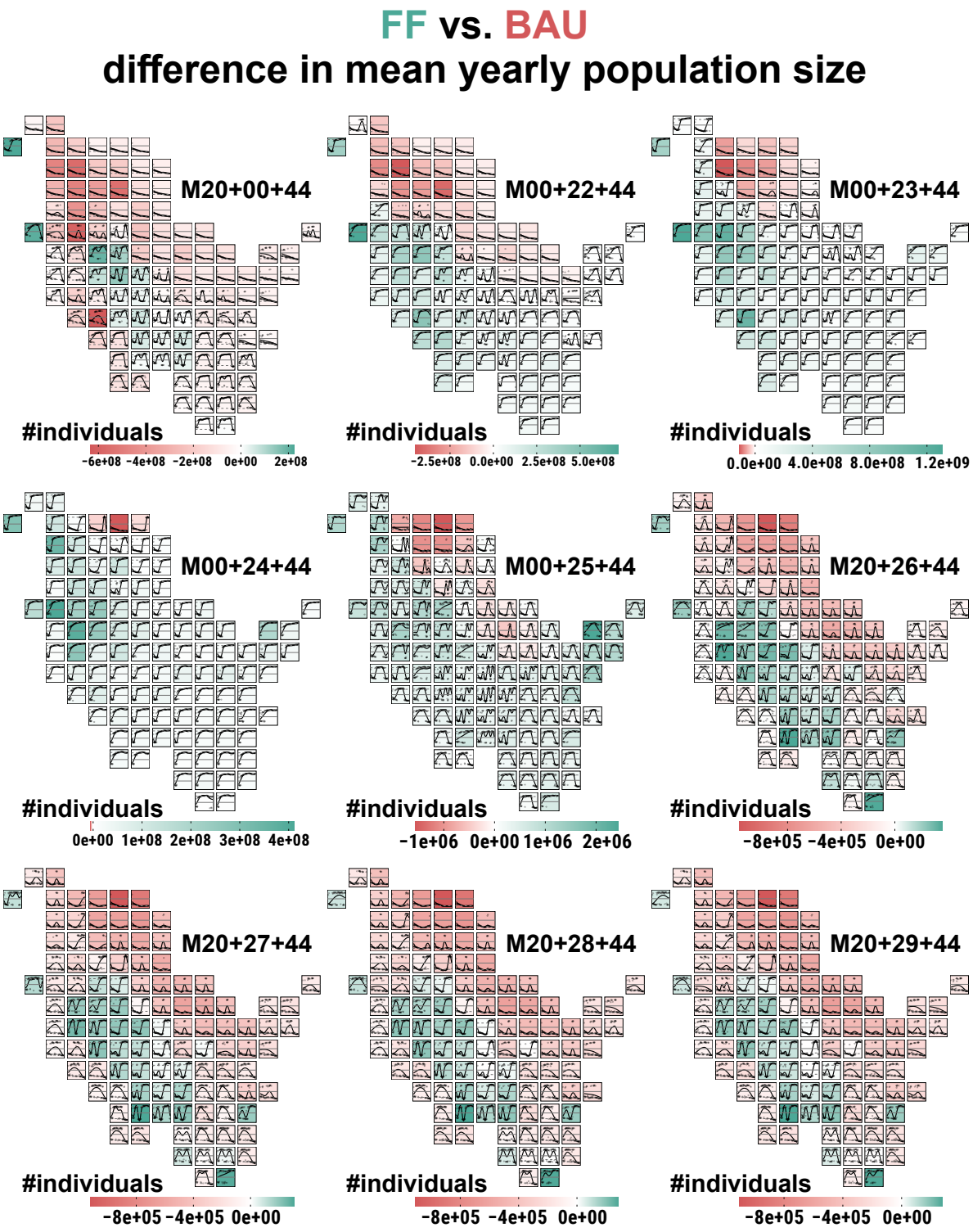

Figure B.27: Map of difference in final population size between scenarios FF and BAU, and mowing schedules M00 and M22-M29

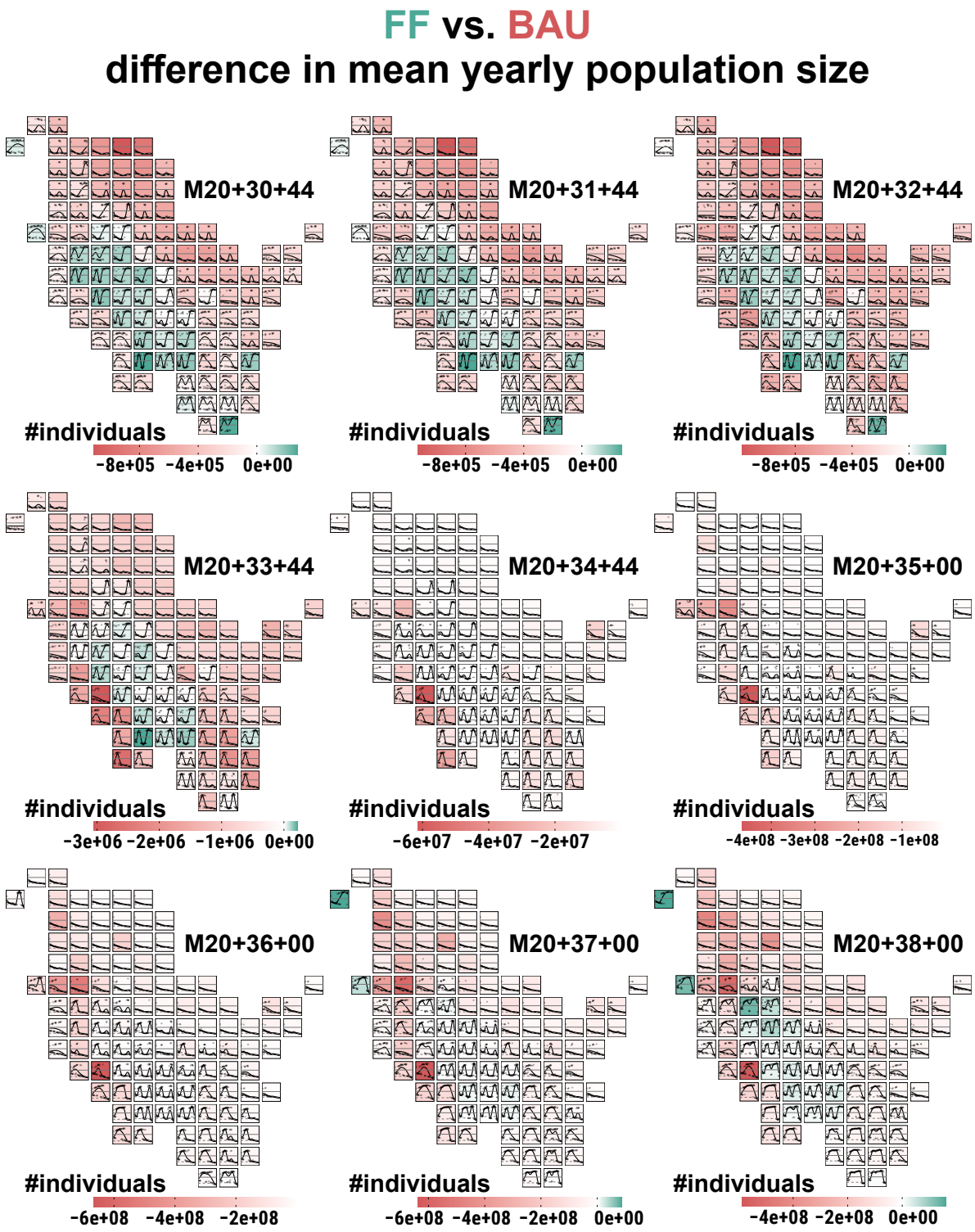

Figure B.28: Map of difference in final population size between scenarios FF and BAU, and mowing schedules M30-M38

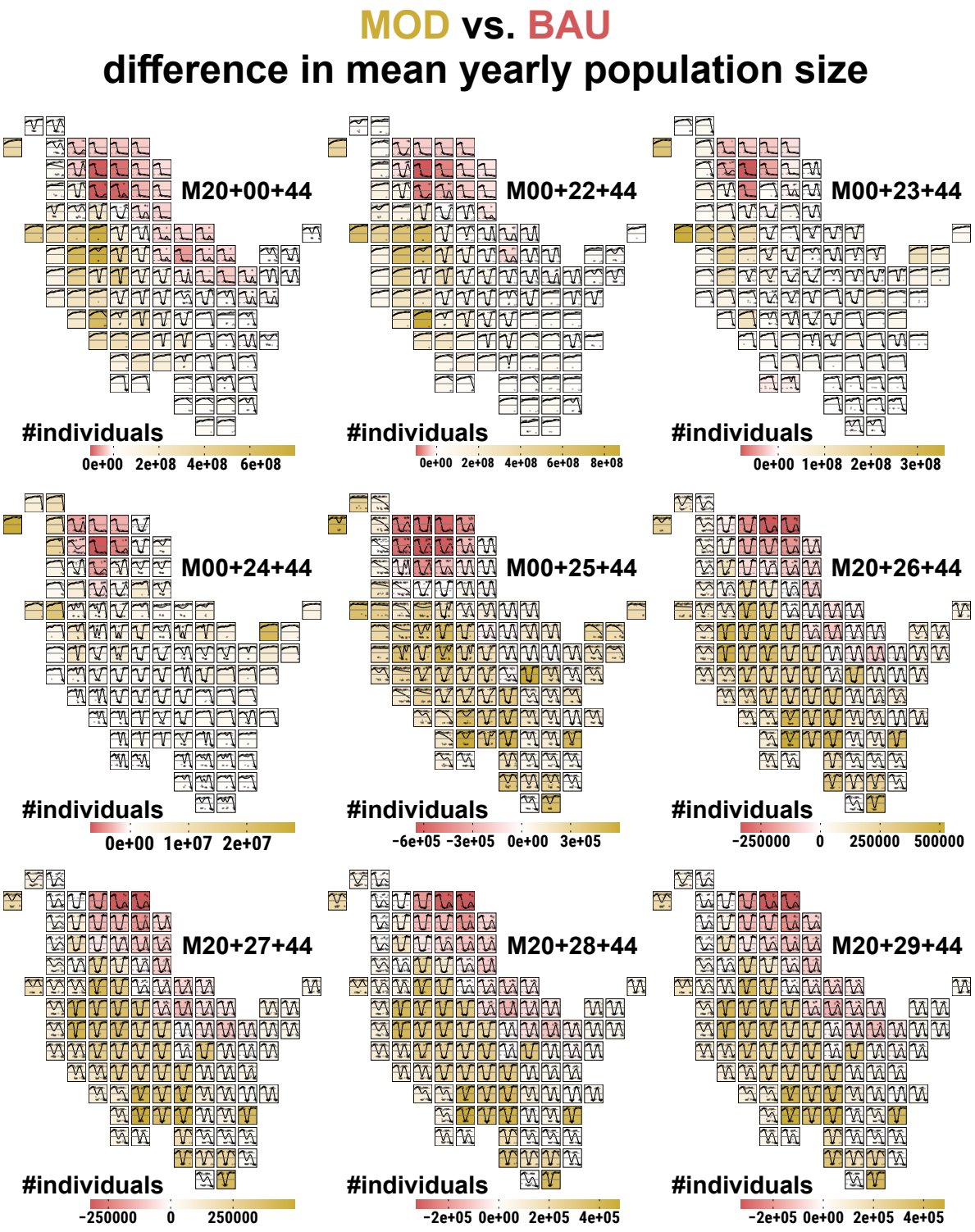

Figure B.29: Map of difference in final population size between scenarios MOD and BAU, and mowing schedules M00 and M22-M29

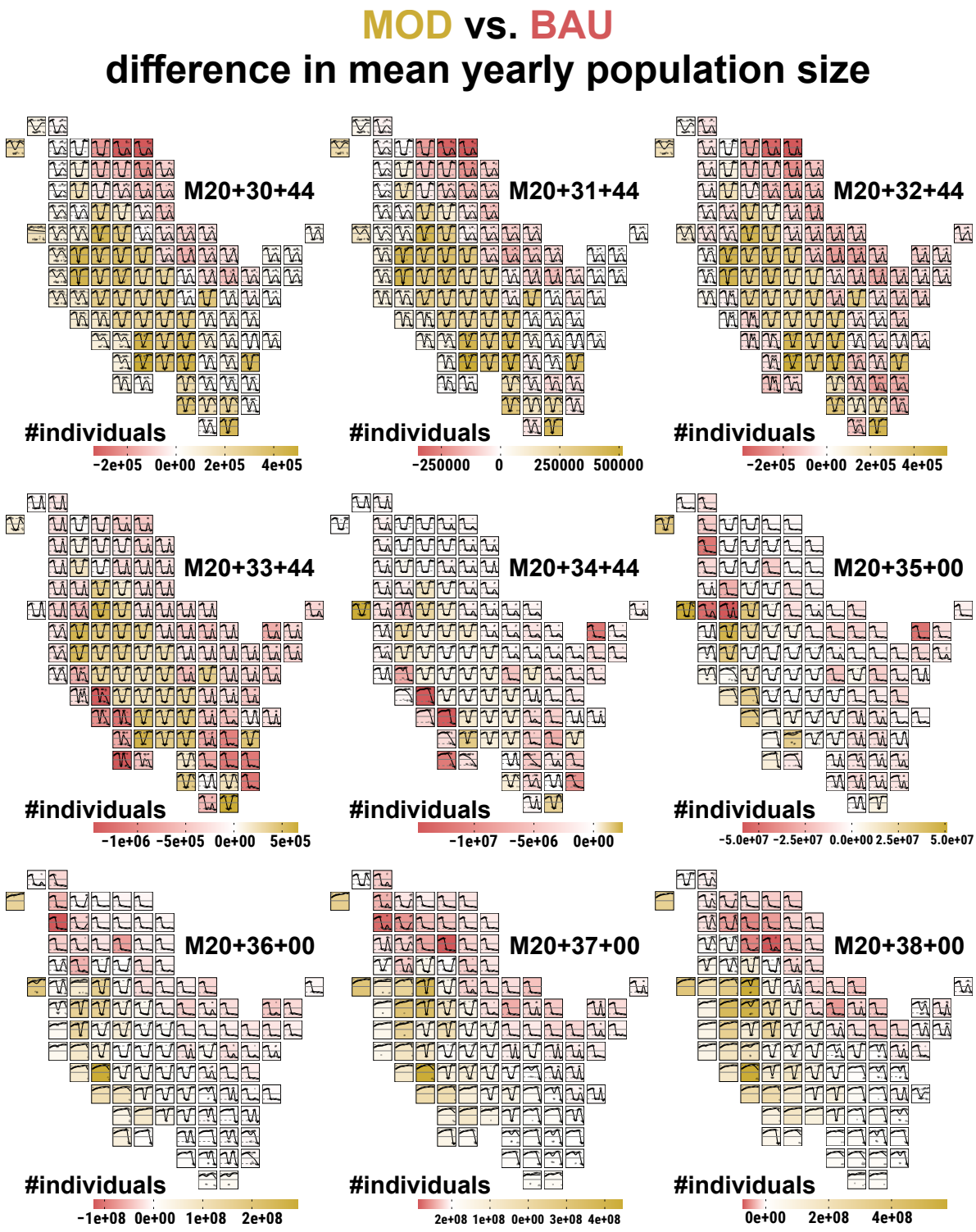

Figure B.30: Map of difference in final population size between scenarios MOD and BAU, and mowing schedules M30-M38

B.2.3 Illustration of Difference in *Population Density*

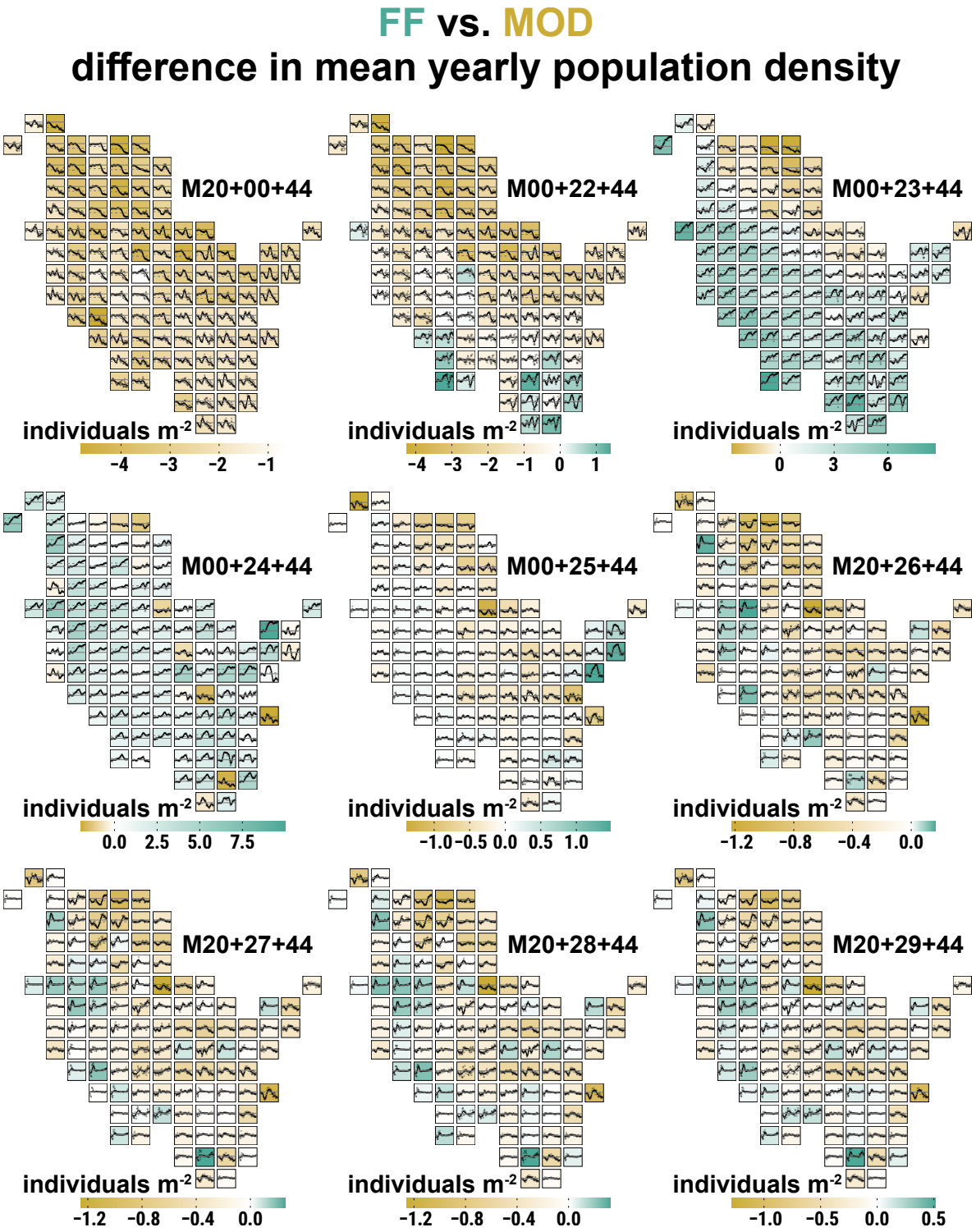

Figure B.31: Map of difference in final population density between scenarios FF and MOD, and mowing schedules M00 and M22-M29

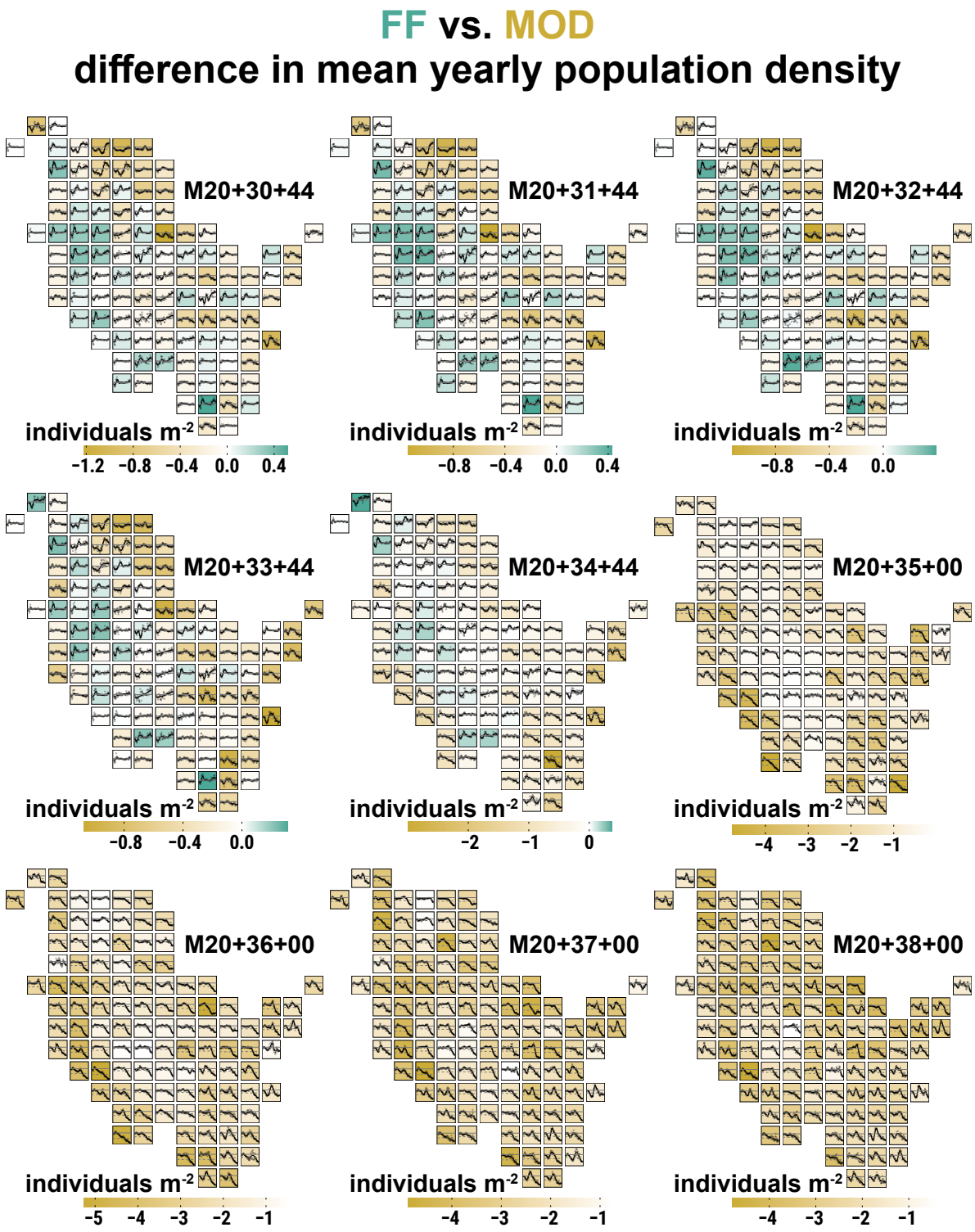

Figure B.32: Map of difference in final population density between scenarios FF and MOD, and mowing schedules M30-M38

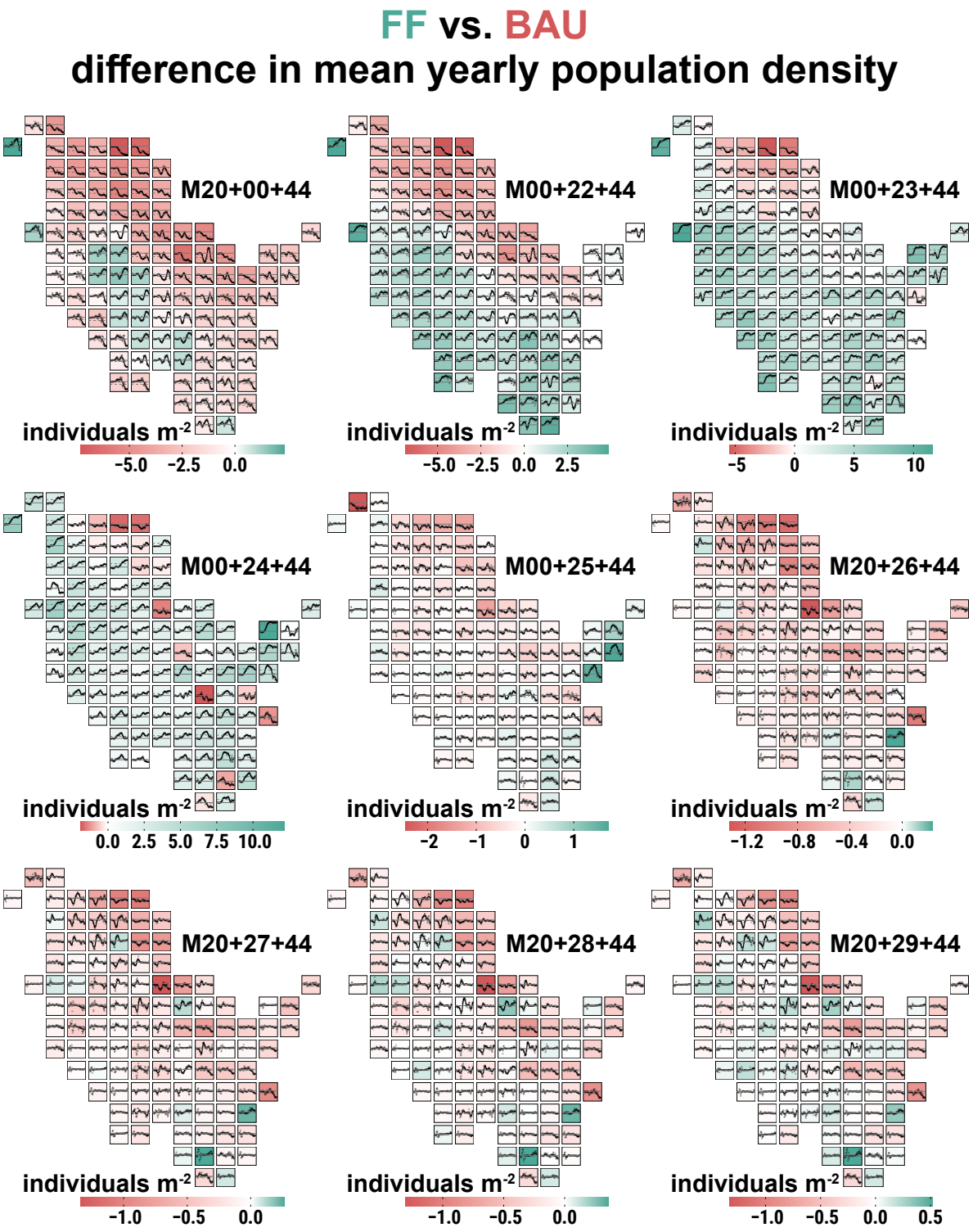

Figure B.33: Map of difference in final population density between scenarios FF and BAU, and mowing schedules M00 and M22-M29

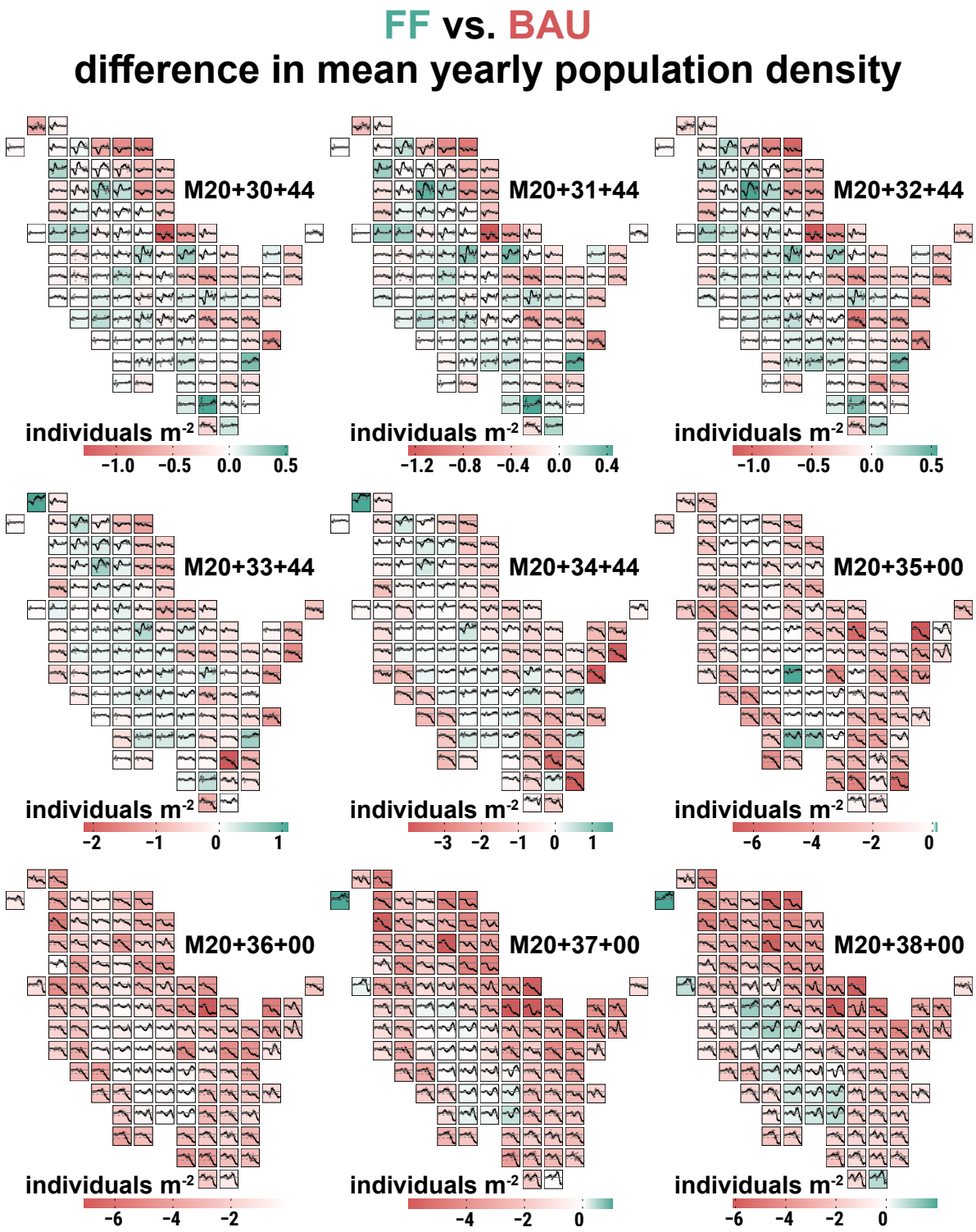

Figure B.34: Map of difference in final population density between scenarios FF and BAU, and mowing schedules M30-M38

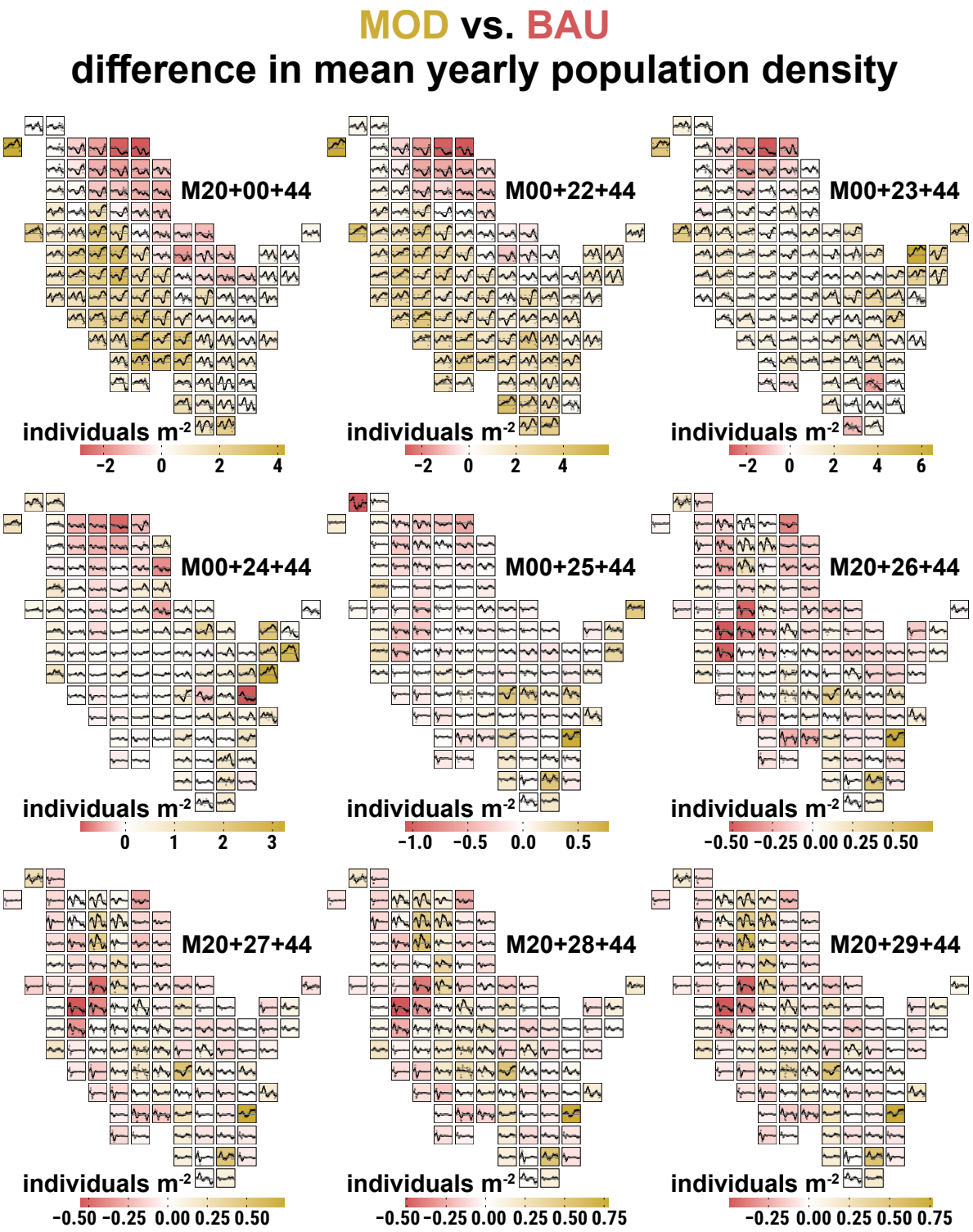

Figure B.35: Map of difference in final population density between scenarios MOD and BAU, and mowing schedules M00 and M22-M29

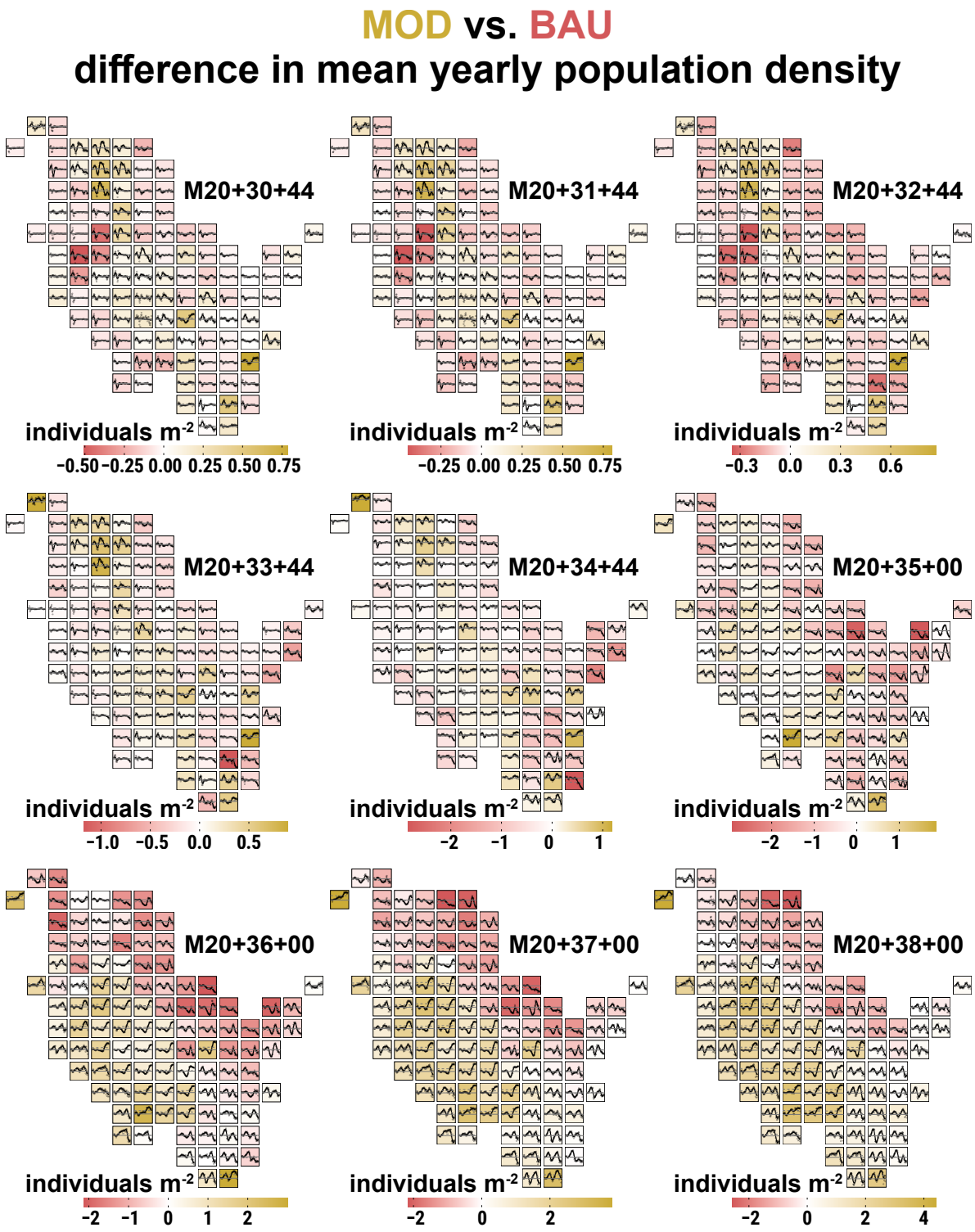

Figure B.36: Map of difference in final population density between scenarios MOD and BAU, and mowing schedules M30-M38

B.3 Mapping and Weights of Climate and Grassland Cells

This document describes the data in CSV files found at ufz.de/record/dmp/archive/11900

File *Supplement_S4-1_climate_cells.csv*:
Specifications per climate cell as defined in Section 4.2 of Chapter 4. The first column assigns a unique identifier (ID) to each cell (cf. Figure 4.2). Columns 2-7 adapt specifications from the applied climate data (Section 4.2.3), where second and third column are the cell's Cartesian coordinates, fourth and fifth their longitude and latitude and sixth and seventh column their longitude and latitude in rotate pole grid coordinates. The last two columns represent a climate cell's geometric center in terms of the Cartesian coordinate system of the grassland cells (Appendix B.1)

File *Supplement_S4-2_grassland_cells.csv*:
Specifications, mapping to climate cells and definition of weights applied for bilinear interpolation per grassland cell (Section 4.2.1). First and second column give the grassland cell's Cartesian coordinate. The remaining columns are subdivided into four three column blocks representing the four potential neighboring climate cells used for bilinear interpolation. Columns labeled ID_x contain the climate cell ID (Table 2.2, Chapter 2) of a respective neighbor, columns labeled DIR_x the cardinal direction of this neighbor and columns labeled w_x the bilinear weight of this neighbor. The 'x' in the previous description is replaced by the numbers 1-4, where the higher numbers represent the closer climate cells. The ID found in column ID_1 is the climate cell the grassland cell geographically belongs to. If ID_2-4, DIR_2-4 and w_2-4 are empty or contain a zero, no respective neighboring climate cell exists.

B.4 Illustration of Correlation between Evaluation Parameters

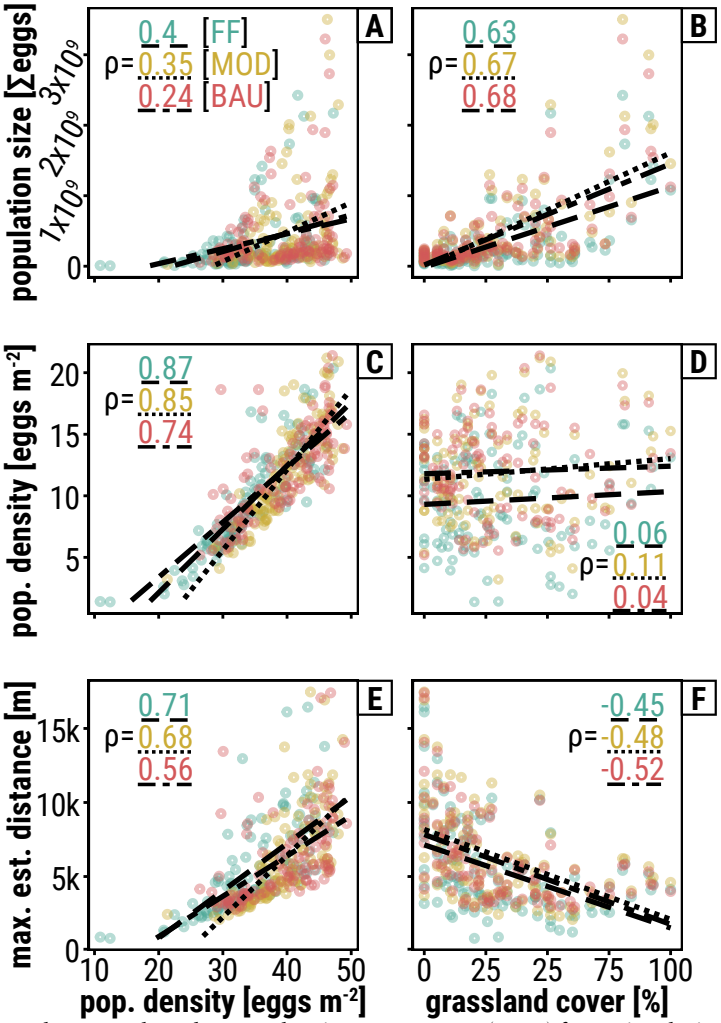

Figure B.37: The scatter plots correlate three evaluation parameters (rows) from simulations with dispersal (population size [$\sum$ *eggs*], population density [*eggs* m^{-2}], maximum established distance [*meters*]) with population density [*eggs* m^{-2}] stemming from simulations without dispersal as well as regional grassland cover [in %] in a radius $\leq 1{,}500$ m of a simulation run's respective habitat of origin (columns). Each colored dot represents the correlated values of INDEPENDENT simulation runs, or rather their mean over 10 replicate runs (5 without dispersal), resulting from the population dynamics and dispersal process of a SINGLE initial population in the center of one out of 107 cells. The dot colors distinguish the three climate change scenarios (CCS) FF (RCP 2.6, green), MOD (RCP 4.5, brown) and BAU (RCP 8.5, pink). The colored numbers give the correlation coefficient ρ for the respective parameter combinations by CCS. The black lines represent the respective linear regression, where dashed=FF, dotted=MOD and dash dotted=BAU

Dankeschön

Auch für das Erreichen eines so großen Meilensteins wie einer Dissertation spielen die Details entlang der Strecke eine nicht zu unterschätzende Rolle. Daher möchte ich nun einigen Menschen danken, die in den vergangen Jahren und Jahrzehnte kleine, mittlere und große – aber immer wichtige – Beiträge geleistet haben, damit ich meinen Weg bis hierhin beschreiten konnte.

Zuvorderst geht ein großer Dank an meinen Betreuerstab am UFZ, ohne den diese Arbeit wohl nicht vollendet worden wäre. Martin Drechsler danke ich dafür, dass er mir diese Promotion ermöglicht hat, für die konstruktiven wissenschaftlichen Diskussionen, den regelmäßigen aber auch kurzfristigen Austausch und die umfangreiche Unterstützung bei der Umsetzung der Promotion. Volker Grimm bin ich dankbar, dass er meinen Fokus immer wieder auf das Wesentliche gelenkt hat, jederzeit für wertvolles Feedback zur Verfügung stand und damit wesentlich zur Verbesserung der Arbeit beigetragen hat. Thomas Banitz danke ich für die zeitnahen und produktiven Diskussionen über die Details der Implementierung und inhaltlicher Aspekte. Bei Jürgen Groeneveld möchte ich mich für die hilfreichen Gespräche und Rat abseits der fachlichen Themen bedanken.

Außerdem danke ich allen Beteiligten im Projekt *Ecoclimb* für die gute Zusammenarbeit, den wissenschaftlichen Austausch und die gemeinsamen Veröffentlichung. Besonders dankbar bin ich Björn Schulz von der *Stiftung Naturschutz Schleswig-Holstein*, der mich immer wieder mit hilfreichen Informationen zur Sumpfschrecke versorgt hat.

Allen Kolleg:innen des Departments *Ökologische Systemanalyse* danke ich für die schöne Zeit, die gute Atmosphäre und dass die Türen jederzeit für wissenschaftlichen, aber auch persönlichen Austausch offen standen. Vor allem möchte ich hier die *ÖSA-Juniors* hervorheben. Ich bin sehr dankbar für den herzlichen Empfang, den ihr mir in Leipzig bereitet habt, und habe unsere regelmäßigen Aktivitäten am UFZ, aber auch nach Feierabend (vgl. Mölkky) sehr genossen.

Meine Freund:innen schätze ich dafür, dass sie gute Wegbegleiter:innen an den vielen Stationen meiner Vita waren und sind. Namentlich nennen möchte ich: Nina, Tobi, Christian, Inga, Annie und Maria. Auch wenn es euch vielleicht nicht bewusst ist, habt ihr mir gerade in den letzten vier Jahren wichtigen Ausgleich abseits des Arbeitsalltags geboten.

Der größte Dank geht an meine Familie, weil sie mein Fundament ist und mir große Sicherheit gibt. Meinen Eltern bin ich sehr dankbar für die Werte, die sie mir vermittelt haben, und dass sie für meinen Weg eine Grundlage geschaffen haben, die kaum besser hätte sein können. Meinen Brüdern danke ich, dass sie sich immer für mich eingesetzt haben und da sind, egal wann und worum es geht. Für meinen Neffen und meine Nichte bin ich dankbar, weil sie mir durch ihre aufgeschlossene und ehrliche Art immer wieder Perspektivwechsel ermöglicht haben. Und zum Schluss danke ich Petra von ganzem Herzen für ihren bedingungslosen Rückhalt in den letzten Jahren und wie sie mich durch die anstrengende Abschlussphase dieser Arbeit getragen hat.